Mechanisms governing the functions of BRCA1-BARD1 complexes during DNA repair

Thesis submitted in partial fulfilment of the requirements for the degree of

Doctor of Philosophy in Medical Sciences



Mary-Anne Durin

Chromatin and Genome Integrity Group

Radcliffe Department of Medicine

And

St Peter's College

University of Oxford

Trinity 2024

Mechanisms governing the functions of BRCA1-BARD1 complexes during DNA repair

Mary-Anne Durin

Radcliffe Department of Medicine and St Peter's College, University of Oxford

Thesis submitted in partial fulfilment of the requirements for the degree of Doctor of Philosophy in Medical Sciences, Trinity 2024

Abstract

The Breast Cancer-Associated protein 1 (BRCA1) forms a heterodimeric complex with BRCA1-associated RING domain protein (BARD1). The BRCA1-BARD1 complex performs important homologous recombination (HR) functions required for tumour suppression. Its dysfunction can lead to hereditary breast, ovarian, prostate, and pancreatic cancers. Furthermore, BRCA1 is required during male germline development. Notably, the BRCA1-BARD1 chromatin interaction domains required for these functions are still unclear. To understand how the BRCA1-BARD1 complex contributes to both genome stability and fertility, it is necessary to understand the molecular mechanism that governs BRCA1-BARD1 complex interactions with chromatin. Using a combination of separation-of-function mutational approaches in a cellular system and *in vivo*, I show that the BARD1 RING-nucleosome binding is dispensable for HR, yet it underpins BARD1 dual reader-independent recruitment of the BRCA1-BARD1 complex that supports its DNA repair functions. Furthermore, while the BARD1 dual reader supports BRCA1 recruitment and DNA double-strand break (DSB) repair by HR, it is dispensable for BRCA1 localisation in mouse spermatocytes and is not required for meiotic sex chromosome inactivation (MSCI). Additionally, this study uncovers a regulatory role of BRCA1-BARD1 in the recruitment of RAP80 to DSB sites, which is influenced by 53BP1 and occurs in a cell cycle-dependent manner. In contrast, the intrinsically disordered region (IDR) of BARD1 is largely dispensable for DNA repair but can support some BARD1 functions, independently of BRCA1. Collectively, this thesis provides new insights into the multifaceted and versatile functions of the BRCA1-BARD1 complex and its critical functions in both somatic and germline contexts, with potential implications for developing therapies targeting BRCA1-deficient cancers in the clinic.

Acknowledgements

The arduous yet exciting journey of my DPhil over the past four years would not have been possible without the support of an ocean of people, to whom I am eternally grateful.

First and foremost, a huge thank you to my supervisor Prof Ross Chapman. Your support and guidance throughout my DPhil have been invaluable. Thank you for the incredible opportunities you have provided over the last four years, which allowed me to share my science with others and learn from them in turn. Thank you for sharing your excitement so wholeheartedly with me whenever I knocked on your door with new results, and for your patience when sometimes things would take a bit longer.

To the entire Chapman group, thank you for the kindness, support and camaraderie that you offered on both the "good days" and the "bad days" of my DPhil, and for all the funny moments we have shared. I learned so much from all of you and had so much fun being a member of our team! I would especially like to thank Lucia and Ash, for always believing in me, even when I was blind to my own achievements, for encouraging me to push through frustrating periods, and for all the inspiring and fun conversations we had during "late-night" hours in the lab and outside of our world in the lab. I learned so much from you on my journey toward becoming an independent researcher!

To my mum and dad, your support throughout my academic life has been immeasurable. Your unconditional patience and unwavering belief that I could achieve anything I set my mind to means the world to me, and it proves that no matter the thousands of kilometres between us, you will always be my home. Being a first-generation student (and now an almost first-generation Dr!), I can imagine that my long monologues about life in the lab and everything that encompassed the topic "thesis" may have sounded abstract at times, but you never failed

to show interest in understanding what I do and support me unconditionally in my academic endeavours. I could not have been able to do this degree without you, thank you for everything you did for me and everything you have sacrificed to allow me to have this life, which has let me work in the field that I am most passionate about. To my sisters, grandma, uncles, and cousins – I am so grateful to have you in my life and for your love that has shaped me into the person I am today.

To all my friends from back home and across the seas, I am so lucky! Thank you for the grounding conversations and the warm words you always had ready for me. You understand me down to my core and your support gave me so much strength to accomplish what I did during my DPhil. I want to especially thank my best friends Anastasia, Elin and Rita – you have always been there for me, no matter the weather, continuously inspiring me and helping me reach the finish line, regardless of the difficulties. And to André, I wish you did not leave us so soon – I often think about all the fun conversations we would have had about all the interesting things in life and my research (now that my DPhil has come to an end!). Your encouraging and supportive words meant more to me than I will ever be able to share with you. To all the friends I made in Oxford, thank you so much for all the fun memories that kept me going throughout the last years! A special thank you to Sanja, for your amazing friendship, for seeing me for who I am and reminding me of it whenever my thesis made me forget.

Thank you to Simone – your special presence in my life and throughout my DPhil has been irreplaceable. Thank you for your comfort, love and patience during the challenging and exciting times, and for sharing all the beautiful and exciting moments in life with me.

My DPhil studies were funded by the MRC WIMM Prize Studentship.

Declaration

I hereby declare that this thesis was composed by myself and has not been submitted for any other degree at the University of Oxford, or elsewhere. The results here presented are of my own work, unless otherwise stated in the text.

Table of Contents

Acknowledgements ii

Declaration iv

List of Abbreviations ix

List of Figures xvi

List of Tables xix

Chapter 1. Introduction 1

1.1 The cellular response to DNA double-strand breaks 1

1.1.1 The DNA damage response (classical paradigm) and the chromatin response to DNA damage 2

1.1.2 DNA double-strand break repair 4

1.1.3 Homologous recombination 5

1.1.4 Non-homologous end joining 8

1.1.5 Alternative repair pathways 10

1.1.6 Checkpoint responses 13

1.1.7 Cell fate decisions following DNA damage 14

1.2 Control of DNA double-strand break repair pathway choice 15

1.2.1 The purpose of DNA double-strand break repair pathway choice 16

1.2.2 Importance of Homologous Recombination and tumour suppression 16

1.2.3 Importance of Non-homologous End Joining in antigen receptor recombination and DNA repair in G0/G1 cells 17

1.2.4 Emergence of backup repair pathways as an important pathway 19

1.2.5 Resection vs. end-protection of DNA double-strand breaks 20

1.2.6 Chromatin regulation of pathway choice 21

1.2.7 Meiotic DNA double-strand break repair 24

1.3 53BP1: a mediator of NHEJ 27

1.3.1 53BP1 protein domains and functions 27

1.3.2 Physiological and pathological functions of 53BP1 30

1.4 BRCA1: a tumour suppressor protein involved in Homologous Recombination repair 31

1.4.1 BRCA1 protein domain architecture 31

1.5 BARD1: the obligate binding partner of BRCA1 36

1.5.1 BARD1 protein domain architecture 36

1.6 The BRCA1 sub-complexes: co-factors of BRCA1 – the BRCA1-A, B and C complexes 40

1.6.1 The BRCA1-A complex 42

1.6.2 Function of RAP80 in DNA repair 44

1.6.3 BRCA1-A dependent recruitment of BRCA1 at DNA double-strand breaks 47

1.7 The biological and physiological functions of BRCA1 and BARD1 48

1.7.1 Tumour suppressor functions: control of HR 48

1.7.2 Additional functions for BRCA1 51

1.7.3 Germline functions of BRCA1: meiosis and meiotic sex chromosome inactivation 53

1.8 Aims 56

Chapter 2. Materials and Methods 58

2.1 Cell culture 58

2.1.1 Cell lines 58

2.2 Mice 58

2.2.1 Mouse strains 58

2.2.2 Mouse genotyping methods 59

2.3 Lentiviral transgene complementation 61

2.3.1 Generation of lentiviral constructs 61

2.3.2 Lentivirus generation and cell infection 66

2.4 SDS-PAGE-Western blot 66

2.5 Cytogenetic methods 67

2.5.1 Sister-chromatid exchange assay 67

2.5.2 Meiotic metaphase spread preparation 69

2.6 Immunofluorescence analysis 70

2.7 Quantitative image-based cytometry 73

2.8 Drug sensitivity assays **74**

2.8.1 Resazurin cell viability assay 74

2.8.2 Clonogenic survival assay 75

2.9 Micronuclei analysis **75**

2.10 Statistical methods **76**

Chapter 3. The importance of BRCA1-BARD1 nucleosome binding in DNA repair **77**

3.1 Introduction **77**

3.2 Results **78**

3.2.1 The role of the BRCA1-BARD1 RING-dependent nucleosome interactions in DNA repair 78

3.2.2 BARD1 RING-nucleosome interactions can support BRCA1-BARD1 DNA repair functionality when the dual reader module is absent 85

3.2.3 The canonical BRCA1-BARD1 complex suppresses RAP80 recruitment to DSB sites in replicating cells 90

3.3 Concluding remarks **95**

Chapter 4. The BRCA1-independent functions of BARD1 **99**

4.1 Introduction **99**

4.2 Results **100**

4.2.1 The BARD1 intrinsically disordered region is not crucial for DNA repair 100

4.2.2 BARD1 has BRCA1-independent functions during DNA repair 104

4.2.3 BRCA1-BARD1 promotes SCEs via HR-dependent and independent mechanisms 112

4.2.4 The involvement of the BARD1 IDR and chromatin binding residues during BRCA1-independent DNA repair 115

4.3 Concluding remarks **123**

Chapter 5. *In vivo* importance of the BARD1 dual-reader domain **127**

5.1 Introduction **127**

5.2 Results **129**

5.2.1 Viability of *Bard1*$^{D700A/D700A}$ mice in *53bp1*$^{L1616A/L1616A}$ and *53bp1*$^{+/+}$ backgrounds 129

5.2.2 *In vivo* functions of the BARD1 dual reader domain in Homologous Recombination: Phenotypic characterisation of *Bard1*$^{D700A/D700A}$ *53bp1*$^{L1616A/L1616A}$ mutant mice 131

5.2.3 *In vivo* functions of the BARD1 dual reader domain in male germline development 134

5.2.4 Meiotic BRCA1 recruitment does not rely on the BARD1 BUDR-dependent recruitment mechanism 136

5.3 Concluding remarks 139

Chapter 6. Discussion 143

6.1 The implications of BARD1 nucleosome binding in supporting somatic DNA repair and BRCA1-dependent functions for MSCI 143

6.2 BARD1 supports additional DNA repair roles independently of BRCA1 148

6.3 Overall Conclusions 150

Chapter 7. References 152

List of Abbreviations

53BP1	p53-Binding Protein 1
9-1-1	RAD9-RAD1-HUS1
AID	Activation-Induced cytidine Deaminase
Alt-EJ	Alternative end-joining
APC/C	Anaphase-Promoting Complex/Cyclosome
ARD	Ankyrin Repeat Domain
ATM	Ataxia Telangiectasia Mutated
ATPase	Adenosine Triphosphatase
ATR	Ataxia Telangiectasia and Rad3-related protein
BARD1	BRCA1-Associated RING Domain protein 1
BAX	Bcl-2 Associated X protein
BBC3	Bcl-2 Binding Component 3
Bcl-2	B-cell lymphoma 2
BIR	Break-Induced Replication
BLM	BLM RecQ like Helicase
BRCA1	Breast Cancer-Associated protein 1
BRCA2	Breast Cancer-Associated protein 2
BRCT	BRCA-1 C-terminus
BSA	Bovine Serum Albumin
BTRR	BLM-TOPIIIα-RMI1-RMI2
BUDR	BRCT-domain-associated Ubiquitin-Dependent Recruitment motif

Cas9	CRISPR-associated protein 9
CDC25A	Cell Division Cycle 25A
CDK	Cyclin-Dependent Kinase
CDK1	Cyclin-Dependent Kinase 1
CDKN1A	Cyclin-Dependent Kinase inhibitor 1A
Chk1	Checkpoint kinase 1
Chk2	Checkpoint kinase 2
CIP1	CDK-Interacting Protein 1
CK2	Casein Kinase 2
CMG	Cdc45-MCM2-7-GINS
cNHEJ	Classical Non-Homologous End Joining
CO	Crossovers
CRISPR	Clustered Regularly Interspaced Short Palindromic Repeats
CSR	Class-Switch Recombination
CST	CTC1-STN1-TEN1
CtIP	CTBP-Interacting Protein
DDR	DNA Damage Response
DEAH	Aspartate-Glutamine-Alanine-Histidine
dHJ	Double Holliday Junction
DMC1	DNA Meiotic recombination protein 1
DMEM	Dulbecco's Modified Eagle's Medium
DNA-PK	DNA-dependent Protein Kinase
DNA2	DNA replication helicase/nuclease 2
DSB	Double-Strand Break

EdU	5-ethynyl-2’-deoxyuridine
EME1	Essential meiotic structure-specific endonuclease 1
ExoI	Exonuclease 1
FBS	Foetal bovine serum
FEN1	5’ flap Endonuclease 1
GADD45A	Growth Arrest and DNA-damage-inducible 45 Alpha
GEN1	Gap-dependent Endonuclease 1
gRNA	Guide RNA
GST	Glutathione S-transferase
H1	Histone 1
H2A	Histone 2A
H2AK13ub	Histone 2A Lysine 13 Ubiquitination
H2AK15	Histone 2A Lysine 15
H2AK15ub	Histone 2A Lysine 15 Ubiquitination
H2AX	Histone 2A variant X
H2B	Histone 2B
H3K36me3	Histone 3 Lysine 36 trimethylation
H3K9me3	Histone 3 Lysine 9 trimethylation
H4	Histone 4
H4K16	Histone 4 Lysine 16
H4K20me2	Histone 4 Lysine 20 dimethylation
HEK	Human Embryonic Kidney
HORMAD1	HORMA Domain-containing protein 1
HORMAD2	HORMA Domain-containing protein 2

HP1	Heterochromatin Protein 1
HR	Homologous Recombination
IAA	Indole-3-Acetic Acid
IDR	Intrinsically Disordered Region
IF	Immunofluorescence
Ig	Immunoglobulin
IR	Ionising Radiation
IRIF	Ionising Radiation-Induced Foci
LEDGF	Lens Epithelium-Derived Growth Factor
Lig1	Ligase 1
Lig3	Ligase 3
Lig4	Ligase 4
LOH	Loss-Of-Heterozygosity
MDC1	Mediator of DNA damage checkpoint protein 1
MERIT40	Mediator of RAP80 and targeting 40 kDa protein
MMBIR	Microhomology-Mediated Break-Induced Replication
MMC	Mitomycin C
MMEJ	Microhomology-Mediated End Joining
MRE11	Meiotic recombination 11
MRN	MRE11-RAD51-NBS1
MSCI	Meiotic Sex Chromosome Inactivation
NHEJ	Non-Homologous End Joining
NLS	Nuclear Localisation Sequence
NOXA	Phorbol-12-myristate-13-acetate-induced protein 1

Opti-MEM	Optimised low serum Minimal Essential Medium
PALB2	Partner and localiser of BRCA2
PAR	Poly (ADP-Ribose)
PARG	Poly (ADP-Ribose) Glycohydrolase
PARP	Poly (ADP-Ribose) Polymerase
PAXX	Paralog of XRCC4 and XLF
PCNA	Proliferating Cell Nuclear Antigen
PCR	Polymerase Chain Reaction
PEI	Polyethylenimine
PLK1	Polo-Like Kinase 1
Polθ	Polymerase theta
PTM	Post-Translational Modification
QIBC	Quantitative-Image Based Cytometry
RAG1	Recombination-Activating Gene 1
RAG2	Recombination-Activating Gene 2
RAP80	Receptor-Associated Protein 80
RB	Retinoblastoma protein
RIF1	Rap-1 Interacting Factor homolog
RING	Really Interesting Gene
RMI1	RecQ-mediated genome instability protein 1
RMI2	RecQ-mediated genome instability protein 2
RNF168	RING Finger 168
RNF4	RING Finger 4
RNF8	RING Finger 8

RPA	Replication Protein A
RSS	Recombination Signal Sequences
SAC	Spindle Assembly Checkpoint
SCE	Sister Chromatid Exchange
SDS-PAGE	Sodium Dodecyl Sulfate-Polyacrylamide Gel Electrophoresis
SDSA	Synthesis-Dependent Single-Strand Annealing
SETD2	SET Domain-containing 2
SHLD1	Shieldin complex subunit 1
SHLD2	Shieldin complex subunit 2
SHLD3	Shieldin complex subunit 3
SIM	SUMO (small ubiquitin-like modifier)-Interacting Motif
SLF1	SMC5/SMC6 complex localization factor 1
SLIM	Short Linear motif
SMX	SLX1-SLX4-Mus81-EME1
SNM1A	Sensitive to Nitrogen Mustard 1A
SOC	Super Optimal broth with Catabolite repression
SCP1	Synaptonemal Complex Protein 1
SCP2	Synaptonemal Complex Protein 2
SCP3	Synaptonemal Complex Protein 3
SSA	Single-Strand Annealing
SSB	Single-Strand Break
ssDNA	Single-Stranded DNA
SUMO	Small Ubiquitin-Like Modifier
TIP60	Tat-Interactive Protein 60

TNF	Tumour Necrosis Factor
TNFR	Tumour Necrosis Factor Receptor
TONSL	Tonsoku-like protein
TOP1	DNA topoisomerase I
TOPBP1	DNA topoisomerase II binding protein 1
TOPIIIα	Topoisomerase IIIα
Ub	Ubiquitin
UBC13	E2 Ubiquitin-Conjugating enzyme 13
UDR	Ubiquitination-Dependent Recruitment
UIM	Ubiquitin-Interacting Motif
V(D)J	Variable, Diversity, Joining
WB	Western Blot
XLF	XRCC4-like factor
XPF	Xeroderma Pigmentosum complementation group F
XRCC4	X-ray Repair Cross-Complementing 4
γH2AX	phosphorylated H2AX

List of Figures

Figure 1.1 The classical paradigm of the DNA damage response to DNA double-strand breaks. 4

Figure 1.2 Homologous recombination and the mechanism of crossover formation. 7

Figure 1.3 Non-homologous end joining. 10

Figure 1.4 The 53BP1 domain architecture. 27

Figure 1.5 The BRCA1 protein domain architecture and BRCA1 protein interactors. 31

Figure 1.6 Cryo-EM structure of the BRCA1-BARD1 RING heterodimer bound to the nucleosome. 32

Figure 1.7 The BARD1 protein domain architecture. 36

Figure 1.8 Cryo-EM structure of the BARD1 ARD-BRCT domain on the nucleosome. 39

Figure 1.9 The BRCA1-associated subcomplexes. 42

Figure 1.10 Overview of the process of meiotic sex chromosome inactivation during meiosis prophase I. 55

Figure 2.1 Representative image of an agarose gel for genotyping *Bard1 D700A* mice. 61

Figure 3.1 Generation of BARD1 RING (W91A) and BRCT (D712A) separation-of-function constructs. 79

Figure 3.2 The BRCA1-BARD1 complex does not rely on BARD1-RING nucleosome binding for DNA repair. 80

Figure 3.3 Generation of BARD1 RING and ARD separation-of-function constructs 81

Figure 3.4 The H4K20me0-binding by BARD1 ARD does not rely on the RING-nucleosome binding function. 82

Figure 3.5 BARD1 RING-nucleosome binding/dual reader mutations do not affect additional DNA repair functions of the BRCA1-BARD1 complex. 83

Figure 3.6 Generation of minimal BARD1 RING constructs. 85

Figure 3.7 BARD1 RING-nucleosome binding supports BRCA1-dependent functions in the absence of the BARD1 dual reader module. 88

Figure 3.8 The BRCA1-BARD1 E3 ligase function is not required for BRCA1-dependent functions in DNA repair. 89

Figure 3.9 Hierarchical suppression of RAP80 recruitment to DSB sites by the BRCA1-BARD1 complex and 53BP1. 92

Figure 3.10 The BRCA1-BARD1 complex suppresses RAP80 recruitment to ionising-radiation-induced DNA DSBs mainly in G2. 94

Figure 4.1 Generation of BARD1 N-terminal, RING and IDR deleted constructs. 101

Figure 4.2 The BARD1 IDR and disordered N-terminal region are not required for the HR repair functions of the BRCA1-BARD1 complex. 103

Figure 4.3 BARD1 supports additional DNA repair roles independently of BRCA1 105

Figure 4.4 Loss of 53BP1 restores HR repair in *BARD1*$^{\Delta RING}$ cells and rescues RAD51 recruitment at sites of DNA DSBs. 107

Figure 4.5 RAD51 recruitment at DNA DSB sites in G2/M is suppressed by 53BP1 109

Figure 4.6 The BARD1 BRCTs and RING domains are essential for BRCA1 recruitment 111

Figure 4.7 DNA repair intermediates levels in 53BP1-deficient and 53BP1-proficient cells. 113

Figure 4.8 Generation of BARD1$^{\Delta RING}$ constructs harbouring mutations in the IDR or chromatin binding modules. 117

Figure 4.9 Redundant BARD1 IDR and chromatin binding features support BRCA1-independent DNA repair functions of BARD1. 119

Figure 4.10 BARD1 recruitment to DSB sites is unaffected by mutations in the IDR in *53BP1*$^{-/-}$ *BARD1*$^{\Delta/\Delta}$ +BARD1$^{\Delta RING}$ cells. 121

Figure 5.1 *Brca1* and *Bard1* genetically engineered mouse models. 129

Figure 5.2 *53bp1*$^{L1616A/L1616A}$ rescues embryonic lethality of *Bard1*$^{D700A/D700A}$ mice and results in mice born at expected Mendelian ratios. 130

Figure 5.3 *Bard1*$^{D700A/D700A}$ *53bp1*$^{L1616A/L1616A}$ mice are not tumour-prone and do not accumulate systemic genomic instability. 133

Figure 5.4 BARD1 H2AK15ub-binding ablation does not cause male germline development defects. 135

Figure 5.5 Loss of BARD1 BUDR-binding is not required for BRCA1 recruitment in germ cells and does not lead to MSCI failure or asynapsis. 138

Figure 6.1. Schematic summary of the multifaceted roles of the BRCA1-BARD1 chromatin binding functions. 151

List of Tables

Table 2.1. gRNA and ssODN sequences used for knock-in genome editing of *53bp1* and *Bard1*. 59

Table 2.2. Genotyping strategy for 53bp1 L1616A and Bard1 D700A mice, using indicated primer pairs. 60

Table 2.3. Primer sequences used for site-directed mutagenesis. 64

Table 2.4. Sequences of the GeneString fragment generated of BARD1 RING constructs. 65

Chapter 1

Introduction

The genome holds all the necessary biological information which ensures an organism's normal physiological function and species' survival. However, the genetic information stored in the nucleus of a cell is fragile and constantly prone to errors and breaks. Consequently, different DNA repair mechanisms have evolved to ensure timely repair and maintenance of genome integrity, coordinated with cell cycle progression signalling pathways.

1.1 The cellular response to DNA double-strand breaks

Cells are subject to the occurrence of diverse kinds of DNA lesions that require different types of DNA repair mechanisms. These DNA lesions include DNA single-strand breaks (SSBs) resulting from oxidative damage or base hydrolysis, DNA double-strand breaks (DSBs), bulky DNA adducts, and base modifications which can result from cytosine deamination, depurination or depyrimidination (Hoeijmakers, 2001). In addition to the DNA DSB repair mechanisms discussed later in this chapter, the nucleotide excision repair (NER) mechanism allows for repair of DNA adducts such as pyrimidine dimers which result from UV light, while base excision repair (BER) can remove DNA lesions that result from base modifications, and mismatch repair (MMR) can remove mis-incorporated nucleotides resulting from DNA replication errors or mismatches that can occur during DNA recombination-dependent strand exchange (Hoeijmakers, 2001).

Although rare, at an estimated frequency of 25 breaks per cell per day, the most toxic types of DNA lesions are DSBs where both DNA strands have broken apart (Tubbs and Nussenzweig, 2017). These can be caused by a variety of exogenous and endogenous sources. Examples of exogenous sources of DNA DSBs are ultraviolet radiation, ionising radiation, and mutagenic chemicals that lead to DNA and DNA-protein crosslinking, for instance. Other sources that lead to DSBs come from cellular events themselves such as replication fork stalling and replication stress, and reactive oxygen species (Tubbs and Nussenzweig, 2017). In addition to two-ended DSBs, DSBs can be one-ended when generated during DNA replication where the replication fork encounters a SSB or DNA polymerase-stalling lesions, e.g. abasic sites or DNA intra- and inter-strand crosslinks, that lead to replication fork collapse (Cannan and Pederson, 2016). Additionally, DSBs can also be induced during meiosis and antigen receptor recombination processes during B and T cell development (Khanna and Jackson, 2001; Jackson and Bartek, 2009). Defective or the lack of DSB repair is highly toxic as it can lead to genome replication and transcription blocks, and loss of genetic information via mutations, deletion of large genomic regions, and genomic rearrangements. This can have detrimental effects on neurological, immunological and germline development and can lead to tumorigenesis. Therefore, cells have evolved tightly regulated DNA damage signalling responses and DSB repair mechanisms (Jackson and Bartek, 2009).

1.1.1 The DNA damage response (classical paradigm) and the chromatin response to DNA damage

DNA DSBs trigger a rapid DNA damage response encompassing a signalling cascade that senses the DNA break and recruits several DNA damage response mediators and transducers

to amplify the signal, modify proximal chromatin and recruit numerous DNA repair effectors (Figure 1.1). Upon the formation of a DNA DSB, the MRN complex comprised of MRE11, RAD50 and NBS1 senses the break and activates the serine/threonine ataxia telangiectasia mutated (ATM) kinase which gets recruited to the DSB site (You *et al.*, 2005). Furthermore, ATM is autophosphorylated on serine 1981 (Bakkenist and Kastan, 2003). Consequently, ATM phosphorylates histone variant H2AX on serine 139, known as γH2AX, which then recruits mediator of checkpoint 1 (MDC1) via the BRCA1 C-terminal (BRCT) domain (Rogakou *et al.*, 1998, 1999; Goldberg *et al.*, 2003; Stewart *et al.*, 2003; Stucki *et al.*, 2005). In addition, ATM activation following DNA damage mediates Chk2 checkpoint activation, ATR-Chk1 activation and p53 transcriptional activation to trigger G1 arrest to genotoxic stress (Matsuoka, Huang and Elledge, 1998; Chaturvedi *et al.*, 1999; Cheng and Chen, 2010). The amplification of the γH2AX signal on damaged chromatin and sequential recruitment and phosphorylation of MDC1 by ATM recruits E3 ubiquitin ligase RING (Really Interesting Gene) finger protein RNF8, which has been reported to catalyse K63-linked ubiquitin chains on histone H1 with ubiquitin-conjugating E2 ligase UBC13 (Lou *et al.*, 2006; Kolas *et al.*, 2007; Mailand *et al.*, 2007). Furthermore, the ATM-dependent phosphorylation of L3MBTL2 and its recruitment by MDC1 to sites of DSBs promotes the ubiquitination of L3MBTL2 by RNF8 (Nowsheen *et al.*, 2018). These events support the recruitment of a second E3 ubiquitin ligase RNF168 which ubiquitinates lysine residues 13/15 on histone H2A and amplifies K63-linked polyubiquitin chains on H2A/H2AX (Doil *et al.*, 2009; Mattiroli *et al.*, 2012; Nowsheen *et al.*, 2018). These and other chromatin modifications set the ground for the recruitment of several DSB repair factors, further discussed in section 1.2.6.

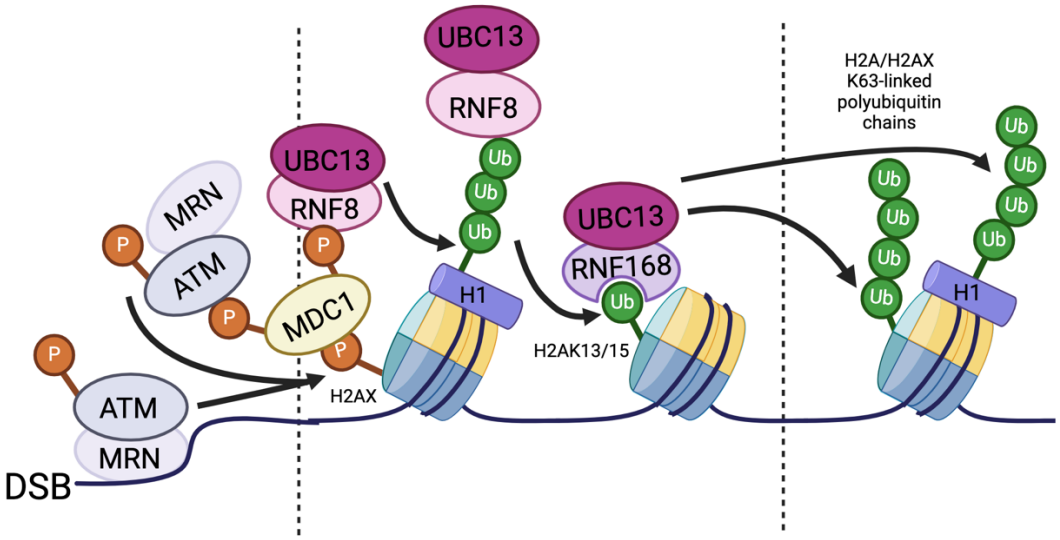


Figure 1.1. Proposed model of the classical paradigm of the DNA damage response to DNA double-strand breaks. Adapted from Panier and Boulton, 2014.

1.1.2 DNA double-strand break repair

Different DNA DSB repair mechanisms are available according to the extent of DNA break processing, cell cycle state, chromatin conformation and cell type. The two main DNA DSB repair pathways are homologous recombination (HR) and classical non-homologous end joining (cNHEJ). Additionally, there are alternative repair pathways such as microhomology-mediated end joining (MMEJ), sometimes known as Alternative end-joining (alt-EJ), single-strand annealing (SSA) and break-induced replication (BIR) (Liu and Malkova, 2022; Groelly *et al.*, 2023).

1.1.3 Homologous recombination

Homologous recombination is considered the most accurate type of DSB repair as it uses the homologous sister chromatid as a repair template. Therefore, it is confined to repairing breaks in replicating cells, during S and G2 phases of the cell cycle. After DNA DSB generation and the DNA damage signalling cascade initiation, the broken DNA ends are resected to create a binding substrate for recombinases (Figure 1.2) (Jasin and Rothstein, 2013).

While Ku70/Ku80 heterodimer binding to DNA ends stabilises DNA termini in preparation for their ligation by NHEJ, the MRN complex is recruited to DSB-proximal sites, where MRE11 creates a nick using its endonucleolytic activity and initiates nucleolytic activities that overcome the Ku70/Ku80 block (Chapman and Jackson, 2008; Garcia *et al.*, 2011; Shao *et al.*, 2012; Anand *et al.*, 2019). Simultaneously, the CDK-dependent phosphorylation of the C-terminal binding protein-interacting protein (CtIP) at serine 327 recruits the MRN complex to activate the 3' to 5' exonucleolytic activity of MRE11 (Paull and Gellert, 1998; Anand *et al.*, 2016; Deshpande *et al.*, 2016). MRN and CtIP then catalyse the short-range end resection at DSB sites to create 3' overhangs (Sartori *et al.*, 2007; Garcia *et al.*, 2011). Furthermore, the BRCA1-BARD1 complex, a key mediator in HR repair, is recruited to DNA DSB sites (discussed in sections 1.2.6 and 1.5) and can interact with CtIP and MRN, as part of the BRCA1-C complex (discussed in section 1.6) (Yu and Chen, 2004; Chen *et al.*, 2008), thereby promoting additional end resection and HR repair. The MRN/CtIP resected ends can be further processed by long-end resection helicases/nucleases such as the 5' to 3' exonuclease, Exonuclease I (EXOI), DNA replication helicase/nuclease 2 (DNA2) and Bloom syndrome RecQ-like helicase (BLM) (Mimitou and Symington, 2008; Zhu *et al.*, 2008).

The long 3' single-stranded DNA is rapidly coated by the replication protein A 1-3 complex (RPA) to prevent DNA degradation, the formation of secondary structures and/or single-strand DNA annealing to regions of microhomology (Chen, Lisby and Symington, 2013; Deng *et al.*, 2014). The BRCA1-BARD1 complex mediates the recruitment of the Partner and Localiser of BRCA2 protein (PALB2) via interactions mediated by coiled-coil domains within BRCA1 and PALB2 (Fan Zhang *et al.*, 2009; Feng Zhang *et al.*, 2009; Sy, Huen and Chen, 2009). In turn, this BRCA1-PALB2 interaction recruits BRCA2 to direct RPA replacement with RAD51 molecules, promoting the formation of RAD51 nucleoprotein filaments. Furthermore, PALB2 recruitment can also be promoted independently of BRCA1 via an interaction with RNF168 (Zong *et al.*, 2019). The RAD51 nucleoprotein filaments direct homology search within adjacent DNA molecules, and subsequently strand invasion, generating a D-loop structure (West, 2003). In addition to PALB2-BRCA2-dependent recruitment, RAD51 recruitment is also promoted by NBS1, regulated by phosphorylation-dependent mechanisms that involve the polo-like kinase 1 (PLK1) and casein kinase 2 (CK2) (Yata *et al.*, 2012). Interestingly, BRCA2 was also shown to facilitate this RAD51 phosphorylation-dependent recruitment mechanism whereby the binding of phosphorylated BRCA2 to PLK1 can further regulate the PLK1-dependent phosphorylation of RAD51, which is particularly important during replication fork protection (Yata *et al.*, 2014). Furthermore, this supports RAD51's roles during mitosis, where it promotes mitotic DNA synthesis of under-replicated chromatin (Wassing *et al.*, 2021).

The D-loop structure can then be further processed by synthesis-dependent strand annealing (SDSA), or form a double Holliday Junction (dHJ) structure (Bzymek *et al.*, 2010; West *et al.*, 2015). One mechanism by which the dHJ structure can be processed is by dHJ dissolution via the BTRR complex, composed of BLM, Topoisomerase IIIα (TOPIIIα), RMI1 and RMI2. The processing of the hemicatenane in the dHJ by the BTRR complex results in non-

crossover products (West *et al.*, 2015). BLM activity is regulated by the cyclin-dependent kinase 1 (CDK1)-dependent phosphorylation of BLM and TOPBP1, which facilitates the

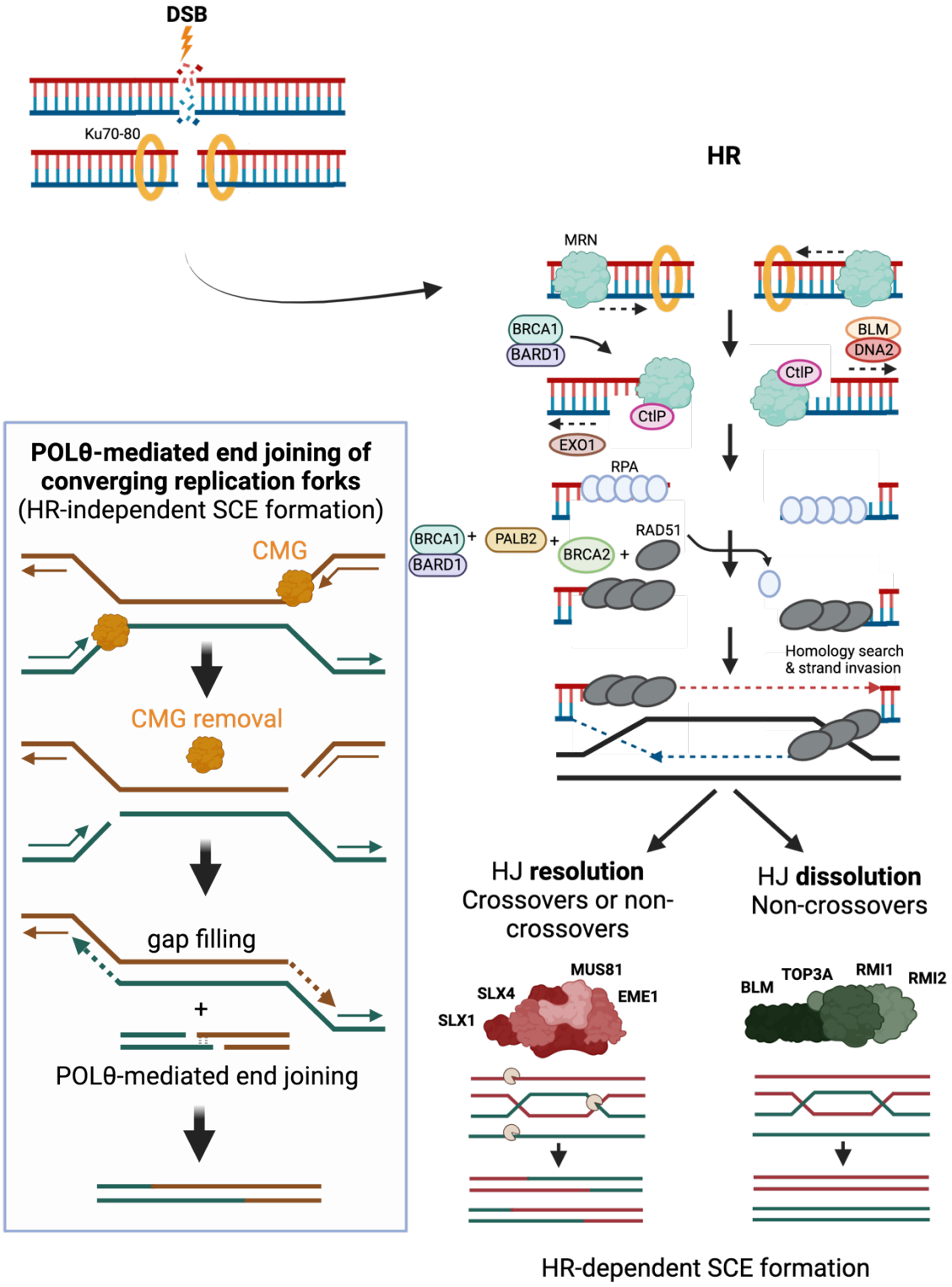


Figure 1.2. Homologous recombination and the mechanism of crossover formation. Adapted from Mirman and Lange, 2020 and Heijink *et al.*, 2022.

interaction of PLK1 and dHJ dissolution to promote crossover-free recombination products in late G2 (Pogliano *et al.*, 2022). dHJ resolution is mediated by the complex, composed of the endonuclease SLX1 and nuclease scaffold protein SLX4 (Fekairi *et al.*, 2009), in concert with MUS81-EME1 (Figure 1.2) (Wyatt *et al.*, 2013). Alternatively, HJ can be resolved by the GEN1 resolvase (Ip *et al.*, 2008). The SMX complex, comprising SLX1-SLX4, MUS81 and the endonuclease XPF introduces nicks in the dHJ which can result in either crossover or non-crossover products and form sister-chromatid exchanges (SCEs) (Figure 1.2) (West *et al.*, 2015). Additionally, recently it was reported that SCEs are able to form independently to the canonical HR machinery, via POLθ-mediated end joining of converging replication forks (Figure 1.2) (Heijink *et al.*, 2022). The POLθ-mediated end joining mechanism is discussed in section 1.1.5.

HR is often referred to as an error-free pathway. However, it is important to regulate HR repair intermediate processing to maintain genome stability as the formation of inter-homolog crossovers by the SMX complex can lead to loss of heterozygosity (LOH) of tumour suppressor genes and compromise genome integrity (LaRocque *et al.*, 2011). Additionally, unregulated end resection leading to hyper-resection of single-strand DNA can lead to loss of genetic information if repaired by MMEJ or SSA, and persistent HR repair intermediates, which, if unresolved can cause chromosomal mis-segregation events in mitosis, resulting in aneuploidy (Truong *et al.*, 2013; Chan, Fugger and West, 2018).

1.1.4 Non-homologous end joining

Non-homologous end joining can be used throughout the cell cycle as this DSB repair mechanism does not rely on a repair template and instead ligates the broken DNA ends

together. Therefore, it is classified as an error-prone repair mechanism as it can lead to loss of genetic information and chromosomal aberrations (Pannunzio, Watanabe and Lieber, 2018). Nevertheless, NHEJ is an important and commonly used DSB repair mechanism and essential in certain cell types to ensure normal physiological functions as discussed later in section 1.2.3.

In NHEJ, DNA DSB ends are bound by the Ku70/Ku80 heterodimer which mediates the recruitment of DNA-dependent protein kinase catalytic subunit (DNA-PKcs) and consequently, Artemis, DNA ligase IV (LIG4) and its scaffolding protein XRCC4 (which are required for LIG4 stability), together with XRCC4-like factor (XLF) and paralogue of XRCC4 and XLF (PAXX) (Wang *et al.*, 2004; Pannunzio, Watanabe and Lieber, 2018) (Figure 1.3). These proteins are part of the long-range synapsis NHEJ ligation complex required to repair the DNA DSB (Pannunzio, Watanabe and Lieber, 2018). The long-range synapsis complex is thought to allow for DNA end trimming and/or polymerase activities in preparation of DNA ends suitable for ligation. The subsequent dissociation of these DNA-PKcs from this complex leads to the formation of a short-range synapsis complex, in which Ku70-80 dimers bring DNA ends in proximity for XRCC4-LIG4-dependent ligation (Yin *et al.*, 2017; Chaplin *et al.*, 2021; Chen *et al.*, 2021, 2023). Central to NHEJ repair is the p53-binding protein 53BP1, which positively promotes DNA end-joining pathway including NHEJ, by binding DSB-proximal nucleosomes to antagonise HR repair by protecting DNA ends from end resection (Chapman, Taylor and Boulton, 2012). These 53BP1 functions will be further discussed in sections 1.2 and 1.3.

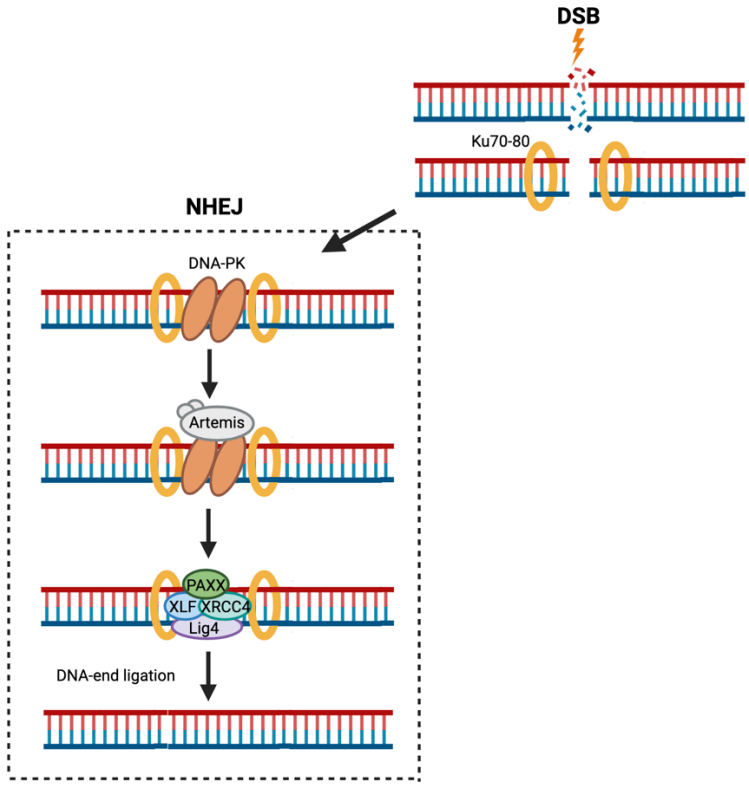


Figure 1.3. Non-homologous end joining. Adapted from Mirman and Lange, 2020.

1.1.5 Alternative repair pathways

In addition to HR and NHEJ, DNA DSBs can be repaired via alternative DNA DSB repair pathways such as single-strand annealing (SSA), break-induced replication (BIR) and microhomology-mediated end joining (MMEJ), also termed Polθ-mediated end joining or alternative end-joining (alt-EJ).

The MMEJ repair pathway relies on microhomology regions proximal to the broken DNA ends which are approximately 20 or fewer nucleotides long to ligate DSB ends (Ma *et al.*, 2003; Corneo *et al.*, 2007; C. T. Yan *et al.*, 2007; Sfeir and Symington, 2015). Therefore, it also requires short-range 5' to 3' resection dependent on the MRN complex and CtIP (Xie, Kwok and Scully, 2009; Lee-Theilen *et al.*, 2011; Zhang and Jasin, 2011; Truong *et al.*, 2013).

Following end resection and RPA recruitment to ssDNA, poly (ADP-ribose) polymerase 1 (PARP1), an ADP-ribose-dependent polymerase involved in the DNA damage response and single-strand break repair, catalyses poly (ADP) ribose chain extension (PARylation) at DNA break sites (Audebert, Salles and Calsou, 2004; Wang *et al.*, 2006; Chaudhuri and Nussenzweig, 2017). This facilitates the recruitment of DNA polymerase theta (Polθ) (Luedeman *et al.*, 2022). However, for efficient Polθ recruitment and function, it was recently reported that PARylated Polθ relies on PARG to remove these PAR chains to activate DNA binding and MMEJ activity of Polθ (Vekariya *et al.*, 2024). Polθ then mediates DNA synapsis of microhomology regions and unloads RPA (Kent *et al.*, 2015, 2016; Mateos-Gomez *et al.*, 2015, 2017). The short 3' DNA flaps generated by Polθ following annealing are removed by flap endonuclease 1 (FEN1), and the broken DNA ends are sealed together by DNA ligases Lig1 and Lig3 (Liang *et al.*, 2005; Simsek *et al.*, 2011; Sharma *et al.*, 2015; Brambati, Barry and Sfeir, 2020). This repair pathway is mutagenic as it can result in DNA insertions, deletions, and chromosomal fusions and translocations (C. T. Yan *et al.*, 2007; Boboila *et al.*, 2010; Mateos-Gomez *et al.*, 2015; Schimmel *et al.*, 2017; Yu *et al.*, 2020). Recent reports have shown that Polθ plays a role in ssDNA gap processing at replication forks in BRCA1/BRCA2-deficient cancers and that Polθ activity is required for cell survival and maintaining replication fork stability which indicates a role of Polθ-mediated end joining in cancer evolution (Ceccaldi *et al.*, 2015; Belan *et al.*, 2022; Mann *et al.*, 2022; Schrempf *et al.*, 2022).

Single-strand annealing requires extensive DNA end resection and therefore, relies on EXO1, DNA2 and BLM to create long 3' DNA overhangs of more than 20 nucleotides (Maryon and Carroll, 1991; Fishman-Lobell, Rudin and Haber, 1992; Mimitou and Symington, 2008; Zhu *et al.*, 2008). These 3' DNA overhangs are coated with RPA to stabilize and protect the DNA ends from further exonuclease activity (Chang *et al.*, 2017; Liang *et al.*, 2024). RAD52 anneals

the 3' single-stranded DNA strands together at homology regions and the xeroderma pigmentosum group F (XPF)-ERCC1 complex cuts the leftover 3' overhangs (Chang *et al.*, 2017). Recent *in vitro* and structural studies on RAD52 have shown that RPA is essential in directing RAD52 to ssDNA sites via the RPA-RAD52 interaction in its open ring form which facilitates RAD52-dependent annealing of homology regions (Liang *et al.*, 2024). The SSA repair pathway is inherently mutagenic due to its deletion events and may also be linked to cancer evolution, as high RAD52 expression levels leading to increased SSA activity have been linked to poor cancer survival rates (Ho *et al.*, 2020).

Break-induced replication (BIR) is used to repair single-ended DSBs that can arise from encountering a ssDNA gap on the replication fork or from fork reversal cleavage, as well as lengthen unprotected telomeres (Roumelioti *et al.*, 2016). This repair pathway involves D-loop ssDNA invasion and subsequent conservative DNA synthesis relying on proliferating cell nuclear antigen (PCNA), DNA polymerase δ subunit POL32 and the DNA polymerase α-primase complex (Lydeard *et al.*, 2007; Donnianni and Symington, 2013; Dilley *et al.*, 2016). Furthermore, the BIR associated with telomere synthesis relies on RAD18-dependent ubiquitination of PCNA to recruit the SNM1A nuclease to telomeres to promote DNA resection and formation of ssDNA required for template switching when an obstacle is encountered during D-loop bubble migration (Zhang *et al.*, 2023). BIR is highly mutagenic and has been reported to lead to chromosomal rearrangements resulting from clustered mutations in yeast (Anand *et al.*, 2014; Sakofsky *et al.*, 2014; Elango *et al.*, 2019). Therefore, BIR could be linked to carcinogenesis as it compromises the integrity of genetic information and is associated with clustered mutations termed *kataegis* in human cancers (Chan and Gordenin, 2015; Liu and Malkova, 2022).

1.1.6 Checkpoint responses

Cell cycle checkpoint responses have evolved to control and regulate cell cycle progression and make sure that a new cell generation is produced faithfully. These ensure that DNA replication and cell division can progress without subsequent accumulating errors in the genome and support the maintenance of the genetic content (Kastan and Bartek, 2004).

The G1/S checkpoint safeguards the integrity of pre-replicative chromatin and allows damaged DNA from the previous cell cycle to be repaired. Therefore, the activation of the G1/S checkpoint impedes damaged DNA from being replicated in S-phase and is dependent on p53 activation. Upon sensing of DNA damage, ATM phosphorylates its effector CHK2 which in turn phosphorylates p53 on serine 20 and prevents p53 ubiquitin-dependent degradation (Banin *et al.*, 1998; Hirao *et al.*, 2000; Kastan and Bartek, 2004). The phosphorylation of CDC25A phosphatase at serine 123 by CHK2 triggers the degradation of CDC25A. Simultaneously, the accumulation of p21 (CIP1/WAF1) by activation of cyclin-dependent kinase inhibitor 1A (CDKN1A) leads to dephosphorylation of cyclin-dependent kinase CDK2 (Harper *et al.*, 1993, 1995; Adams *et al.*, 1996; Poon *et al.*, 1996; Falck *et al.*, 2001). Ultimately, the inactivation of these G1-related cyclin-dependent kinases blocks the progression to S-phase and arrests cells in G1.

The G2/M checkpoint ensures that cells do not progress into mitosis if incompletely replicated DNA or unrepaired DNA damage is encountered in G2, although in some cases replication of under-replicated DNA can occur in mitosis (MiDAS) (Kastan and Bartek, 2004). ATR and its effector kinase CHK1 phosphorylate CDC25c causing its degradation (Khanna and Jackson, 2001). Together with the p53-dependent activation of growth arrest and DNA-damage-inducible 45 alpha (GADD45A) and 14-3-3 sigma proteins this leads to inhibition of

dephosphorylation of Cdk2/cyclin B1 which is required to progress into mitosis (Hermeking *et al.*, 1997; Wang *et al.*, 1999). Ultimately, this results in G2 arrest.

1.1.7 Cell fate decisions following DNA damage

Despite the effort to revert DNA damage and restore chromatin integrity via cell cycle checkpoint responses, some cells do not release checkpoint arrest. In these cases, cells can undergo senescence or apoptosis to maintain cellular homeostasis and prevent the accumulation of genetic errors that could lead to tumorigenesis (Kastan and Bartek, 2004).

Senescence can be triggered by oncogene activation, oxidative stress, genotoxic stress and critical telomere shortening. These cells do not undergo further DNA replication and are permanently arrested halting future cell growth (Huang *et al.*, 2022). Senescence is mediated via two pathways: the p53/$p21^{CIP1/WAF1}$ and the $p16^{INK4A}$/pRB pathways (Dai and Enders, 2000; Huang *et al.*, 2022). In the $p16^{INK4A}$/pRB pathway, the formation of cyclin D-CDK4/6 complex is inhibited by cyclin-dependent kinase inhibitor 2A (p16) (Russo *et al.*, 1998). The inhibition of cyclin D-CDK4/6 complex formation prevents RB phosphorylation, leading to RB-E2F complex formation. This inhibits the transcription of cell-cycle genes halting cell growth and inducing a senescent state (Weinberg, 1995; Alcorta *et al.*, 1996). During the p53/$p21^{CIP1/WAF1}$ pathway, the induction of p53 leads to the DREAM complex formation (Quaas, Müller and Engeland, 2012). This upregulates $p21^{CIP1/WAF1}$ which dephosphorylates CDK2 and prevents RB phosphorylation. The hypophosphorylated state of RB then binds to E2F, repressing transcription of cell-cycle genes required for cell growth (Brown, Wei and Sedivy, 1997; Chicas *et al.*, 2010; Quaas, Müller and Engeland, 2012). Additionally, the p21-dependent nuclear

retention of cyclin B1 in G2 arrested cells also plays into the senescent switch (Krenning *et al.*, 2014).

Apoptosis is the process that leads to programmed cell death which is induced after irreparable cellular lesions. It is controlled by p53-dependent mechanisms, governed by the intrinsic and the extrinsic pathways. The intrinsic pathway requires p53-dependent upregulation of pro-apoptotic target genes PUMA/BBC3, BAX and NOXA and inhibition of the anti-apoptotic B-cell lymphoma 2 (Bcl-2) family members (Youle and Strasser, 2008). This triggers the permeabilization of the outer mitochondrial membrane and activates the apoptotic caspase cascade leading to cell death (Aubrey *et al.*, 2018). The extrinsic pathway is governed by death receptor activation. Here, death receptor ligands such as FASL and tumour necrosis factor (TNF) bind to the extracellular domain of tumour necrosis factor receptor (TNFR) family members. This eventually results in the activation of the caspase cascade and cell death (Fulda and Debatin, 2006).

1.2 Control of DNA double-strand break repair pathway choice

Non-homologous end joining and homologous recombination are both important DNA DSB repair mechanisms which are involved in normal physiological functions. However, in cellular contexts where both NHEJ and HR can be employed, a refined and regulated mechanism of DNA DSB repair pathway choice is required. This ensures accurate DSB repair and cell survival and limits the accumulation of mutations, which can lead to tumorigenesis and neurological and immunological diseases (Jackson and Bartek, 2009). Different factors such as cell type, cell cycle phase, complexity of the DSB and chromatin post-translational marks (PTMs) dictate pathway choice (Chapman, Taylor and Boulton, 2012).

1.2.1 The purpose of DNA double-strand break repair pathway choice

HR has important roles in genome maintenance and tumour suppression however it can also lead to loss of heterozygosity (LOH) leading to homozygotic loci (Moynahan and Jasin, 1997). On the other hand, NHEJ is available throughout interphase to repair DSBs and is important during B and T cell development and antigen receptor recombination (discussed in section 1.2.3) (Chapman, Taylor and Boulton, 2012). However, NHEJ repair can lead to small substitutions, insertions and deletions, and translocations if two broken chromosomes are ligated together, or from repair of replication-associated one-ended DNA breaks, which can all compromise the integrity of the genome (Lieber, 2010).

Understanding how the DNA DSB repair pathway choice between HR, NHEJ and the alternative repair pathways are regulated and fine-tuned is crucial in understanding how HR-deficient cancers can be exploited therapeutically. However, these mechanisms remain to be fully understood.

1.2.2 Importance of Homologous Recombination and tumour suppression

HR is required to maintain genome stability and repair DSBs accurately without causing the loss of genetic information or chromosomal aberrations. It is also needed during gametogenesis for meiotic recombination to increase genetic diversity (Jasin and Rothstein, 2013). Several HR factors are essential in the downstream processes for recruiting HR proteins and initiating strand invasion to allow accurate DSB repair and prevent tumorigenesis. Germline mutations in homologous recombination genes such as breast cancer gene 1 (*BRCA1*), breast cancer gene 2 (*BRCA2*), BRCA1-associated RING domain protein 1 (*BARD1*), partner and localiser of BRCA2 (*PALB2*), *ATM*, *CHK2* and BRCA1 Interacting Helicase 1 (*BRIP1*

also known as *FANCJ* or *BACH1*, here forth *BACH1*) are linked to familial breast, ovarian, pancreatic and prostate cancer (Rahman *et al.*, 2007; Weber-Lassalle *et al.*, 2019; Yamamoto and Hirasawa, 2021; Incorvaia *et al.*, 2024) emphasising the essentiality of their DNA repair functions during HR and tumour suppression function. The importance of the tumour suppression functions of the BRCA1-BARD1 complex will be discussed in section 1.7.1.

1.2.3 Importance of Non-homologous End Joining in antigen receptor recombination and DNA repair in G0/G1 cells

Despite being an error-prone pathway, NHEJ remains a crucial mechanism for repairing DNA DSBs in non-dividing cells and is essential for the repair of induced DSBs in the immune system (Lieber, 2010). Here, NHEJ is required in diversifying the immune repertoire, generating antigen receptor diversity and during B and T lymphocyte development. These processes involve variable, diversity and joining (V(D)J) recombination and immunoglobulin (Ig) heavy chain class switch recombination (CSR) (Dudley *et al.*, 2005).

V(D)J recombination is an important process for B and T lymphocyte activation occurring in the bone marrow and the thymus, respectively, where the immunoglobulin gene and T cell receptors are generated. This involves the induction of DSBs by Recombination Activating Gene 1 and 2 (RAG1/2) endonucleases at recombination signal sequences (RSS) which flank the variable, diversity and joining gene segments, generating hairpin-like structures. Ku70/80 are recruited to the generated DSBs and the hairpin-like structures are opened by the endonuclease Artemis, activated by the DNA-dependent protein kinase (DNA-PK) complex. XRCC4 and ligase IV ligate the generated DNA ends (Wang, Lee and Zha, 2020). The physiological importance of NHEJ in V(D)J recombination is evident from mutations in several

NHEJ factors in humans and mice, leading to failure in B and T lymphocyte maturation and severe combined immune deficiency. Examples include mutations in important classical NHEJ factors Artemis, DNA-PKcs, XRCC4 and LIG4 which are essential for V(D)J recombination, and to a lesser extent 53BP1, whose loss in mice lead mild T/B-cell lymphopenia owing to loss of long-range joining events during V(D)J recombination (Gao, Chaudhuri, *et al.*, 1998; Taccioli *et al.*, 1998; Moshous *et al.*, 2001; Difilippantonio *et al.*, 2008; Ghezraoui *et al.*, 2018).

CSR occurs in immature B cells and generates new immunoglobulin (Ig; antibody) isotypes. This process occurs in so-called switch (*S*) regions, large GC-rich repeat sequences located within introns positioned upstream of each antibody isotype-encoding constant *(C)* exon. At these switch regions, clusters of cytosine residues are deaminated to uracil by activation-induced cytidine deaminase (AID). The generated mismatch is repaired via base excision repair (BER) and mismatch repair (MMR), which can turn into DSBs and then be repaired by cNHEJ and/or alt-EJ (Bregenhorn *et al.*, 2016). CSR relies on the 53BP1/Rap1-interacting factor 1 (RIF1)/REV7-dependent DNA end-joining to mediate deletional recombination events within the immunoglobulin constant heavy chain *(igh)* locus during Ig class-switching (Manis *et al.*, 2004; Ward *et al.*, 2004; Chapman *et al.*, 2013; Ghezraoui *et al.*, 2018; Setiaputra *et al.*, 2022). Accordingly, 53BP1-deficient mice have lower titres of CSR-dependent Ig isotypes such as IgA and IgG (Manis *et al.*, 2004). The recently discovered Shieldin complex composed of SHLD1, SHLD2, SHLD3 and REV7 proteins, which binds to ssDNA, is also essential during CSR, and is required for polymerase-α (Polα)-primase-dependent fill-in synthesis with CTC1-STN1-TEN1 (CST) to render ssDNA-tailed DNA termini double-stranded in preparation of DSB ligation (Ghezraoui *et al.*, 2018; Gupta *et al.*, 2018; Noordermeer *et al.*, 2018; Mirman *et al.*, 2022; King *et al.*, 2024). SHLD1-deficient mice are defective in generating wild-type serum levels of IgG1 antibodies (Vincendeau *et al.*, 2022) and equally SHLD2-deficient mice have lower Ig

levels (Ling *et al.*, 2020). However, loss of Shieldin had less drastic effects on CSR than 53BP1 loss, as 53BP1 has upstream functions to the Shieldin complex (Vincendeau *et al.*, 2022; King *et al.*, 2024). In contrast, Shieldin is not important during V(D)J recombination, possibly because shieldin/CST-dependent fill-in synthesis is not required at RAG1/2-induced DSBs (King *et al.*, 2024).

NHEJ is also an important DSB repair pathway in G0/G1 cells. This includes cells undergoing CSR and V(D)J recombination in G1 and in non-dividing cells such as post-mitotic neurons. Indeed, LIG4 or XRCC4-deficient mice had high levels of apoptosis of post-mitotic neuronal cells (Gao, Sun, *et al.*, 1998; McKinnon, 2013; Wang, Lee and Zha, 2020). Additionally, NHEJ is an important repair pathway during G1 when sister chromatids are unavailable to ensure that DSBs can be repaired before cells progress into S phase (Lieber, 2010).

1.2.4 Emergence of backup repair pathways as an important pathway

Although the previously introduced MMEJ repair pathway is mutagenic, recent research on the mechanism of Polθ-mediated end-joining repair has shown that MMEJ is required during mitosis to repair DNA breaks and prevent the accumulation of DNA damage into the next cell cycle (Messer and Fox, 2024). This is important as both HR and NHEJ are suppressed in mitosis via PLK1 and CDK1-dependent phosphorylation of 53BP1, and PLK1 and CDK1/Aurora A-dependent phosphorylation of CtIP, promoting MMEJ repair (Benada *et al.*, 2015; Wang *et al.*, 2018).

MMEJ in mitosis is activated by the PLK1-dependent phosphorylation of Polθ and of the RHINO complex, which is an interactor of the 9-1-1 (RAD9A-RAD1-HUS1) complex and regulates Polθ activity in mitosis by being involved in Polθ recruitment to mitotic DSBs

(Brambati *et al.*, 2023; Gelot *et al.*, 2023). Loss of Polθ in cells with DSBs resulted in micronuclei formation following mitosis which indicated increased genome instability (Brambati *et al.*, 2023). Furthermore, Polθ was also shown to be involved in stalled replication fork protection and gap filling in BRCA1/2-deficient cells (Belan *et al.*, 2022; Mann *et al.*, 2022; Schrempf *et al.*, 2022).

HR-deficient cells rely on MMEJ to repair DSBs for survival, as loss of Polθ in BRCA1/BRCA2-deficient cells leads to synthetic lethality (Ceccaldi *et al.*, 2015; Mateos-Gomez *et al.*, 2015). The synergy between inhibition of Polθ and PARPi makes it an attractive avenue to treat HR-deficient cancers in the clinic (Zhou *et al.*, 2021; Ronson *et al.*, 2023).

1.2.5 Resection vs. end-protection of DNA double-strand breaks

The choice of DSB repair pathway depends on whether the DNA ends of the break are protected or resected. Super-resolution microscopy has shown that 53BP1 is localised adjacently to BRCA1 ionising-radiation induced foci (IRIF), indicating that 53BP1 and BRCA1 have antagonistic properties at chromatin recruitment (Chapman *et al.*, 2012). Therefore, understanding the antagonistic relationship between 53BP1 and BRCA1-BARD1 is crucial to better understand how DSB repair pathway choice is regulated.

The BRCA1-BARD1 complex by interacting with CtIP through the BRCA1 BRCT domain (see section 1.6) mediates end resection at DSB sites to direct HR repair (Chen *et al.*, 2008). Additionally, the BRCA1-BARD1 complex was recently shown to promote long-range resection mediated by CtIP, EXO1 and DNA2 and promote DNA unwinding mediated by the Werner (WRN) or BLM helicases (Ceppi *et al.*, 2024; Salunkhe *et al.*, 2024). Interestingly, these BRCA1-BARD1-mediated resection functions were shown to be dependent on the RAD51

concentration at ssDNA as RAD51 inhibits further DNA degradation promoted by BRCA1-BARD1 (Ceppi *et al.*, 2024). In parallel, work recently published by the Patrick Sung laboratory corroborates that BRCA1-BARD1 promotes DNA end resection by interacting with EXO1, WRN and BLM, which rely on DNA-binding activity mediated by lysine residues in BARD1 within amino acid residues 124-270 (Salunkhe *et al.*, 2024).

These end resection functions promoted by the BRCA1-BARD1 complex were proposed to be important for counteracting the 53BP1-Shieldin-mediated end protection and the CST-Polα-mediated fill-in synthesis activities of DNA ends which block end resection and promote classical NHEJ (Dev *et al.*, 2018; Ghezraoui *et al.*, 2018; Mirman *et al.*, 2018, 2022; Noordermeer *et al.*, 2018; Ceppi *et al.*, 2024). Furthermore, loss of 53BP1 in BRCA1-mutant cells reinstates DNA end resection indicating that 53BP1 antagonises HR by blocking long-range 5' to 3' end resection (Bothmer *et al.*, 2010, 2011; Bouwman *et al.*, 2010; Bunting *et al.*, 2010). These 53BP1 anti-resection functions are further supported by 53BP1 interaction with RIF1, and REV7 (Chapman *et al.*, 2013; Zimmermann *et al.*, 2013; Boersma *et al.*, 2015; Xu *et al.*, 2015). The DNA end protection mechanisms governed by 53BP1 and the protein complexes Shieldin and CST will be further introduced and discussed in section 1.3.

1.2.6 Chromatin regulation of pathway choice

The chromatin organisation and epigenetic post-translational modification marks on histones play an important role in DNA DSB repair pathway choice. Following the initiation of DNA DSB damage response, MDC1 is phosphorylated by ATM allowing the recruitment of the E3 ubiquitin ligase Really Interesting Gene (RING) finger protein 8 (RNF8) to create lysine 63 and lysine 48-linked ubiquitin chains on linker histone H1 with E2 ubiquitin-conjugating

enzyme UBC13 (Goldberg *et al.*, 2003; Stewart *et al.*, 2003; Kolas *et al.*, 2007; Mailand *et al.*, 2007; Thorslund *et al.*, 2015). Following the RNF8-mediated K63-linked polyubiquitin chain formation, E3 ubiquitin ligase RING finger protein 168 (RNF168) is recruited to chromatin to deposit mono-ubiquitin at lysines 13 and 15 on histone H2A (H2AK13ub and H2AK15ub) with the E2 ubiquitin-conjugating enzyme UbcH5c and UBC13 (Doil *et al.*, 2009; Gatti *et al.*, 2012; Mattiroli *et al.*, 2012; Thorslund *et al.*, 2015; Qi Hu *et al.*, 2024). Additionally, RNF168 amplifies the K63-linked polyubiquitin signal on histones H2A and H2AX (Doil *et al.*, 2009). These post-translational modifications (PTMs) and the amplification of their signal from the initial DNA DSB site are necessary to recruit several DNA repair proteins to initiate repair. The amplification of the ubiquitin signal catalysed by RNF8 and RNF168 form substrates for binding of 53BP1, RAD18, RNF169 and RAP80 proteins, the BRCA1-BARD1 complex and RNF168 itself (Hu *et al.*, 2017; Kitevski-LeBlanc *et al.*, 2017; Chen and Tyler, 2022). The H2AK15ub mark serves as a substrate for both 53BP1 and BARD1, determining pathway choice between NHEJ and HR, respectively (Fradet-Turcotte *et al.*, 2013; Becker *et al.*, 2021; Hu *et al.*, 2021). In addition to the DNA damage mark deposited on chromatin by RNF8/RNF168, DNA DSB repair pathway choice is also determined by the cell cycle phase and the consequent presence of unmethylated lysine 20 tails of histone H4 (H4K20me0) in newly replicated chromatin and mono or di-methylation present in G1, and re-established during late G2/M phase by the SETD8 and SUV4-20H1/2 lysine methyl-transferases (Schotta *et al.*, 2004; Couture *et al.*, 2005). While 53BP1 recognises the ubiquitously distributed mono-/di-methylated lysine 20 histone H4 (H4K20me1/2) histone PTM in G1, its simultaneous binding to H2AK15ub specifically at DSB sites stimulates repair by NHEJ (Botuyan *et al.*, 2006; Fradet-Turcotte *et al.*, 2013; Pellegrino *et al.*, 2017). Conversely, BARD1 directs BRCA1 to promote HR repair by binding to H4K20me0 in newly assembled nucleosomes which are deposited on both nascently

generated daughter strands during DNA replication, and therefore demark post-replicative chromatin (Nakamura *et al.*, 2019). The binding of both cell cycle and DNA damage histone marks by BARD1 inhibits 53BP1 and consequently antagonises NHEJ, directing DNA DSB repair towards HR (Pellegrino *et al.*, 2017; Nakamura *et al.*, 2019; Becker *et al.*, 2021; Krais *et al.*, 2021).

RNF8/RNF168-mediated extension of K63-linked polyubiquitin chains on H2A forms the binding substrate for receptor-associated protein 80 (RAP80) which can recruit BRCA1 to DNA DSB sites part of the BRCA1-A complex (Stewart *et al.*, 2009). In addition, super-resolution microscopy showed that the E3 ubiquitin ligase RAD18, usually involved in translesion DNA synthesis, is recruited to H2AK15ub chromatin sites together with the SMC5/SMC6 complex localization factor 1 (SLF1) which binds to H4K20me0, to exclude 53BP1 from DNA DSB sites in similar fashion to BRCA1-BARD1 and antagonise NHEJ (Hu *et al.*, 2017; Palek *et al.*, 2024). Similarly, the RING finger protein 169 (RNF169) is also recruited to H2AK15ub at DSB-associated chromatin, inhibiting the recruitment of 53BP1 and RAP80 on DSBs to promote end resection for HR and SSA (Poulsen *et al.*, 2012; Hu *et al.*, 2017; Kitevski-LeBlanc *et al.*, 2017; An *et al.*, 2018). How DNA DSB repair relies on 53BP1, BARD1 and RAP80 interacting with the PTMs mentioned in this section will be further discussed in sections 1.3.1, 1.5 and 1.6 of this chapter.

In addition, BARD1 has been reported to interact with the conserved chromatin binding protein heterochromatin protein 1 (HP1) bound at H3K9me2, in facultative heterochromatin, via a conserved PxVxL motif in its tandem BRCTs domain, to maintain BRCA1 bound at DSB-proximal chromatin sites and promote HR (Lee *et al.*, 2013; Wu *et al.*, 2015). In eukaryotes, H3K36me3, trimethylated by SETD2, is required to promote DSB repair towards HR in regions of active gene transcription in euchromatin through H3K36me3-binding factor

LEDGF-CtIP interaction and PALB2-MRG15 interaction for RAD51 recruitment (Hayakawa *et al.*, 2010; Aymard *et al.*, 2014; Clouaire *et al.*, 2018). As well as histone ubiquitination and methylation, histone acetylation plays a role in DSB pathway choice, as interaction of the repressive histone mark H3K9me3 with acetyltransferase TIP60 leads to the acetylation of H4K16 and reduces the binding affinity of 53BP1, thereby blocking repair by NHEJ and promoting BRCA1 foci formation at DSB sites (Sun *et al.*, 2009; Tang *et al.*, 2013; Alagoz *et al.*, 2015). Additionally, TIP60 was reported to acetylate H2AK15, consequently blocking ubiquitination by RNF168 and 53BP1 binding in constitutive heterochromatin (Jacquet *et al.*, 2016).

DSB repair pathway choice is also regulated by poly (ADP-ribose) polymerases (PARPs) which catalyse the formation of poly (ADP-ribose) (PAR) chains onto specific amino acid residues on PARP1 itself and other proteins during DNA damage responses, forming important process during DNA repair protein recruitment (Chaudhuri and Nussenzweig, 2017). Interestingly, PARP1 was shown to regulate DNA end resection by blocking EXO1/DNA2-mediated resection via Ku80 recruitment to PAR chains (Caron *et al.*, 2019). Contrarily, PARP2 promotes DNA end resection via CtIP by inhibiting 53BP1 at DNA damage sites, independently of PARylation activity to suppress NHEJ repair (Fouquin *et al.*, 2017).

1.2.7 Meiotic DNA double-strand break repair

During germline development, programmed DNA double-strand breaks are induced during the first stage of meiosis prophase I, in leptotene cells, by the meiosis-specific endonuclease SPO11, which is conserved among species (Bergerat *et al.*, 1997; Keeney, Giroux and Kleckner, 1997). These SPO11-induced DSBs are repaired mainly by HR as it is essential

for the formation of crossovers generated by the homologous recombination machinery. Crossovers (COs) consist of exchanges of genetic material between the parental and maternal homologs and are required for correct homolog alignment for subsequent chromosome segregation, and genetic diversity (Paigen and Petkov, 2010). In mammals, these SPO11-induced DSBs are directed to specific locations across the genome (referred to as DSB hotspots) by the DNA-binding methyltransferase PRDM9, which is essential in facilitating DSB repair between homologs to generate crossovers and support meiotic recombination events (Davies *et al.*, 2016; Paiano *et al.*, 2020). In addition to homologous recombination which involves the genetic exchange between identical DNA sequences, the term homoeologous recombination describes recombination events that occur between DNA sequences which are not fully homologous (Spies and Fishel, 2015). This can result in mismatched nucleotides in the recombined DNA duplex that result from sequence differences between the parental chromosomes (Spies and Fishel, 2015). These resulting mismatches can be repaired via the MMR mechanism and limits the occurrence of recombination between highly heterologous sequences, e.g. during interspecies recombination (Tham *et al.*, 2013; Spies and Fishel, 2015).

These DSB sites are then subjected to end resection by the MRN complex (in *Saccharomyces cerevisiae* bidirectional end resection is mediated by both MRE11 and EXO1), which removes SPO11 from the 5' DSB site covalently bound to a short SPO11 oligonucleotide (SPO11 oligo) with further 5' to 3' resection directed by CtIP, ultimately resulting in 3' ssDNA overhangs (Neale, Pan and Keeney, 2005; Garcia *et al.*, 2011; Zhang *et al.*, 2020; Arter and Keeney, 2024). Interestingly, resection by EXO1 is largely dispensable during meiotic end resection in mice (Paiano *et al.*, 2020; Yamada *et al.*, 2020). The abundance of SPO11-induced DSBs was also found to be regulated by ATM, which also regulates MRE11 activation for end

processing and phosphorylates H2AX on serine 139 (γH2AX) together with ATR (Lange *et al.*, 2016; Lukaszewicz *et al.*, 2018; Widger *et al.*, 2018; Abe *et al.*, 2020; Paiano *et al.*, 2020).

The 3' ssDNA overhangs are bound by RPA and subsequently substituted by RAD51 and the meiosis-specific paralog DMC1 on ssDNA to direct homolog search and ssDNA strand invasion (Pittman *et al.*, 1998; Yoshida *et al.*, 1998; Tarsounas *et al.*, 1999; Xu *et al.*, 2003; Brown and Bishop, 2014; Dai *et al.*, 2017). The requirement of BRCA1 for meiotic recombination requires further investigation as some reports have shown RAD51 recruitment deficiency in spermatocytes from *Brca1*$^{\Delta 11/\Delta 11}$ *p53*$^{+/-}$ mice while others have shown that meiotic recombination in conditional, germline-specific *Brca1* exon 11 deleted mice had no severe defects (Xu *et al.*, 2003; Broering *et al.*, 2014). In *Caenorhabditis elegans*, the BRCA1-BARD1 complex was found to be required for RAD51 recruitment and supporting meiotic DNA repair (Janisiw *et al.*, 2018). Interestingly, DMC1 was shown to bind proximally to DSB sites while RAD51 is found further away, with DMC1 directing strand exchange between homologs (Hinch *et al.*, 2020). Consequently, this leads to the formation of a dHJ which is processed by HJ resolvases, involving the SMX complex, which results in crossover formation (Cromie *et al.*, 2006). The meiosis-specific MutS homologue MSH4 promotes crossover formation and the MutL homologue MLH1 marks the crossover sites on the chromosome (Edelmann *et al.*, 1996; Kneitz *et al.*, 2000). However, not all meiotic DSBs and the resulting HR repair intermediates are processed into crossovers, with the vast majority of DSBs being processed into non-crossovers (Li *et al.*, 2019). These non-crossover events rely on phosphorylated BLM and its associated BTRR complex in meiosis, altogether revealing an intricate regulation between the number of recombination events and their processing outcomes (Grigaitis *et al.*, 2020). The repair and recombination of meiotic DSBs is essential for homolog synapsis and therefore meiotic progression (Pittman *et al.*, 1998; Yoshida *et al.*, 1998; Bugreev *et al.*, 2011).

Interestingly, during spermatogenesis, the X and Y chromosomes are also subjected to SPO11-induced DSBs despite homolog repair not being possible in the unsynapsed regions. These DSBs can also be found in the minimal homologous region where synapsing does occur, termed the pseudoautosomal region (PAR) (Kauppi *et al.*, 2011; Acquaviva *et al.*, 2020). As these chromosomes remain almost fully unsynapsed, the X and Y chromosomes are subjected to chromatin-wide transcriptional silencing, termed meiotic sex chromosome inactivation (MSCI), marked by the formation of a sex body in pachytene (meiosis prophase I cell stage where complete chromatin condensation and synapsis of all autosomes takes place) (Turner, 2007). The MSCI process will be further discussed in section 1.7.3.

1.3 53BP1: a mediator of NHEJ

1.3.1 53BP1 protein domains and functions

53BP1, briefly introduced in sections 1.1.4 and 1.2.3, is an important mediator in the NHEJ repair pathway and a chromatin-binding protein.

The 53BP1 protein domain architecture is composed of the N-terminal tail, an oligomerisation domain (OD), a glycine and arginine-rich (GAR) motif, a tandem Tudor domain, a ubiquitination-dependent recruitment (UDR) domain and a tandem BRCT domain (Figure 1.4) (Panier and Boulton, 2014).

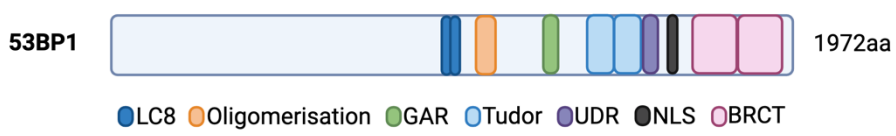


Figure 1.4. The 53BP1 domain architecture.

The N-terminal tail is an unstructured region in 53BP1, which contains two 8 kDa dynein light chain (LC8) binding motifs that mediate the interaction of 53BP1 with dynein light chain LC8 type 1 (DYNLL1) (West *et al.*, 2019). This 53BP1-DYNLL1 interaction, together with ASCIZ, the transcriptional regulator of DYNLL1, supports 53BP1 oligomerisation and its functions in NHEJ, CSR and p53 regulation (Becker *et al.*, 2018). Additionally, the N-terminal tail has 28 serine/threonine-glutamine residues which contain ATM-dependent phosphorylation sites required for the recruitment of RAP1-interacting Factor 1 (RIF1) and Pax transactivation domain-interacting protein (PTIP) to DNA damage sites (Silverman *et al.*, 2004; Gong *et al.*, 2009). RIF1 is an important 53BP1 interacting protein in NHEJ, which is involved in DNA end protection and HR block and is required for CSR functions of 53BP1 (Chapman *et al.*, 2013; Virgilio *et al.*, 2013; Zimmermann *et al.*, 2013; Setiaputra *et al.*, 2022), while the 53BP1-PTIP interaction is dispensable for CSR but involved in dysfunctional telomere fusion and restricting end resection (Callen *et al.*, 2013).

Furthermore, the 53BP1-RIF1 binding mediates the 53BP1-RIF1 interaction with the Shieldin complex, consisting of Shieldin 1 (SHLD1), Shieldin 2 (SHLD2), Shieldin 3 (SHLD3) and revertibility protein 7 (REV7) which localises Shieldin to DNA DSBs (Dev *et al.*, 2018; Ghezraoui *et al.*, 2018; Gupta *et al.*, 2018; Noordermeer *et al.*, 2018). The oligosaccharide/oligonucleotide binding (OB) folds in SHLD2 bind to ssDNA and block 5'-3' resection mediated by EXO1 and DNA2/BLM (Noordermeer *et al.*, 2018). Following the recruitment of Shieldin to DNA, the CTC1-STN1-TEN1 (CST) complex and Polymerase α-primase (Polα-primase) complex are recruited to DSBs which directs fill-in synthesis (Barazas *et al.*, 2018; Mirman *et al.*, 2018; King *et al.*, 2024). The interaction between Shieldin and the CST complex was recently shown to be dependent on DNA damage dependent ATM signalling (King *et al.*, 2024). Interestingly, 53BP1-REV7/shieldin cooperation, while being required for

DNA end joining during CSR, it is dispensable for 53BP1-dependent NHEJ during V(D)J recombination (Ghezraoui *et al.*, 2018; King *et al.*, 2024).

The oligomerisation domain in 53BP1 is required for the assembly of 53BP1 dimers and multimers (Adams *et al.*, 2005). However, loss of the OD in 53BP1 only leads to moderately defective dysfunctional telomeres fusions, whereas it is required for CSR and promotes 53BP1 recruitment to DSB sites at IR-induced breaks (Ward *et al.*, 2006; Zgheib *et al.*, 2008; Bothmer *et al.*, 2010; Lottersberger *et al.*, 2013). The GAR motif is methylated by protein arginine N-methyltransferase 1 (PRMT1) which was reported to support 53BP1 DNA-binding function (Adams *et al.*, 2005; Boisvert *et al.*, 2005).

The focus-forming region of 53BP1 consists of the oligomerisation domain, the tandem Tudor domain and the UDR (Mirman and Lange, 2020). 53BP1 binds to the cell cycle-specific post-translational modification on histone H4 mono- and di-methylated lysine 20 (H4K20me1/2) via its tandem Tudor domain to direct 53BP1 to chromatin sites (Botuyan *et al.*, 2006; Wilson *et al.*, 2016). The 53BP1 chromatin recruitment to sites of DSBs is directed via its UDR domain which binds to H2AK15ub (Fradet-Turcotte *et al.*, 2013; Wilson *et al.*, 2016).

The 53BP1 tandem BRCT domain is not required for CSR, protection of DNA ends from end resection and localisation of 53BP1 to sites of DSBs (Ward *et al.*, 2006; Bothmer *et al.*, 2011). However, 53BP1 interacts with p53 through the tandem BRCT domain and with USP28 which supports p53-dependent transcriptional responses (Derbyshire *et al.*, 2002; Joo *et al.*, 2002; Cuella-Martin *et al.*, 2016). In addition, 53BP1 can also interact with γH2AX through the tandem BRCT domain (Kleiner *et al.*, 2015).

1.3.2 Physiological and pathological functions of 53BP1

As discussed in sections 1.2.3 and 1.3.1, 53BP1-dependent NHEJ is required to repair programmed DSBs for the immune repertoire development and DNA end-joining events at DSBs. However, 53BP1 is not a classical NHEJ factor as it does not bind to DNA ends directly and instead acts as a chromatin insulator which drives classical NHEJ by protecting DNA ends from end resection and facilitating DNA fill-in synthesis (Bothmer *et al.*, 2010; Mirman and Lange, 2020).

Furthermore, 53BP1-deficient mice in addition to being immunodeficient, are also radiation sensitive and prone to tumour development, indicating that 53BP1-mediated NHEJ in also required for genome maintenance (Ward *et al.*, 2003). 53BP1 through mediating interactions with the Shieldin complex and the CST complex at ssDNA is required at unprotected telomeres for Polα-mediated DNA fill-in synthesis, and was shown to be required for dysfunctional telomere fusions (Dimitrova *et al.*, 2008; Mirman *et al.*, 2022).

However, 53BP1-mediated NHEJ as it is error-prone, drives oncogenesis in BRCA1-deficient/mutant cells, where the unstrained activity of NHEJ drive the formation of chromosomal aberrations and genome rearrangements leading to genome instability and cancer development (Bunting *et al.*, 2010; Chapman *et al.*, 2012; Callen *et al.*, 2013). Additionally, the pathological 53BP1 functions in BRCA1-deficient cells were shown to be dependent on the CST-Polα-primase fill-in synthesis (Mirman *et al.*, 2022). Loss of 53BP1 but not of Lig4 in BRCA1-deficient cells leads to HR restoration, indicating that the DSB repair pathway choice between NHEJ and HR is mediated by 53BP1 and BRCA1 (Bunting *et al.*, 2010). Furthermore, 53BP1, independently of Shieldin is the driver of genome instability in BRCA1-deficient cells (Bouwman *et al.*, 2010; Bunting *et al.*, 2010; Xu *et al.*, 2015; King *et al.*, 2024).

These pathological functions of 53BP1 can be exploited in therapy by treating HR-deficient cancers with PARPi which takes advantage of the mutagenic repair driven by 53BP1-mediated NHEJ in HR-deficient cells, ultimately leading to cell death (Farmer *et al.*, 2005; Kass, Moynahan and Jasin, 2010). Furthermore, 53BP1-mediated NHEJ is also involved in chromothripsis events that arise from mitotic errors which further contribute to the genome instability associated with HR-deficient cancers (Qing Hu *et al.*, 2024).

1.4 BRCA1: a tumour suppressor protein involved in Homologous Recombination repair

1.4.1 BRCA1 protein domain architecture

The BRCA1 protein consists of 1863 amino acids and is composed of the RING domain at its N-terminus, a long unstructured region within exon 11, a coiled-coil domain (CCD) and a tandem BRCTs repeat domain (Figure 1.5) (Tarsounas and Sung, 2020).

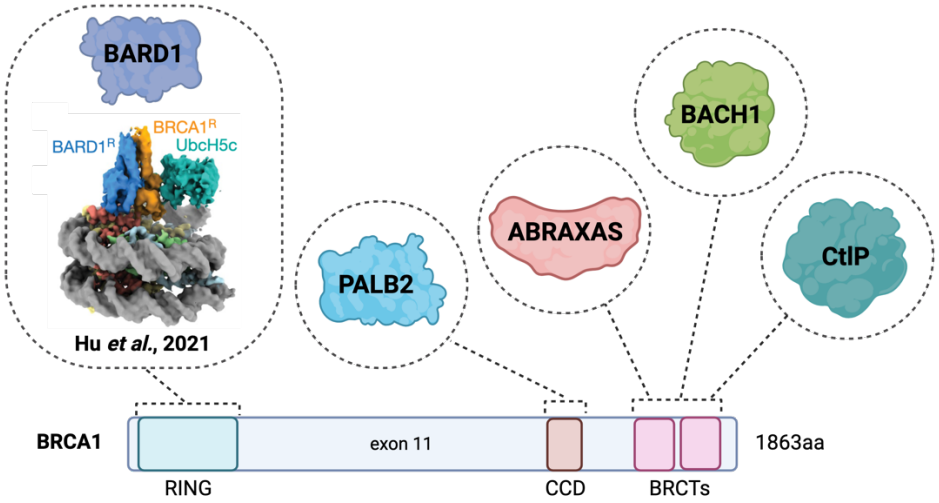


Figure 1.5. The BRCA1 protein domain architecture and BRCA1 protein interactors.

The BRCA1 RING domain spans amino acids 1-109 and forms a binding platform for the RING domain in BARD1, which interact via their α-helices creating a four-helix assembly to form the BRCA1-BARD1 heterodimer (Figure 1.5 and 1.6) (Wu *et al.*, 1996; Brzovic *et al.*, 2001; Morris, Keep and Solomon, 2002). Without BRCA1-RING/BARD1-RING binding, the hydrophobic core within the helices in the RING domain is exposed, tagging the BRCA1 protein for proteasomal degradation (Brzovic *et al.*, 2001; Hashizume *et al.*, 2001).

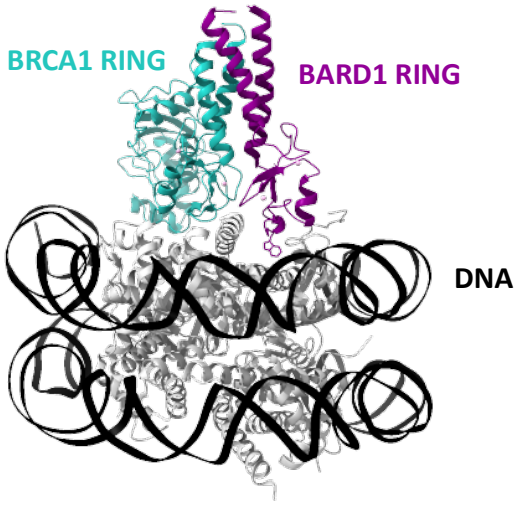


Figure 1.6. Cryo-EM structure of the BRCA1-BARD1 RING heterodimer bound to the nucleosome. PDB: 7JZV, Witus *et al.*, 2021.

Additionally, the BRCA1-BARD1 RING heterodimer contains an E3 ligase function which ubiquitinates histone H2A on lysine residues 125/127/129 and was also reported to have autoubiquitination functions by catalysing lysine 6-linked polyubiquitination (Baer and Ludwig, 2002; Brzovic *et al.*, 2003; Kalb *et al.*, 2014; Witus *et al.*, 2022). Recently, it was also reported that BRCA1-BARD1 ubiquitinates PCNA on lysine 164 for replication fork protection and suppression of ssDNA gaps at replication forks in cells under stochastic conditions (Salas-Lloret *et al.*, 2024). Moreover, several additional BRCA1-BARD1 E3 ligase substrates involved in cell cycle regulation, transcriptional regulation, and DNA repair have been previously

reported (Witus, Stewart and Klevit, 2021). These include Aurora Kinase B, cyclin B and Cdc25C, where it was shown that ubiquitination by BRCA1-BARD1 was required for Aurora B degradation and turnover, and ubiquitination of cyclin B and Cdc25C was involved in G2/M cell cycle checkpoint regulation, respectively (Ryser *et al.*, 2009; Shabbeer *et al.*, 2013). In addition, ubiquitination of oestrogen receptor α on lysine 302 by BRCA1-BARD1 was reported to be required for repression of oestrogen receptor α transcriptional activity, while CtIP ubiquitination by BRCA1-BARD1 was shown to be required for its association with chromatin following DNA damage and G2/M cell cycle checkpoint regulation (Yu *et al.*, 2006; Witus, Stewart and Klevit, 2021). However, the function of the autoubiquitination and of H2AK125/127/129 ubiquitination in DNA DSB repair remains to be clearly understood due to previous contrasting findings. Previous reports using siRNA to knockdown BARD1 have indicated that the BRCA1-BARD1 E3 ligase activity is required for the recruitment of SMARCAD1, a chromatin remodeller, to DNA DSB sites to promote long-range end resection and HR repair (Densham and Morris, 2016; Uckelmann *et al.*, 2018), claiming that the E3 ligase function of the BRCA1-BARD1 complex is required for RAD51 recruitment and survival to some genotoxic agents such as irradiation, olaparib, camptothecin and etoposide (Densham *et al.*, 2016). Other reports have shown that a BRCA1 triple mutant harbouring I26A/L63A/K65A point mutations abrogates all E3 ligase function and E2 ubiquitin-conjugating enzyme interactions while still being able to heterodimerise with BARD1 (Stewart *et al.*, 2017; Wang *et al.*, 2023). The expression of this BRCA1 'E3 ligase dead' mutant following shRNA knockdown of endogenous BRCA1 in HeLa cells reduced RAD51 IRIF and caused olaparib and cisplatin sensitivity which indicated that the BRCA1-BARD1 E3 ligase activity was required for HR repair (Wang *et al.*, 2023). However, this contradicts previous reports, including work from our laboratory that assessed the importance of the BRCA1-BARD1 E3 ligase function in DNA

repair and found that the BARD1 RING mutant arginine 99 to glutamic acid (R99E), which abrogates the interaction of the BRCA1-BARD1 RING heterodimer E3 ligase with E2 ubiquitin-conjugating enzymes, does not confer olaparib sensitivity in HCT116 cells (Nakamura *et al.*, 2019). Additionally, mice harbouring a homozygous mutation in which isoleucine 26 is converted to alanine (*Brca1*$^{I26A/I26A}$) were not prone to tumour development but displayed male sterility, which indicates that the BRCA1-BARD1 RING E3 ligase is dispensable for the tumour suppression and is likely to be required for the H2A ubiquitination functions during male germline development (Shakya *et al.*, 2011). Although transient expression of the BRCA1 I26A mutation in 293T cells lead to cisplatin sensitivity in another report (Anantha *et al.*, 2017). The contradicting conclusions on the importance of the BRCA1-BARD1 E3 ligase role in DNA repair could be due to the difference in cell lines or the penetrance of the E3 ligase mutations studied in each report, as the BARD1 R99E and the BRCA1 I26A E3 ligase mutant proteins were shown to retain residual E3 ligase activity (Stewart *et al.*, 2017; Wang *et al.*, 2023). Additionally, while recent reports which studied the BRCA1 I26A/L63A/K65A protein showed that complete loss of E3 ligase function led to DNA repair deficiency, the impact of the BRCA1 I26A/L63A/K65A mutations was not studied *in vivo* to conclude on the importance of the BRCA1-BARD1 E3 ligase function in tumour suppression (Wang *et al.*, 2023). Therefore, the physiological importance of the E3 ligase activity of the BRCA1-BARD1 RING heterodimer in tumour suppression and DNA repair remains to be fully clarified.

Furthermore, the BRCA1 RING domain interacts with the nucleosome acidic patch via residues lysine 70 (K70) and arginine 71 (R71) by interacting with the side chains from H2A residues glutamic acid 64, glutamic acid 61, aspartic acid 90 and glutamic acid 92 (Hu *et al.*, 2021; Witus *et al.*, 2021). When mutated to alanine (K70A and R71A) caused reduced H2A ubiquitination activity and abrogated nucleosome binding (McGinty, Henrici and Tan, 2014;

Hu *et al.*, 2021; Witus *et al.*, 2022). Work by the Dan Durocher laboratory investigated the BRCA1 IRIF formation in RPE-1 hTERT *p53*$^{-/-}$ *BRCA1*$^{-/-}$ BRCA1$^{K70A\ R71A}$ mutant-expressing cells and found that BRCA1 localisation to IR-induced DSB sites was RAP80-dependent (Sherker *et al.*, 2021). However, the importance of the BRCA1 RING-nucleosome binding in DNA repair has not been further explored.

The BRCA1 exon 11 is an unstructured region found between the BRCA1 RING domain and the CCD domain which covers over 65% of the BRCA1 sequence (Clark *et al.*, 2012). Mice which are homozygous for *Brca1* exon 11 deletion (*Brca1*$^{\Delta 11/\Delta 11}$) die during embryonic development from embryonic development day E12.5 (Xu *et al.*, 2001). However, loss of one *p53* allele was able to rescue embryonic development, yielding viable mice albeit tumour-prone (Xu *et al.*, 2001). Furthermore, deletion of *53bp1* was also found to rescue embryonic development in *Brca1*$^{\Delta 11/\Delta 11}$ mice and lowered tumour incidence in comparison to *p53* loss (Cao *et al.*, 2009; Bunting *et al.*, 2010). Cells derived from *53bp1*$^{-/-}$ *Brca1*$^{\Delta 11/\Delta 11}$ mice displayed lower chromosomal abnormalities compared to *Brca1*$^{\Delta 11/\Delta 11}$ *p53*$^{-/-}$, rescued PARPi resistance and restored HR, independently to p53, indicating that the BRCA1 exon 11 could be required for tumour suppressive roles of the BRCA1-BARD1 complex (Bunting *et al.*, 2010). Additionally, previous reports showed that the exon 11 is involved in promoting DNA end resection for HR repair by counteracting RIF1 (Nacson *et al.*, 2020). However, much of the function in exon 11 is not understood.

As discussed in detail in section 1.1.3, the BRCA1 coiled-coil domain (CCD) interacts with the coiled-coil domain in PALB2, which mediates the recruitment of BRCA2 for downstream HR events and relies on leucine 1407 in the BRCA1 CCD for PALB2 interaction (Figure 1.5) (Fan Zhang *et al.*, 2009; Feng Zhang *et al.*, 2009; Sy, Huen and Chen, 2009; Pulver *et al.*, 2021). The BRCA1 BRCT domain consists of two tandem BRCT repeats, spanning amino acids 1650 to

1863, which are connected by a 22 amino acid linker (Williams, Green and Glover, 2001). This domain interacts with phospho-binding proteins to form the BRCA1-A, BRCA1-B and BRCA1-C complexes, which are covered in further detail in section 1.6 (Figure 1.5) (Yu *et al.*, 2003; Yu and Chen, 2004; Kim, Huang and Chen, 2007).

1.5 BARD1: the obligate binding partner of BRCA1

1.5.1 BARD1 protein domain architecture

BARD1 is an essential protein which forms a heterodimeric complex with BRCA1 and thereby constitutes the obligate binding partner of BRCA1. Together with BRCA1, BARD1 plays a critical role in the maintenance of genome stability and directing DSB repair towards HR (Tarsounas and Sung, 2020). Accordingly, loss of *Bard1* in mice leads to embryonic lethality between embryonic day E7.5-E8.5 (McCarthy *et al.*, 2003). Therefore, studying the domain structure of BARD1 is fundamental to understanding its functions in DNA repair mechanisms, tumour suppression and germline development.

The BARD1 protein is composed of a RING domain, an intrinsically disordered region (IDR), ankyrin repeat domains (ARD) and the tandem BRCT repeats domain (Figure 1.7) (Tarsounas and Sung, 2020).



Figure 1.7. The BARD1 domain architecture.

As already introduced in section 1.4.1, BARD1 contains an N-terminal RING domain that spans amino acids 26-122, which together with BRCA1 constitutes the BRCA1-BARD1 E3 ligase function and is required for stability of the BRCA1-BARD1 complex. Interestingly, both the Rachel Klevit and Georges Mer laboratories reported that BARD1 binds to nucleosomes via proline 89 (P89) and tryptophan 91 (W91) residues (Hu *et al.*, 2021; Witus *et al.*, 2021). However, it was reported that the BARD1 RING domain can bind to both the H2B/H4 nucleosome cleft and the H2B αC helix indicating that the BARD1 RING domain can bind to the nucleosome in two different conformations, where both binding modes position the E2 ubiquitin-conjugating enzyme away to facilitate selective ubiquitination of the H2AK127 residue (Hu *et al.*, 2021; Witus *et al.*, 2021). The BARD1 RING domain nucleosome interaction was shown to rely on van der Waals contacts between proline 89 and the H2B residue threonine 115, and between tryptophan 91 and H2B residues lysine 108 and serine 112 (Hu *et al.*, 2021), and on the contact of the tryptophan 91 side chain with a pocket surrounding H3 residue phenylalanine 78/lysine 79, H4 residue valine 70/threonine 71/glutamic acid 74 and H2B residue arginine 99 (Witus *et al.*, 2021). Interestingly, it was also reported that the BARD1 RING nucleosome interaction by P89 and W91 facilitates H2A ubiquitination (Witus *et al.*, 2021, 2023; Wang *et al.*, 2023). Additionally, more recent biochemical assays performed on the BARD1 RING-domain P89A and W91A mutants showed that while these mutations disrupted the H2A ubiquitination, the nucleosome binding affinity was minimally affected (Witus *et al.*, 2023). Furthermore, the BARD1 RING nucleosome binding by both P89 and W91 residues was reported to be required for RPA and RAD51 loading in IR-treated HeLa cells treated with shBARD1 (Wang *et al.*, 2023). However, the physiological importance of the BARD1 RING nucleosome interaction during DNA repair needs to be further studied.

Little is known about the functions and importance of the intrinsically disordered region (IDR) in BARD1 which spans 300 residues, whether it mediates DNA repair functions and/or if it is a linker between the BARD1 RING and ARD domains to support its nucleosome binding functions (Mark *et al.*, 2005). Recent structural studies have identified a region located between residues 141-216 and 194-216 within the IDR which supports nucleosome DNA binding and promotes the BRCA1/BARD1-RING mediated H2A ubiquitination activity (Witus *et al.*, 2023). Furthermore, HeLa cells treated with shBARD1 to deplete endogenous BARD1 that re-expressed a shBARD1 construct harbouring deletions between residues 194-216 were sensitive to PARPi olaparib and had fewer BARD1 foci upon olaparib treatment (Witus *et al.*, 2023). Moreover, the IDR region between residues 123-162 was identified to contain a RAD51 interacting motif which facilitates RAD51-ssDNA invasion (Zhao *et al.*, 2017) and a SLX4-interacting motif, situated around serine 148 in BARD1 contained within the IDR, which is involved in the processing of HR repair intermediates that have not been dissolved by the BLM helicase (Tsukada *et al.*, 2024). However, the physiological importance of the IDR and its importance during DNA repair have not been thoroughly investigated. Interestingly, this unstructured region within BARD1 seems to be important to facilitate the bridging of the BRCA1-BARD1 complex binding to two nucleosomes via the BRCA1-BARD1 RING domain and the BARD1 ARD-BRCT domain to bind to nucleosomes which have both H4K20me0 and H4K20me1/2 status in newly replicated chromatin associated to DSBs (Burdett *et al.*, 2023).

The BARD1 ARD and tandem BRCTs domain in BARD1 directly associate with chromatin upon DNA DSB formation through the dual-reader module and play crucial functions in HR repair by directing BRCA1 recruitment to DSB sites (Figure 1.8) (Nakamura *et al.*, 2019; Becker *et al.*, 2021). The recognition of unmethylated histone H4 lysine 20 (H4K20me0) by BARD1 ARD via glutamic acid 467, asparagine 470 and aspartic acid 500 residues is essential to recruit

the BRCA1-BARD1 complex to DNA DSB sites, which are found in post-replicative chromatin (Nakamura *et al.*, 2019; Becker *et al.*, 2021). This BARD1 ARD binding directs the BRCA1-BARD1 complex to DNA DSB sites in cells that have a sister chromatid available in S/G2 for HR. The BARD1 tandem BRCTs domain contains a recently discovered BRCT ubiquitin-dependent recruitment motif (BUDR) (Becker *et al.*, 2021; Krais *et al.*, 2021). The BUDR is localised in the inter-β2'-β3' loop of the second BRCT in BARD1 and mediates the recognition of the RNF168-dependent ubiquitination of histone H2A lysine 15 (H2AK15ub) which competes with 53BP1 for binding and is essential for BRCA1 recruitment to DSB sites and NHEJ antagonization (Becker *et al.*, 2021; Dai *et al.*, 2021; Hu *et al.*, 2021; Krais *et al.*, 2021). The mutation of aspartic acid 712 residue to alanine (D712A) in the BARD1 BUDR abrogates the electrostatic interaction of D712 with H2B residues serine 109 and lysine 113/lysine 116, which are required to promote BARD1 BUDR-H2AK15ub interaction (Dai *et al.*, 2021; Hu *et al.*, 2021). Additionally, it was shown that the nucleosome binding by BARD1 ARD-BRCTs domain stimulates H2A ubiquitination by the BRCA1-BARD1 RING domains, indicating that the linker region in BARD1 (IDR) supports bi-functional roles of BRCA1-BARD1 that involve chromatin

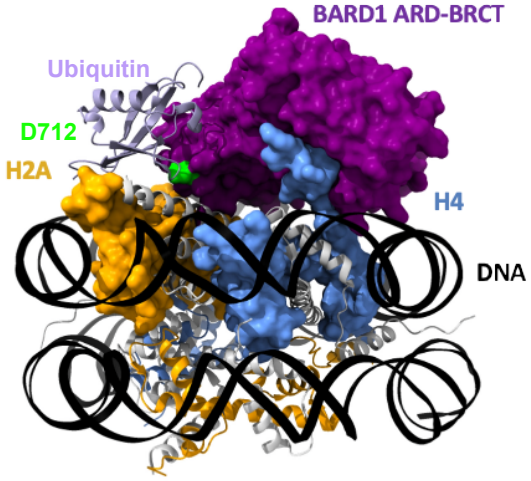


Figure 1.8. Cryo-EM structure of the BARD1 ARD-BRCT domain on the nucleosome. The BARD1 ARD binds to H4K20me0, while the BARD1 BRCT domain binds to H2AK15ub. PDB: 7LYC, Hu *et al.*, 2021.

anchoring via H4K20me0/H2AK15ub-binding and the BRCA1-BARD1 E3 ubiquitin ligase activity (Burdett *et al.*, 2023; Witus *et al.*, 2023).

1.6 The BRCA1 sub-complexes: co-factors of BRCA1 – the BRCA1-A, B and C complexes

In addition to the BRCA1-BARD1 complex, BRCA1 associates with three other complexes via its BRCT domain with phosphorylated proteins ABRAXAS, BACH1 and CtIP resulting in BRCA1-A, BRCA1-B and BRCA1-C complexes, respectively (Figure 1.9) (Yu *et al.*, 2003; Greenberg *et al.*, 2006; Wang *et al.*, 2007). The formation of these BRCA1 sub-complexes depends on the BRCA1 BRCT phospho-peptide binding domain which recognises the phospho-serine-proline-X-phenylalanine (p-SPxF, where x is variable) motif (Manke *et al.*, 2003; Rodriguez *et al.*, 2003).

The BRCA1-B complex is composed of BRCA1-BARD1, DNA topoisomerase 2-binding protein 1 (TOPBP1) and BACH1, also known as BRIP1 or FANCJ, which is phosphorylated on serine 990 by CDK from S to M phase (Yu *et al.*, 2003; Yu and Chen, 2004). BACH1 is bound by BRCA1 via serine 1655 and lysine 1702 in the BRCT domain which are essential for the BRCA1-BACH1 complex formation and function (Cantor *et al.*, 2001; Botuyan *et al.*, 2004; Shiozaki *et al.*, 2004). The BRCA1-B complex is required during replication checkpoint control and cell cycle checkpoint control at S/G2 to accumulate cells at the G2 phase and control cell cycle progression following DNA damage (Yu and Chen, 2004; Gong *et al.*, 2010). Phosphorylation of threonine 1133 in BACH1 mediates the TOPBP1 interaction, required for RPA loading onto ssDNA strands following replication stress and ATR activation to consequently activate the S-phase checkpoint (Gong *et al.*, 2010). Furthermore, BACH1 is a member of the DEAH helicase

family and a DNA-dependent ATPase, as well as a Fanconi Anaemia protein which plays a role in DNA interstrand crosslink repair (Cantor *et al.*, 2001, 2004; Litman *et al.*, 2005). In addition, mutations in the helicase domain of BACH1 or the BRCA1 interacting motif in the BRCT domain were found in breast and ovarian cancer which indicates that its function together with BRCA1 in the BRCA1-B complex might be required for important tumour suppressive roles (Cantor and Guillemette, 2011; Rafnar *et al.*, 2011). In fact, mutations in the BACH1 helicase domain led to HR deficiency and increased chromosome radials and breaks in cells treated with the genotoxic agent mitomycin C (MMC), which causes DNA interstrand crosslinks (Litman *et al.*, 2005). Furthermore, the tumour suppressor functions of the BRCA1-B complex might be mediated by the repression of MMEJ repair by BRCA1-BACH1, which is dependent on the interaction of BACH1 with BRCA1 via serine 990 (Dohrn *et al.*, 2012).

The BRCA1-C complex is composed of BRCA1-BARD1, CtIP, and MRN which function in DNA DSB end resection with exonucleases EXO1 and DNA2, required for HR repair (Greenberg *et al.*, 2006). BRCA1 interacts with CtIP by binding the BRCA1-BRCT domain to the CDK-mediated phosphorylated serine 327 residue in CtIP (Yu and Chen, 2004). While the function of CtIP in DNA end resection depends on the CDK-dependent phosphorylation of CtIP at threonine 847 during S/G2 upon DNA damage (Huertas and Jackson, 2009), it does not entirely rely on the BRCA1 interaction as it was shown that MEFs carrying a mutation in the residue equivalent to S327 in humans had no end resection deficiency (Reczek *et al.*, 2013). In contrast, the T847A mutation reduced RAD51 recruitment at IR-induced DSBs and resulted in HR deficiency (Polato *et al.*, 2014). The non-crucial functions of BRCA1 in CtIP's end resection roles are further supported by reports indicating that disrupting the CtIP-BRCA1 interaction did not lead to tumour formation in mice (Reczek *et al.*, 2013). Nevertheless, the BRCA1-C complex has been shown to support the CtIP-mediated end resection mechanism by accelerating resection

(Cruz-García, López-Saavedra and Huertas, 2014). Furthermore, BRCA1-C is also found to mediate CHK1 phosphorylation and regulate the G2/M cell cycle checkpoint (Yu and Chen, 2004; Greenberg *et al.*, 2006), as well as play a role in DNA DSB repair pathway choice by repressing RIF1 recruitment to DSB sites in S/G2 to promote end resection for HR repair (Escribano-Díaz *et al.*, 2013).

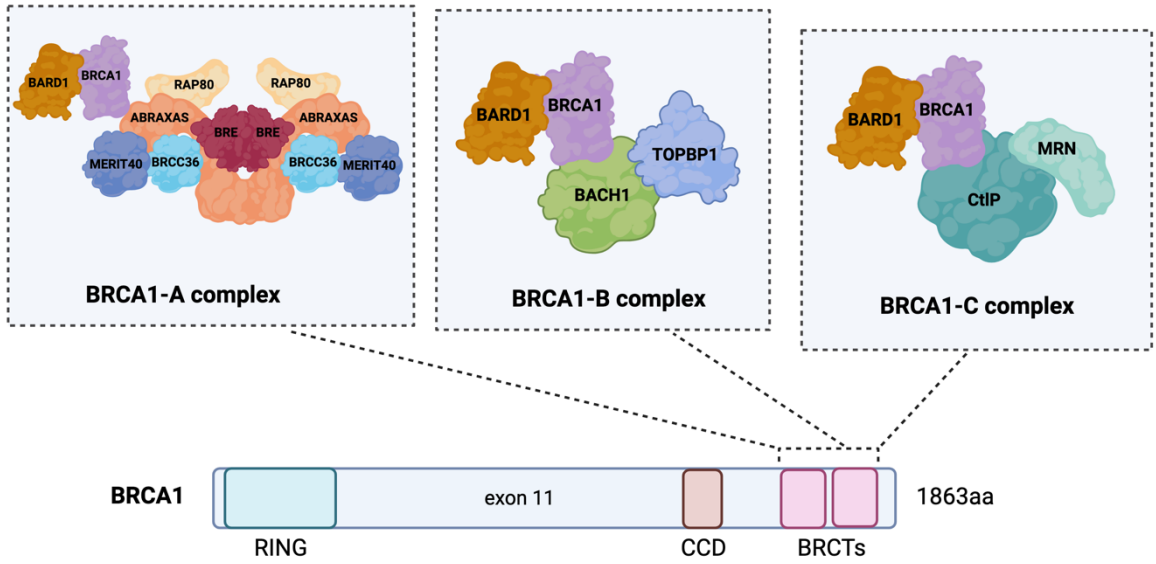


Figure 1.9. The BRCA1-associated subcomplexes. The BRCA1 tandem BRCT domain binds to ABRAXAS, forming the BRCA1-A complex, BACH1 forming the BRCA1-B complex and to CtIP forming the BRCA1-C complex.

1.6.1 The BRCA1-A complex

The BRCA1-A complex is constituted of BRCA1-BARD1, receptor-associated protein 80 (RAP80), MERIT40 (also known as NBA1), BRCC36, BRE (also known as BRCC45) and ABRAXAS (also known as CCDC98, Abra1, FAM175A) (Dong *et al.*, 2003; Kim, Huang and Chen, 2007; Sobhian *et al.*, 2007; Wang and Elledge, 2007; Wang *et al.*, 2007, 2009). ABRAXAS is the adaptor protein for the BRCA1-A complex, which binds to the pSPxF motif in the BRCA1-BRCT domain via phosphorylated serine 406 (Kim, Huang and Chen, 2007; Wu *et al.*, 2016). Although the ABRAXAS-BRCA1 interaction is not required for RAP80-ABRAXAS interaction (Liu,

Wu and Yu, 2007; Wang *et al.*, 2007), it is essential for repairing DSBs in cells exposed to IR and functions in recruiting BRCA1 to DSB sites (Liu, Wu and Yu, 2007; Castillo *et al.*, 2014). Furthermore, work done in *Abraxas*$^{-/-}$ mice showed that while ABRAXAS is not required for embryonic development and while *Abraxas*$^{-/-}$ mice are viable, these mice are IR-sensitive and become tumour-prone between 17-24 months of life, on average (Castillo *et al.*, 2014). The MEFs derived from these mice are hypersensitive to MMC, PARPi olaparib and IR, and have reduced SCEs, supporting the role of ABRAXAS in genome stability (Castillo *et al.*, 2014). These findings are in line with reports of breast and ovarian cancer cases that carry mutations in *Abraxas* or copy losses (Solyom *et al.*, 2012; Castillo *et al.*, 2014).

Upon DNA damage, RAP80 binds to the RNF8/RNF168 K63-linked polyubiquitin chains (discussed in section 1.2.6) via its two ubiquitin-interacting motif (UIM) domains, which recruits ABRAXAS-BRCA1 to DSB sites, whereas RAP80 and ABRAXAS bind through the Abraxas-interacting region (AIR) located at amino acids 270-400 (Sobhian *et al.*, 2007; Wang and Elledge, 2007). Furthermore, ABRAXAS localisation to DSB sites is BRCA1-independent and so is RAP80 recruitment. However, ABRAXAS loss compromises both BRCA1 and RAP80 foci formation suggesting that the BRCA1-A complex could have BRCA1-independent roles in DNA repair in different repair contexts (Wang *et al.*, 2007). BRCC36 is a deubiquitinase (DUB) enzyme which degrades K63-polyubiquitin chains and interacts with ABRAXAS via their coiled-coil domains (Sobhian *et al.*, 2007; Wang and Elledge, 2007). On the other hand, MERIT40 (mediator of RAP80 interactions and target 40kDa) is required for the integrity of the complex and facilitating ubiquitin binding together with BRE (brain and reproductive organ-expressed), which is also involved in BRCA1 sequestration (Feng, Huang and Chen, 2009; Shao *et al.*, 2009; X. Hu *et al.*, 2011; Rabl *et al.*, 2019). Furthermore, MERIT40 associates with ABRAXAS via the

N-terminal region in ABRAXAS, and together with BRE mediates the association with RAP80 and BRCC36 (Wang *et al.*, 2009; Rabl *et al.*, 2019).

Equally to ABRAXAS, the depletion of BRCC36 and BRE increased the IR-sensitivity in HeLa cells and affected the G2/M checkpoint, indicating that the integrity of the complete BRCA1-A complex is required for these DNA repair response functions (Dong *et al.*, 2003). Interestingly, structural studies of the BRCA1-A complex have shown that it is assembled by two copies of each protein component, with ABRAXAS acting as a scaffolding protein (Kyrieleis *et al.*, 2016; Rabl *et al.*, 2019). BRCA1-A is required to regulate HR repair by restricting DNA end resection as well as in regulation of the G2/M checkpoint (Liu, Wu and Yu, 2007; Wang *et al.*, 2007, 2009; Coleman and Greenberg, 2011). The K1702M mutation in the BRCA1-BRCT domain reduces the ability of BRCA1 to bind to the BRCT interacting proteins and was reported to increase RPA and RAD51 levels indicating hyper-recombination (Dever *et al.*, 2011). Intriguingly, the BRCA1-A complex is also involved in meiosis during male germline development, where BRCA1, ABRAXAS, MERIT40 and RAP80 are found on unsynapsed chromosomes during meiotic prophase I, localising in an MDC1/H2AX/RNF8-independent manner (Lu *et al.*, 2013). Nevertheless, it is not responsible for BRCA1 recruitment in meiosis as *Rap80*$^{-/-}$ male mice are fertile and have no meiotic progression defects, and ABRAXAS is absent from unsynapsed XY chromosomes where BRCA1 is localised (Wu *et al.*, 2012; Lu *et al.*, 2013). However, the exact physiological role of the BRCA1-A complex is not clear yet.

1.6.2 Function of RAP80 in DNA repair

As mentioned in the previous section, RAP80 contains two UIM domains which bind to K63-linked polyubiquitin chains on H2A and H2AX deposited by RNF168 (Sobhian *et al.*,

2007). This promotes BRCA1 recruitment to DSBs, discussed in section 1.6.2. RAP80 also contains a SUMO (small ubiquitin-like modifier)-interacting motif (SIM) that contributes to the recruitment of BRCA1 to DSBs and depends on the E3 ligase RNF4 (Guzzo *et al.*, 2012; Hu, Paul and Wang, 2012). *Rap80*$^{-/-}$ mice are tumour-prone and hypersensitive to ionizing radiation indicating major DNA DSB repair defects, in line with reports of germline mutations in RAP80 found in familial breast cancer (Akbari *et al.*, 2009; Wu *et al.*, 2012). Furthermore, the loss of RAP80 eliminated residual recruitment of BRCA1 in cells carrying the BARD1-BUDR mutation, indicating that RAP80 contributes partially to DNA repair by supporting BARD1 dual reader domain-independent BRCA1 recruitment mechanisms via K63-linked polyubiquitin chain-dependent recruitment of RAP80 to DSBs (Becker *et al.*, 2021). In contrast, loss of RAP80 in cells with wild-type BRCA1-BARD1 only reduced BRCA1 foci levels slightly (Shao *et al.*, 2009; Y. Hu *et al.*, 2011; Becker *et al.*, 2021). Additionally, RAP80 loss did not affect BRCA1 protein levels and that of its interacting proteins BACH1, CtIP or RAD51 (Y. Hu *et al.*, 2011). Apart from its BRCA1 DSB site-recruitment roles, RAP80 was also reported to suppress excessive HR activity, limit DNA end resection, and accumulate toxic HR repair intermediates (Y. Hu *et al.*, 2011). BACH1 (FANCJ) and RAP80 loss increased chromosomal instability and resulted in cell cycle checkpoint defects due to compromised repair of ICL-induced HR repair intermediates, exacerbated by excessive end resection (Awate *et al.*, 2020). RAP80 could also suppress chromosomal instability by mechanisms independent of BRCA1-BARD1's role in DNA repair by limiting CtIP-supported MMEJ and repairing DSBs on chromatin sites with a topoisomerase-cleavage complex (Iijima *et al.*, 2010; Lee-Theilen *et al.*, 2011; Zhang and Jasin, 2011). Besides, RAP80 has multiple ATM-phosphorylation sites as well as an ATR phosphorylation site at serine 205, required for checkpoint control and DNA repair which suggests that RAP80 could have DNA repair functions independently to BRCA1 (J. Yan, Kim, Yang, Li, *et al.*, 2007; Yan *et al.*,

2008). In addition, *Brcc36* inactive mice which inactivates the deubiquitinating enzyme function of the BRCA1-A complex lead to increased chromosomal abnormalities after mitomycin C treatment but not following PARP inhibition (Jiang *et al.*, 2022).

Recent structural studies investigated the chromatin binding mechanisms by the BRCA1-BARD1 complex and reported that BARD1 binding to H2AK15ub blocked K63-linked ubiquitin chain extension (Hu *et al.*, 2021). However, BARD1 H2AK15ub binding was not prevented by the presence of K63-linked ubiquitin chains (Burdett *et al.*, 2023). So far it has not been shown if this suppresses RAP80 recruitment to DSB sites, and the mechanism that regulates RAP80 activity and its importance is still unclear.

Recently, RAP80 and other components of the BRCA1-A complex were found to be recruited at camptothecin-damaged replication forks and this mechanism was dependent on the suppression of ATM signalling. This hints at distinct RAP80-related functions at broken replication forks which are involved in the interplay between NHEJ and HR repair at single-ended DSBs (Balmus *et al.*, 2019; Nakamura *et al.*, 2021). In addition, ABRAXAS was found to limit DNA end resection at camptothecin-induced DNA damage sites by inhibiting SLX4/MUS81 recruitment, and restrict break-induced replication in mitosis in MEFs (Wu and Wang, 2021). Break-induced replication and the associated mitotic DNA synthesis are mediated by the cleavage of collapsed replication forks at common fragile sites by MUS81 (Minocherhomji *et al.*, 2015). Consequently, this implies that ABRAXAS and RAP80 could have separate roles in genome stability which are independent of each other highlighting the complexities of the BRCA1-A complex that remain to be fully understood.

1.6.3 BRCA1-A dependent recruitment of BRCA1 at DNA double-strand breaks

The BRCA1 BRCT-ABRAXAS S406 interaction allows the BRCA1-BARD1 complex to be recruited in a K63-linked polyubiquitin chain-dependent fashion via RAP80 (Sobhian *et al.*, 2007; Castillo *et al.*, 2014). This interaction is required to support BRCA1 recruitment to DSB-associated chromatin sites at later stages following DNA damage, in addition to the first mode of recruitment via the BARD1 dual reader module (Kim, Chen and Yu, 2007; Wang *et al.*, 2007; Y. Hu *et al.*, 2011; Becker *et al.*, 2021). Furthermore, RAP80 was found to be involved in oestrogen receptor alpha binding which might indicate that the BRCA1-A dependent recruitment of BRCA1 might support its functions in oestrogen signalling (J. Yan, Kim, Yang, Albers, *et al.*, 2007). Nevertheless, BRCA1 recruitment by RAP80 is not required for RAD51 foci formation (Li *et al.*, 2024). Interestingly, while the BRCA1-A complex can recruit BRCA1 to DNA DSB sites to support BRCA1-BARD1 activity in cells harbouring mutations in the BARD1-chromatin interacting domains required for HR (Becker *et al.*, 2021), other reports have shown that the BRCA1-A complex limits the hyper-recombination activity stimulated by BRCA1 and the end resection machinery, as loss of RAP80 lead to increased RPA and RAD51 foci levels following IR treatment and increased BRCA1-CtIP interaction (Coleman and Greenberg, 2011; Y. Hu *et al.*, 2011) and a mutation in the BRCA1-BRCT protein interaction motif (K702M) resulted in hyper-recombination shown to rely on the BRCA1 RING ubiquitination activity (Dever *et al.*, 2011). This would suggest that the BRCA1-A dependent recruitment of BRCA1 could play a role in positioning it further away from DSB sites to limit the extent of end-resection. This could be important in G1 to prevent recombination and to restrict BIR and mitotic DNA synthesis which if unregulated leads to chromosomal instability (Y. Hu *et al.*, 2011; Minocherhomji *et al.*, 2015).

Notably, BRCA1-A dependent recruitment of BRCA1 is not required during spermatogenesis to localised BRCA1 on unsynapsed XY chromosomes as BRCA1 recruitment was still observed in *Rap80*$^{-/-}$ spermatocytes, contrarily to ABRAXAS which was ablated from the XY chromosomes (Lu *et al.*, 2013). Therefore, the biological context in which BRCA1 recruitment via the BRCA1-A complex is essential, for instance at stalled replication forks, and if the restriction of DNA end resection is specifically important in certain regions of the genome, such as common fragile sites, remains to be understood.

1.7 The biological and physiological functions of BRCA1 and BARD1

1.7.1 Tumour suppressor functions: control of HR

The previously described DNA repair functions of the tumour suppressor complex BRCA1-BARD1 are pivotal in maintaining genome stability (Tarsounas and Sung, 2020). Germline mutations in the *BRCA1* and *BARD1* genes account for hereditary breast, ovarian, prostate and pancreatic cancers (Weber-Lassalle *et al.*, 2019; Yamamoto and Hirasawa, 2021). Carriers of mutations in *BRCA1* have a lifetime risk of up to 90% of developing breast cancer and 40%-50% of developing ovarian cancer (Rahman and Stratton, 1998).

Brca1 heterozygous mice which are also heterozygous for *p53* (*Brca1*$^{+/-}$ *p53*$^{+/-}$) developed breast tumours when exposed to ionizing radiation indicating that the loss of p53 checkpoint control further drives tumorigenesis associated with BRCA1 loss (Cressman *et al.*, 1999). Furthermore, loss of the BRCA1 BRCT phosphoprotein binding function in mice via the serine-1598-phenylalanine mutation, which interrupts the interaction of a hydrogen bond with the phosphate group of the BRCA1-interacting phospho-ligands, led to tumour formation (Shakya

et al., 2011). Equally, cells derived from *Brca1* mutant mice harbouring an in-frame deletion spanning amino acids 1361-1363 in the coiled-coil domain had no RAD51 foci, while the mice displayed Fanconi Anaemia phenotypes and were predisposed to cancer (Nacson *et al.*, 2020). Mutations in *BARD1* for instance, which lack the RING domain due to the loss of exons 2 and 3 and lead to the expression of the BARD1 β-isoform were found to contribute to neuroblastoma tumorigenesis (Bosse *et al.*, 2012), likely because of the loss of the BRCA1 tumour suppressive functions resulting from the inability to heterodimerise with BARD1 and form a stable BRCA1-BARD1 complex. Mutations that cluster in the BRCA1 RING domain have been reported to be associated with breast and ovarian cancer (Castilla *et al.*, 1994; Friedman *et al.*, 1994). One of those mutations, the cysteine 61 to glycine (C61G) substitution in the BRCA1 RING domain, affects the heterodimerisation with the BARD1 RING domain (Hashizume *et al.*, 2001). The BRCA1-C61G mutation is reported to affect the tumour suppressive functions of BRCA1-BARD1 and cause cisplatin resistance in a *Brca1* mouse mammary tumour model carrying the C61G mutation (*K14cre;Brca1*$^{F/C61G}$*;p53*$^{F/F}$), suggesting that residual BRCA1 functions could be responsible for cisplatin resistance (Drost *et al.*, 2011). Furthermore, the two most common frameshift mutations in *BRCA1* (*BRCA1*^{185delAG} and *BRCA1*^{5832insC}) when expressed in the *K14cre;Brca1*$^{F/F}$*;p53*$^{F/F}$ mouse mammary tumour model led to tumour formation, and mice expressing *Brca1*^{185stop} where shown to have poorer olaparib responses than *Brca1*^{5832stop} mice and the BRCA1-deficient *KB1P* mice (Drost *et al.*, 2016). Additionally, loss of exon 2 in *Brca1* was shown to cause chromosomal aberrations upon olaparib and cisplatin treatment, despite normal RAD51 recruitment (Li *et al.*, 2016). Interestingly, in the absence of 53BP1, *Brca1*$^{\Delta 2/\Delta 2}$ mice lacking exon 2 did not have an increased susceptibility to tumour development, indicating that residual BRCA1-BARD1 functions mediate genome maintenance (Li *et al.*, 2016).

The HR deficiency of *BRCA1/BARD1*-mutated cancers can be therapeutically targeted with PARPi and platinum-based drugs such as cisplatin which generate replication stress, chromosomal instability and consequent cell death as they rely on mutagenic repair of NHEJ and MMEJ for survival (Bryant *et al.*, 2005; Farmer *et al.*, 2005; Ceccaldi *et al.*, 2015; Ashworth and Lord, 2018). The PARP1/2 catalytic inhibitor olaparib causes DNA DSBs by blocking PARP1/2-dependent single-strand break (SSB) repair and the catalysis-dependent PARP1/2 release from SSBs (often referred to as PARP trapping), leading to replication fork collapse or stalling following the encounter with unrepaired SSBs or trapped PARP1/2-SSB complexes (Rose *et al.*, 2020). BRCA1/BRCA2-deficient cells are hypersensitive to the PARPi olaparib as they are HR deficient and rely on the error-prone NHEJ pathway to repair DSBs (Bryant *et al.*, 2005; Farmer *et al.*, 2005). Loss of 53BP1 in BRCA1/2-deficient cells restores PARPi sensitivity (Bouwman *et al.*, 2010; Jaspers *et al.*, 2013). In addition to olaparib, BRCA1-deficient cells are also sensitive to platinum-based drug cisplatin and TOP1 inhibitor camptothecin (Bhattacharyya *et al.*, 2000; Fedier *et al.*, 2003; Farmer *et al.*, 2005; Bartz *et al.*, 2006; Bouwman *et al.*, 2010). Cisplatin introduces intrastrand crosslinks, which introduce transcription and replication fork conflicts due to DNA crosslinks that result in DNA DSBs upon replication fork collapse (Deans and West, 2011). Camptothecin is a DNA topoisomerase I (TOP1) inhibitor that by blocking the release of TOP1 cleavage complexes (TOP1ccs) on DNA, can lead to the persistence of TOP1-bound SSBs that can be later converted to DSBs during replication and/or transcription (Cleary *et al.*, 2020).

However, secondary mutations in *BRCA1* or *BARD1* which re-express these functional proteins, or mutations which cause the loss of 53BP1 function and consequent HR restoration pose challenges in cancer treatment, as they mediate drug resistance (Tarsounas and Sung, 2020). Furthermore, the efficacy of Polθ inhibitors in killing 53BP1-deficient *BRCA1/BRCA2*

mutant cells was shown to depend on RAD52 activity (Ronson *et al.*, 2023). Based on recent findings using mouse models it was also reported that the BRCA1-Polθ synthetic lethality depends on the end resection proficiency of *Brca1* mutant cells, as cells with active end resection relied more on Polθ for cell survival (Krais *et al.*, 2023). This highlights the importance of investigating how the BRCA1-BARD1 protein domains and their engagement with chromatin at DSB sites are required for their tumour-suppressive roles, and the mechanism by which HR restoration takes place in 53BP1-deficient and BRCA1/2-deficient cells. This is so that new cancer therapies can be developed which exploit the DNA repair mechanisms that *BRCA1/BARD1*-mutant cancers rely on for survival.

1.7.2 Additional functions for BRCA1

Beyond its well-characterised role in HR, BRCA1 is also involved in protecting stalled replication forks from nuclease-mediated degradation and promoting fork reversal and restart with a subset of other DNA repair factors (Schreuder *et al.*, 2024). BRCA1 works together with PALB2-BRCA2 to promote RAD51 stabilisation at ssDNA at stalled replication forks and protect these sequences from extensive MRE11-mediated end resection (Hashimoto *et al.*, 2010; Schlacher *et al.*, 2011; Lemaçon *et al.*, 2017; Whelan *et al.*, 2018). Furthermore, the MMS22L-TONSL complex and the Fanconi Anaemia protein FANCD2 were also reported to support RAD51 recruitment at stalled replication forks to promote fork reversal and restoration (Schlacher, Wu and Jasin, 2012; Piwko *et al.*, 2016). In addition to its RAD51 recruitment functions, BRCA1 was reported to be required for unloading of the CMG complex (CDC45-MCM-GINS) at the stalled replication forks (Long *et al.*, 2014), this function has since been dismissed in unpublished experiments published by the same group. Subsequently, RAD51

and MRE11 mediate reloading of a functional CMG replisome by loading Polε and GINS, and are therefore required for replication fork restart (Hashimoto, Puddu and Costanzo, 2012).

Fittingly with the requirement of BRCA1 at blocked replication forks, BRCA1 haploinsufficiency caused stalled replication fork repair defects which were instead repaired by the mutagenic microhomology-mediated break-induced replication (MMBIR) mechanism, mediated by MUS81-processing of replication forks (Pathania *et al.*, 2014; Deshpande *et al.*, 2022). Furthermore, stalled replication forks in BRCA1/BRCA2-deficient tumours were shown to also rely on Polθ-mediated alt-EJ repair which is promoted by FANCD2 (Ceccaldi *et al.*, 2015; Mateos-Gomez *et al.*, 2015; Kais *et al.*, 2016). Therefore, loss of FANCD2 in BRCA1/BRCA2-deficient cells was reported to result in loss of fork protection and restart, and consequently cell death (Kais *et al.*, 2016). Interestingly, other reports have also indicated that BRCA1 promotes its replication fork protection functions via its interaction with BARD1, which is driven by the phosphorylation-directed prolyl isomerase PIN1 to support RAD51 recruitment (Daza-Martin *et al.*, 2019). Additionally, loss of replication fork protection was observed in cells derived from *Brca1* mutant mice harbouring the S1598F mutation in the BRCT domain and relied on the PAR-dependent recruitment of BRCA1-BARD1 by the BARD1 BRCT domain (Billing *et al.*, 2018). Therefore, further investigation into the function of the BRCA1-BARD1 complex domains is required to understand how BRCA1 supports replication fork protection to promote genome stability.

1.7.3 Germline functions of BRCA1: meiosis and meiotic sex chromosome inactivation

Meiosis is the cell division process that results in the production of gametes for sexual reproduction. It requires a highly regulated system to faithfully segregate chromosomes and transmit the species' genetic information to the next generation. After DNA replication, before the first meiotic cell division, meiosis prophase I marks crucial events for meiotic progression such as synapsis and meiotic recombination of the parental chromosomes, and transcriptional silencing events (Grey and Massy, 2021). Meiosis prophase I has four cell progression stages: leptotene, zygotene, pachytene and diplotene (Figure 1.10). The onset of chromatin condensation begins in leptotene where also induction of DNA DSBs by the meiosis-specific endonuclease SPO11 occurs (Grey and Massy, 2021). In zygotene, the parental chromosomes start to synapse, forming the chromosome axes between them. The axial elements are formed by the synaptonemal protein complex comprised of synaptonemal complex proteins 1, 2 and 3 (SCP1, SCP2 and SCP3) and the HORMA-domain proteins HORMAD1 and HORMAD2 (Grey and Massy, 2021). In pachytene, autosomes have fully synapsed and chiasma have formed at recombination regions, however as the sex chromosomes are not homologous, these only synapse in a small region called the pseudoautosomal region (PAR). For normal meiotic progression, the sex chromosomes get transcriptionally silenced which is coupled with the formation of the sex body. This process is termed Meiotic Sex Chromosome Inactivation (MSCI) and it relies on the DNA damage signalling response (Figure 1.10) (Turner, 2015). In diplotene, the synaptonemal complex starts to dissolve and homologs remain linked to one another via the chiasmata and at centromeres, which is important for the subsequent chromosome segregation (Grey and Massy, 2021).

In addition to the tumour suppressor functions of BRCA1 and its role in DNA DSB repair in somatic cells, BRCA1 also has crucial roles during meiosis, specifically during MSCI which is a transcriptional silencing event of the X and Y chromosomes, required during spermatogenesis (Turner *et al.*, 2004, 2005; Royo *et al.*, 2010; Broering *et al.*, 2014). Accordingly, male *Brca1* mutant mice are infertile and undergo apoptosis in mid-pachynema (Xu *et al.*, 2003; Turner *et al.*, 2004; Broering *et al.*, 2014). However, it is not fully understood to which BRCA1-BARD1 protein domain functions these meiotic roles are attributed.

During leptotene, BRCA1 and Ataxia Telangiectasia and Rad3-related (ATR) serine-threonine kinase are recruited to the axial elements, indicating that their recruitment is DSB dependent (Turner *et al.*, 2004, 2005). Furthermore, ATR phosphorylates H2AX (γH2AX) at sites of DNA breaks and is required for the onset of meiotic silencing (Royo *et al.*, 2013). In pachytene, BRCA1, ATR and its binding partner ATR-interacting peptide (ATRIP) and DNA topoisomerase II binding protein 1 (TOPBP1) which plays a role in the activation of ATR, are localised to the sex chromosomes, where BRCA1 mediates the recruitment of ATR and the amplification of both ATR and TOPBP1 signal in the sex body (Scully *et al.*, 1997; Turner *et al.*, 2004, 2005; Refolio *et al.*, 2011; Royo *et al.*, 2013). *H2ax* or *Mdc1*-knockout male mice are infertile due to defects in the formation of the sex body and amplification of γH2AX signal on the asynapsed non-autosomal chromosomes for MSCI, respectively (Fernandez-Capetillo *et al.*, 2003; Baarends *et al.*, 2005; Ichijima *et al.*, 2011). Therefore, the MDC1-dependent amplification of the γH2AX signal in the sex body is crucial for MSCI. Mutations in *Brca1* mutant mice that disrupt the exon 11 fail to amplify the ATR-TOPBP1 signal on sex chromosomes and have aberrant γH2AX signalling on the sex body and autosomes, resulting in failed MSCI (Turner *et al.*, 2004). Interestingly, the BRCA1 BRCT domain was reported to be required for BRCA1 localisation to the sex chromosomes, indicating that the BRCA1 BRCT-

phosphobinding protein interactions might have important functions in mediating meiotic BRCA1 roles (Lu *et al.*, 2013). Accordingly, male *Brca1* mice harbouring a mutation in the BRCT domain were infertile (Shakya *et al.*, 2011). Furthermore, mice with a *Palb2* mutation that disrupts the BRCA1-PALB2 interaction had reduced fertility due to DSB break repair-dependent synapsis defects (Simhadri *et al.*, 2014). As DSBs remain unrepaired on the sex chromosomes due to the lack of a homolog and large asynapsis, it is plausible that BRCA1's recruitment to these regions and the downstream DDR signalling events are required to initiate transcriptional silencing of unrepaired DSBs, which involve a set of DNA damage response-dependent histone PTMs (Burgoyne, Mahadevaiah and Turner, 2009; Abe *et al.*, 2020, 2022).

Consequently, the purpose of MSCI might be to target unsynapsed chromatin with unrepaired DSBs to prevent toxic repair outcomes of X and Y chromosome-associated DSBs with non-homologous chromosomes which would lead to aberrant chiasma-like structures and incorrect chromosome separation, or for the silencing of the expression of lethal genes on chromosome Y (Turner, 2007; Alavattam *et al.*, 2022).

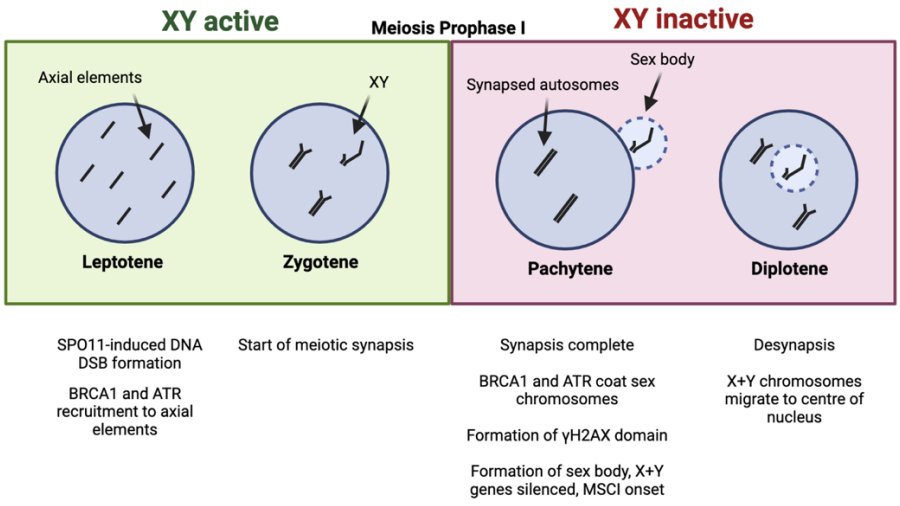


Figure 1.10. Overview of the process of meiotic sex chromosome inactivation during meiosis prophase I. Adapted from Turner, 2007**.**

1.8 Aims

In this thesis, I outlined approaching four years of research that aimed to disentangle, investigate and better understand the various functions of the BRCA1-BARD1 complex in DNA repair and genome maintenance. As described above, BRCA1 operates in many different contexts, and interacts within a variety of distinct sub-complexes, the function of which are mostly poorly understood. In recent work, by investigating the function of BRCA1's obligate binding partner BARD1, my host laboratory discovered a dual-reader domain comprising its C-terminal ARD and BRCT repeat domain, that through binding the H4K20me0/H2AK15ub, DSB-associated, histone PTM states in post-replicative chromatin engages with the nucleosome to evict 53BP1 and enable DSB repair by HR (Chapman *et al.*, 2012; Nakamura *et al.*, 2019; Becker *et al.*, 2021). Interestingly, however, the BARD1 dual reader architecture represents only one of the BRCA1-BARD1 complex's domain features that confer chromatin reader function: The BRCA1-BARD1 RING heterodimer has been noted to closely resemble an analogous RING heterodimer in the RING1B-BMI1 polycomb repressor complex 1 (PRC1), which engages the nucleosome face through direct contacts with the acidic patch on H2A-type histones (McGinty, Henrici and Tan, 2014; Hu *et al.*, 2021; Witus *et al.*, 2021). This function enables PRC1-dependent mono-ubiquitination of H2A on lysine 119, a PTM state associated with transcriptionally silent chromatin (Cao, Tsukada and Zhang, 2005). Indeed, analogous contacts between the BRCA1-BARD1 RING heterodimer and the nucleosome have been reported and reconstituted *in vitro*, where they have been shown to mediate H2A ubiquitination on lysines 127/129 (Kalb *et al.*, 2014; Hu *et al.*, 2021; Witus *et al.*, 2021). Recent follow-up data also implicate additional DNA-chromatin functions to the Intrinsically Disordered Region (IDR) in BARD1 that link its structured N-terminal RING and C-terminal dual

reader ARD-BRCT repeat domain (Witus *et al.*, 2023). Thus, akin to the case for the BRCA1 E3 ligase activity, the function of BRCA1-BARD1's associated RING-mediated nucleosome binding remains ill-defined.

Similarly, as discussed above (sections 1.6.1 and 1.6.2), BRCA1's interaction with the BRCA1-A complex constitutes a third chromatin reader function of the BRCA1-BARD1 complex, in which RAP80-binding to K63 polyubiquitin chains promotes BRCA1 recruitment to DSB sites, in a mechanism that is mechanistically separable from the BARD1 dual-reader domain (Becker *et al.*, 2021). The function of this domain, and its importance for DNA repair and genome stability remains to be fully understood.

Whether each of the nucleosome binding functions of the BRCA1-BARD1 complexes allow for DNA damage recognition, in isolation, or in cooperation had not yet been functionally dissected. The overarching aim of this thesis was to tackle this question, and define the functions, and specific cellular contexts, in which each of these modes of chromatin interaction are most important. In pursuit of this, the following results chapters describe experiments in which a suite of mutational complementation approaches was used both in cells and in the mouse, to uncouple and study each of these three chromatin binding modes in cells for the first time. The ultimate aim was to advance the field's understanding of BRCA1's various contributions to genome maintenance in somatic cells, and its importance for programmed diversification of the germline.

Chapter 2

Materials and Methods

2.1 Cell culture

2.1.1 Cell lines

HCT116 human colorectal carcinoma and human embryonic kidney (HEK) cells were cultured in high-glucose Dulbecco's modified Eagle's Medium (DMEM) (Sigma-Aldrich or Life Technologies) supplemented with 10% (v/v) foetal bovine serum (Sigma-Aldrich), 50 units/ml Penicillin (Merck Life Science), 50 µg/ml Streptomycin (Sigma-Aldrich) and 2 mM L-glutamine (Merck Life Sciences), in a humidified atmosphere at 37 ˚C with 5% CO_2 supply.

2.2 Mice

2.2.1 Mouse strains

The mouse strains used throughout this thesis were generated on a C57BL/6 background. All experiments, where otherwise indicated, involved 8-12 week old mice and sex-matched littermate control animals. The *53bp1*$^{-/-}$ mice (MGI: 2654201; on C57BL/6 background) and the *Brca1*$^{-/-}$ mice (MGI: 104537) were generated as described elsewhere (Ward *et al.*, 2003; Liu *et al.*, 2007; Chen *et al.*, 2020). The *53bp1*$^{L1616A/L1616A}$ and *Bard1*$^{+/D700A}$ mice were commissioned by the Ben Davies group and generated using the CRISPR/Cas9 technology. In brief, point mutations were introduced by homology-directed repair by microinjection of Cas9 ribonucleoprotein complexes, to introduce the leucine 1616 to alanine substitution in *53bp1* and the aspartic acid 500 to alanine substitution in *Bard1* using the single-stranded oligodeoxynucleotide (ssODN) sequences, and the corresponding guide RNA (gRNA)

sequences which target the exons containing the corresponding residues of choice, shown in Table 2.1.

All experiments were approved by the University of Oxford Ethical Review Committee and performed under a UK Home Office Licence, complying with animal use guidelines and ethical regulations.

gRNA sequences	
Target exon (mutation)	**Sequence (5'-3')**
53bp1 exon 22 (L1616A)	AAGGCAGCAGATATCAGCTT
Bard1 exon 13 (D700A)	GTCTGAGTCACATCACTGTC
ssODN sequences	
Target exon (mutation)	**Sequence (5'-3')**
53bp1 exon 22 (L1616A)	AGAGAGCAATATGGGCTTGGCCCATATGAAGC TGTCACACCGCTCACGAAGGCAGCAGATATCT CTGCAGGTAAGACTTTCCTGAACAACTGCCTG TGGATCCAGGCTTCGCTTAAAGGGAGGAATG GTTCCCAGGATA
Bard1 exon 13 (D700A)	GGGGGGAAACTTCAAGCATCATCCAAGGGAT GACCTCCTTAAGCTCATTGCTGCAGCAGGAGG CAAAGTCCTGAGTCGCAAGCCCAAGCCAGATA GCGCTGTGACTCAGACCATCAACACGGTTGCA TACCATGCCAAGCCTGAGTCGGATCAGCGCTT CTGTACGCAGTACATCGTCTACGAAGACCTGTT TAACTGTC

Table 2.1. gRNA and ssODN sequences used for knock-in genome editing of *53bp1* and *Bard1*, and for insertion of the desired point mutations by homology-directed repair, respectively.

2.2.2 Mouse genotyping methods

The mice used in this project were genotyped by polymerase chain reaction (PCR) amplification of the target genomic region. DNA extraction was performed on mouse ear clips, using the hotshot protocol. In brief, ear clips were incubated in 75 µl of alkaline lysis reagent (pH 12) composed of 25 mM NaOH and 0.2 mM disodium EDTA, at 95 ℃ for 30 minutes. Then, DNA samples were cooled to 4 ℃ and neutralised with 75 µl of 40 mM Tris-HCl (pH 5) solution. PCR amplification was carried out in 20 µl reactions using the OneTaq® Quick-Load® 2x Master

Mix (New England Biolabs) following the manufacturer's instructions, using the primer pairs detailed in Table 2.2. PCR products were run on a 2% (w/v) agarose gel at 120 V for 35 minutes (Figure 2.1). To detect the *Bard1*^{D700A} mutation, specific primers were designed over the mutated site, to use in a two-step PCR procedure. Mouse genotyping was performed by Dr Jean Metson.

Genotype	Primer sequence		Nomenclature	Notes
53bp1 L1616A	Fwd	agggacagccaagttcagccca	-	-
	Rev	ccgataggaggagaaaggccag		
Bard1 D700A	Fwd	gcccaagccagacagtga	WT_F1	To detect wild-type *Bard1*
	Rev	ccagaaatatcacaatggccgt	R1	
	Fwd	aattggctctttctgacacgtg	F1	
	Rev	ggtctgagtcacatcactg	WT_R1	
	Fwd	gcccaagccagatagcgc	MUT_F1	To detect *Bard1* with D700A mutation
	Rev	ccagaaatatcacaatggccgt	R1	
	Fwd	aattggctctttctgacacgtg	F1	
	Rev	tggtctgagtcacagcgcta	MUT_R1	
	Fwd	ctttcttgttatttcagttgcc	F2	See note in table legend
	Rev	ggtctgagtcacatcactg	WT_R1	
	Fwd	ctttcttgttatttcagttgcc	F2	
	Rev	tggtctgagtcacagcgcta	MUT_R1	

Table 2.2. Genotyping strategy for 53bp1 L1616A and Bard1 D700A mice, using indicated primer pairs.
Primer F2 was never used for genotyping purposes as it gave a weak signal.

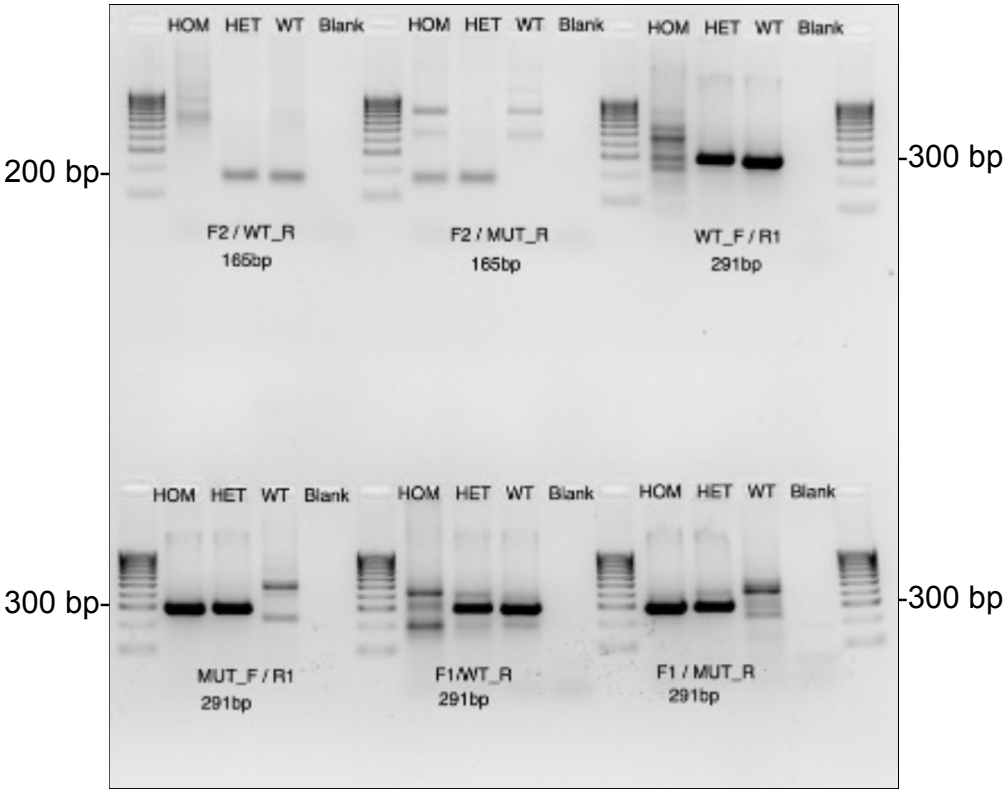


Figure 2.1. Representative image of an agarose gel for genotyping *Bard1 D700A* mice. PCR reactions were performed using the primer combinations detailed in Table 2.2.

2.3 Lentiviral transgene complementation

2.3.1 Generation of lentiviral constructs

All constructs generated in this project were made using the recombination-based Gateway cloning technology.

To generate the BARD1 separation-of-function mutants used in this project, the donor vector pDONR221 with cloned full-length BARD1 (host laboratory) was used for site-directed mutagenesis reactions using primer pairs and template plasmids detailed in Table 2.3. Site-directed mutagenesis was performed using the Q5® Site-Directed Mutagenesis Kit (New England Biolabs) according to manufacturer's instructions, and NEBaseChanger™ was used to generate specific primer pairs. PCR product size was verified by agarose gel electrophoresis

before being transformed into chemically competent DH5α *E. coli* cells. Following transformation, bacteria were plated on corresponding antibiotic-containing LB-agar plates and incubated at 37 ˚C overnight. Single colonies were grown in LB medium containing the corresponding antibiotic and incubated at 37 ˚C overnight in a shaking incubator. The plasmid DNA was purified using the NucleoSpin Plasmid Kit (Macherey-Nagel), following manufacturer's instructions and the final pDONR221 vectors were verified by restriction digestion and Sanger sequencing, and stored at -20 ˚C. Then, pDONR221 inserts were cloned into lentiviral destination vectors, either pLenti-PGK-puro (Addgene 19068) or pLenti-PGK-puro FLAG-HA, using the Gateway® LR Clonase® II Enzyme Mix (Invitrogen) and transformed into chemically competent Stbl3 *E. coli* cells, according to manufacturer's instructions. The final products were obtained as described before and were verified by restriction digestion and stored at -20 ˚C.

The BARD1^{RING} and BARD1$^{RING\ R99E}$ constructs were generated by synthesizing a GeneString, that includes the attB recombination sites, a FLAG-HA tag and the open reading frame of the BARD1 RING domain, the sequence of which is detailed in Table 2.4. These were cloned into pDONR221 using the Gateway® BP Clonase® Enzyme Mix (Invitrogen), according to the manufacturer's instructions. The final pDONR221 products were amplified and further processed as described above.

The pDONR221 BARD1$^{W91A\ ARD3A}$ and pDONR221$^{W91A\ ARD3A\ D712A}$ constructs were made using the T4 DNA ligase (New England Biolabs) following manufacturer's instructions, at a 3:1 insert to vector ratio. Previous to the T4 DNA ligation, 2 µg of pDONR221 BARD1^{ARD3A} (Nakamura *et al.*, 2019) and pDONR221 BARD1$^{ARD3A\ D712A}$ (Becker *et al.*, 2021) were digested using BamHI and NdeI restriction enzymes (New England Biolabs) in a 40 µl reaction, following manufacturer's instructions. The resulting 4.3 kb band was purified from 2% (w/v) agarose gel

using the NucleoSpin Gel extraction and PCR clean up kit (Macherey-Nagel). Simultaneously, 20 ng of pDONR221 BARD1^{W91A} were amplified by PCR using following primer pairs (Fwd - TGTAAAACGACGGCCAGT; Rev - gatccCTCTAAATTCCATTTTTGGTTGATTTCAG) using Q5 polymerase (New England Biolabs), following manufacturer's instructions, and the resulting product was purified as before. Then 1 µg of resulting PCR product was digested with BamHI and NdeI restriction enzymes (New England Biolabs), and the 500 bp band was purified as previously described.

BARD1 construct	**Template DNA**	**Primer sequences 5' to 3'**	
W91A	pDONR221 BARD1 (Becker *et al.*, 2021)	Fwd	CACCCCGGCCgccATACAAGACTTG
		Rev	TAACACACTGGACATCCAG
RING^{W91A}	pDONR221 FLAG-HA BARD1 RING	Fwd	CACCCCGGCCgccATACAAGACTTG
		Rev	TAACACACTGGACATCCAG
W91A D712A	pDONR221 BARD1 D712A (Becker *et al.*, 2021)	Fwd	CACCCCGGCCgccATACAAGACTTG
		Rev	TAACACACTGGACATCCAG
Spot-tag BARD1	pDONR221 BARD1 (Becker *et al.*, 2021)	Fwd (1)	ATGCCAGACCGCGTGCGCGCC GTGAGCCATTGGAGCAGCGGC AGCcctagatctATGccggataatcggcag
		Rev (1)	GGGGACCACTTTGTACAAGAAAG CTGGGTtcagctgtcaagaggaag
		Fwd (2)	GGGGACAAGTTTGTACAAAAA AGCAGGCTTCACCATGCCAGACCGCGTGCGC
		Rev (2)	GGGGACCACTTTGTACAAGAAAGCTG GGTtcagctgtcaagaggaag
D712A	pDONR221 spot-tag BARD1	Fwd	GCCAGACAGTgccGTGACTCAGA
		Rev	TTGGGCTTTCTACTGAGGATC
ΔN	pDONR221 spot-tag BARD1	Fwd	cggtATGGAACCGGATGGTCGC
		Rev	gatccAGATCTAGGGCTGCCGCT
ΔIDR1	pDONR221 spot-tag BARD1	Fwd	cggtGCTTCAGTGCAAACCCAG
		Rev	gatccATTAAACAAACTTTTCCTAGGTTTATC
ΔIDR2		Fwd	cggtGAGGCAGAAAAAGAAGATG

	pDONR221 spot-tag BARD1	Rev	gatccACTTGCATCTTTTTTTATTGC
ΔIDR3	pDONR221 spot-tag BARD1	Fwd	cggtTCACCAGGTACACCACCT
		Rev	gatccCTCTAAATTCCATTTTTGGTTGATTTCAG
Δ133-140	pDONR221 spot-tag BARD1	Fwd	cggtAATTCAATTAAAATGTGGTTTAG
		Rev	gatccCAAACTTTTCCTAGGTTTATC
ΔRING	pDONR221 spot-tag BARD1	Fwd	TccaaaaaagaagagaaaggtaggatccggtAAT GATGCAGGAAACAAGAAGAATTCAATT AAAATGTGGTTTAGCCCTC
		Rev	tctaccttcctcttttttcttaggaccggatccGG CGGGCGCGGAACGAGG
ΔRING SLIM1	pDONR221 spot-tag BARD1 ΔRING	Fwd	TGCCGCTCGAAGTAAGAAAGTCAGATATGTTG
		Rev	GCCCACGCTTTAATTGAATTCTTCTTGTTTCC
ΔRING SLIM2	pDONR221 spot-tag BARD1 ΔRING	Fwd	TCATATGCGTCTTGCTGAGCACTTGC
		Rev	AGCTGTTGCCCCAAGTCCTCCTGCAG
ΔRING SLIM3	pDONR221 spot-tag BARD1 ΔRING	Fwd	tatgttgtgAGTAAAGCTTCAGTGCAAAC
		Rev	tgcggctttCTTACTTCGAGGGCTAAAC
ΔRING SLIM4	pDONR221 spot-tag BARD1 ΔRING	Fwd	atcgcccaaAAATGGAATTTAGAGGCAG
		Rev	ttcagctgcAGTTTTCTTTTTTTGCTTTTTTC
ΔRING SLIM5	pDONR221 spot-tag BARD1 ΔRING	Fwd	tgtagccaaCCATCTGTTATCTCCAGTC
		Rev	ggcggatgcCAGCTTTTGCTTAGATTC
ΔRING ARD3A	pDONR221 BARD1 ARD3A (Becker *et al.*, 2021)	Fwd	TccaaaaaagaagagaaaggtaggatccggtAAT GATGCAGGAAACAAGAAGAATTCAATT AAAATGTGGTTTAGCCCTC
		Rev	tctaccttcctcttttttcttaggaccggatccGG CGGGCGCGGAACGAGG
ΔRING D712A	pDONR221 spot-tag BARD1 D712A	Fwd	TccaaaaaagaagagaaaggtaggatccggtAAT GATGCAGGAAACAAGAAGAATTCAATT AAAATGTGGTTTAGCCCTC
		Rev	tctaccttcctcttttttcttaggaccggatccGG CGGGCGCGGAACGAGG
ΔRING K619A	pDONR221 BARD1 K619A (Nakamura *et al.*, 2019)	Fwd	TccaaaaaagaagagaaaggtaggatccggtAAT GATGCAGGAAACAAGAAGAATTCAATT AAAATGTGGTTTAGCCCTC
		Rev	tctaccttcctcttttttcttaggaccggatccGG CGGGCGCGGAACGAGG

Table 2.3. Primer sequences used for site-directed mutagenesis. Enclosed is also the plasmid that was used as the template DNA to generate the indicated BARD1 constructs. pDONR221 spot-tagged BARD1 plasmids were

generated using a two-step PCR protocol, in which primer pairs from (1) add the spot-tag sequence to the N-terminal end of BARD1, and the primer pairs from (2) add the attB1 recombination sequence to the N-terminal end of the spot-tag BARD1 sequence to make it suitable for Gateway® BP cloning.

Construct	Template DNA	GeneString sequence 5'-3'
$BARD1^{RING}$	pDONR221	GGGGACAAGTTTGTACAAAAAAGCAGGCTTCA CCatgGACTACAAGGATGACGATGACAAGCTCG ATGGAGGATACCCATACGATGTTCCAGATTAC GCTGCTCGAGGTTATCAAcctaagaaaaagaggaag gtagatccaaaaaagaagagaaaggtaTCCGGAAGCG GTATGGAACCGGATGGTCGCGGTGCCTGGGCC CACAGTCGCGCCGCGCTCGACCGCCTGGAGAA GCTGCTGCGCTGCTCGCGTTGTACTAACATTCT GAGAGAGCCTGTGTGTTTAGGAGGATGTGAG CACATCTTCTGTAGTAATTGTGTAAGTGACTGC ATTGGAACTGGATGTCCAGTGTGTTACACCCC GGCCTGGATACAAGACTTGAAGATAAATAGAC AACTGGACAGCATGATTCAACTTTGTAGTAAGC TTCGAAATTTGCTACATGACAATGAGCTGTCAG ATTTGAAAGAAGATAAACCTAGGAAAAGTTTG TGAACCCAGCTTTCTTGTACAAAGTGGTCCCC
$BARD1^{RING\ R99E}$	pDONR221	GGGGACAAGTTTGTACAAAAAAGCAGGCTTCA CCatgGACTACAAGGATGACGATGACAAGCTCG ATGGAGGATACCCATACGATGTTCCAGATTAC GCTGCTCGAGGTTATCAAcctaagaaaaagaggaag gtagatccaaaaaagaagagaaaggtaTCCGGAAGCG GTATGGAACCGGATGGTCGCGGTGCCTGGGCC CACAGTCGCGCCGCGCTCGACCGCCTGGAGAA GCTGCTGCGCTGCTCGCGTTGTACTAACATTCT GAGAGAGCCTGTGTGTTTAGGAGGATGTGAG CACATCTTCTGTAGTAATTGTGTAAGTGACTGC ATTGGAACTGGATGTCCAGTGTGTTACACCCC GGCCTGGATACAAGACTTGAAGATAAATGAAC AACTGGACAGCATGATTCAACTTTGTAGTAAGC TTCGAAATTTGCTACATGACAATGAGCTGTCAG ATTTGAAAGAAGATAAACCTAGGAAAAGTTTG TGAACCCAGCTTTCTTGTACAAAGTGGTCCCC

Table 2.4. Sequences of the GeneString fragment generated of BARD1 RING constructs.

2.3.2 Lentivirus generation and cell infection

To generate lentivirus for stable HCT116 *BARD1*$^{AID/AID}$ transgene complementation, HEK293T (human embryonic kidney cells) were co-transfected with 3.2 µg of the lentiviral expression construct of interest and the lentiviral packaging components comprised of 0.16 µg pHDM-tat1b, 0.32 µg pHDM-G, 0.16 µg pRC/CMV-rev1b and 0.16 µg pHDM-Hgpm2. Briefly, 2x10^6 HEK293T cells were plated in a 6 cm dish the day before transfection in antibiotic-free DMEM with 10% FBS. The next day, cells were transfected with the transfection master mix prepared with 1.29 µg polyethyleneimine (PEI) per µg of DNA in Opti-MEM (Thermo Fisher). The morning after, media was replaced for fresh media containing antibiotics. 5x10^5 HCT116 *BARD1*$^{AID/AID}$ cells were transduced 48 hours and 72 hours after transfection, with syringe-filtered (0.45 µm) viral supernatant collected from HEK293T cells, containing 4 µg/ml polybrene. 24 hours after the last round of transduction, cells were selected with antibiotics (700 µg/ml neomycin or 1 µg/ml puromycin) until a non-transduced control population was completely dead. Stably transduced cell lines were cultured in the presence of selective antibiotic.

2.4 SDS-PAGE-Western blot

Whole-cell protein extracts were isolated using Benzonase buffer [25 mM Tris (pH 8.0), 40 mM NaCl, 0.05% SDS, 2 mM $MgCl_2$, 10 U/ml Benzonase (Sigma-Aldrich) and Complete™ EDTA-free protease inhibitor (Roche)], then incubated on ice for 10 minutes to allow for DNA digestion. Protein concentration quantification was determined using the Bio-Rad Protein Assay Dye Reagent Concentrate (Biorad) and a bovine serum albumin (BSA) standard curve as a reference. For protein denaturation, whole-cell lysate protein samples were diluted in 3x Laemmli buffer and boiled for 5 minutes at 95 ˚C. To perform Sodium dodecyl sulfate-

polyacrylamide gel electrophoresis (SDS-PAGE), NuPAGE® Novex® 4-12% gradient acrylamide gels were used (Life Technologies), ran at 80V for 10 minutes, then at 110V for approximately 80 minutes. The wet-transfer method was performed using 0.45 µM nitrocellulose membrane (Life Technologies) using the Biorad wet-transfer system for 60 minutes at 100 V or for 16 hours at 0.05 mA. Membranes were blocked for 30 minutes in 5% (w/v) milk in 0.01% (v/v) Tween20/PBS prior to incubation with primary antibodies, diluted in 3% BSA in 0.05% (v/v) Tween20/PBS, overnight at 4 ˚C or at RT for 3-4 hours on a tube roller. The membranes were washed 3x in 0.01% (v/v) Tween20/PBS for 5 minutes at RT and incubated with HRP-conjugated secondary antibodies diluted in blocking buffer, for 1 hour at RT. Following 3 washes as before, the membrane was incubated with enhanced chemiluminescence (ECL) reagent (Biorad) and signals were acquired digitally with the Biorad Gel Doc™ XR system (Biorad). The following antibodies were used: rabbit anti-53BP1 (Novus Biologicals NB100-304, 1:2500), mouse anti-BRCA1 D-9 (Santa Cruz sc-6954, 1:400), rabbit anti-histone H3 (abcam ab1791, 1:5000), mouse anti-RPA32 (abcam ab16855, 1:500), mouse anti-Tat-1 (tubulin) (Sigma 00020911, 1:10000), rabbit anti-BARD1 (abcam ab64164, 1:500), rabbit anti-BARD1 (Bethyl A300-263A, 1:4000), rabbit anti-HA-tag (Cell Signalling 3724, 1:1000), mouse anti-HA.11 (BioLegend 901501, 1:2000), mouse anti-HRP (Thermo Fisher 31432, 1:50000) and rabbit anti-HRP (Thermo Fisher 31462, 1:50000).

2.5 Cytogenetic methods

2.5.1 Sister-chromatid exchange assay

Cells were seeded on a 6 cm dish at densities of $3x10^5$ cells/dish. At the time of seeding, cells were treated with 1 µg/ml doxycycline (MP Biomedicals) and 1 µg/ml puromycin (InvivoGen). The following day, cells were treated with 1 mM IAA, and with 10 µM BrdU 1 h

later for the duration of two cell doublings. Cells were treated with 50 mg/ml KaryoMAX™ Colcemid™ (Life Technologies) for 3 hours before harvesting cells for metaphase spreads. For the olaparib sister-chromatid exchange assay, cells were treated with 50 nM olaparib (AZD2281) (Stratech Scientific Ltd) following 1 mM Indole-3-acetic-acid (IAA) treatment. 24 hours following olaparib treatment, cells were treated with 10 µM BrdU for the duration of two cell doublings. Cells were treated with 50 mg/ml KaryoMAX™ Colcemid™ (Life Technologies) for 3 hours before harvesting cells for metaphase spreads. Metaphase spreads were prepared by collecting the medium in a corning tube. The cells were washed with 1x PBS and PBS was collected into the same corning tube. The cells were then detached with 1x TrypLE™ Express Enzyme (Gibco) for 3 minutes at room temperature (RT) and collected into the same tube. Cells were centrifuged at 309 x g for 10 minutes, and supernatant was removed as gently as possible. The pellet was resuspended by gently flicking the tube. Cells were then incubated for 15 minutes at 37 ˚C following the addition of 10 ml of hypotonic solution pre-heated to 37 ˚C (75 mM KCl). Cells were centrifuged at 309 x g for 10 minutes and the supernatant was removed as gently as possible. The pellet was again resuspended by gently flicking the tube. A few drops of ice-cold fixative (Carnoy's fixative solution, 3:1 methanol : glacial acetic acid) were then added to the suspension before fixative was topped up to 10 ml. Cells were then incubated for 30 minutes at RT and centrifuged at 309 x g for 10 minutes. The supernatant was removed, and the pellet was resuspended in 10 ml of ice-cold fixative, followed by RT incubation for 10 minutes. The cells were then centrifuged at 309 x g for 10 minutes and the supernatant removed. The cell pellet was finally resuspended in 0.25 to 0.5 ml of cold fixative and 20 µl of cell preparation was dropped onto a clean slide, and dried on a hot plate (37 ˚C). The metaphase cell suspension was stored at -20 ˚C with 3 ml of cold fixative for long-term storage. Slides were subsequently aged at RT for 2-4 days. For

sister-chromatid exchange staining, metaphase slides were stained with 0.5 ml of 10 µg/ml Hoechst 33258 (BioTechne) in PBS for 30 minutes at RT, followed by a rinsing step in freshly prepared Sorenson buffer (1:1 0.1M Na_2HPO_4: 0.1M NaH_2PO_4). Slides were mounted with 350 µl of Sorenson buffer under 24 x 50 coverslips, placed on a hot plate (55 ˚C) and exposed to longwave UV light (354 nm) at a distance of approximately 5 cm for 10 minutes. Then, slides were incubated at 50 ˚C between 30 minutes-1 hour in 1x SSC buffer preheated to 50 ˚C. Slides were stained using 10% KaryoMAX™ Giemsa stain solution (Gibco) diluted in Sorenson buffer, for 30 minutes at RT. This was followed by sequential washes in double-distilled H_2O (2x-3x). Slides were dried overnight, protected from light, before mounting with 20 µl of Mowiol mounting media (composed of 10% Mowiol 4-88 (Merck), 25% glycerol, 100 mM Tris-HCl, pH 8.5). At least 50 images per sample were acquired using the Olympus BX60 microscope and the 100x immersion oil objective. Number of exchanges per chromosome was counted for each image and the mean exchanges per chromosome was calculated. Data points were plotted as a superplot on Graphpad Prism, with data points from each of the three biological repeats displayed in a different colour.

2.5.2 Meiotic metaphase spread preparation

Following the mouse culling, testes were dissected and placed into a Petri dish with MEM (non-essential amino acids solution; Life technologies). The tunica albuginea from the testes was removed and seminiferous tubules were chopped with a flat razor blade in a 5 cm Petri dish. 0.5 ml of 1x PBS with cOmplete™ EDTA-free protease inhibitor (Roche) was added and pipetted up and down to resuspend, before transferring to a corning tube. Spermatocyte suspension was left on ice for 10 minutes until large pieces had settled at the bottom. Then, 1 ml of spermatocyte suspension was pipetted into 1.5 ml Eppendorf tubes and centrifuged

for 5 minutes at 5800 x g. During centrifugation, SuperFrost slides were placed in a humid chamber, each with 65 µl of 1% PFA (paraformaldehyde). The supernatant was removed and 40 µl of 0.1 M sucrose was added to resuspend the cell pellet. Then 20 µl of spermatocyte/sucrose suspension was distributed onto the slide. The slides with the spermatocyte suspension were incubated in the humid chamber for 3 hours, then rinsed with 0.4% Photo-Flo 200 (Kodak). For long-term storage, slides were stored at -80 ˚C, ready for immunofluorescence staining.

2.6 Immunofluorescence analysis

For meiotic immunofluorescence staining, slides with meiotic metaphase spreads stored at -80 ˚C were placed in 50 ml of RT blocking/antibody dilution (B/ABD) buffer in a Coplin jar. The B/ABD buffer is composed of 0.2% BSA (Sigma), 0.2% gelatin from cold water fish skin (Sigma) and 0.05% Tween20 in 1x PBS. Slides were blocked for 1 hour at RT on a shaker platform. Then, slides were incubated with primary antibodies diluted in 100 µl of B/ABD buffer, placed in a humid chamber with parafilm on top of slides, and incubated at 4 ˚C overnight. The following primary antibodies were used in meiotic immunofluorescence staining: mouse anti-BRCA1 (gift from Andre Nussenzweig, 1:100), rabbit anti-phospho-H2AX (Cell Signalling 9718, 1:400), mouse anti-SCP3 (Santa Cruz sc-74569, 1:100), rabbit anti-SCP3 (BioTechne NB300-231, 1:500) and rabbit anti-HORMAD2 (Santa Cruz sc-82192, 1:100). The next morning, slides were washed 4x for 5 minutes at RT with B/ABD in Coplin jars on a shaker platform for gentle agitation. The secondary antibodies were diluted in 100 µl of B/ABD per slide, and slides were incubated with secondary antibodies for 30 minutes at 37 ˚C in a humid chamber. From now on, all steps were carried out with samples protected from light. The following secondary antibodies were used: AlexaFluor™ 568 Goat anti-rabbit (Life

Technologies A11036, 1:250) and AlexaFluor™ 488 Goat anti-mouse (Life Technologies A11029, 1:250). Following secondary antibody incubation, slides were washed 3x for 5 minutes at RT in B/ABD buffer with gentle agitation and washed once in double-distilled H_2O for 2-3 minutes. Then, slides were air-dried for 3 minutes and mounted with 15-20 µl of Prolong GOLD antifade mounting reagent with DAPI (Life Technologies) and a 24 x 50 coverslip. Slides were dried overnight, protected from light before proceeding with microscope acquisition.

For immunofluorescence staining performed on interphase nuclei, 13 mm glass coverslips were placed in a tissue-culture treated 6-well plate, and coated with 4 µg/ml Fibronectin (Sigma F47459) diluted in 1x PBS for 45 minutes at RT. 4.5-5x10^5 cells/well, previously strained through a 70 µm cell strainer and treated with 1 µg/ml doxycycline for up to 24 hours, were then seeded in the presence of 1 µg/ml doxycycline and 1 µg/ml puromycin, and returned to the incubator for 1 hour. Cells were subsequently treated with 1 mM IAA for between 20 and 24 hours. The next day, cells were treated with 40 µM EdU (Abcam ab146186) for 10 minutes before EdU was washed out with fresh medium, replaced with complete medium and cells irradiated (5Gy) using a calibrated Faxitron X-ray generator. Cells were then fixed in 2% PFA following a predetermined irradiation recovery period. For pre-extraction fixation, the medium was removed and cells were washed with RT 1x PBS. Following gentle aspiration of the media, cells were fixed with pre-chilled cytoskeletal buffer (CSK) composed of 10 mM PIPES pH 6.8, 300 mM sucrose, 50 mM NaCl, 3 mM EDTA, 0.5% Triton X-100 and cOmplete™ EDTA-free protease inhibitor (Roche), enough to cover coverslips. Following a 5 minutes incubation on ice, CSK was gently removed by aspiration and cells were washed once in RT 1x PBS before adding 2% PFA (diluted in PBS pH 7.4) and fixing cells for 15 minutes at RT. Then, 2 washes were performed in PBS and coverslips were stored at 4 ˚C for short-term storage, in

4 ml PBS. For immunofluorescence staining, cells were blocked with 3% BSA, 0.1% Triton X-100 in 1x PBS, for 15 minutes at RT. Then, cells were washed 3x for 5 min at RT with 0.1% Triton X-100/PBS (washing buffer). For EdU-positive cell labelling, the Click-iT EdU Cell Proliferation Kit, Alexa Fluor 647 (Thermo Fisher, C10340) was used according to the manufacturer's protocol. Following the EdU-labelling step, cells were washed 3x for 5 minutes at RT with washing buffer before being incubated with 35 µl of primary antibody diluted in blocking buffer, for 1 hour at RT in a humid chamber and protected from light (overnight at 4 ˚C for the RAP80 staining). The following primary antibodies were used: rabbit anti-HA tag (Cell Signalling 3724, 1:500), rabbit anti-phospho-H2AX (Cell Signalling 9718, 1:400), mouse anti-phospho-H2AX (Millipore 05-636, 1:1000), mouse anti-BRCA1 D-9 (Santa Cruz sc-6954, 1:40), rabbit anti-RAP80 (Bethyl A300-763A, 1:600) and rabbit anti-RAD51 (BioAcademia 70-001, 1:1000). Following primary antibody incubation, coverslips were washed 3x for 5 minutes at RT with washing buffer and then incubated with 35 µl per coverslip of secondary antibodies diluted in blocking buffer, for 1 hour at RT protected from light. The following secondary antibodies were used: AlexaFluor™ 568 Goat anti-rabbit (Life Technologies A11036, 1:500) and AlexaFluor™ 488 Goat anti-mouse (Life Technologies A11029, 1:500). Coverslips were washed 3x for 5 minutes at RT with washing buffer, then washed once in RT 1x PBS and dipped into deionised H_2O, before mounting on a glass slide with Prolong GOLD antifade mounting reagent with DAPI (Life Technologies).

Immunofluorescence images were acquired on a Leica DMi8 Thunder widefield microscope, using the HC PL APO 63x/1.40-0.60 oil objective, and the Leica software platform LAS X (Leica Application Suite X). Foci number was quantified using CellProfiler 4.2.1 (Broad Institute) and Graphpad Prism was used for data presentation.

2.7 Quantitative image-based cytometry

For quantitative image-based cytometry (QIBC), cells were prepared as previously described in section 2.6, with the exception that 12 mm glass coverslips were used. Following 20-24 hours treatment with 1 mM IAA, cells were treated with 40 µM EdU for 30 minutes, EdU was washed out with medium and replaced with complete medium, and cells on coverslips were irradiated with 1Gy or 5Gy and allowed to recover. For analysis of BRCA1 immunofluorescence, cells were pre-extracted and fixed with 4% PFA, and stained as detailed in section 2.6. For RAP80 and RAD51 immunofluorescence analysis by QIBC, cells on coverslips were fixed post-permeabilization by gently aspirating the media, washing the cells with ice-cold 0.2% Tween20/PBS, followed by 4% PFA fixation at RT for 15 minutes. Then, cells were washed once more with ice-cold 0.2% Tween20/PBS and incubated on ice with ice-cold 0.2% Triton X-100/PBS for 1-2 minutes. Finally, cells were washed 1x with ice-cold 0.2% Tween20/PBS and stored at 4 ℃ in 1x PBS for short-term storage. Following fixation, cells were blocked using complete DMEM + 10% FBS, at 37 ℃ for 1 hour (blocking buffer and antibody diluent). Then, coverslips were gently washed once in 0.2% Tween20/PBS and incubated at RT for 30 minutes with 35 µl of the EdU Click-iT solution, prepared according to the manufacturer's instructions. Following a single wash with 0.2% Tween20/PBS, coverslips were placed in a dark, humid chamber and incubated with 35 µl of primary antibodies diluted in complete DMEM for 1 hour at RT (or overnight at 4 ℃ for RAP80 immunofluorescence staining). Following incubation with primary antibodies, coverslips were gently washed 3x with RT 0.2% Tween20/PBS and incubated with secondary antibodies and 0.5 µg/ml DAPI in complete DMEM for 30 minutes at RT, protected from light. Coverslips were then washed 3x with RT 0.2% Tween20/PBS and 2x with deionised H_2O, before mounting coverslips on glass slides with 10 µl of Mowiol mounting media (composed of 10% Mowiol 4-88 (Merck), 25% glycerol, 100

mM Tris-HCl, pH 8.5). Slides were dried ON at RT, protected from light before proceeding with microscope analysis. QIBC was performed using the Olympus ScanR inverted microscope and the Olympus UPLXAPO 20x, NA 0.80, WD 0.6 mm, AIR/Dry objective. Images were acquired, processed and analysed using the ScanR acquisition and image analysis software (Olympus, version 3.2.0). BRCA1, RAP80 and RAD51 foci were processed using a virtual mask. The in-built object detection module was used to segment nuclei and foci based on intensity and size inclusion criteria. Downstream data analysis and data visualization was performed using TIBCO Spotfire software (version 16.6.0). Total number of analysed cells per sample were filtered to under 2000 cells per sample, in a randomised manner. Gates to visualise cells in G1, S and G2 phases were generated using scatter plot profiles of total DAPI intensity and log scale mean EdU intensity. The data points of each gate entailing the sum intensity of foci analysed was exported from TIBCO Spotfire as a table and plotted as a scatter plot on Graphpad Prism.

2.8 Drug sensitivity assays

2.8.1 Resazurin cell viability assay

Cells were seeded in triplicate between 300 and 1200 cells/well depending on the cell line, in 96-well plates in the presence of 1 µg/ml doxycycline, and 1 µg/ml puromycin or 700 µg/ml neomycin to maintain antibiotic selection of the stably transduced cell lines. The next day, cells were treated with 1 mM IAA or with the carrier dimethyl sulfoxide (DMSO) for 1 hour before treating cells with indicated concentrations of olaparib, cisplatin or camptothecin. 7 days later, the media was replaced with phenol-red free DMEM (Thermo Fisher), supplemented with penicillin and streptomycin, 2 mM L-glutamine and 10% FBS, containing 10 µg/ml Resazurin dye (Sigma). Plates were returned to the incubator for 3 to 4 hours and relative fluorescence (560 nm excitation) was measured with the BMG LABTECH CLARIOstar

plate reader. Relative fluorescence data points were exported from the BMG Labtech MARS software and relative viability to DMSO was calculated on Microsoft Excel and plotted on Graphpad Prism.

2.8.2 Clonogenic survival assay

Cells were seeded in duplicate between $1x10^4$ and $4.5x10^4$ cells/well depending on the cell line, in 12-well plates in the presence of 1 µg/ml doxycycline and 1 µg/ml puromycin. The next day, cells were treated with 1 mM IAA or with DMSO (carrier) for 1 hour. Then, cells were treated with 500 nM olaparib and returned to the incubator for 7 days. 7 days later, the media was aspirated and cells were fixed and stained with 0.5% crystal violet in 25% methanol for at least 15 minutes on a shaking platform. The plates were washed twice in deionised H_2O and air-dried. The next day, the stained cells were dissolved with 1 ml/well of 2% SDS and absorbance (570 nm) was measured with the BMG LABTECH CLARIOstar plate reader. Relative viability to DMSO was calculated on Microsoft Excel and plotted on Graphpad Prism.

2.9 Micronuclei analysis

Micronuclei from peripheral blood samples were analysed as described by (Balmus *et al.*, 2015). Approximately 50 µl of tail-vein blood was collected into 300 µl heparin solution and 150 µl heparin-blood mix was fixed in 2 ml cold methanol in a 15 ml tube. Samples were stored at -80 ˚C until processing. To process samples for micronuclei analysis, 12 ml of cold bicarbonate buffer was added to each tube and inverted to mix. Then, samples were centrifuged at 500 x g for 5 minutes at 4 ℃. The supernatant was discarded and 200 µl of cold bicarbonate buffer was added. The cell pellet was resuspended by gently pipetting up and down. 20 µl of sample was transferred to each well in a 96-deep-well-plate. 20 µl of any sample was transferred to 1.5 ml microcentrifuge tubes to prepare unstained, propidium

iodide-only and CD71-FITC-only controls to set up the flow cytometry setup. Samples in the 96-well plate were stained with CD71 (BioLegend 113805, 1:400) and 1 µl (1 mg/ml) propidium iodide by adding 80 µl of CD71-FITC/RNase solution to each test sample. Plate was incubated for 45-60 minutes at 4 ℃ with gentle agitation on a shaker, covered with foil to protect from light. Samples were washed with 600 µl cold bicarbonate buffer and centrifuged at 500 x g for 5 minutes at 4 ℃, then 200 µl of bicarbonate buffer-resuspended cell pellet was transferred to fresh flat-bottom 96-well plate and processed by flow cytometry. Micronuclei analysis was performed by Dr Jean Metson.

2.10 Statistical methods

For statistical analysis of the datasets included in this study, the Graphpad Prism software (version 10) was used. The applied statistical test for each experiment, where *n*=3 biological replicates, is described in the corresponding figure legend. For QIBC-derived data, visual representation of the data as scatter plots and its trend was used for data interpretation, as done similarly in previous papers (Ochs *et al.*, 2016; Tsukada *et al.*, 2024).

Chapter 3

The importance of BRCA1-BARD1 nucleosome binding in DNA repair

3.1 Introduction

By binding to chromatin, the BRCA1-BARD1 complex directs activities and protein recruitment events that are vital for DSB repair by HR. Therefore, it is important to understand how BRCA1-BARD1 complexes engage with chromatin, the nucleosome binding domains that mediate this interaction, and what importance they play in DNA repair and tumour suppression.

There are three known modes in which the BRCA1-BARD1 complex can interact with nucleosomes. These are through the BRCA1/BARD1 RING domains, the dual reader module in the C-terminal domain of BARD1, and indirectly via the BRCA1-A complex. BRCA1 binds to the H2A acidic patch on nucleosomes using residues lysine 70 (K70) and arginine 71 (R71) in its RING domain (McGinty, Henrici and Tan, 2014; Hu *et al.*, 2021; Witus *et al.*, 2021). BARD1 also contributes to nucleosome binding using residues proline 89 (P89) and tryptophan 91 (W91) in its RING domain, that contact histone 2B (H2B) and histone 4 (H4) cleft or the H2B αC helix (Hu *et al.*, 2021; Witus *et al.*, 2021). Both BRCA1/BARD1-RING nucleosome binding functions were shown to be required for efficient histone binding and facilitating H2A ubiquitination *in vitro* (Figure 3.1A-B) (Hu *et al.*, 2021; Witus *et al.*, 2021). However, it was unknown if these nucleosome binding domains were required for the DNA repair functions of BRCA1-BARD1 complex. Furthermore, it is not clear if BARD1 inter-domain cooperation supports DNA repair functions of the BRCA1-BARD1 complex and if BARD1 chromatin binding can regulate BRCA1-A complex activities at DNA DSB sites. Experiments in this chapter aimed to address these

questions, using the HCT116 *BARD1*$^{AID/AID}$ human colorectal carcinoma cell line engineered to have a biallelic knock-in auxin-inducible degron tag on *BARD1* (Natsume *et al.*, 2016; Nakamura *et al.*, 2019), and lentiviral complementation studies with BARD1 separation-of-function mutants. The ultimate aim was to determine to what extent each of the three different chromatin binding modes of the BRCA1-BARD1 complex support DNA repair, either working together, or in isolation.

3.2 Results

3.2.1 The role of the BRCA1-BARD1 RING-dependent nucleosome interactions in DNA repair

To test if the BARD1 RING H2B-H4 cleft/H2B αC helix binding is required for the DNA repair functions of BRCA1-BARD1, I selected the tryptophan 91 (W91) residue for mutagenesis, based on *in vitro* biochemical assays which showed a W91A mutated BRCA1^{RING}- BRCA1^{RING}-UbcH5c complex had reduced affinity nucleosome core particle (NCP) binding (Figure 3.1A-B), and was unable to promote ubiquitination of nucleosomal H2A (Hu *et al.*, 2021). Therefore, I generated lentiviral constructs encoding full-length BARD1 containing a tryptophan 91 substitution to alanine (W91A) in the RING domain, the aspartic acid 712 substitution to alanine (D712A) in the BRCT-BUDR domain, previously shown to be required for HR repair by promoting BARD1 BRCT-H2AK15ub binding via the electrostatic interaction of the carboxylate of D712 with H2B serine 109/lysine 113/lysine 116 (Becker *et al.*, 2021; Dai *et al.*, 2021; Hu *et al.*, 2021), and the double-mutant W91A D712A to test the inter-domain cooperation of the BARD1 RING and BARD1 BUDR nucleosome binding in DNA repair (Figure 3.1C). These *BARD1* transgenes were stably expressed via lentiviral transduction in HCT116 *BARD1*$^{AID/AID}$ cells

previously described by our laboratory (Nakamura *et al.*, 2019; Becker *et al.*, 2021), and the BRCA1-BARD1 heterodimer stability was tested via western blot. As expected, auxin-treated HCT116 *BARD1*$^{AID/AID}$ cells (depleted on endogenous BARD1 protein – hereforth referred to as *BARD1*$^{\Delta/\Delta}$) complemented with (control) glutathione S-transferase (GST) resulted in BRCA1 destabilisation due to the loss of BARD1 protein expression. In contrast, BRCA1 stability did not change in *BARD1*$^{\Delta/\Delta}$ +BARD1^{W91A}/+BARD1^{D712A}/+BARD1$^{W91A\ D712A}$ cells, according to the BRCA1 protein expression levels (Figure 3.1D).

To test if the BARD1 RING-nucleosome interaction is required for BRCA1-BARD1-mediated DNA repair, and determine if it supports the H2AK15ub-binding mediated by the BARD1 tandem BRCTs domain, cell survival assays were performed using PARPi olaparib, platinum-based drug cisplatin and TOP1 inhibitor camptothecin, which are genotoxic agents known to sensitise *BRCA1/BARD1*-deficient cells (refer to section 1.7.1).

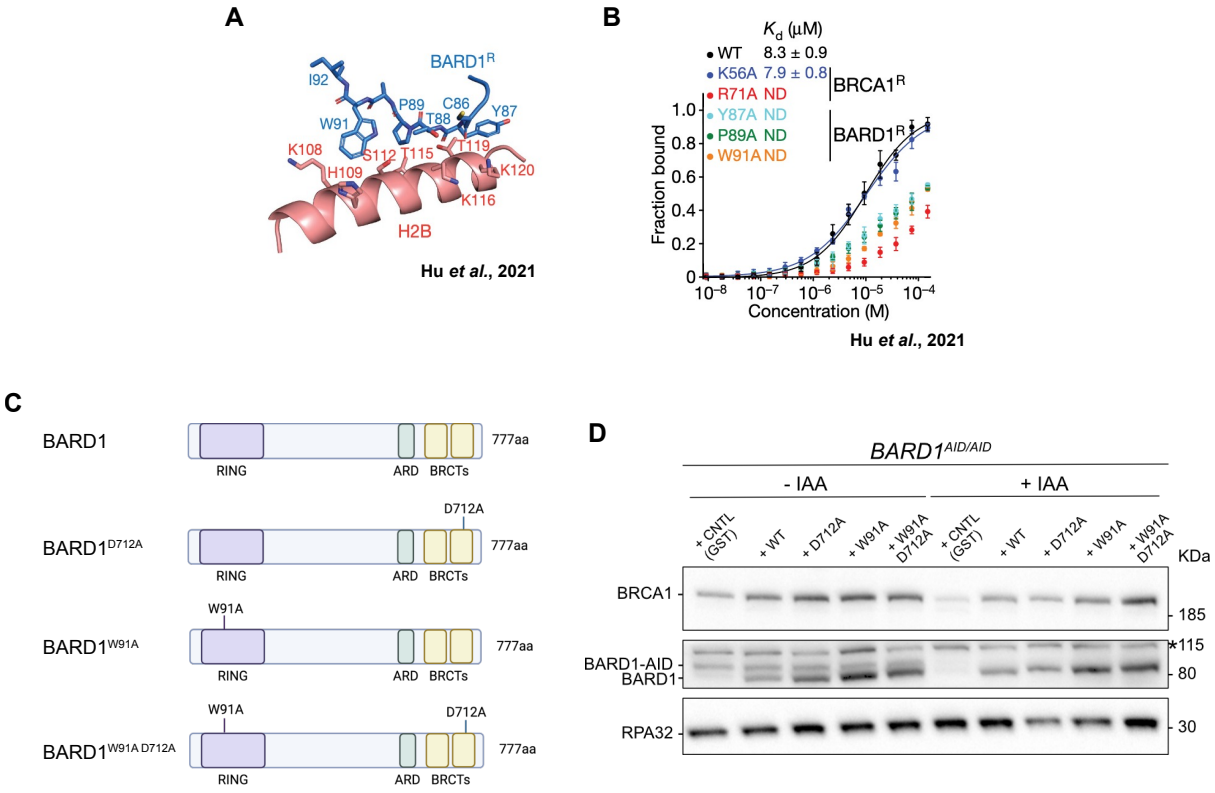


Figure 3.1 Generation of BARD1 RING (W91A) and BRCT (D712A) separation-of-function constructs. (A, B) Structure of BARD1 RING interaction with histone H2B and fluorescence polarisation binding curve which shows weak nucleosome core particle binding by BRCA1 and BARD1 RING nucleosome binding mutants (Hu *et al.*, 2021. Reproduced with permission from Springer Nature). (C) Schematic representation of BARD1 constructs generated for lentiviral complementation: full-length wild-type BARD1, BARD1^{D712A}, BARD1^{W91A} and BARD1$^{W91A\ D712A}$. (D) Western blot of HCT116 *BARD1*$^{AID/AID}$ cells complemented with *BARD1* transgenes showing BRCA1 protein expression and of *BARD1* transgenes, in the absence or presence of auxin (indole-3-acetic acid (IAA)) treatment for 24 hours. RPA32, loading control. BRCA1 (sc-6954), BARD1 (ab64164), RPA32 (ab16855). Asterisk (*) indicates a non-specific band.

As expected, and previously reported (Becker *et al.*, 2021), *BARD1*$^{\Delta/\Delta}$ cells expressing BARD1^{D712A} are HR-deficient, and accordingly exhibit hypersensitivity to olaparib, cisplatin and camptothecin similarly to *BARD1*$^{\Delta/\Delta}$ +GST (control) cells (Figure 3.2). This was in contrast to *BARD1*$^{\Delta/\Delta}$ cells reconstituted with BARD1^{W91A} expression which indicated resistance to all three treatments to the same degree as wild-type (*BARD1*$^{\Delta/\Delta}$ +BARD1) cells (Figure 3.2). Therefore, these results suggest that the RING-nucleosome binding by BARD1 is not required for the repair of DNA damage caused by these agents, which includes PARP1/2 trapped DNA lesions (olaparib), DNA intrastrand crosslink (ICL) damage (cisplatin), and trapped TOP1 cleavage complexes (camptothecin). Furthermore, as observed by the cell survival assays in Figure 3.2, combined BARD1$^{W91A\ D712A}$ mutation did not synergise over BARD1^{D712A} alone, indicating that the RING-nucleosome binding and the BRCT-ubiquitin binding domain are unlikely to show inter-domain cooperativity during DNA repair.

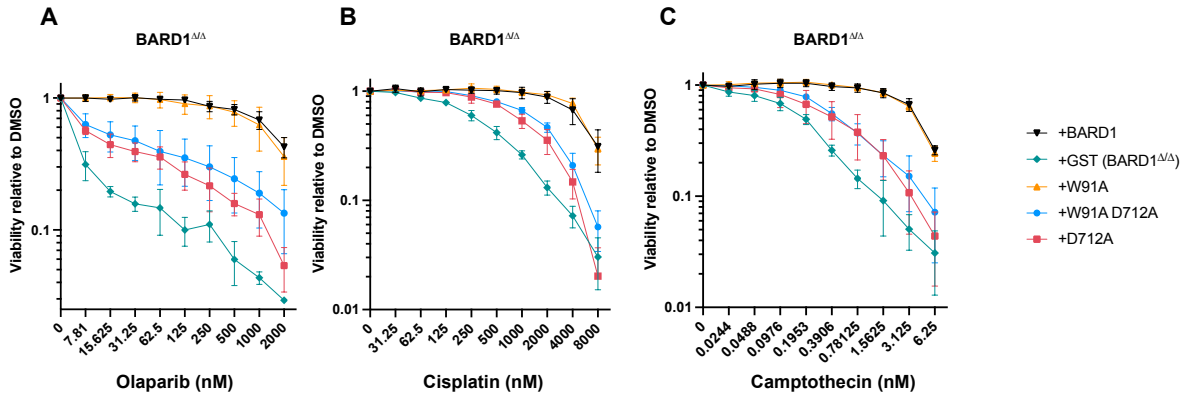


Figure 3.2 The BRCA1-BARD1 complex does not rely on BARD1-RING nucleosome binding for DNA repair. (A-C) Cell survival assays of indicated *BARD1*$^{\Delta/\Delta}$ cell lines grown for 7 days in indicated concentrations of olaparib, cisplatin and camptothecin, respectively. Cells were grown in doxycycline (1 µg/ml) for 16 h, IAA (1 mM) was added the following day and olaparib, cisplatin or camptothecin was added 1 h later. Cell viability was measured by resazurin 7 days later. Mean ± S.D., *n*=3 biological experiments.

Next, I evaluated if the RING-nucleosome binding mediated by the amino acid residue W91 supported the second chromatin binding function in the dual reader module of BARD1, situated in the ARD. It was previously discovered that the ARD contains three important residues (asparagine 470, glutamic acid 467, aspartic acid 500) which bind to H4K20me0 and together with H2AK15ub-binding by the BUDR allow for efficient BRCA1 recruitment to DSB sites and HR repair (Nakamura *et al.*, 2019; Becker *et al.*, 2021). *BARD1*$^{\Delta/\Delta}$ cells complemented with *BARD1*^{ARD3A} transgenes which express point mutations of the three previously mentioned amino acid residues to alanine (N470A, E467A, D500A) are hypersensitive to olaparib and cisplatin and have deficient BRCA1 IRIF formation (Nakamura *et al.*, 2019; Becker *et al.*, 2021).

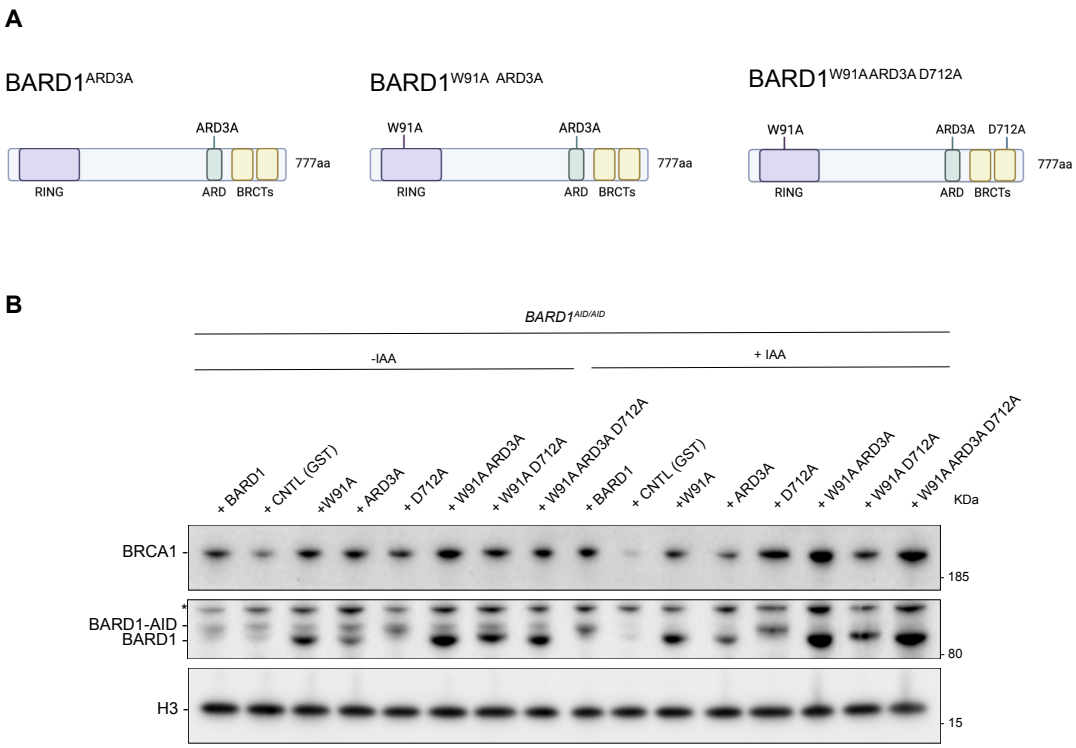


Figure 3.3 Generation of BARD1 RING and ARD separation-of-function constructs. (A) Schematic representation of BARD1 separation-of-function mutants generated to complement HCT116 *BARD1*$^{AID/AID}$ cells via lentiviral transduction: BARD1 ARD3A harbouring point mutations N470A, E467A and D500A and respective

cell line were previously generated by Dr. Jordan Becker (Nakamura *et al.*, 2019); BARD1 W91A ARD3A harbours the RING-nucleosome binding mutant and the H4K20me0-binding mutant; BARD1 W91A ARD3A D712A harbours the previously mentioned point mutations and the BUDR-mutation D712A. (B) Western blot showing BRCA1 and BARD1 protein levels in *BARD1*$^{AID/AID}$ cell lines stably transduced with BARD1 mutant constructs. Cells were grown in the constant presence of selection marker puromycin (1 µg/ml) or neomycin for *BARD1*$^{AID/AID}$ +ARD3A (700 µg/ml), doxycycline (1 µg/ml) and IAA (1 mM) 16 h later for 24 h before harvesting whole-cell lysates for SDS-PAGE/WB. Histone H3, loading control. BRCA1 (sc-6954), BARD1 (ab64164), H3 (ab1791). Asterisk (*) indicates a non-specific band.

Therefore, I generated the BARD1$^{W91A\ ARD3A}$ construct that harbours the BARD1 RING-nucleosome binding mutation (W91A) and the BARD1 ARD-H4K20me0 binding mutation (ARD3A) to test if these two chromatin binding domains show cooperativity. Additionally, I generated the BARD1$^{W91A\ ARD3A\ D712A}$ construct which lacks all of the three reported BARD1 chromatin binding residues to test if the BARD1 dual reader domain relied on the BARD1 RING-nucleosome binding for DNA repair (Figure 3.3A). The stability of the BRCA1-BARD1 heterodimer in *BARD1*$^{\Delta/\Delta}$ cells expressing the previously mentioned BARD1 constructs was confirmed by western blot to check for BRCA1 protein expression (Figure 3.3B). As reported

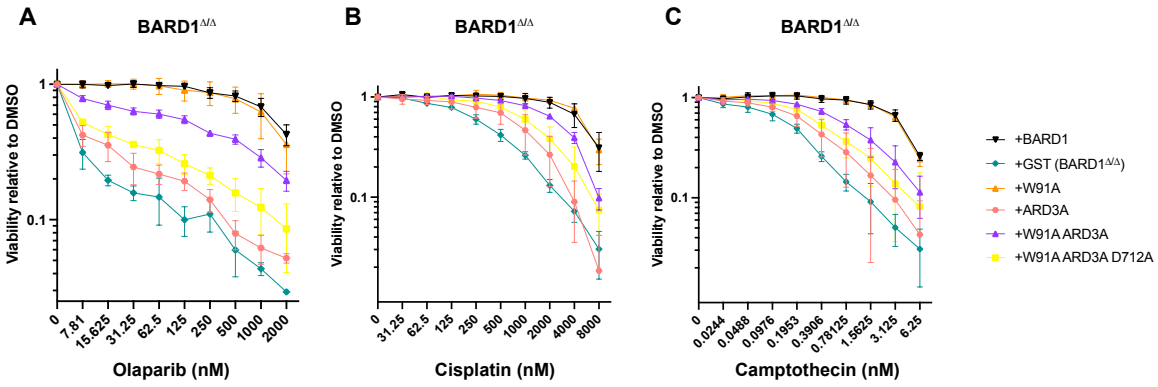


Figure 3.4 The H4K20me0-binding by BARD1 ARD does not rely on the RING-nucleosome binding function. (A, B, C) Cell survival assays of indicated *BARD1*$^{\Delta/\Delta}$ cell lines complemented with indicated BARD1 constructs and GST control, were grown for 7 days in the indicated concentrations of olaparib, cisplatin, and camptothecin, respectively. Cells were grown in selection marker puromycin (1 µg/ml) or neomycin for *BARD1*$^{AID/AID}$ +BARD1^{ARD3A} (700 µg/ml), doxycycline (1 µg/ml) for 16 h, IAA (1 mM) was added the following day and olaparib, cisplatin or camptothecin was added 1 h later. Cell viability was measured by resazurin 7 days later. Mean ± S.D., *n*=3 biological experiments. Control data points (*BARD1*$^{AID/AID}$ cells complemented with wild-type BARD1 and GST constructs) from Figure 3.3 are the same as in Figure 3.4 since these data points originate from the same experiment performed simultaneously with all depicted cell lines. Data points regarding the function of W91 in connection to BARD1 ARD and BRCT are presented on separate graphs for clarity and simplicity of interpretation and visualization.

previously, *BARD1*$^{\Delta/\Delta}$ +BARD1^{ARD3A} cells are hypersensitive to olaparib and cisplatin (Nakamura *et al.*, 2019; Becker *et al.*, 2021), as well as camptothecin, as H4K20me0-binding by BARD1 is required for BRCA1 recruitment to DSB sites (Figure 3.4). Unexpectedly, *BARD1*$^{\Delta/\Delta}$ +BARD1$^{W91A\ ARD3A}$ cells displayed slightly increased resistance to DNA damaging agents, particularly in olaparib survival assays (Figure 3.4). This could suggest that H2AK15ub-binding by the BARD1 BRCT domain facilitates DNA repair in *BARD1*$^{\Delta/\Delta}$ +BARD1^{ARD3A} cells which lack the BARD1 RING-nucleosome binding feature. On the other hand, *BARD1*$^{\Delta/\Delta}$ +BARD1$^{W91A\ ARD3A\ D712A}$ cells displayed similar olaparib, cisplatin and camptothecin sensitivity responses as *BARD1*$^{\Delta/\Delta}$ +BARD1^{ARD3A} cells (Figure 3.4), indicating that the BARD1 RING-nucleosome binding is generally dispensable for the dual reader-mediated chromatin binding during DNA repair.

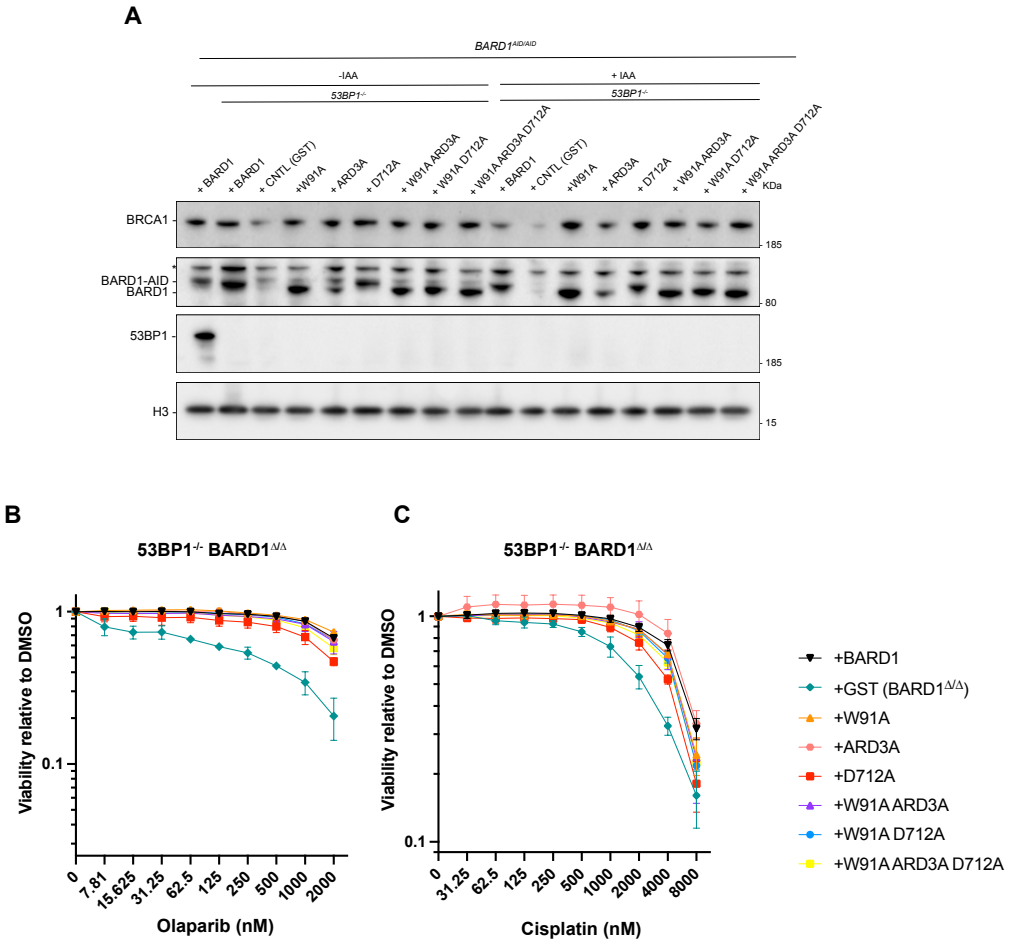


Figure 3.5 BARD1 RING-nucleosome binding/dual reader mutations do not affect additional DNA repair functions of the BRCA1-BARD1 complex. (A) Western blot indicating expression of BRCA1 protein and *BARD1* transgenes in *53BP1*$^{-/-}$ *BARD1*$^{AID/AID}$ cells. HCT116 *BARD1*$^{AID/AID}$ *53BP1*$^{-/-}$ cell line was previously generated in the laboratory (Becker *et al.*, 2021). H3, loading control. BRCA1 (sc-6964), BARD1 (ab64164), 53BP1 (NB100-304), H3 (ab1791). Asterisk (*) indicates a non-specific band. (B and C) Cell survival assays of *53BP1*$^{-/-}$ *BARD1*$^{\Delta/\Delta}$ cell lines complemented with indicated BARD1 and GST (control) constructs, treated with increasing concentrations of olaparib and cisplatin, respectively. Cells were treated with respective selection marker antibiotics mentioned above, doxycycline (1 µg/ml) for 16 h before treatment with IAA (1 mM). Olaparib and cisplatin treatment was added to the culture 1 h after IAA treatment. Cell viability was measured 7 days later by resazurin. Mean ± S.D., *n*=3 biological experiments.

To test if the *BARD1*$^{\Delta/\Delta}$ cells complemented with the BARD1 chromatin binding mutant constructs (BARD1$^{W91A\ ARD3A}$, BARD1$^{W91A\ D712A}$, BARD1$^{W91A\ ARD3A\ D712A}$) could support DNA repair functions following 53BP1 loss, *53BP1*$^{-/-}$ *BARD1*$^{AID/AID}$ cell lines complemented with the previously mentioned BARD1 constructs were generated. As previously confirmed, BRCA1-BARD1 heterodimer stability was not affected by the BARD1 protein mutants according to the protein expression level (Figure 3.5A).

Loss of 53BP1 restored olaparib and cisplatin resistance in *BARD1*$^{\Delta/\Delta}$ +BARD1^{ARD3A} and +BARD1^{D712A} to wild-type (*BARD1*$^{\Delta/\Delta}$ +BARD1) levels, as previously reported (Becker *et al.*, 2021). Interestingly, *53BP1*$^{-/-}$ *BARD1*$^{\Delta/\Delta}$ +BARD1$^{W91A\ ARD3A}$/+BARD1$^{W91A\ D712A}$/+BARD1$^{W91A\ ARD3A\ D712A}$ cells all restored olaparib and cisplatin resistance, contrary to *53BP1*$^{-/-}$ *BARD1*$^{\Delta/\Delta}$ +GST (control) cells which displayed noticeable residual olaparib and cisplatin sensitivity (Figure 3.5B-C), in accordance with previous reports (Becker *et al.*, 2021; King *et al.*, 2024). This suggests that the additional DNA repair functions in BRCA1-BARD1 are independent of the BARD1 chromatin binding domains, and could instead rely on interactions with additional binding proteins, including BRCA1 BRCT domain interactors (e.g. BRCA1-A, CtIP and/or BACH1). Therefore, based on the observed resistance to the DNA damaging agents olaparib, cisplatin and CPT, my results indicate that the BARD1 RING-nucleosome interactions mediated

by the W91 residue are dispensable for the associated DNA damage repair functions of the BRCA1-BARD1 complex.

3.2.2 BARD1 RING-nucleosome interactions can support BRCA1-BARD1 DNA repair functionality when the dual reader module is absent

W91 in the BARD1 RING is important for H2B-H4 nucleosome cleft/H2B αC helix binding and facilitating H2A ubiquitination as evidenced by recent biochemical *in vitro* reports (Hu *et al.*, 2021; Witus *et al.*, 2021). However, in the aforementioned survival assays it was found to be dispensable for DNA repair roles of the complete BRCA1-BARD1 complex. Therefore, I hypothesised that BARD1 RING-nucleosome binding might support the function of DNA repair complexes assembled through domains within BRCA1. To test this hypothesis, I generated transgenes encoding wild-type and W91A mutated BARD1 fragments that were truncated following the RING domain, so that they lacked the intrinsically disordered region, and C-terminal ARD and tandem BRCTs domains (Figure 3.6A). As expected, based on the BRCA1 protein expression levels, the expression of the BARD1 RING domain alone still allows for

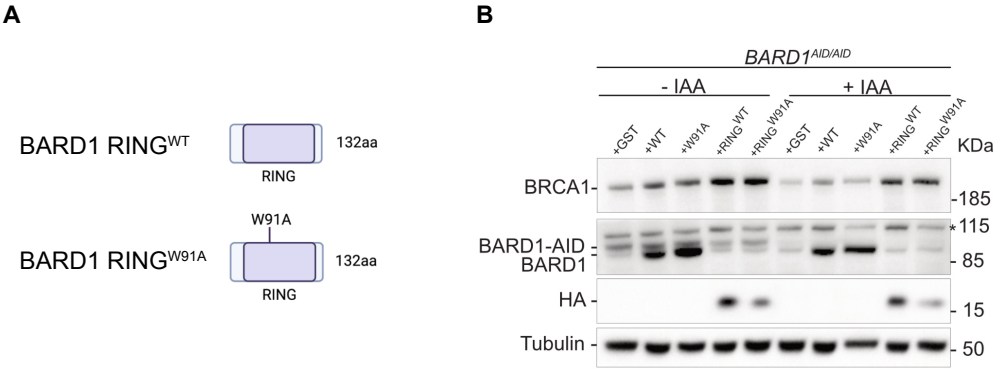


Figure 3.6 Generation of minimal BARD1 RING constructs. (A) Schematic representation of minimal BARD1 RING wild-type and nucleosome-binding mutant W91A constructs, both contain an N-terminal FLAG-HA tag. (B) Western blot showing BRCA1, BARD1 and HA-BARD1^{RING} protein expression levels. Cells in culture were treated with puromycin (1 μg/ml) to keep constant antibiotic selection, and doxycycline (1 μg/ml) for 16 h, followed by

DMSO or IAA (1 mM) for 24 h before harvesting whole-cell protein lysates. GST-complemented *BARD1*$^{AID/AID}$ are used as *BARD1*$^{\Delta/\Delta}$ control cells. α-Tubulin, loading control. BRCA1 (sc-6954), BARD1 (ab64164), HA (901501), tubulin (00020911). Asterisk (*) indicates a non-specific band.

heterodimerisation with the BRCA1 RING domain and the formation of the BRCA1-BARD1^{RING} complex, in line with previous reports (Brzovic *et al.*, 2001; Densham *et al.*, 2016; Sherker *et al.*, 2021) (Figure 3.6B).

BARD1$^{\Delta/\Delta}$ cells that express the *BARD1 RING*^{W91A} transgene, while being able to express BRCA1, were found to be hypersensitive to olaparib, which equalled that of *BARD1*$^{\Delta/\Delta}$ +GST negative control cells, implying HR-deficiency (Figure 3.7A). Remarkably, this contrasted with *BARD1*$^{\Delta/\Delta}$ +BARD1^{RING} cells, which displayed increased resistance to olaparib treatments, and an intermediate overall PARPi sensitivity profile (Figure 3.7A). I speculate that the implied residual HR proficiency in *BARD1*$^{\Delta/\Delta}$ +BARD1^{RING} cells is likely due to RAP80-dependent recruitment of BRCA1 to DSB sites, which was previously shown to sustain some DNA repair activity to BRCA1-BARD1^{D712A} complexes disrupted BARD1 dual-reader activity (Becker *et al.*, 2021). Therefore, the BARD1 RING-nucleosome binding could reinforce BRCA1-dependent functions which rely on RAP80-dependent DNA repair within the BRCA1-A complex.

To assess the efficiency of BRCA1 recruitment at DNA DSB sites in *BARD1*$^{\Delta/\Delta}$ +BARD1$^{W91A\ D712A}$/+BARD1^{RING}/+BARD1$^{RING\ W91A}$ cells, I irradiated cells with 5Gy and recovered them for either 2 h or 8 h to analyse BRCA1 ionising-radiation induced foci (IRIF). The 8 h timepoint allows me to assess secondary BRCA1 recruitment mechanisms via the BRCA1-A complex, as the BARD1 H4K20me0/H2AK15ub-mediated BRCA1 recruitment is the primary (direct) mode of BRCA1 recruitment. As expected from the olaparib hypersensitivity observed in Figure 3.2 and Figure 3.7A, BRCA1 recruitment was completely abrogated in *BARD1*$^{\Delta/\Delta}$ +GST (control) cells. By contrast, *BARD1*$^{\Delta/\Delta}$ +BARD1^{D712A}/+BARD1^{RING}/+BARD1$^{RING\ W91A}$ cells displayed reduced BRCA1 IRIF which appeared unstable and is in line with previous reports showing the

importance of the BARD1 dual reader chromatin binding for efficient BRCA1 recruitment (Figure 3.7B-C) (Becker *et al.*, 2021). Conversely, 8 h post-irradiation, BRCA1 IRIF was rescued in *BARD1*$^{\Delta/\Delta}$ +BARD1^{D712A} cells similarly to wild-type (*BARD1*$^{\Delta/\Delta}$ +BARD1) cells (Figure 3.7D-E), attributed to RAP80-dependent recruitment of BRCA1 (Becker *et al.*, 2021). Equally, *BARD1*$^{\Delta/\Delta}$ +BARD1^{RING} cells rescued BRCA1 IRIF formation to slightly higher levels than *BARD1*$^{\Delta/\Delta}$ +BARD1 cells (Figure 3.7D-E). However, *BARD1*$^{\Delta/\Delta}$ cells complemented with BARD1$^{RING\ W91A}$ and BARD1$^{W91A\ D712A}$ constructs were not able to restore BRCA1 IRIF (Figure 3.7D-E). This indicates that the BARD1 RING-nucleosome binding could support BRCA1-dependent functions in DNA repair which rely on the BRCA1-A complex and is abrogated in *BARD1*$^{\Delta/\Delta}$ +BARD1$^{RING\ W91A}$ and *BARD1*$^{\Delta/\Delta}$ +BARD1$^{W91A\ D712A}$ cells.

The R99 residue is required for the transfer of ubiquitin from the BRCA1-interacting E2 enzyme and mutation to R99E was reported to inactivate E3 ligase function, although recent reports have shown the BARD1 R99E retains residual E3 ligase activity which could account for the contrasting findings on the role of the BRCA1-BARD1 E3 ligase in DNA repair (Densham *et al.*, 2016; Wang *et al.*, 2023). A previous report from our laboratory having demonstrated that BARD1^{R99E}-complemented HCT116 cells showed normal levels of olaparib resistance and HR functionality (Nakamura *et al.*, 2019), as well as work from the Neil Johnson laboratory which found that MCF7 cells expressing BARD1 R99E had no RAD51 recruitment deficiency and were PARPi resistant (Krais *et al.*, 2021). However, Densham et al reported that HeLa cells depleted of endogenous BARD1 using siRNA, yet expressing siRNA-resistant BARD1-R99E transgenes were sensitive to irradiation, olaparib, etoposide and camptothecin but not to hydroxyurea, cisplatin or aphidicolin (Densham *et al.*, 2016). Therefore, to assess if the BRCA1-BARD1 E3 ligase function is required for BRCA1-dependent roles in DNA repair, I engineered

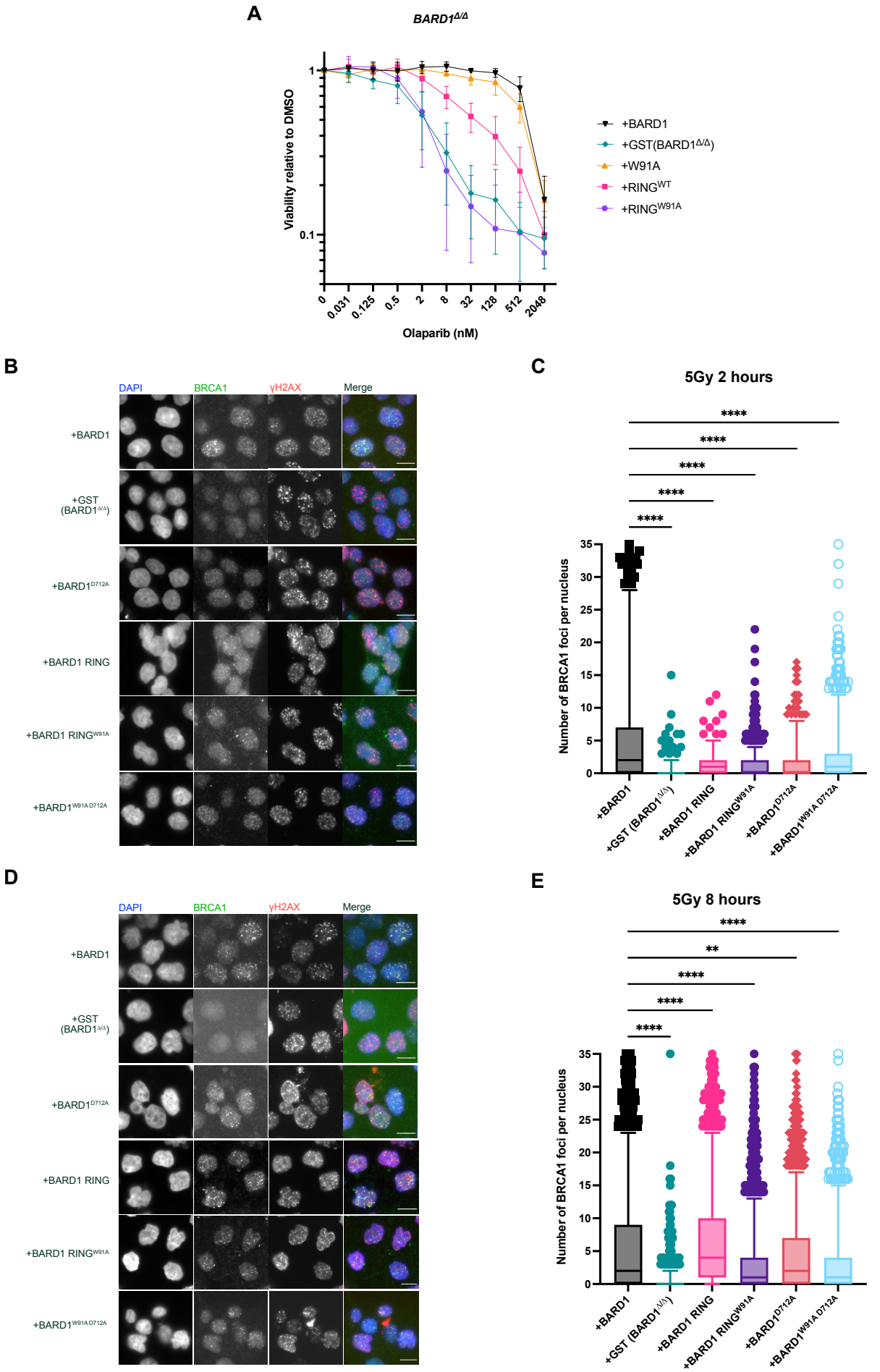

A
BARD1Δ/Δ
Viability relative to DMSO
1
0.1
0
0.031
0.125
0.5
2
8
32
128
512
2048
Olaparib (nM)
+BARD1
+GST(BARD1Δ/Δ)
+W91A
+RINGWT
+RINGW91A
B
DAPI
BRCA1
γH2AX
Merge
+BARD1
+GST (BARD1Δ/Δ)
+BARD1D712A
+BARD1 RING
+BARD1 RINGW91A
+BARD1W91A D712A
C
5Gy 2 hours
****
Number of BRCA1 foci per nucleus
35
30
25
20
15
10
5
0
+BARD1
+GST (BARD1Δ/Δ)
+BARD1 RING
+BARD1 RINGW91A
+BARD1D712A
+BARD1W91A D712A
D
DAPI
BRCA1
γH2AX
Merge
+BARD1
+GST (BARD1Δ/Δ)
+BARD1D712A
+BARD1 RING
+BARD1 RINGW91A
+BARD1W91A D712A
E
5Gy 8 hours
****
**
Number of BRCA1 foci per nucleus
35
30
25
20
15
10
5
0
+BARD1
+GST (BARD1Δ/Δ)
+BARD1 RING
+BARD1 RINGW91A
+BARD1D712A
+BARD1W91A D712A

Figure 3.7 BARD1 RING-nucleosome binding supports BRCA1-dependent functions in the absence of the BARD1 dual reader module. (A) Cell survival assay of *BARD1*$^{AID/AID}$ cells stably transduced with previously described constructs, treated with increasing concentrations of olaparib. At the start of the experiment, cells were treated with puromycin (1 µg/ml) as the selection marker and doxycycline (1 µg/ml) for 16 h before treatment with IAA (1 mM). Olaparib treatment was added to the culture 1 h after IAA treatment. Cell viability was measured 7 days later by resazurin. Mean ± S.D., *n*=3 biological experiments. (B) Representative images of immunofluorescence analysis of BRCA1 foci formation in respective complemented *BARD1*$^{AID/AID}$ cells treated with 5Gy irradiation and 2 h recovery. Scale bar, 10µm. (C) Quantification of BRCA1 IRIF from (B) using CellProfiler. Boxes, median ±25th-75th percentiles; whiskers, 10th-90th percentiles. Statistical significance was determined using the two-sided Kruskal–Wallis H test with Dunn's correction for multiple comparisons. ****P ≤ 0.0001. *n*=2 biological experiments. (D) Same as in (B) but cells were treated with 5Gy irradiation and 8 h recovery. Scale bar, 10µm. (E) Same as in (C), *n*=3 biological experiments.

an arginine to glutamic acid substitution at residue R99 in the BARD1 RING domain fragment (R99E) (Figure 3.8A). The *BARD1*$^{Δ/Δ}$ +BARD1$^{RING\ R99E}$ cells had no BRCA1-BARD1 RING heterodimerisation defects as confirmed via western blot (Figure 3.8B). *BARD1*$^{Δ/Δ}$ +BARD1$^{RING\ R99E}$ cells were moderately sensitive to olaparib, similar to *BARD1*$^{Δ/Δ}$ +BARD1^{RING} cells (Figure 3.8C). Consequently, these results suggest that the BRCA1-BARD1 RING E3 ligase activity mediated by the R99 residue has minimal influence on the DNA repair functions of the BRCA1-BARD1^{RING} complex, deduced from the olaparib resistance profile, possibly due to the residual E3 ligase activity that might be present in the BRCA1-BARD1$^{RING\ R99E}$ complex (Wang *et al.*, 2023).

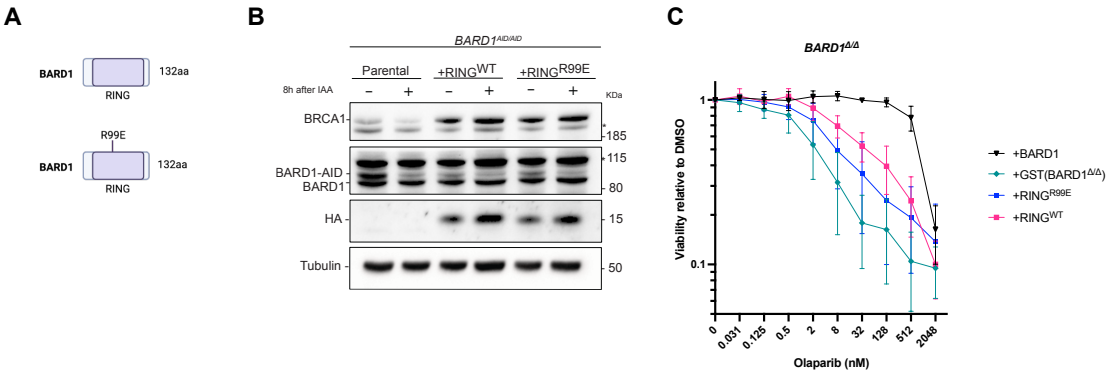


Figure 3.8 The BRCA1-BARD1 E3 ligase function is not required for BRCA1-dependent functions in DNA repair. (A) Schematic representation of minimal BARD1 RING wild-type and E3 ligase activity mutant R99E constructs, both contain an N-terminal FLAG-HA tag. (B) Western blot indicating BRCA1 protein expression levels and of indicated *BARD1* transgenes expressed in *BARD1*$^{AID/AID}$ cells. Cell in culture were treated with puromycin (1 µg/ml) to keep constant antibiotic selection of complemented cells, and doxycycline (1 µg/ml) for 16 h, followed by DMSO or IAA (1 mM) for 8 h before harvesting whole-cell protein lysates. Tubulin, loading control. BRCA1 (sc-6954), BARD1 (ab64164), HA (901501), tubulin (00020911). Asterisk (*) indicates a non-specific band. (C) Cell

survival assay of *BARD1*$^{AID/AID}$ cells stably transduced with indicated BARD1 constructs, treated with increasing concentrations of olaparib. At the start of the experiment, cells were treated with puromycin (1 μg/ml) as the selection marker and doxycycline (1 μg/ml) for 16 h before treatment with IAA (1 mM). Olaparib treatment was added to the culture 1 h after IAA treatment. Cell viability was measured 7 days later by resazurin. Mean ± S.D., *n*=3 biological experiments.

3.2.3 The canonical BRCA1-BARD1 complex suppresses RAP80 recruitment to DSB sites in replicating cells

Previous results indicated that BRCA1 recruitment to DSB-associated chromatin sites can be supported by RAP80, in addition to the BARD1 H4K20me0/H2AK15ub chromatin binding modes and in accordance with previous reports (Figure 3.7E) (Becker *et al.*, 2021). Next I wanted to investigate how RAP80 recruitment is regulated at sites of DNA damage to better understand how BRCA1-A functions are regulated in cells. I therefore analysed RAP80 recruitment in BARD1-depleted *BARD1*$^{\Delta/\Delta}$ control (+GST) cells, and contrasted this to *BARD1*$^{\Delta/\Delta}$ cell complemented with wild-type BARD1 or BARD1^{D712A} expression, 2 h following irradiation with 5Gy. Cells were immunostained with antibodies against RAP80 and γH2AX (as a DNA damage marker), and EdU counter-labelling allowed me to distinguish cells in S-phase from non-replicating cells. In wild-type (*BARD1*$^{\Delta/\Delta}$ +BARD1) cells, RAP80 IRIF were efficiently formed in G1/G2-staged (EdU negative) cell populations, yet were dramatically reduced in frequency in S-phase (EdU-positive) cells (Figure 3.9A-B). By contrast, BRCA1-BARD1 depletion in *BARD1*$^{\Delta/\Delta}$ +GST cells resulted in increased RAP80 recruitment in both EdU-negative and -positive cell populations, indicating that the BRCA1-BARD1 complex suppresses RAP80's recruitment at DSB-associated chromatin sites (Figure 3.9B). Similarly, RAP80 recruitment in S-phase cells was significantly elevated in *BARD1*$^{\Delta/\Delta}$ +BARD1^{D712A} cells, where it supported maximal RAP80 IRIF frequencies in both EdU-negative and EdU-positive cells (Figure 3.9A-B). Interestingly, this indicates that the canonical BRCA1-BARD1 complex recruitment via direct

binding of BARD1 to H2AK15ub at DSB sites suppresses the recruitment of RAP80/BRCA1-A. Additionally, equivalent experiments with *53BP1*$^{-/-}$ *BARD1*$^{\Delta/\Delta}$ cells showed 53BP1 further imposed a barrier to RAP80 IRIF formation (Figure 3.9B): 53BP1 loss increased the recruitment of RAP80 both in G1/G2 (EdU-negative) and S-phase (EdU-positive) staged cell populations, exerting a greater effect in the G1/G2 population (Figure 3.9B). Ultimately, loss of both BRCA1-BARD1 and 53BP1 in *53BP1*$^{-/-}$ *BARD1*$^{\Delta/\Delta}$ +GST cells led to maximal RAP80 IRIF formation across both populations, revealing that BARD1-mediated suppression of RAP80 recruitment is most pronounced to S-phase cells (Figure 3.9B).

Altogether, this data indicates that through the binding of H2AK15ub BRCA1-BARD1 suppresses RAP80 recruitment in S/G2, while 53BP1 plays an equivalent role in suppressing RAP80 recruitment in G1. Therefore, I was interested in understanding where RAP80 IRIF accumulate in the cell cycle in response to DNA DSBs, and how this gets regulated by the chromatin interaction functions of the BRCA1-BARD1 complex. Negatively-stained EdU cells cannot discriminate G1 and G2 phases of the cell cycle, so I next analysed RAP80 IRIF using quantitative image-based cytometry (QIBC). This automated widefield microscopy technique facilitates the analysis of the recruitment of DNA repair proteins at different stages of the cell cycle within large cell populations (over 1000 cells per sample) (Michelena *et al.*, 2021). Interestingly, in wild-type (*BARD1*$^{\Delta/\Delta}$ +BARD1) cells, RAP80 recruitment was mostly confined to G1 (Figure 3.10A). The presence of BRCA1-BARD1 appeared to block most of RAP80 IRIF formation in early and mid S-phase and G2 cell cycle stages, with a similar trend also observed in *BARD1*$^{\Delta/\Delta}$ +BARD1^{D712A} cells (Figure 3.10A-B). As expected, 53BP1-loss led to the accumulation of RAP80 recruitment in G1 and G2, and upon BARD1-depletion in *53BP1*$^{-/-}$ *BARD1*$^{\Delta/\Delta}$ +GST cells, RAP80 recruitment to DNA DSBs accumulated across all cell cycle stages,

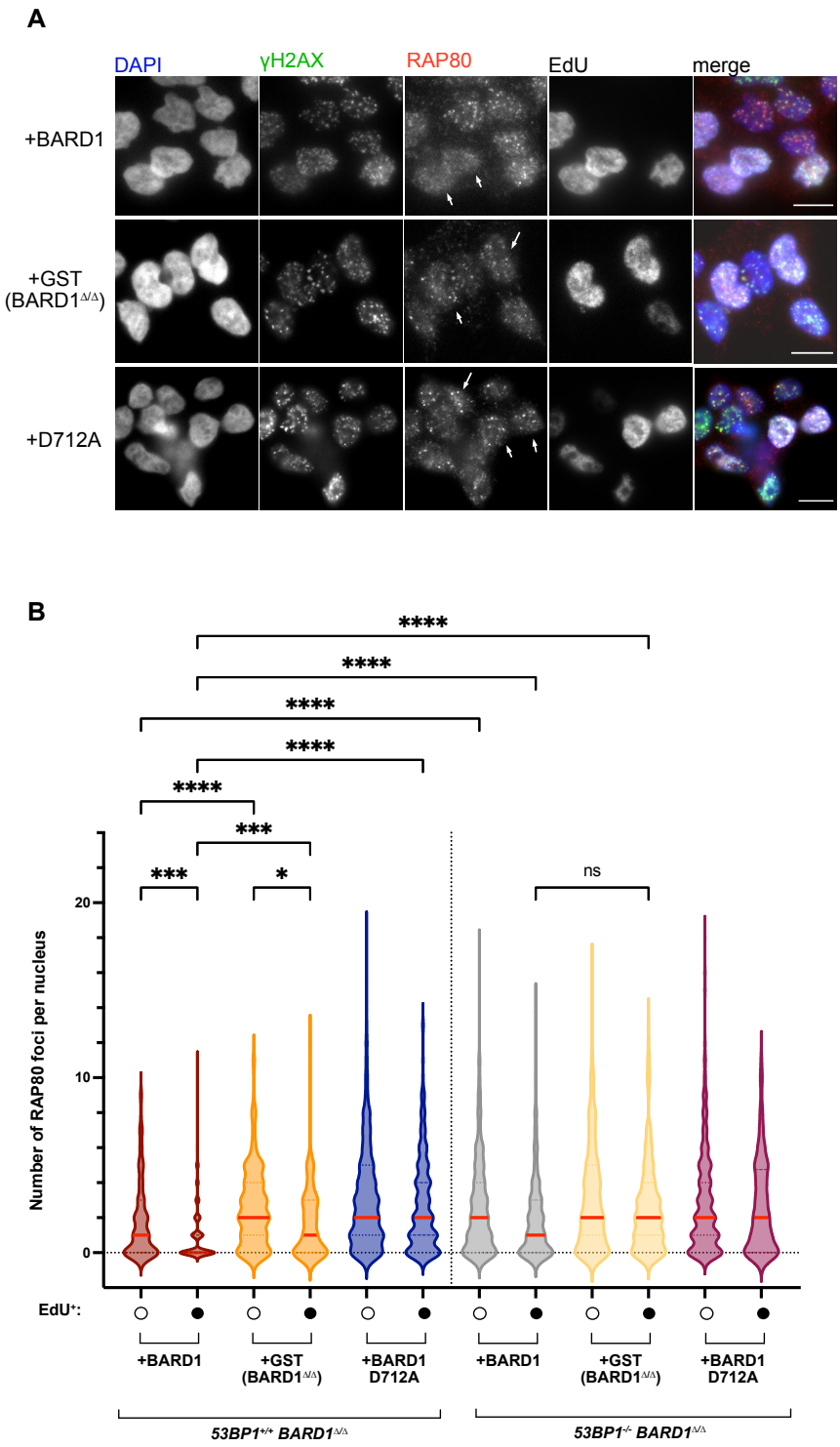


Figure 3.9 Hierarchical suppression of RAP80 recruitment to DSB sites by the BRCA1-BARD1 complex and 53BP1. (A) Representative images of immunofluorescence analysis of RAP80 IRIF formation in *BARD1*$^{AID/AID}$ cell lines expressing wild-type BARD1, GST or BARD1^{D712A} mutant transgenes. Cells were treated with 5Gy of ionising radiation and recovered for 2 h before fixation and immunofluorescence staining. Arrows indicate RAP80 recruitment in nuclei according to non-replicating/replicating cell cycle stage, determined by the EdU staining pattern. Scale bar, 10µm. (B) Violin plot showing the quantification of number of RAP80 foci from experiment in (A) using CellProfiler, including complemented *BARD1*$^{AID/AID}$ cell lines in *53BP1*$^{-/-}$ background. Median levels are indicated in red. EdU-positive indicated in black dots. EdU-negative indicated in white dots. The two-sided Kruskal-Wallis test with Dunn's correction for multiple comparisons was used as the statistical test to determine significance. ***P ≤ 0.0001. *n*=3 biological experiments.

with the most pronounced effect in S-phase and G2 (Figure 3.10A, C). A similar trend was observed in the *53BP1*$^{-/-}$ *BARD1*$^{\Delta/\Delta}$ +BARD1^{D712A} cells (Figure 3.10C). QIBC analysis reassuringly recapitulated what was previously seen in the RAP80 immunofluorescence analysis shown in Figure 3.9B, and together these experiments indicate a hierarchy in the recruitment of BRCA1-BARD1, 53BP1 and RAP80 to sites of DNA DSBs, with H2AK15ub-binding by BRCA1-BARD1 and 53BP1 contributing to the suppression of RAP80 recruitment, during the S and G1/G2 phases, respectively.

5Gy is an ionising radiation dose that leads to numerous DNA DSBs and can lead to DNA repair protein exhaustion (Ochs *et al.*, 2016), so I was interested to investigate RAP80 recruitment dynamics shortly after induction of DNA DSBs by a lower dose of IR to detect possible subtle differences in RAP80 recruitment across different control and BARD1 wild-type and mutant complemented conditions in *53BP1*$^{-/-}$ and *53BP1*$^{+/+}$ backgrounds. Therefore, cells were irradiated with 1Gy and then recovered for 15 minutes. Surprisingly, increased intensity of RAP80 IRIF was detected in wild-type (*BARD1*$^{\Delta/\Delta}$ +BARD1) cells irradiated with lower doses and recovered for shorter periods, although no apparent trend differences between cell cycle phase could be observed (Figure 3.10D). This data suggests that RAP80 itself can get recruited to DNA DSB sites rapidly following DNA damage, then repressed by the BRCA1-BARD1 complex in S and G2 phases (Figure 3.10D). As previously observed in Figure 3.10B, loss of H2AK15ub-binding by BARD1 in *BARD1*$^{\Delta/\Delta}$ +BARD1^{D712A} cells continued to display repressive functions over RAP80 recruitment to DSB sites, mainly in G2 (Figure 3.10D). Loss of 53BP1 was also seen to increase RAP80 recruitment in G2 cells, in line with the previous data in Figure 3.10B,E. Combined loss of both 53BP1 and BARD1 in *53BP1*$^{-/-}$ *BARD1*$^{\Delta/\Delta}$ +GST cells led to maximal

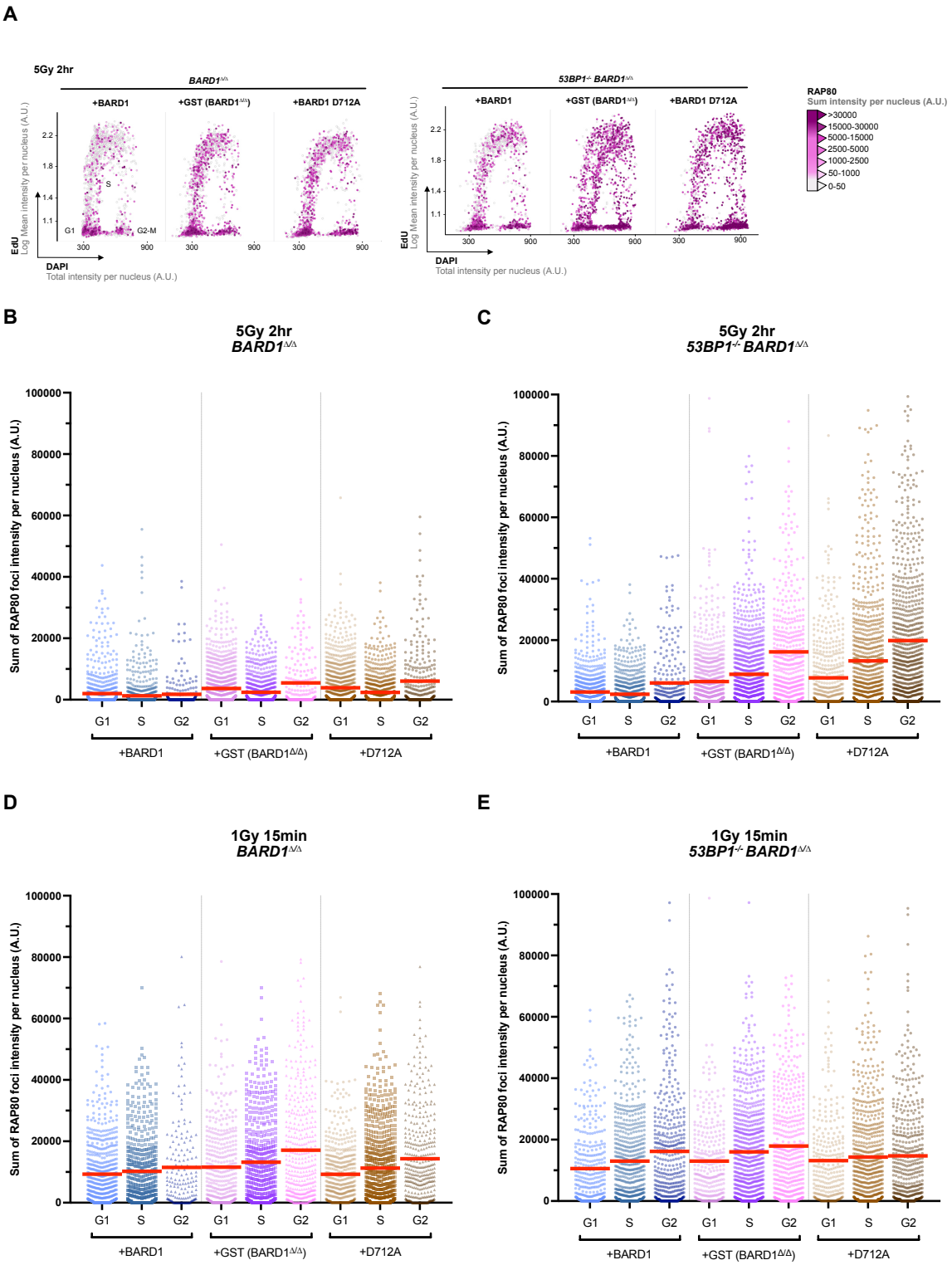


Figure 3.10 The BRCA1-BARD1 complex suppresses RAP80 recruitment to ionising-radiation-induced DNA DSBs mainly in G2. (A) QIBC of RAP80 recruitment at IRIF in *BARD1*$^{AID/AID}$ and *53BP1*$^{-/-}$ *BARD1*$^{AID/AID}$ cells complemented with BARD1 mutant D712A, with GST-control constructs or reconstituted with wild-type BARD1. The log mean EdU intensity per nucleus was plotted over the total DAPI intensity per nucleus. The heat map indicates the Sum intensity of RAP80 per nucleus. Cells were pulse-labelled with EdU for 30 minutes before 5Gy irradiation and post-permeabilization fixation after 2 h recovery. Nuclei were stained for RAP80 and counterstained with DAPI and EdU for cell cycle content. Each sample contains at least 1000 analysed cells. *n*=3 biological experiments (B and C) Quantification of sum intensity of RAP80 foci detected in (A) in *BARD1*$^{AID/AID}$ and *53BP1*$^{-/-}$ *BARD1*$^{AID/AID}$ cells,

respectively, expressing indicated BARD1 constructs. Cells were gated by DAPI and EdU intensity to distinguish cell populations in G1, S-phase and G2. Mean levels are indicated in red. *n*=3 biological experiments. (D and E) Same as in (A-C) however here cells were treated with 1Gy irradiation and recovered for 15 minutes before fixation and nuclei staining. *n*=2 biological experiments.

RAP80 recruitment, most pronouncedly in G2, whereas in *53BP1*$^{-/-}$ *BARD1*$^{\Delta/\Delta}$ +BARD1^{D712A} cells, RAP80 recruitment was not enhanced in the same fashion as by loss of the BRCA1-BARD1 complex altogether (Figure 3.10E).

Interestingly, these results could indicate that besides H2AK15ub binding by BARD1 BUDR, other BARD1 chromatin binding or BRCA1-related functions in DNA repair might have additional roles in regulating RAP80 activity at DNA damage sites.

3.3 Concluding remarks

The ability of the BRCA1-BARD1 complex to interact with the nucleosome core particle was recently discovered through structural work on the BRCA1 and BARD1 RING domains (Hu *et al.*, 2021; Witus *et al.*, 2021). The BARD1 RING residues W91 and P89 were discovered to have van der Waals contact with the H2B-H4 nucleosome cleft/H2B αC helix. These residues when mutated to alanine caused decreased H2A ubiquitination levels and lower binding affinity between the BARD1 RING domain and the nucleosome while it did not change BARD1 RING domain conformation or the BRCA1 RING-BARD1 RING fold (Hu *et al.*, 2021; Witus *et al.*, 2021). However, the importance of these RING-nucleosome binding features for DNA repair roles of the BRCA1-BARD1 complex was previously poorly explored. In this chapter, I investigated the role of the BARD1 RING domain binding H2B-H4 nucleosome cleft/H2B αC helix in supporting DNA repair and BRCA1 recruitment to DNA DSB sites. Via separation-of-function mutants, my data showed that the BARD1 RING chromatin binding mutant

BARD1^{W91A} did not destabilise BRCA1 stability, in line with previously reported biochemical results on the BARD1 RING W91A mutant (Witus *et al.*, 2021). Furthermore, I showed that the W91A mutation did not sensitise cells to olaparib, cisplatin or camptothecin and thus indicating that it could be dispensable for the repair of DNA damage caused by these agents. It is worth considering that residual BARD1 RING-nucleosome binding may be supported by the P89 residue, which was shown to contribute to BARD1 RING-nucleosome binding and facilitate H2A ubiquitination along with W91 (Hu *et al.*, 2021; Witus *et al.*, 2021). Furthermore, recent reports have found that HeLa-shBARD1 P89A W91A cells had reduced RPA and RAD51 recruitment following IR and reduced cell survival to olaparib (Wang *et al.*, 2023). Future experiments assessing the DNA repair proficiency of BARD1 P89A and BARD1 W91A, compared to the double-mutant BARD1 P89A W91A, will provide deeper insight into the role of BARD1 RING-nucleosome binding mediated by the P89 W91 residues.

The dual reader module in BARD1, localised in the ARD and BRCT domains, is vital for efficient BRCA1 recruitment to DSB sites, inhibition of 53BP1 and promoting HR repair (Nakamura *et al.*, 2019; Becker *et al.*, 2021; Dai *et al.*, 2021; Krais *et al.*, 2021). However, it was previously not understood if the BARD1 dual reader module was supported by other BARD1 chromatin binding domains. The cell survival data in response to olaparib, cisplatin and camptothecin shown in Figure 3.2 and 3.4 indicates that there is no inter-domain cooperativity between the BARD1 BRCT domain and the BARD1 RING domain. Additionally, no inter-domain cooperation between the BARD1 RING-nucleosome interaction and any of the BARD1 ARD and BRCT chromatin reader interfaces were observed. This suggests that the BARD1 RING-chromatin binding functions are not essential for DNA repair, and are therefore dispensable for dual reader-mediated chromatin binding by BARD1. Furthermore, my data suggest that reduced H2A ubiquitination, due to the disruption of the BARD1 RING-nucleosome interaction

in BARD1 W91A, does not affect HR-associated BRCA1-BARD1 functions, as indicated by the resistance to olaparib, cisplatin, and CPT in comparison to *BARD1*$^{\Delta/\Delta}$ +GST (control) cells (Figure 3.2). However, my results did not assess the impact of reduced H2A ubiquitination, mediated by both BARD1 P89 and W91 interactions with the nucleosome core particle, on DNA repair proficiency.

Additionally, the previously reported residual E3 ligase activity in BARD1 R99E classifies the BRCA1-BARD1$^{RING\ R99E}$ complex studied here as E3 ligase-defective rather than E3 ligase-dead, which may challenge investigations into the role of BRCA1-BARD1 E3 ligase function in DNA repair (Densham *et al.*, 2016; Stewart *et al.*, 2017; Wang *et al.*, 2023). Recent findings on BRCA1 I26A/L63A/K65A showed that HeLa-shBRCA1 cells expressing this 'E3 ligase dead' BRCA1 mutant were sensitive to the genotoxic agents which included mitomycin C, CPT, cisplatin and olaparib, and exhibited impaired HR and SSA (Wang *et al.*, 2023). Future studies should examine the impact of the 'E3 ligase dead' BRCA1 I26A/L63A/K65A mutations on BRCA1-BARD1 DNA repair functions using alternative systems, such as degron-engineered cell lines that allow for conditional knockout of endogenous BRCA1, rather than shRNA technology. Additionally, it will be interesting to study the effect of these BRCA1 mutations on the tumour suppressive functions of the BRCA1-BARD1 complex in the future by, for instance, *in vivo* mouse models.

An alternative speculation of the function of the BARD1-RING nucleosome binding is that it could be required in other biological contexts such as BRCA1-BARD1 functions during male germline meiosis which seems to rely on the E3 ligase function of BRCA1-BARD1, since male mice homozygous for a homozygous E3 ligase mutation (I26A) were reported to be sterile (Shakya *et al.*, 2011). Remarkably, the fact that the W91A mutation neutralised all drug-resistance in *BARD1*$^{\Delta/\Delta}$ +BARD1^{RING} cells, indicated that the BARD1 RING-nucleosome binding

might support BRCA1-A-dependent recruitment of BRCA1 to DSBs for DNA repair, as neither these, nor the *BARD1*$^{\Delta/\Delta}$ +BARD1$^{W91A\ D712A}$ cells, were also unable to recruit BRCA1 to sites of DNA DSBs even several hours post-IR (Figure 3.7E).

Interestingly, my results uncovered a hierarchical regulation of RAP80 recruitment by the BRCA1-BARD1 complex and 53BP1 protein at DSB sites. In the S and G2 phases of the cell cycle, the presence of the BRCA1-BARD1 complex at DSB sites suppressed the recruitment of RAP80. It was the particular binding of the post-translational ubiquitination mark on H2AK15 by the BARD1 BRCT domain which indicated to suppress RAP80 foci formation at DNA DSB sites. The subsequent loss of 53BP1 further enhanced RAP80 accessibility to DNA DSB sites in BRCA1/BARD1-proficient cells in G2, which could suggest that 53BP1 is involved in regulating RAP80 activity at these cell cycle phases. It was previously unknown if the BRCA1-BARD1 complex itself could regulate the functions related to RAP80. However, it was recently shown that the H2AK15ub-binding by the BARD1 tandem BRCTs domain could block K63-linked polyubiquitin chain extension required for RAP80 binding (Hu *et al.*, 2021), while the BARD1 tandem BRCTs domain's binding to H2AK15ub was not prevented by the presence of K63-linked polyubiquitin chains (Burdett *et al.*, 2023). Therefore, this data indicates that the co-existence of RAP80 and BRCA1-BARD1 on DNA DSB sites is regulated by H2AK15ub-binding via BARD1, and 53BP1 in a cell cycle-dependent manner.

Chapter 4

The BRCA1-independent functions of BARD1

4.1 Introduction

In the previous chapter, I examined the role of the BARD1 RING domain in nucleosome binding during DNA repair. I found that the interaction between the W91 amino acid residue in the BARD1 RING domain and the H2B/H4 cleft or H2B αC helix is not crucial for the HR functions of the BRCA1-BARD1 complex. This implies that BRCA1/BARD1 RING heterodimer-mediated interactions with nucleosomes could be involved in different functions of BRCA1-BARD1, and that they operate separately from the C-terminal BARD1 dual chromatin reader modules. To further investigate the function of BARD1's under-studied chromatin binding mechanisms, and to identify the minimal sequences and domains within the BARD1 polypeptide that are necessary for BRCA1 recruitment at DNA DSB sites, I decided to focus on the intrinsically disordered region (IDR) of BARD1. The function of this highly disordered region, consisting of approximately 300 amino acids, remains largely underexplored (Witus *et al.*, 2023).

It is unclear if the BARD1 IDR is required during DNA repair by supporting the BRCA1-BARD1 chromatin binding functions for HR or if it supports DNA repair via other protein-protein interactions. Recent structural and biochemical work by the Rachel Klevit laboratory (Witus *et al.*, 2023) identified BARD1 IDR regions proximal to the BARD1 RING domain, which supports the BRCA1-BARD1 RING E3 ligase H2A ubiquitination activity via interaction with nucleosomes and free double-stranded DNA. Using the auxin-inducible degron HCT116 cell line to conditionally knockout BARD1, I have used complementation studies in order to deduce

the importance of the BARD1 IDR region, and determine its importance for HR and supporting DNA damage recognition by the BRCA1/BARD1 complex. These results are described in this chapter.

4.2 Results

4.2.1 The BARD1 intrinsically disordered region is not crucial for DNA repair

Following analysis of the BARD1 amino acid sequence conservation within the disordered N-terminal region and the IDR, using the ConSurf server (Berezin *et al.*, 2004), I generated lentiviral constructs encoding full-length BARD1 with deletions in disordered but highly conserved regions (Figure 4.1A). Within the BARD1 IDR, deletions were selected for amino acid positions 135-160 ($BARD1^{\Delta IDR1}$, see (A2) in Figure 4.1A), 175-220 ($BARD1^{\Delta IDR2}$, see (A4) in Figure 4.1A) or 222-390 ($BARD1^{\Delta IDR3}$, see (A5) in Figure 4.1A). These deleted sequences were substituted with a short glycine-serine-glycine linker to mitigate the possibility of introducing structural protein folding defects. In addition to deletions within the IDR, an N-terminally truncated BARD1 construct was generated lacking amino acids 1-25 (hereforth referred to as $BARD1^{\Delta N}$; see (A1) in Figure 4.1A), a RING-proximal disordered region in BARD1 which contained conserved residues that were predicted to be functional in ConSurf multiple sequence alignment analysis. In addition, to examine the potential for BRCA1-independent functions of BARD1, a $BARD1^{\Delta RING}$ transgene was generated which encoded a RING domain-deleted BARD1 polypeptide in which the RING-encoding amino acids (a.a. 26-132) were substituted with two SV40-derived nuclear localisation sequences (NLS; see (A6) in Figure 4.1A). These NLS insertions were to safeguard against the possibility that a RING-less BARD1 protein was not efficiently localised into the nucleus due to disrupted complex formation with

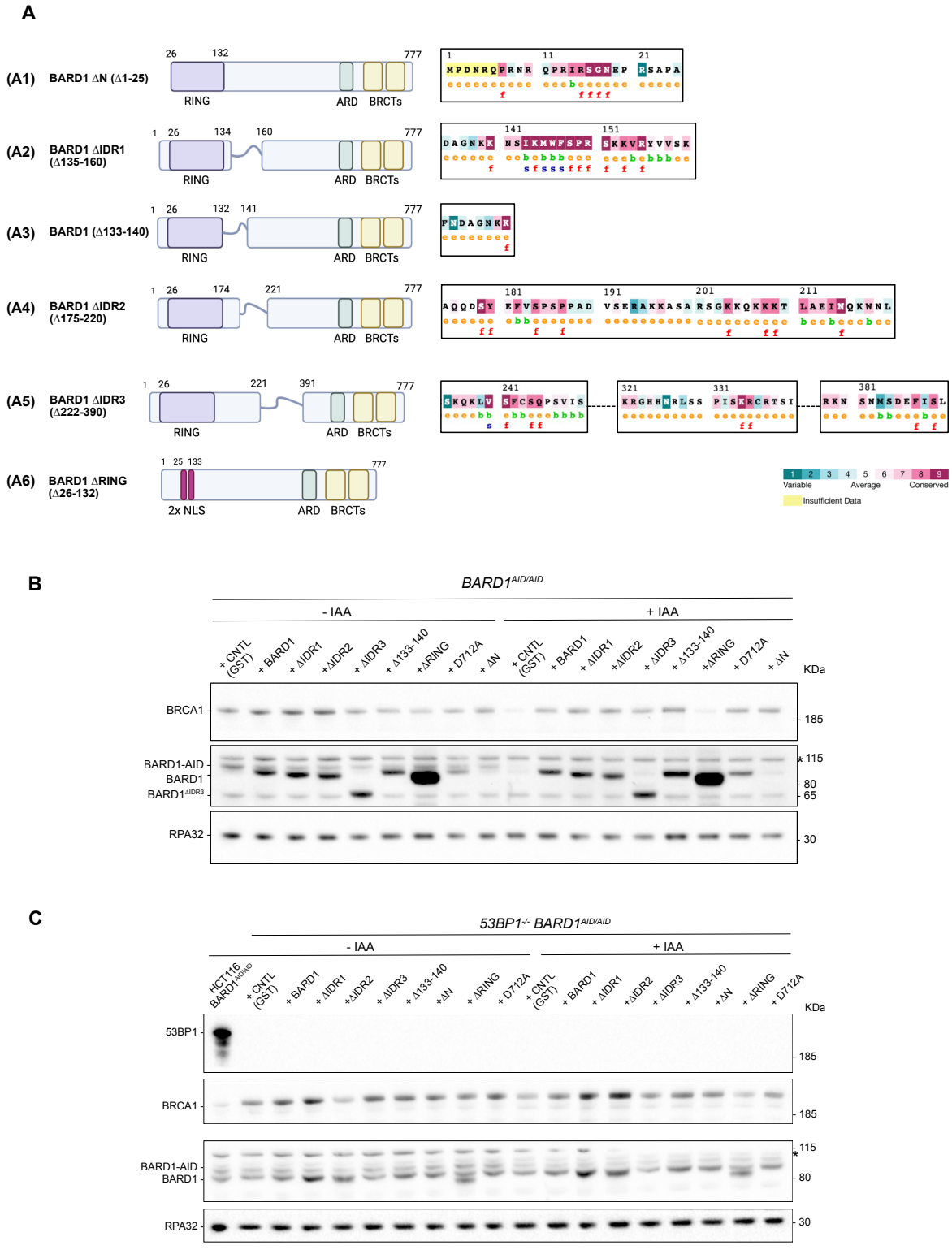


Figure 4.1 Generation of BARD1 N-terminal, RING and IDR deleted constructs. (A) Schematic diagram illustrating the design of the deleted BARD1 constructs generated to study DNA repair-related functions of the N-terminal region from amino acids 1-25 and four different IDR regions (IDR1, IDR2, IDR3 and a.a. 133-140). The respective ConSurf results detailing conservation scores of the deleted residues in the selected areas are shown respectively to the different BARD1 constructs. Functional, f; Structural, s; Exposed, e; Buried, b. (B and C) Western blot indicating expression of BRCA1 protein and of *BARD1* transgenes, and in *53BP1*$^{-/-}$ cell lines in (C). RPA32, loading

control. BRCA1 (sc-6954), BARD1 (ab64164), 53BP1 (NB100-304), RPA32 (ab16855). Asterisk (*) indicates a non-specific band.

BRCA1. Previous biochemical studies found that BARD1 has a RAD51-interaction motif localised within the IDR, corresponding to amino acids 123-162 in BARD1, which contained residues that were not highly conserved. A mutant ablated for these amino acids blocked the BARD1-RAD51 interaction and caused defects in *in vitro* D-loop formation and RAD51-mediated strand invasion assays (Zhao *et al.*, 2017). So, to test the importance of this BARD1-RAD51 interaction motif during DNA repair using *BARD1*$^{AID/AID}$ cell survival assays, I engineered a BARD1$^{\Delta 133\text{-}140}$ construct deleted for the identified conserved residues required for RAD51 association in this study (see (A3), in Figure 4.1A). Also of interest, serine 184 and serine 186 residues in BARD1 were previously identified as mitotic phosphorylation sites (Choudhury *et al.*, 2005), so a deletion within residues 175-220 (BARD1$^{\Delta IDR2}$, see (A4) in Figure 4.1A) was introduced into BARD1 to remove these residues to test the impact on DNA repair (Figure 4.1A).

These *BARD1* deletion-mutant transgenes were stably integrated into HCT116 *BARD1*$^{AID/AID}$ cells via lentiviral transduction and the BRCA1-BARD1 heterodimer stability was assessed via western blot. Neither the N-terminal truncation in BARD1 nor the IDR truncations affected BRCA1-BARD1 heterodimer stability (Figure 4.1B). However, as expected, BRCA1 was destabilized in auxin-treated HCT116 *BARD1*$^{AID/AID}$ +BARD1$^{\Delta RING}$ cells to the same level as was observed in *BARD1*$^{\Delta/\Delta}$ control cells complemented with a control (GST-encoding) transgene (Figure 4.1B). The loss of BRCA1 protein expression upon deletion of the BARD1 RING domain highlights the requirement of the binding of the BRCA1-RING/BARD1-RING domains for overall protein complex stability, and was expected since BARD1 expression is known to be required for BRCA1 stability (Brzovic *et al.*, 2001; Hashizume *et al.*, 2001). Additionally, these

constructs were stably complemented into *53BP1*$^{-/-}$ cell lines (Figure 4.1C). Next, I questioned the importance of these amino acid sequences within the unstructured BARD1 protein during HR repair via cell survival assays.

In contrast to complete BARD1 loss in control GST-complemented *BARD1*$^{\Delta/\Delta}$ cells, none of the generated BARD1 IDR deletions resulted in hypersensitivity to either olaparib or cisplatin in resazurin survival assays (Figure 4.2A-B). In turn, the BARD1$^{\Delta N}$ mutation had no impact on olaparib or cisplatin sensitivity, indicative of preserved HR as in wild-type BARD1 reconstituted cells (Figure 4.2A-B). I also assessed the functionality of BARD1$^{\Delta IDR}$ mutants in 53BP1-deficient cells in similar cell viability assays. As in wild-type BARD1 reconstituted cells, all of the BARD1$^{\Delta IDR}$-expressing *53BP1*$^{-/-}$ *BARD1*$^{\Delta/\Delta}$ cells displayed wild-type olaparib sensitivity profiles, again indicating that the BARD1 IDR does not have crucial DNA repair functions (Figure 4.2C).

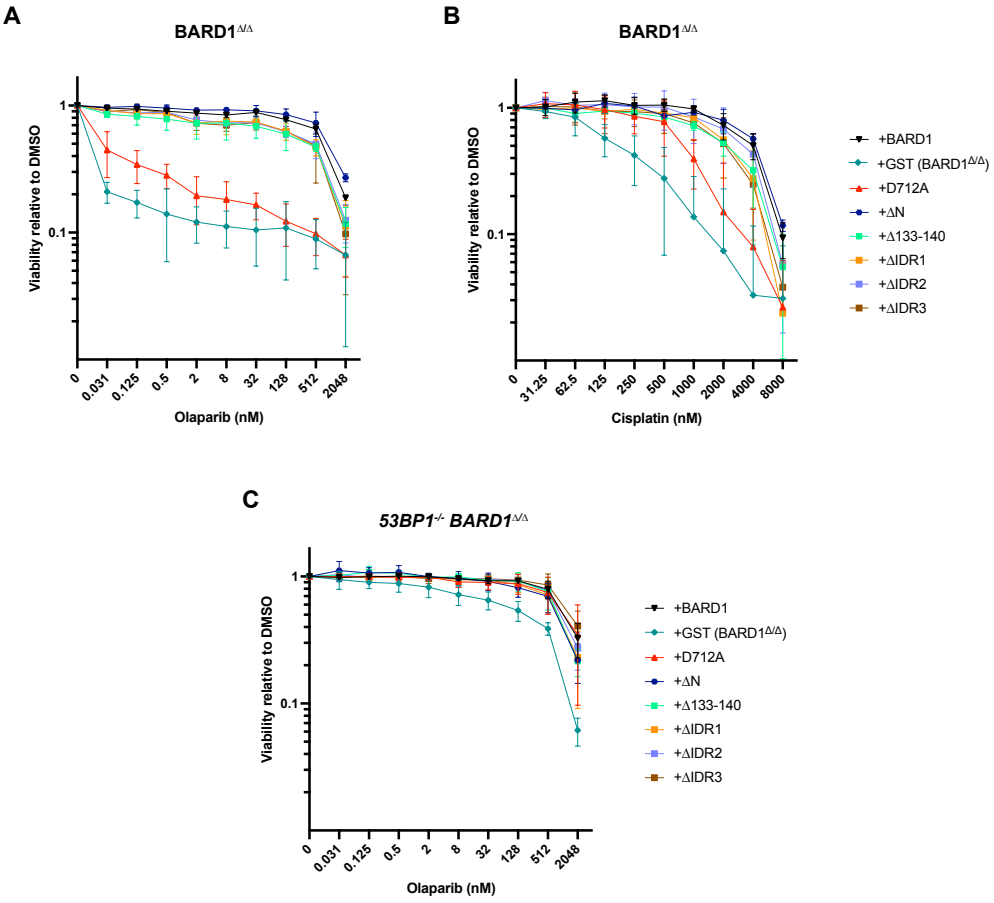


Figure 4.2 The BARD1 IDR and disordered N-terminal region are not required for the HR repair functions of the BRCA1-BARD1 complex. (A and B) Cell survival assays of *BARD1*$^{AID/AID}$ cell lines complemented with indicated constructs grown for 7 days in the presence of increasing concentrations of olaparib and cisplatin, respectively. Cells were treated with doxycycline (1 µg/ml) 16 h before adding auxin (1 mM). Olaparib or cisplatin was added 1 h after IAA treatment. Cell viability was measured by resazurin 7 days later. Mean ± S.D., *n*=3 biological experiments. (B) Olaparib cell survival assay of *53BP1*$^{-/-}$ *BARD1*$^{AID/AID}$ cell lines complemented with indicated constructs, treated as detailed previously.

Nevertheless, all of the four BARD1$^{\Delta IDR1}$, BARD1$^{\Delta IDR2}$, BARD1$^{\Delta IDR3}$ and BARD1$^{\Delta 133\text{-}140}$ mutations showed identical sensitivity profiles following DNA-damaging treatments with olaparib and cisplatin, with a consistent trend toward slightly increased sensitivity towards both agents (Figure 4.2A-B). These results suggest that the BARD1 IDR region as a whole is not essential for mediating DNA repair in response to these DNA-damaging agents. However, it could have auxiliary functions in supporting optimal BRCA1-BARD1 complex interactions with chromatin, or other factors, perhaps by affecting structural conformation and/or the positioning of the BRCA1-BARD1 complex at DNA DSB sites.

4.2.2 BARD1 has BRCA1-independent functions during DNA repair

While the previous results showed that the BARD1 IDR region itself is not essential for the DNA repair functions of the BRCA1-BARD1 complex, I was interested in asking if BARD1 alone can promote other DNA repair functions. Therefore, I assessed the viability of BARD1$^{\Delta RING}$-expressing *BARD1*$^{\Delta/\Delta}$ cells, hereforth described as *BARD1*$^{\Delta RING}$ cells, after olaparib and cisplatin treatment. As expected, BRCA1 destabilisation was observed in *BARD1*$^{\Delta RING}$ cells (Figure 4.1B), and this correlated to a hypersensitivity to both olaparib and cisplatin, equivalent to that seen in BARD1-depleted *BARD1*$^{\Delta/\Delta}$ cells (Figure 4.3A-B). The BARD1$^{\Delta RING}$ protein is nuclear-localised (Figure 4.9A) in *BARD1*$^{\Delta/\Delta}$ cells, yet cannot interact with, or stabilise BRCA1. Thus, it is independent of BRCA1/BARD1-depleted *BARD1*$^{\Delta/\Delta}$ cells.

Previous reports, including work from our laboratory, have shown that deletion of *53BP1* in *BRCA1/BARD1*-null cells leads to HR restoration, and consequently a dramatic restoration of olaparib resistance (Jaspers *et al.*, 2013; Belotserkovskaya *et al.*, 2020; Becker *et al.*, 2021; King *et al.*, 2024). Nevertheless, these cells remain partially sensitive to olaparib (Becker *et al.*, 2021; King *et al.*, 2024). Remarkably, BARD1$^{\Delta RING}$ expression in *53BP1*$^{-/-}$ *BARD1*$^{\Delta/\Delta}$ cells resulted in a complete rescue of olaparib resistance to wild-type levels (Figure 4.3C). This data indicates that BARD1 alone, independently of BRCA1, can counteract residual olaparib toxicity observed in 53BP1-deficient *BARD1*$^{\Delta/\Delta}$ cells.

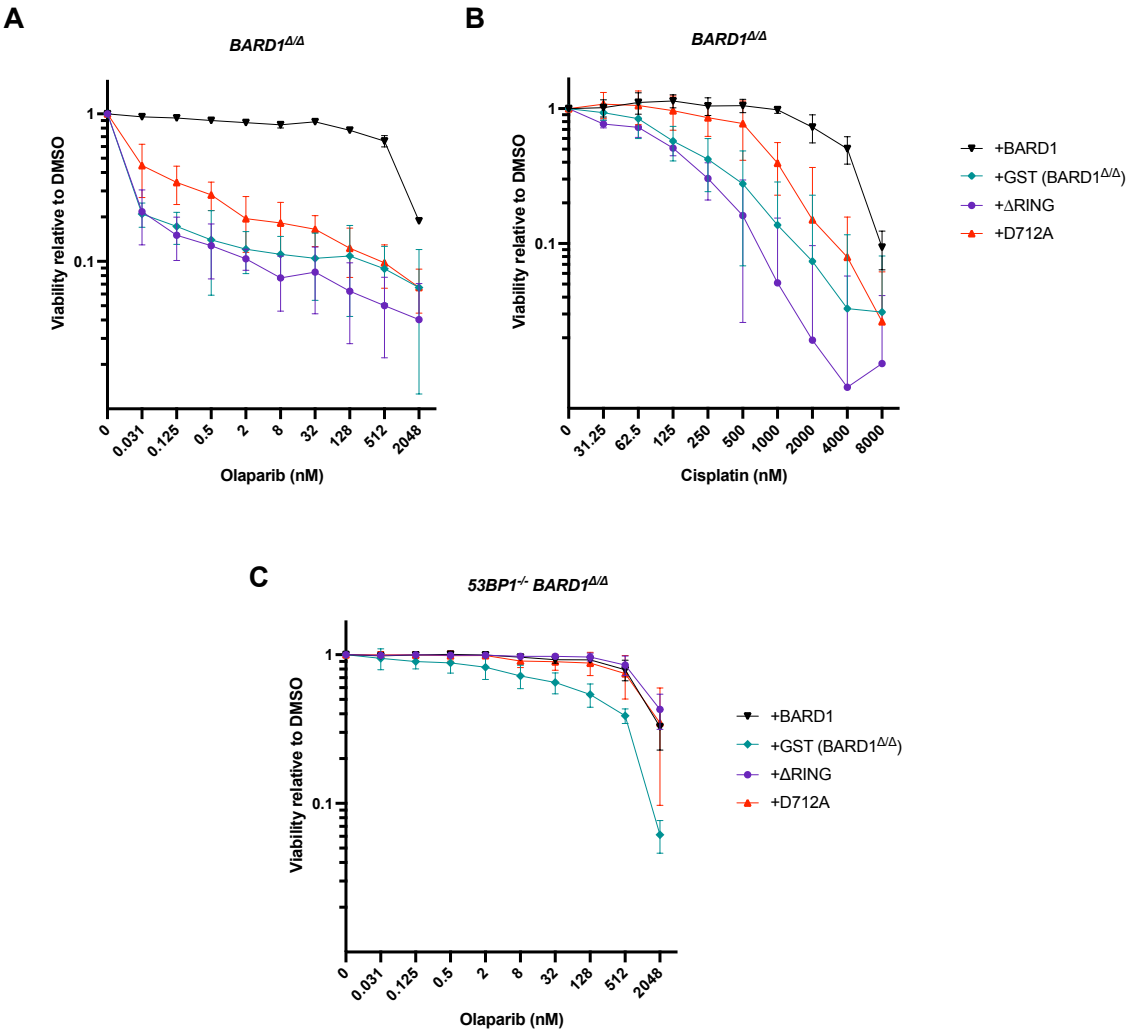


Figure 4.3 BARD1 supports additional DNA repair roles independently of BRCA1. (A-B) Cell survival assays of transduced *BARD1*$^{AID/AID}$ cells treated with selection marker puromycin (1 µg/ml), doxycycline (1 µg/ml) and IAA

(1mM) as detailed previously. Cells were treated with indicated concentrations of olaparib and cisplatin, respectively, for 7 days. Cell viability was measured using resazurin 7 days later. Mean ± S.D., *n*=3 biological experiments. (C) Olaparib cell survival assay of transduced *53BP1*$^{-/-}$ *BARD1*$^{AID/AID}$ cells, treated as detailed previously. Mean ± S.D., *n*=3 biological experiments.

These surprising results prompted me to analyse RAD51 recruitment to DSB sites in 53BP1-deficient cells and 53BP1-proficient *BARD1*$^{\Delta RING}$ cells. The recruitment of BRCA1-BARD1 to DNA DSB sites promotes the formation of RAD51 nucleoprotein filaments, involving the coiled-coil domain-dependent BRCA1-PALB2 interaction, which enables the downstream recruitment of BRCA2. BRCA2 can then recruit RAD51 which replaces RPA proteins coating the 3' resected ssDNA strands (Jasin and Rothstein, 2013). RAD51 recruitment is also supported in BRCA1-independent mechanisms mediated by an interaction between PALB2 and the E3 ubiquitin ligase RNF168 (Luijsterburg *et al.*, 2017; Zong *et al.*, 2019; Krais *et al.*, 2021). Based on the previous data showing DNA repair proficiency in 53BP1-deficient *BARD1*$^{\Delta RING}$ cells, I questioned if restoration of RAD51 recruitment to DNA DSB sites was observed to levels as in wild-type BARD1 reconstituted cells. RAD51 levels were measured in *BARD1*$^{\Delta/\Delta}$ cells reconstituted wild-type BARD1, or with GST (control), BARD1^{D712A} or BARD1$^{\Delta RING}$ expression, and the equivalent experiments were additionally performed in a 53BP1-deficient background. In a preliminary experiment and in agreement with the olaparib and cisplatin survival data in Figure 4.3A-B, the BARD1^{D712A} and BARD1$^{\Delta RING}$- complement *BARD1*$^{\Delta/\Delta}$ cells were deficient in RAD51 recruitment to IR-induced DNA DSB sites, as the GST-expressing *BARD1*$^{\Delta/\Delta}$ cells (Figure 4.4A-B). Loss of RAD51 recruitment to IRIF was rescued after 53BP1 loss at equivalent, wild-type levels, in GST, BARD1^{D712A}, and BARD1$^{\Delta RING}$-complemented *BARD1*$^{\Delta/\Delta}$ cells (Figure 4.4A-B). Interestingly, *53BP1*$^{-/-}$ *BARD1*$^{\Delta/\Delta}$ cells reconstituted with either GST or wild-type BARD1 expression showed higher frequencies of RAD51 foci than did 53BP1-proficient *BARD1*$^{\Delta/\Delta}$ cells complemented with the equivalent transgenes (Figure 4.4A-B).

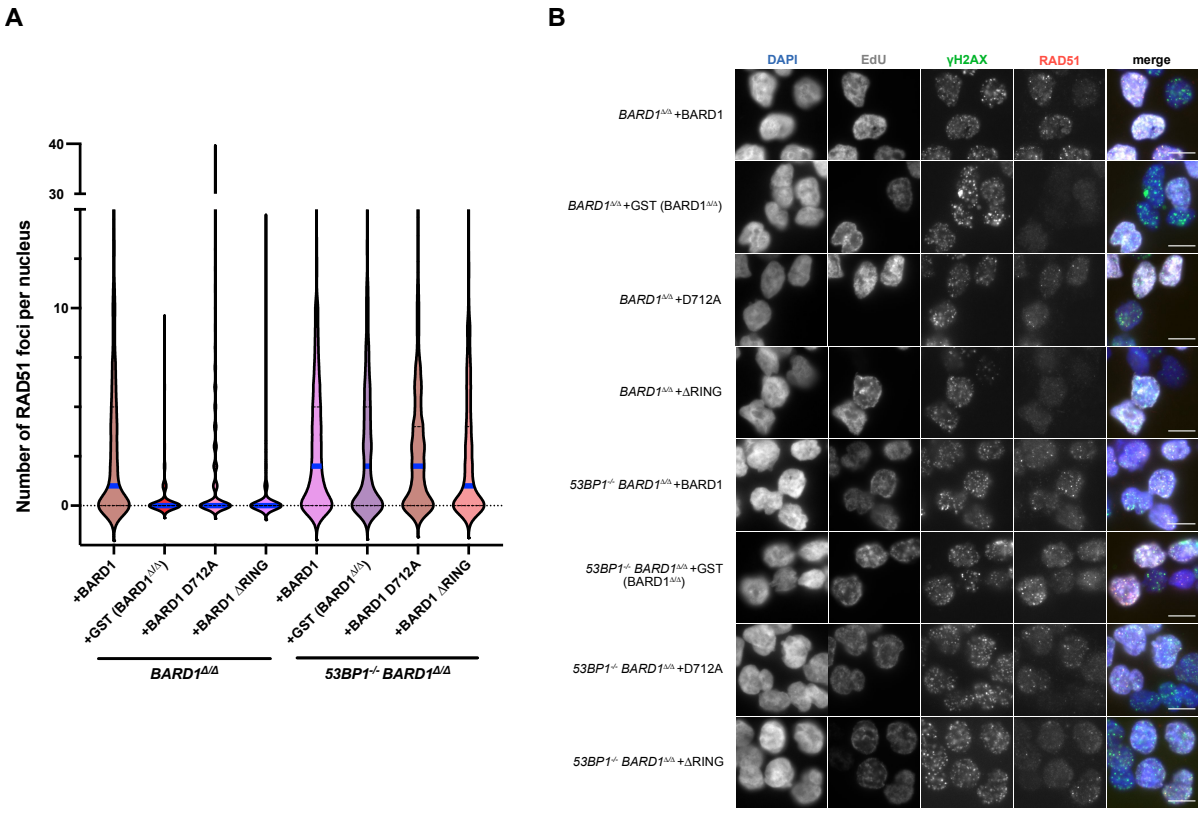


Figure 4.4 Loss of 53BP1 restores HR repair in *BARD1$^{\Delta RING}$* cells and rescues RAD51 recruitment at sites of DNA DSBs. (A) Immunofluorescence analysis of RAD51 IRIF formation in total nuclei of *BARD1$^{AID/AID}$ 53BP1$^{+/+}$* and *53BP1$^{-/-}$* cells transduced with the indicated BARD1 or GST (control) constructs, irradiated with 5Gy and recovered for 2 hours. RAD51 IRIF counts are displayed as violin plots. Median levels are indicated in blue. Quantification of RAD51 IRIF was performed using CellProfiler. *n*=1 biological experiment, three technical repeats. (B) Representative images of RAD51 IRIF formation in cells irradiated with 5Gy and recovered for 2 hours. S-phase nuclei were detected by EdU incorporation. Scale bar, 10 µm.

The notable exception was *53BP1$^{-/-}$ BARD1$^{\Delta/\Delta}$* cells upon BARD1$^{\Delta RING}$ complementation, where RAD51 IRIF frequencies were attenuated to levels equivalent to the wild-type (*BARD1$^{\Delta/\Delta}$* +BARD1) scenario (Figure 4.4A-B). This data suggests that additional BARD1 functions in DNA repair could be regulating RAD51-ssDNA recruitment at DSB sites independently of BRCA1. In 53BP1-deficient cells RAD51 recruitment is hyperregulated by BRCA1-mediated end resection activity while in *53BP1$^{-/-}$ BARD1$^{\Delta/\Delta}$* cells it could be driven by alternative pro-resection mechanisms which are not suppressed by the end protection roles of 53BP1. To analyse the accumulation of RAD51 foci in bigger cell populations and investigate the cell cycle stages in which RAD51 foci accumulate upon DNA DSB induction, QIBC microscopy was performed in

experiments akin to that in Figure 4.4A. Following the optimization of irradiation doses administered to cells to induce DNA DSBs, I decided to irradiate cells with 1Gy which prevents DNA repair protein exhaustion observed at irradiation doses of 5Gy (Ochs *et al.*, 2016). By integrating EdU-fluorescence labelling intensity, from cells pulse labelled with EdU for 30 minutes prior to cell-irradiation, the resulting plot generated allows visualization of the distribution of the sum intensity of RAD51 foci per nucleus according to the cell cycle stage of each single cell. This high-throughput QIBC analysis recapitulated the trends that were previously observed in the immunofluorescence analysis of RAD51 IRIF formation in Figure 4.4A, with the added benefit of being able to discriminate cells in the G1 and G2 phases. Most of the RAD51 foci were found predominantly in mid-S phase population of wild-type (*BARD1*$^{\Delta/\Delta}$ +BARD1) cells (Figure 4.5A-B), in line with previous reports (Ochs *et al.*, 2016), while HR-deficient genotypes (including *BARD1*$^{\Delta/\Delta}$ +GST/+BARD1^{D712A}/+BARD1$^{\Delta RING}$) were deficient in recruiting RAD51 (Figure 4.5A-B). By contrast, loss of 53BP1 dramatically increased the focal accumulation of RAD51 in G2 cells (Figure 4.5A-B). Notably, BARD1$^{\Delta RING}$ complementation into *53BP1*$^{-/-}$ *BARD1*$^{\Delta/\Delta}$ cells resulted in higher focal RAD51 levels than BARD1-depleted 53BP1-deficient cells (*53BP1*$^{-/-}$ *BARD1*$^{\Delta/\Delta}$ +GST) in S and G1 phases, contrary to what was observed in Figure 4.4A (Figure 4.5A-B). This discrepancy could be due to differences in the irradiation doses and/or the different methods of quantifying RAD51 foci: Figure 4.4A quantifies the number of RAD51 foci, indicating the number of DNA DSB sites with RAD51 engagement, while Figure 4.5 quantifies RAD51 foci intensity, which reflects the level of RAD51 concentration at ssDNA filaments (Ochs *et al.*, 2016). Equally, loss of 53BP1 in BARD1-null (*BARD1*$^{\Delta/\Delta}$ +GST) and *BARD1*$^{\Delta/\Delta}$ +D712A cells restored RAD51 foci, not only in S-phase but also in G2 (Figure 4.5A-B). The striking RAD51 recruitment in G2 could indicate that 53BP1 chromatin binding at DSBs and H4K20me2 re-establishment after S phase are required to suppress RAD51 recruitment

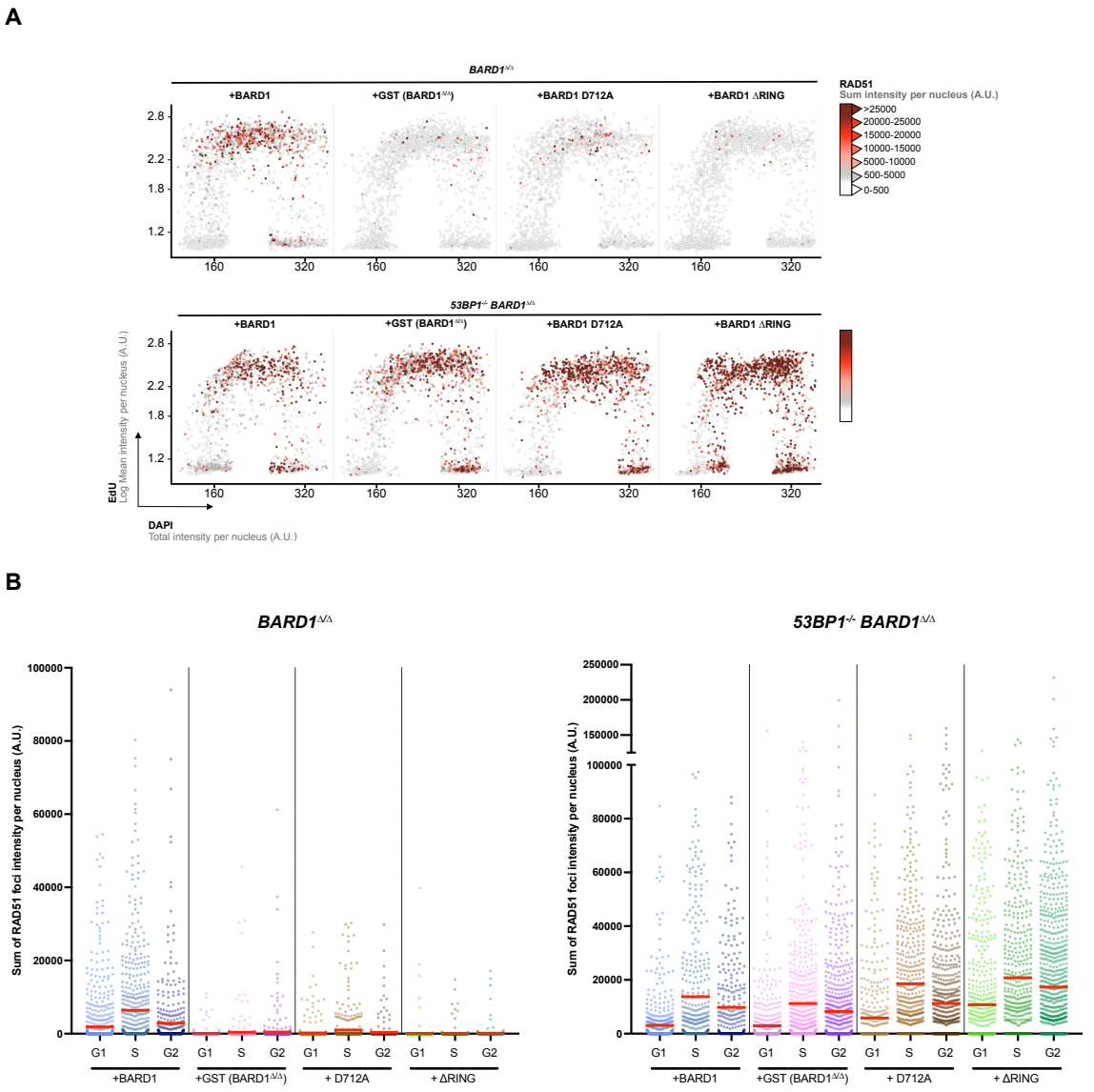


Figure 4.5 RAD51 recruitment at DNA DSB sites in G2/M is suppressed by 53BP1. (A) QIBC of RAD51 IRIF formation in *BARD1*$^{AID/AID}$ and *53BP1*$^{-/-}$ *BARD1*$^{AID/AID}$ cells complemented with wild-type BARD1, GST-complemented controls, BARD1^{D712A} or BARD1$^{\Delta RING}$ constructs. Cells were pulse-labelled with EdU for 30 minutes before 1Gy irradiation and post-permeabilization fixation after 2 h recovery. Nuclei were stained for RAD51 and counterstained with DAPI and EdU for cell cycle content. The log mean EdU intensity per nucleus was plotted over the total DAPI intensity per nucleus. The heat map indicates the sum intensity of RAD51 per nucleus. Each sample contains at least 1000 analysed cells. *n*=2 biological experiments. (B) Quantification of sum intensity of RAD51 foci detected in (A) in *BARD1*$^{AID/AID}$ and *53BP1*$^{-/-}$ *BARD1*$^{AID/AID}$ cell lines, respectively, expressing the indicated BARD1 constructs. Cells were gated by DAPI and EdU intensity to distinguish cell populations in G1, S-phase and G2. Mean levels are indicated in red. *n*=2 biological experiments.

in G2/M. Additionally, RAD51 IRIF were detected at elevated levels in G1 in *53BP1*$^{-/-}$ *BARD1*$^{\Delta/\Delta}$ +BARD1$^{\Delta RING}$ cells. Although HR is suppressed in G1 as there is no available sister-chromatid to repair DNA DSBs, the RAD51-BRCA1-BRCA2 complex can be recruited to centromeric DSBs

during G1 via the interaction of CENP-A and the chaperone HJURP with deubiquitinase USP11 to promote HR (Yilmaz *et al.*, 2021).

To monitor the ability of BRCA1 to be recruited to DNA DSB sites in these experiments, BRCA1 foci were analysed by QIBC, in cells irradiated with 5Gy and recovered for 2 h. As expected from the western blot analysis of BRCA1 expression levels, *BARD1*$^{\Delta/\Delta}$ +BARD1$^{\Delta RING}$ had no BRCA1 IRIF, comparable to *BARD1*$^{\Delta/\Delta}$ +GST cells (Figure 4.6A-B). In contrast, *BARD1*$^{\Delta/\Delta}$ +BARD1^{D712A} cells had very low BRCA1 IRIF (Figure 4.6A-B), supporting the importance of the BARD1 ubiquitin-binding domain for BRCA1 recruitment and HR repair. These residual BRCA1 IRIF depend on the BRCA1-A complex via RAP80-dependent recruitment (Becker *et al.*, 2021). The BRCA1 recruitment defects were restored after reconstituting wild-type BARD1 in *BARD1*$^{\Delta/\Delta}$ cells (Figure 4.6A-B). Loss of 53BP1 in *BARD1*$^{\Delta/\Delta}$ +BARD1^{D712A} cells resulted in only minimal BRCA1 IRIF formation (Figure 4.6A-B), as 53BP1 is not bound to DSB-associated chromatin which could allow for better RAP80 chromatin accessibility, reflecting the data shown in Chapter 3 indicating that 53BP1 can, in part, suppress RAP80 recruitment. Additionally, most BRCA1 foci were found in mid S-phase in HR-proficient BRCA1/BARD1-wild type cells (Figure 4.6C). Intriguingly, 53BP1-deficient *BARD1*$^{\Delta/\Delta}$ cells expressing either the *GST*- control or *BARD1*$^{\Delta RING}$ transgenes showed permissible BRCA1 foci formation. Although in these cell lines, BRCA1 is destabilised and undergoes proteasomal degradation as observed by western blot analysis (Figure 4.1C), the loss of endogenous BARD1 protein levels does not lead to absolute BRCA1 degradation. Therefore, residual amounts of unstable BRCA1 protein likely remains. This technical caveat might explain the BRCA1 foci observed in these cells, which appeared unstable and scarce in numbers (Figure 4.6A). However, most of the S-phase cells (EdU positive nuclei) lack observable BRCA1 foci (Figure 4.6A).

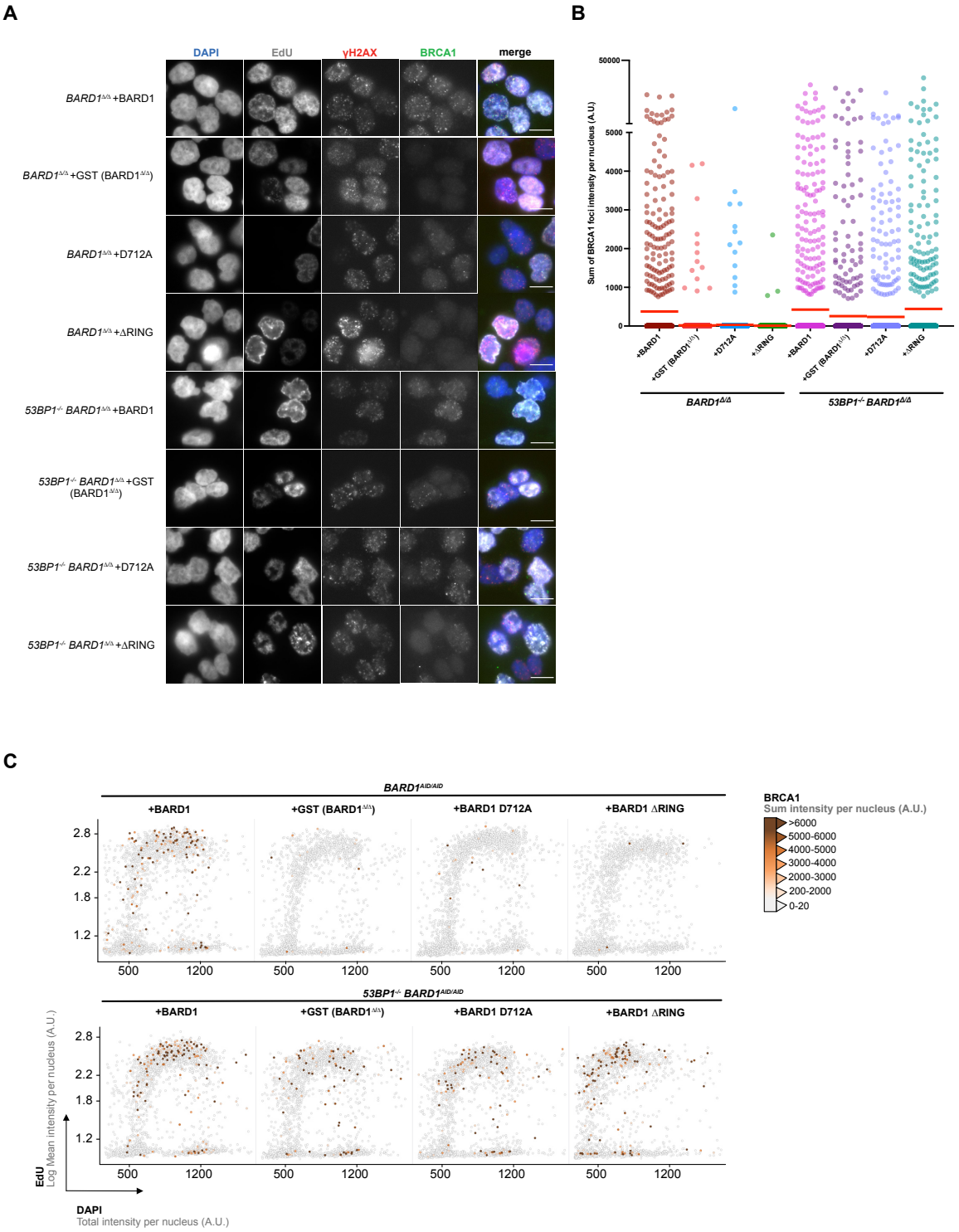


Figure 4.6 The BARD1 BRCTs and RING domains are essential for BRCA1 recruitment. (A) Representative images of BRCA1 IRIF formation in cells irradiated with 5Gy and recovered for 2 h. S-phase nuclei were detected by EdU incorporation. Scale bar, 10 µm. (B) Quantification of sum intensity of BRCA1 foci measured in (C) in *BARD1*$^{AID/AID}$ and *53BP1*$^{-/-}$ *BARD1*$^{AID/AID}$ cell lines, respectively, expressing the indicated BARD1 constructs. Cells were gated by DAPI and EdU intensity to distinguish cell populations in G1, S-phase and G2. Mean levels are indicated in red. *n*=3 biological experiments. (C) QIBC of BRCA1 IRIF formation in *BARD1*$^{AID/AID}$ and *53BP1*$^{-/-}$ *BARD1*$^{AID/AID}$ cells complemented with wild-type BARD1, GST-complemented controls, BARD1^{D712A} or BARD1$^{\Delta RING}$ constructs. Cells were pulse-labelled with EdU for 30 minutes before 5Gy irradiation and post-permeabilization fixation after 2 h recovery. Nuclei were stained for BRCA1 and counterstained with DAPI and EdU for cell cycle content. The log

mean EdU intensity per nucleus was plotted over the total DAPI intensity per nucleus. The heat map indicates the sum intensity of BRCA1 foci per nucleus. Each sample contains at least 1000 analysed cells. *n*=3 biological experiments.

Thus, the observed RAD51 restoration in Figure 4.4 and 4.5 and HR rescue in 53BP1-deficient BARD1$^{\Delta RING}$ cells in Figure 4.3, is independent of the BRCA1-PALB2 mechanism and relies on other BRCA1-independent mechanisms.

4.2.3 BRCA1-BARD1 promotes SCEs via HR-dependent and independent mechanisms

Next, I questioned if elevated RAD51 levels in BRCA1/BARD1-proficient 53BP1-deficient cells (Figure 4.4 and Figure 4.5) would increase toxic HR repair intermediates. To test this, I used the sister-chromatid exchange (SCE) assay which measures the frequency of recombination-mediated crossover events between sister chromatids. The processing of a double Holliday Junction following HR repair can result in non-crossovers if it is 'dissolved' via the BTRR helicase complex (BLM-TOPIIIα-RMI1-RMI1) or potentially cause crossovers if it is 'resolved' via the SMX nuclease complex (SLX1-SLX4-MUS81-EME1) or GEN1 nuclease (West *et al.*, 2015). SCEs can occur naturally in the absence of DNA-damaging agents, as a result of replication fork breakage (Wilson and Thompson, 2007). Therefore, to measure the baseline levels of exchanges per chromosome, SCEs were scored in untreated cells. Basal SCE levels were low in 53BP1-proficient and deficient cells, regardless of the BRCA1-BARD1 status (Figure 4.7A, C). That said, a mild increase in basal SCE frequency was reproducibly observed in *53BP1*$^{-/-}$ *BARD1*$^{\Delta/\Delta}$ cells complemented with wild-type BARD1 expression, and to a similar degree upon complementation with BARD1^{D712A} (Figure 4.7A). Although these differences do not show statistical significance potentially due to sample size or the visible outlier, this data could indicate that 53BP1 typically suppresses the occurrence of spontaneous SCE events, which

depend on an intact BRCA1/BARD1 complex, yet surprisingly not the BARD1-dependent interaction with H2AK15ub at DSB sites.

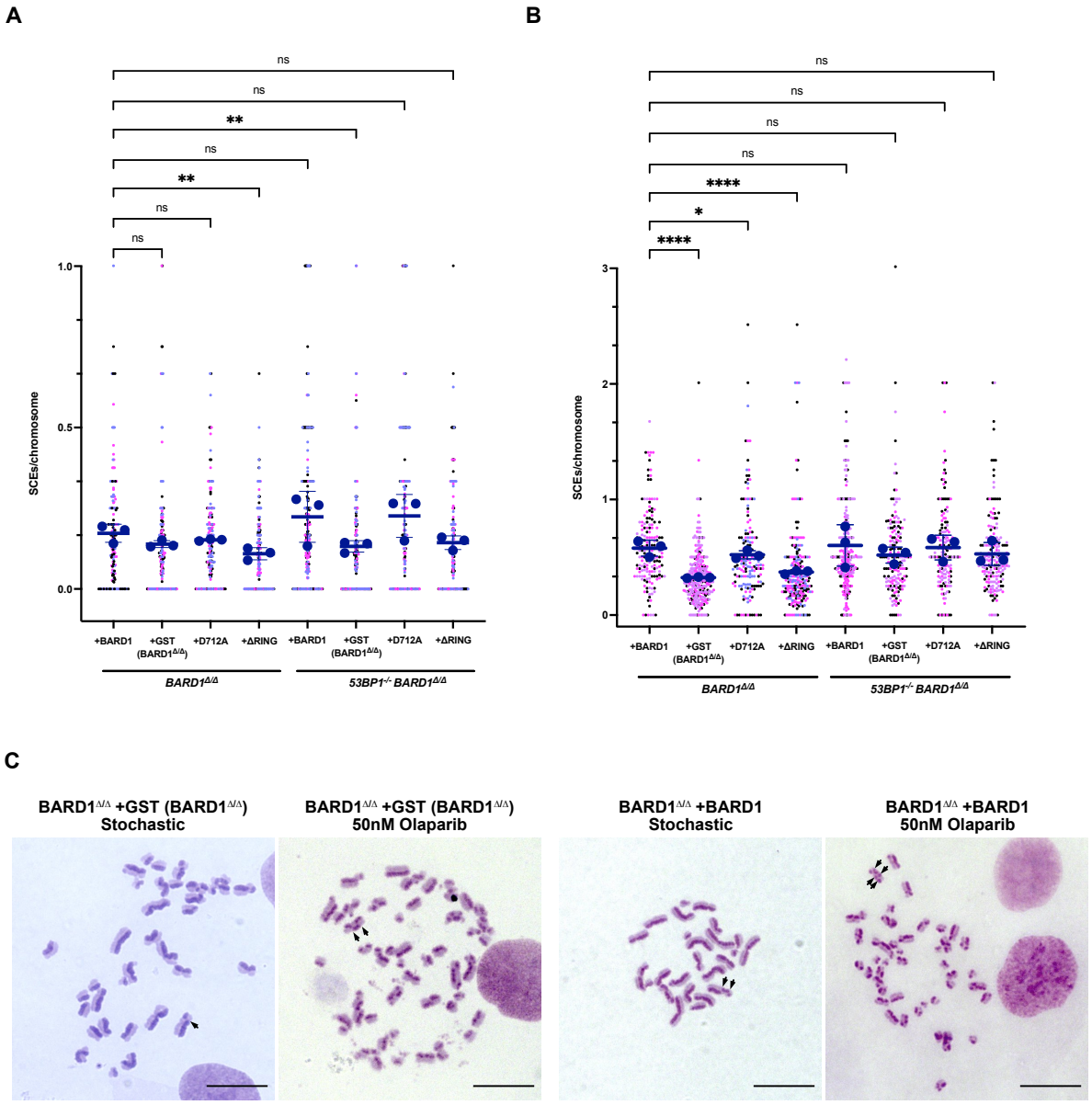


Figure 4.7 DNA repair intermediates levels in 53BP1-deficient and 53BP1-proficient cells. (A) Superplot showing stochastic sister-chromatid exchange (SCE) levels per chromosome in untreated *BARD1*$^{\Delta/\Delta}$ cells complemented with wild-type BARD1, GST (control), BUDR-mutant BARD1^{D712A} or BARD1$^{\Delta RING}$ constructs, in *53BP1*$^{+/+}$ or *53BP1*$^{-/-}$ backgrounds. Mean ± SD. Each circle represents the mean SCE/chromosome per biological experiment, *n*=3. The two-sided Kruskal-Wallis test with Dunn's correction for multiple comparisons was used as the statistical test to determine significance. ****P < 0.0001. (B) Superplot showing SCE levels per chromosome after treatment with olaparib (50 nM). (C) Representative images of SCEs in GST-complemented BARD1$^{\Delta/\Delta}$ cells and reconstituted wild-type BARD1 cells either untreated or treated with 50 nM olaparib. Arrows indicate one SCE. Scale bar, 5 µM.

In olaparib-treated cells, SCE frequencies were increased dramatically across all the different cell lines (Figure 4.7B). These SCEs were also highly dependent on BARD1 and the intact BRCA1-BARD1 complex, as evidenced by equivalently reduced SCE frequencies in *BARD1*$^{\Delta/\Delta}$ cells complemented with control (GST) or BARD1$^{\Delta RING}$ proteins, when compared to the rescued SCE frequencies in BARD1-complemented *BARD1*$^{\Delta/\Delta}$ cells (Figure 4.7B). Interestingly, expression of the HR-deficient BARD1^{D712A} mutant protein significantly increased SCE frequencies in *BARD1*$^{\Delta/\Delta}$ cells, albeit not to wild-type (+BARD1) frequencies. This indicates that a significant proportion of BRCA1-BARD1-dependent SCEs are mediated by an HR- and H2AK15ub-independent mechanism.

In contrast, SCEs frequencies in *53BP1*$^{-/-}$ *BARD1*$^{\Delta/\Delta}$ cells remained fairly consistent across the different control and BARD1 wild-type and mutant complemented conditions, with perhaps only a mild decrease in their frequency in control (GST) and BARD1$^{\Delta RING}$ complemented *53BP1*$^{-/-}$ *BARD1*$^{\Delta/\Delta}$ cell line (Figure 4.7B). This would again be consistent on BARD1-dependent SCEs occurring through HR-dependent and independent mechanisms, with the former sensitive to 53BP1 status, and the latter being additive in an HR-restored *53BP1*$^{-/-}$ *BARD1*$^{\Delta/\Delta}$ background.

Altogether, these experiments provide compelling support for HR-dependent and independent functions of the BRCA1-BARD1 complex being involved in SCE generation under unchallenged and PARPi-treatment conditions. The fact that the BARD1^{D712A} mutant cannot recognise DSBs through binding to H2AK15ub/H4K20me2-bimodified nucleosomes, yet is competent to significantly stimulate SCE formation, implicates different DNA damage recognition modules in the BRCA1-BARD1 complex which promote DNA repair, perhaps via functionally distinct BRCA1-BARD1 complexes. This conclusion also aligns with the previous

RAD51 data, where only wild-type BARD1, but not BARD1^{D712A} could promote RAD51 recruitment in *BARD1$^{\Delta/\Delta}$* cells (Figure 4.4A and 4.5A-B).

4.2.4 The involvement of the BARD1 IDR and chromatin binding residues during BRCA1-independent DNA repair

Intrigued by the ability of a RING-less BARD1 mutant protein to mediate some DNA repair functionality, independently to BRCA1 in 53BP1-deficient cells (in Figure 4.5 and 4.7B above), I hypothesized that these BRCA1-independent functions could be supported by functional sequences within the BARD1 IDR and potential protein-protein interactions. It was recently reported that BARD1 has a short linear motif (SLIM) located in the IDR region, deleted in my BARD1$^{\Delta IDR1}$ mutant protein introduced in Figure 4.1A, which interacts with SLX4 and MUS81 to process HR repair intermediates which have not been processed by BLM helicase (Tsukada *et al.*, 2024). This SLX4-interacting motif is centred around the serine 148 residue in BARD1 and is phosphorylation-dependent (Tsukada *et al.*, 2024). Therefore, to study the importance of SLIMs in the IDR in supporting BRCA1-independent functions of BARD1 during DNA repair, five different SLIM regions were mutated bearing alanine substitutions at highly conserved residues in the *BARD1$^{\Delta RING}$* transgene as depicted in Figure 4.8A. Additionally, the previously studied BARD1 chromatin binding residues in the ARD and tandem BRCTs domains were also mutated in the *BARD1$^{\Delta RING}$* transgene to ARD3A and D712A, respectively. Here, I hypothesized that the chromatin binding to H4K20me0 and H2AK15ub is essential for the functions of RING-less BARD1, as previous data in Chapter 3 and previous work from our lab have shown (Nakamura *et al.*, 2019; Becker *et al.*, 2021). Lastly, a BARD1 tandem BRCTs point mutation on residue lysine 619, substituted to alanine (K619A), was included as another BARD1 RING-less

chromatin binding mutant. This reported poly (ADP-ribose) (PAR) binding module in the BARD1 tandem BRCTs domain was shown to be required for stalled replication fork protection (Li and Yu, 2013; Billing *et al.*, 2018). The point mutation K607A in mice, equivalent to K619A in humans, ablated the BARD1-PAR chain binding and the ability of BRCA1/BARD1 localisation at stalled replication forks in hydroxyurea-treated mouse embryonic fibroblasts. At the same time, it did not affect BRCA1 and RAD51 recruitment or cause HR deficiency in mice (Billing *et al.*, 2018). Similarly, the expression of BARD1 BRCTs-mutant K619A did not sensitise HCT116 cells to olaparib treatment (Nakamura *et al.*, 2019; Becker *et al.*, 2021). Therefore, I questioned if the BARD1 tandem BRCTs-PAR binding module supported DNA repair in RING-less BARD1 cells. The *BARD1*$^{\Delta RING}$ transgenes harbouring the point mutations detailed in Figure 4.8A were stably integrated into *53BP1*$^{-/-}$ *BARD1*$^{\Delta/\Delta}$ cells and as previously observed in Figure 4.1B-C, expression of RING-less BARD1 destabilised endogenous BRCA1 expression upon auxin-induced depletion of endogenous BARD1 protein (Figure 4.8B).

To identify the BARD1 amino acid sequences involved in DNA repair in RING-less BARD1 cells and to assess the role of chromatin binding and of the SLIM regions within the IDR, I performed olaparib clonogenic survival assays to evaluate the response to olaparib-induced DNA damage as a readout for DNA repair proficiency in cells expressing mutations in BARD1$^{\Delta RING}$. In line with previous reports (Bouwman *et al.*, 2010; Bunting *et al.*, 2010; Nacson *et al.*, 2018; Becker *et al.*, 2021; King *et al.*, 2024) and the olaparib survival data shown in Figure 4.2C, loss of 53BP1 rescues olaparib resistance in BARD1-deficient cells (Figure 4.9). However, this rescue is incomplete and residual olaparib toxicity was still evident in *53BP1*$^{-/-}$ *BARD1*$^{\Delta/\Delta}$ cells (Figure 4.9). In contrast, reconstitution of *53BP1*$^{-/-}$ *BARD1*$^{\Delta/\Delta}$ cells with wild-type BARD1 or BARD1$^{\Delta RING}$ fully rescued olaparib sensitivity, as observed in the previous olaparib and cisplatin survival assays (Figure 4.9 and Figure 4.3C). Interestingly, all SLIM

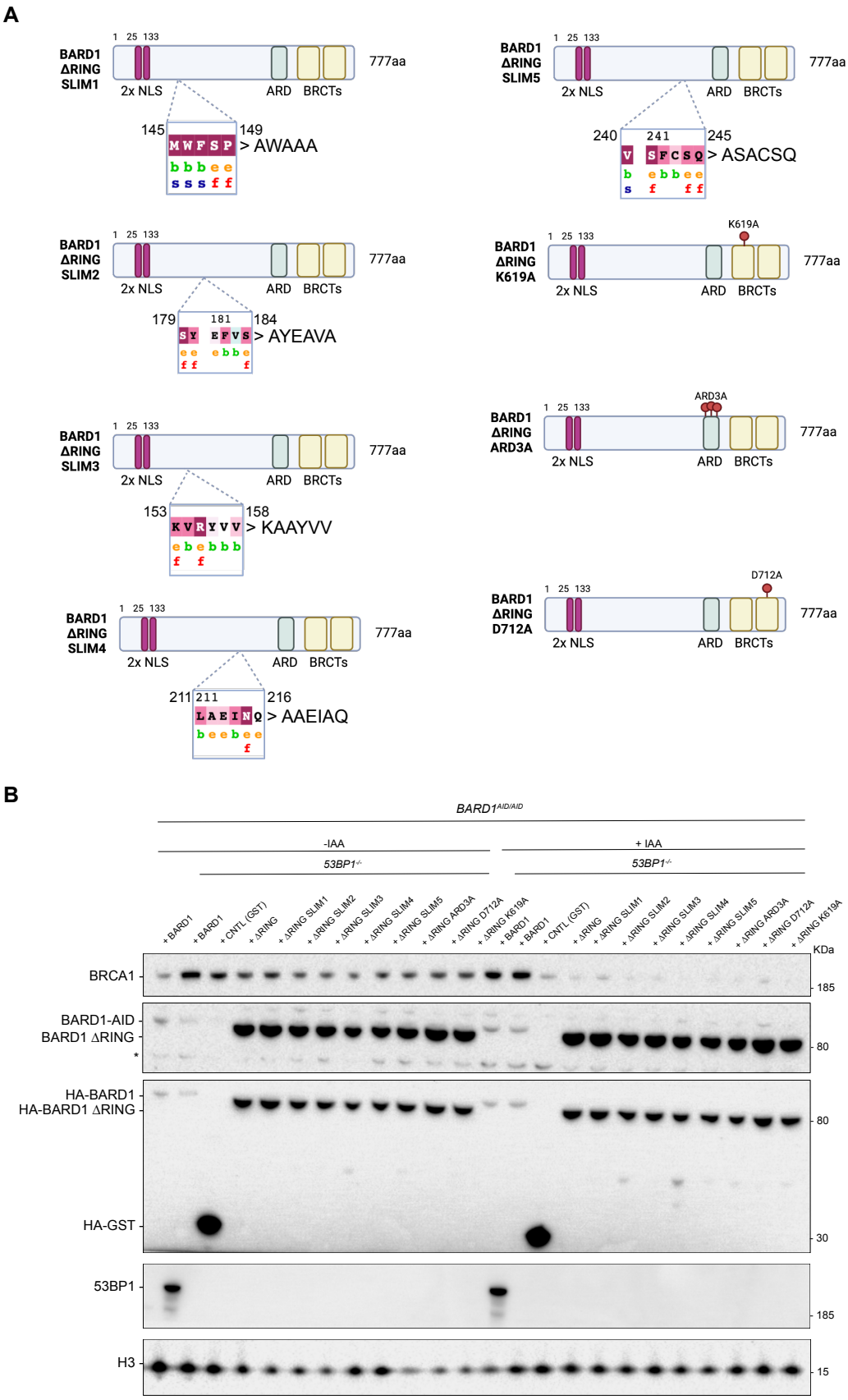


Figure 4.8 Generation of BARD1$^{\Delta RING}$ constructs harbouring mutations in the IDR or chromatin binding modules. (A) Schematic diagram illustrating the design of the RING domain deleted BARD1 constructs with alanine substitutions in the indicated SLIM regions or harbouring designated point mutations in the ARD or BRCT domains. SLIM1 was substituted to residues AWAAA; SLIM2 was substituted to residues AYEAVA; SLIM3 was

substituted to residues KAAYVV; SLIM4 was substituted to residues AAEIAQ; SLIM5 was substituted to residues ASACSQ. The respective ConSurf results detailing conservation scores of the selected SLIM regions are shown. Functional, f; Structural, s; Exposed, e; Buried, b. (B) Western blot indicating expression of BRCA1 and of the BARD1 endogenous and complemented transgenes. H3, loading control. BRCA1 (sc-6954), BARD1 (A300-263A), HA (3724), H3 (ab1791), 53BP1 (NB100-304). Asterisk (*) indicates a non-specific band.

mutations expressed in BARD1$^{\Delta RING}$ in *53BP1*$^{-/-}$ *BARD1*$^{\Delta/\Delta}$ cells collectively rendered hypersensitivity to olaparib (Figure 4.9). This suggests that the BARD1 IDR SLIMs could be supporting the restoration of DNA repair in 53BP1-deficient BARD1 RING-less cells in a cooperative manner to either promote the recruitment of DNA repair factors, or aid chromatin binding via the BARD1 ARD-BRCTs domains.

This prompted the question of whether *53BP1*$^{-/-}$ *BARD1*$^{\Delta/\Delta}$ +BARD1$^{\Delta RING}$ cells harbouring mutations in IDR sequences supported DNA repair functions of BARD1 by assisting BARD1 chromatin binding via the ARD-BRCTs domains. To analyse this, the auxin-treated *53BP1*$^{-/-}$ *BARD1*$^{\Delta/\Delta}$ cells expressing HA-tagged *BARD1*$^{\Delta RING\ mutated}$ transgenes were irradiated with 5Gy to induce DNA DSBs, and stained against HA-BARD1 and BRCA1. The drastic loss of BRCA1 and BARD1 IRIF in *BARD1*$^{\Delta/\Delta}$ +GST (control) cells was restored by re-expression of full-length BARD1 (Figure 4.10A). However, reconstituting *BARD1*$^{\Delta/\Delta}$ cells with BARD1^{D712A} only resulted in partial BRCA1 and BARD1 IRIF formation, in line with previous findings from our laboratory (Figure 4.10A) (Becker *et al.*, 2021). In comparison, *BARD1*$^{\Delta/\Delta}$ +BARD1$^{\Delta RING}$ cells support BARD1 recruitment to DNA damage sites in S-phase to the same degree as *BARD1*$^{\Delta/\Delta}$ +BARD1 cells (Figure 4.10A). RING-less BARD1 recruitment to DSB-associated chromatin sites is dependent on the nucleosome binding by the BARD1 ARD and tandem BRCTs, as BARD1$^{\Delta RING\ ARD3A}$ and BARD1$^{\Delta RING\ D712A}$ fully abrogated its localisation into IRIF (Figure 4.10B). Contrastingly, BARD1$^{\Delta RING\ K619A}$ did not render cells sensitive to olaparib due to deficient BARD1 recruitment to DNA damage sites, as its IRIF were still observed in EdU-positive cells (Figure 4.10B). This data indicates that PAR chain binding by the BARD1 tandem BRCTs is not required for BARD1

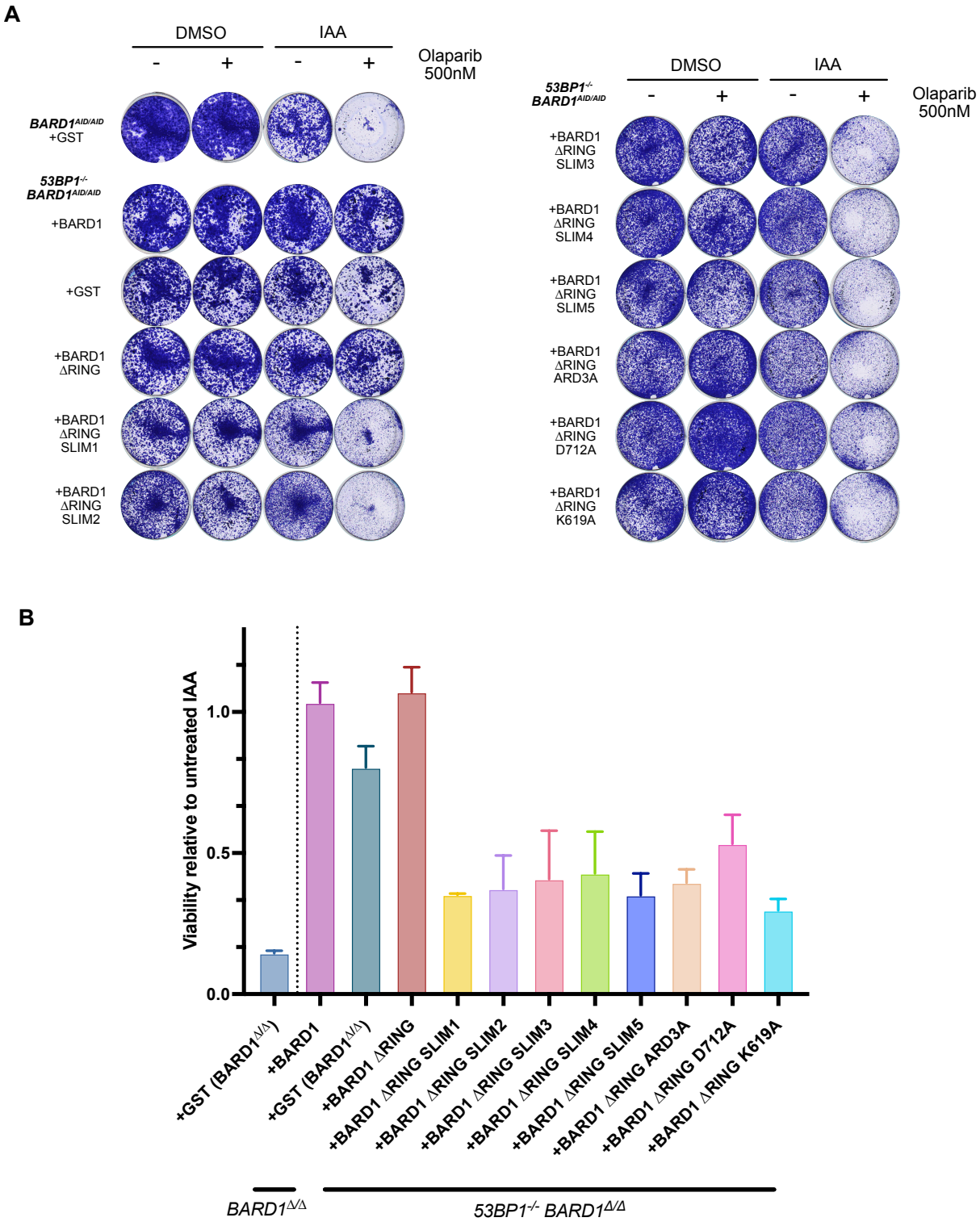
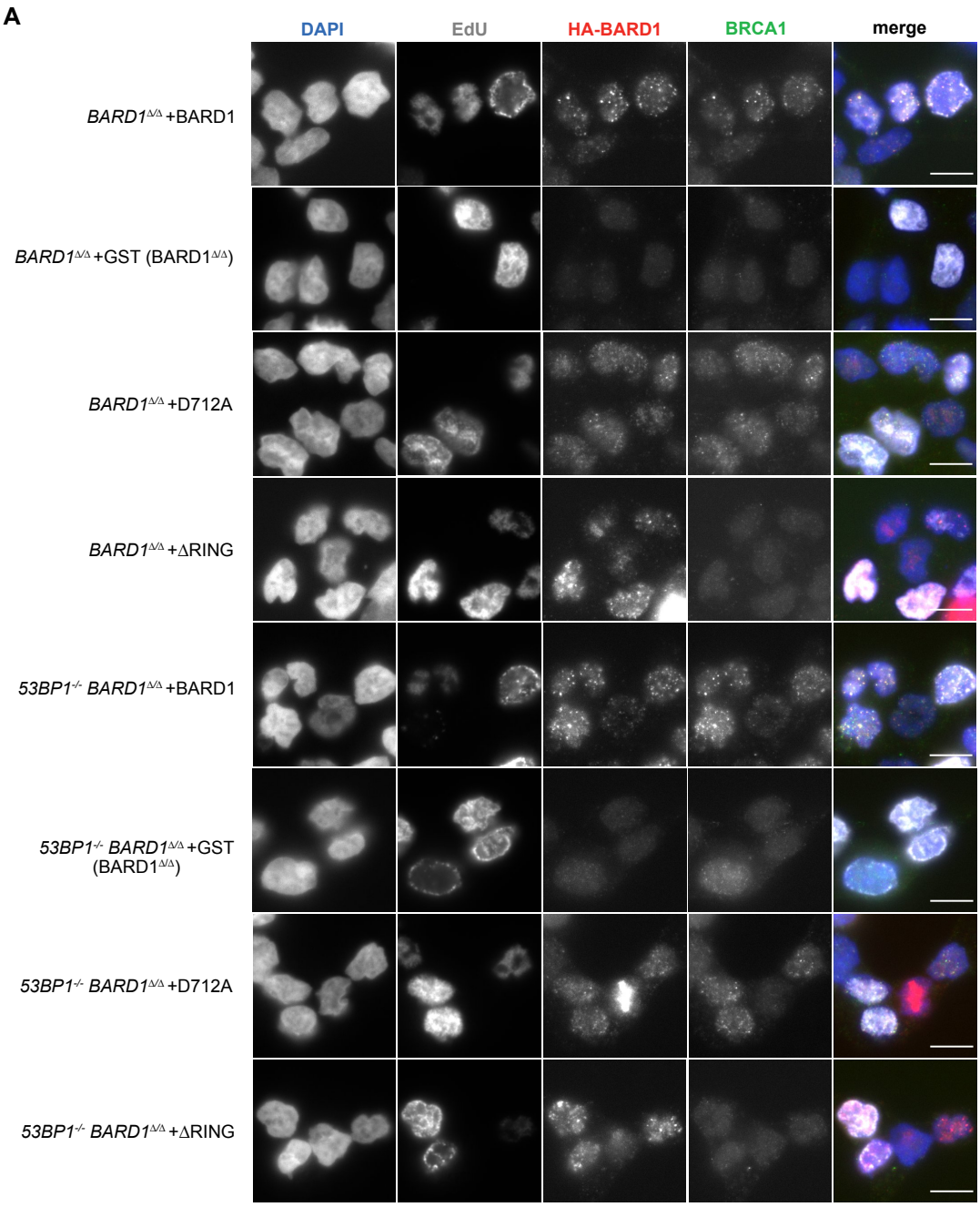


Figure 4.9 Redundant BARD1 IDR and chromatin binding features support BRCA1-independent DNA repair functions of BARD1. (A) Representative image of 7-day clonogenic survival assay of *53BP1*$^{-/-}$ *BARD1*$^{AID/AID}$ cells expressing *BARD1*$^{\Delta RING\ mutant}$ transgenes and the respective control cell lines. (B) Quantification of (A). Mean ± SD. *n* = 2 biological experiments, plated in duplicate.

recruitment to DSB sites. Interestingly, none of the IDR SLIM mutations in BARD1$^{\Delta RING}$ conferred BARD1 localisation defects (Figure 4.10B), indicating that the minimal sequence features required for BARD1 IRIF accumulation region are likely to correspond to a region spanning the C-terminal ARD and tandem BRCT domains (Becker *et al.*, 2021). Additionally, this data suggests that the DNA repair deficiency in *53BP1*$^{-/-}$ *BARD1*$^{\Delta/\Delta}$ cells complemented with *BARD1*$^{\Delta RING\ IDR\ mutated}$ transgenes is not due to ablation of BARD1 localisation at DNA damage-associated chromatin and indicates that these SLIMs do not support chromatin interactions crucial for BARD1 chromatin recruitment. Instead, it could be speculated that the BARD1 IDR sequences support additional DNA repair roles via nucleosomal DNA binding or by yet unknown protein-protein interactions.


A
DAPI
EdU
HA-BARD1
BRCA1
merge
BARD1Δ/Δ +BARD1
BARD1Δ/Δ +GST (BARD1Δ/Δ)
BARD1Δ/Δ +D712A
BARD1Δ/Δ +ΔRING
53BP1-/- BARD1Δ/Δ +BARD1
53BP1-/- BARD1Δ/Δ +GST (BARD1Δ/Δ)
53BP1-/- BARD1Δ/Δ +D712A
53BP1-/- BARD1Δ/Δ +ΔRING

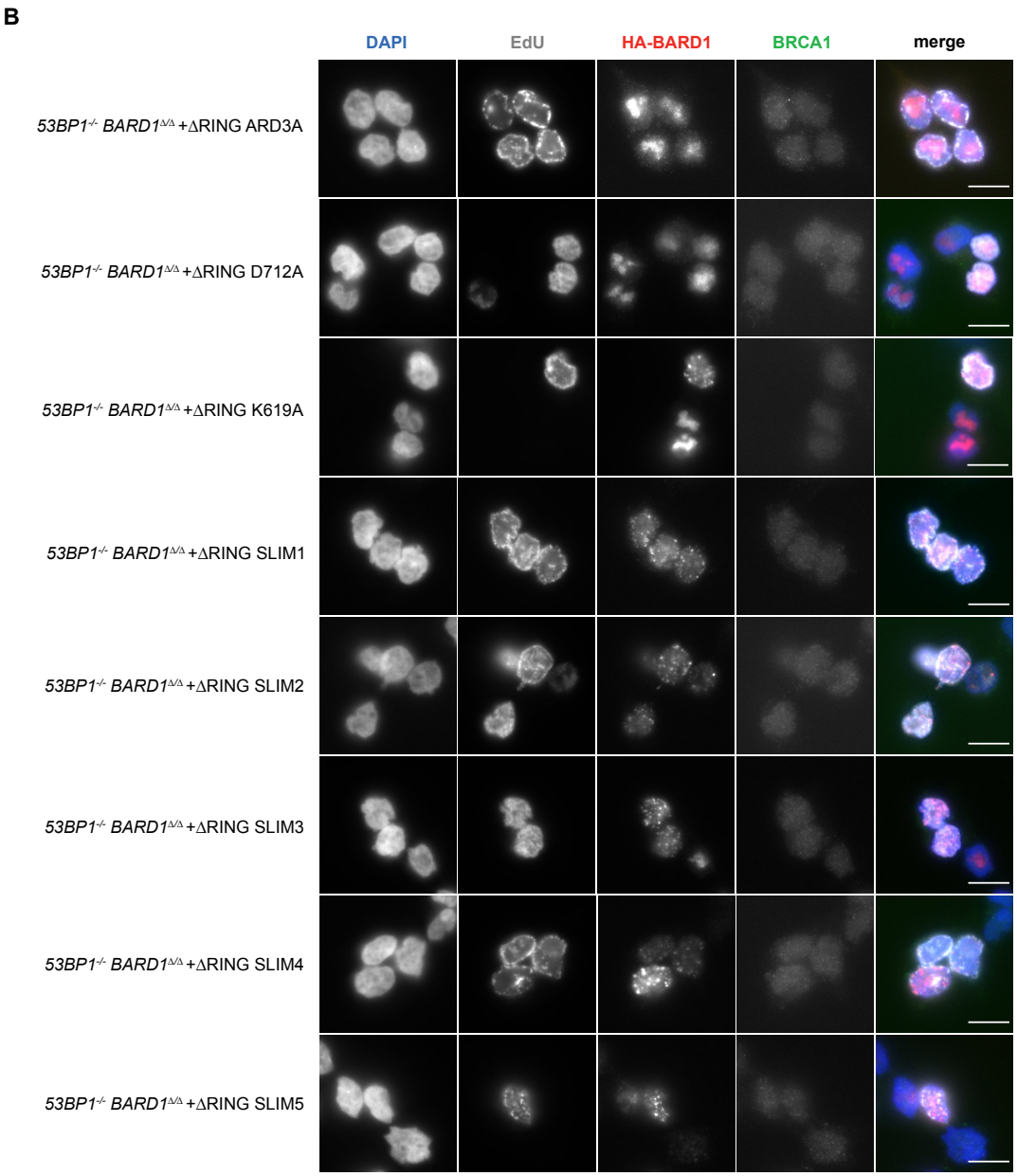


Figure 4.10 BARD1 recruitment to DSB sites is unaffected by mutations in the IDR in *53BP1*$^{-/-}$ *BARD1*$^{\Delta/\Delta}$ +BARD1$^{\Delta RING}$ cells. (A and B) Representative immunofluorescence images of BARD1 IRIF at DSB sites in *53BP1*$^{-/-}$ *BARD1*$^{\Delta/\Delta}$ +BARD1$^{\Delta RING\ mutated}$ cells. Cells were pulse-labelled with EdU for 10 minutes before being irradiated with 5Gy and recovered for 2 h. Scale bar, 10 µM. *n* = 3 biological experiments.

4.3 Concluding remarks

The importance of the BARD1 IDR in DNA repair has remained unclear. Previous reports indicated that the IDR has a RAD51-interacting motif required for D-loop formation and strand invasion (Zhao *et al.*, 2017), while other more recent reports identify a DNA-interacting motif within the IDR involved in promoting H2A ubiquitination catalysed by the BRCA1/BARD1-RING domains (Witus *et al.*, 2023). The findings presented in this chapter examined the contribution of IDR amino acid sequences in HCT116 cells and their resistance to DNA damaging agents olaparib and cisplatin to study the impact on DNA repair, and shed new light on both the non-essential functions of the BARD1 IDR and its intriguing ability to mediate some DNA repair activities, in an HR-restored *53BP1/BARD1*-double knockout background, independently of BRCA1.

Deletions within the highly conserved but disordered IDR region of BARD1 revealed that these cells remained resistant to PARPi olaparib and platinum-based drug cisplatin and did not affect BRCA1-BARD1 heterodimer protein expression levels, implying that this region is not crucial for efficient DNA double-strand break (DSB) repair. Deletions of $BARD1^{\Delta IDR1}$, or $BARD1^{\Delta 133\text{-}140}$ which repealed the BARD1-RAD51 interacting motif, did not result in olaparib hypersensitivity, and instead led to an extremely subtle sensitization, contrary to what was reported in cell survival assays by the Patrick Sung laboratory using BARD1 siRNA in HeLa cells (Zhao *et al.*, 2017). This indicates that this RAD51 interaction with BARD1 is not of fundamental importance during DNA repair, and might instead exert more subtle influences during D-loop formation. Additionally, while these IDR deletions did not result in sensitivity to olaparib or cisplatin, it cannot be ruled out that these motifs play important roles in other DNA repair contexts or cellular contexts, as it was recently reported that BARD1 contains an

SLX4-interacting motif required to promote resolution of HR and DNA replication intermediates via the SMX complex, the loss of which together with BLM deficiency leads to synthetic sickness in a *BRCA1/BARD1*-depleted setting (Tsukada *et al.*, 2024). Furthermore, it was recently shown that the IDR in BARD1 supports the BRCA1/BARD1-RING E3 ligase activity and caused olaparib and cisplatin sensitivity, and reduced BARD1 foci formation in olaparib-treated HeLa-shBARD1 cells expressing a BARD1 truncation between residues 194-216 (Witus *et al.*, 2023). Therefore, based on my results it could also hypothesized that these functions are crucial for BRCA1 localisation to sex chromosomes in meiosis during male germline development, but dispensable during somatic cell DNA repair, at least in MMR-defective HCT116 cells.

Additionally, the findings presented in this chapter highlighted the BRCA1-independent functions of BARD1 during DNA repair. *BARD1*$^{\Delta/\Delta}$ BARD1$^{\Delta RING}$-expressing cells were hypersensitive to olaparib and cisplatin, confirming that the loss of BRCA1 destabilizes the BRCA1-BARD1 complex leading to complete loss of its DNA repair functions. Interestingly, in a 53BP1-deficient background, *BARD1*$^{\Delta RING}$ cells rescue olaparib sensitivity to wild-type levels. This finding is particularly significant as it demonstrates that BARD1, even without BRCA1, promotes DNA repair functions outside of HR. The observation that 53BP1 loss led to RAD51 hyperaccumulation in BRCA1/BARD1-proficient cells is likely due to the loss of 53BP1-Shieldin-mediated DNA end fill-in synthesis which suppresses end resection (King *et al.*, 2024). However, 53BP1 loss in *BARD1*$^{\Delta/\Delta}$ +BARD1 cells did not lead to the accumulation of toxic HR repair intermediates according to the SCE levels in PARPi olaparib-treated cells. The observation that the loss of BARD1 H4K20me0/H2AK15ub chromatin binding upon loss of 53BP1 promotes SCE formation under stochastic conditions indicates that SCEs can result from HR-dependent and HR-independent mechanisms. Interestingly, a recent report showed that

SCE formation does not only depend on HR factors but can also result from replication-associated perturbations which result in under-replicated DNA and rely on Polθ-mediated repair (Heijink *et al.*, 2022). Therefore, the endogenous SCE levels observed in 53BP1-deficient *BARD1*$^{\Delta/\Delta}$ +D712A cells could be supported by POLθ and/or BRCA1-A dependent DNA repair functions at under-replicated DNA. This would align with my previous findings showing that BARD1^{D712}-H2AK15ub interaction can suppress RAP80 at DNA DSB sites (Figure 3.9 and Figure 3.10).

The chromatin-binding properties of BARD1, particularly its interaction with H4K20me0 and H2AK15ub, were critical. Contrarily, the short linear motifs (SLIMs) within the IDR are not required for BARD1 recruitment to chromatin but perhaps could support the structural conformation of the BARD1 RING and ARD-tandem BRCTs domains binding onto the nucleosome core particle, acting as a linker between the N-terminal and C-terminal domains of BARD1 (Burdett *et al.*, 2023; Witus *et al.*, 2023). Interestingly, the DNA binding region between amino acids 194-216 in the BARD1 IDR was reported to be important for BARD1 IRIF formation in cells treated with olaparib, and loss of this region lead to cisplatin and olaparib sensitivity in HeLa-shBARD1 cells (Witus *et al.*, 2023). Therefore, further studies on the physiological relevance of the BARD1 IDR in different cellular contexts will be of interest.

In conclusion, this chapter characterised the importance of the BARD1 disordered regions and their functional cooperation with BARD1 chromatin binding domains during DNA repair, highlighting that the IDR is not crucial for HR repair mediated by the BRCA1-BARD1 complex in the HCT116 *BARD1*$^{AID/AID}$ cell line model based on the response to DNA DSB damage-inducing agents olaparib and cisplatin, and likely plays a role in alternative DNA repair contexts. Furthermore, the future characterization of the mechanism that supports the previously unknown independent HR-promoting functions of BARD1 in NHEJ-deficient cells

will be of future interest. These findings not only expand the known functional repertoire of BARD1 but also suggest potential therapeutic implications, particularly in targeting BRCA1-independent repair mechanisms in cancers with BARD1 RING domain deletion mutations or 53BP1 deficiencies.

Chapter 5

In vivo importance of the BARD1 dual-reader domain

5.1 Introduction

The exact BRCA1-BARD1 chromatin-interacting regions necessary for male spermatogenesis are still not fully understood. It is also unclear whether BRCA1's role in this process depends on BARD1 recognizing and binding to H2AK15ub. This interaction might be important for recruiting BRCA1 to meiotic DSBs and unsynapsed chromosome segments, which are crucial for MSCI and normal meiotic progression, in addition to the somatic DNA repair functions.

Previous work showed that mice homozygous for the isoleucine 26 to alanine mutation in the BRCA1 RING domain (*Brca1*$^{I26A/I26A}$), which by blocking binding to E2 enzymes selectively inactivates the BRCA1-BARD1 E3 ligase activity without disrupting the BRCA1-BARD1 interaction, did not have an increased predisposition for developing tumours, although male mice were infertile (Shakya *et al.*, 2011). To consider is that the BRCA1 I26A mutant was shown to retain residual E3 ligase activity (Stewart *et al.*, 2017; Wang *et al.*, 2023), while it was also shown to sensitise cells to genotoxic agents in HeLa-shBRCA1 cells (Wang *et al.*, 2023), and cause cisplatin sensitivity in 293T cells although the BRCA1 I26A mutation was also shown to destabilise BARD1 expression in these cells (Anantha *et al.*, 2017). Contrastingly, the serine-1598-phenylalanine (S1598F) mutation that disrupts the phosphoprotein recognition by the BRCA1 tandem BRCT domain led to tumour-prone mice as well as male infertility in *Brca1*$^{S1598/S1598}$ mice (Shakya *et al.*, 2011). This suggests that the BRCA1 E3 ligase function is dispensable for tumour suppression in mice, contrarily to the BRCA1-tandem BRCT domain, while both

domains play a role in spermatogenesis. Furthermore, the C61G mutation in the BRCA1 RING disrupts both the E3 ligase activity and the heterodimerization with the BARD1 RING domain (Hashizume *et al.*, 2001). The C61G mutation resulted in embryonic lethality at E12.5 and contributed to tumour development in the *K14cre;Brca1$^{F/C61G}$;p53$^{F/F}$* (*KB1C61GP*) mouse mammary tumour model (Drost *et al.*, 2011). Interestingly, *53bp1$^{-/-}$* mice harbouring exon 2 mutations in *Brca1* which result in a RINGless BRCA1 isoform displayed male infertility and ectopic γH2AX staining outside of the sex body indicating defective meiotic DNA DSB repair (Li *et al.*, 2016). These reports suggest that the chromatin binding domains in BARD1 or the BRCA1-BARD1 RING heterodimer might have additional roles required for spermatogenesis.

The work presented in the previous chapters and previous work from the lab (Becker *et al.*, 2021) have shown the importance of the BARD1 dual-reader domain in promoting HR repair via recruitment of BRCA1 to DNA DSB sites and in regulating chromatin accessibility for RAP80 recruitment. What remained unexplored were the *in vivo* functions of the BARD1 H2AK15ub-binding domain for tumour suppression and male spermatogenesis.

Loss of *Brca1* and *Bard1* leads to early embryonic lethality at E7.5-E8.5 (Hakem *et al.*, 1996; Ludwig *et al.*, 1997; McCarthy *et al.*, 2003). Given that DNA damage-dependent H2AK15ub binding by the tandem BRCTs domain in BARD1 is essential for BRCA1-BARD1 heterodimer recruitment to chromatin (Becker *et al.*, 2021; Krais *et al.*, 2021), we generated the *Bard1$^{D700A/D700A}$ 53bp1$^{L1616A/L1616A}$* genetically engineered mouse model to study the *in vivo* importance of the BARD1 dual-reader domain in tumour suppression and male fertility. The *Bard1$^{D700A/D700A}$ 53bp1$^{L1616A/L1616A}$* mouse model harbours the homozygous D700A mutation (equivalent to BARD1-BUDR D712A in humans) in the tandem BRCTs domain, and the homozygous L1616A mutation in *53bp1* located in the UDR domain (equivalent to 53BP1 UDR-L1619A in humans) (Figure 5.1B). The corresponding L1619A substitution in human 53BP1 was

previously found to abrogate the binding of RNF168-dependent H2AK15ub, blocking 53BP1 focus formation, disrupting CSR and 53BP1-dependent NHEJ, with the mutations I1617A and L1619A having the most pronounced impact on 53BP1 focus formation (Zgheib *et al.*, 2008; Fradet-Turcotte *et al.*, 2013). Additionally, in this chapter I examined the *Brca1*$^{\Delta 5\text{-}13/\Delta 5\text{-}13}$ *53bp1*$^{-/-}$ genetically engineered mouse model, hereafter *Brca1*$^{-/-}$ *53bp1*$^{-/-}$, which contains *Brca1* exon 5 to 13 deletions ablating all BRCA1 protein expression (Liu *et al.*, 2007) and *53bp1* exon 18 deletion (Figure 5.1A) (Ward *et al.*, 2003).

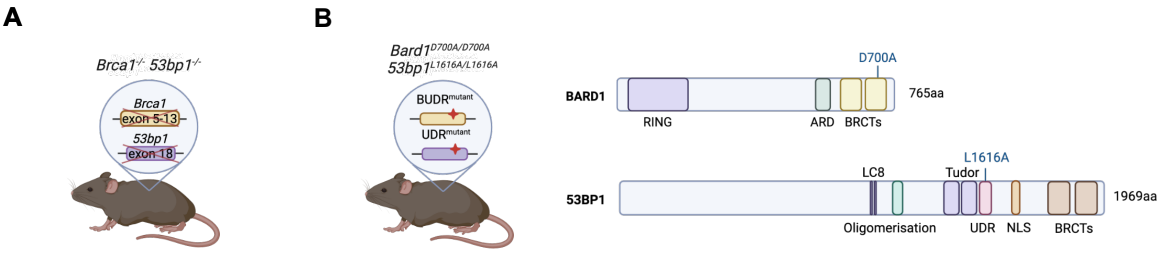


Figure 5.1 *Brca1* and *Bard1* genetically engineered mouse models. (A) Schematic diagram of the double-knockout *Brca1* (homozygous exon 5-13 deletion) and *53bp1* (homozygous exon 18 deletion) mouse. (B) Schematic diagram of the double-mutant *Bard1* (homozygous D700A mutation) and *53bp1* (homozygous L1616A mutation) mouse with the respective protein domain architecture diagram showing the domain location of these point mutations.

5.2 Results

5.2.1 Viability of *Bard1*$^{D700A/D700A}$ mice in *53bp1*$^{L1616A/L1616A}$ and *53bp1*$^{+/+}$ backgrounds

We interbred heterozygous *Brca1*$^{+/\Delta 5\text{-}13}$ (*Brca1*$^{+/-}$), homozygous *53bp1*$^{-/-}$ mice to obtain *Brca1* and *53bp1* double-knockout mice. In line with previous reports, 53BP1 loss rescued embryonic lethality of BRCA1-deficient mice (Chen *et al.*, 2020; King *et al.*, 2024), yielding embryos of developmental stage E12.5 at expected frequencies. However, *Brca1*$^{-/-}$ *53bp1*$^{-/-}$ mice were born at lower Mendelian ratios, with only approximately 9% of the expected

A

***Brca1*$^{+/-}$ *53bp1*$^{-/-}$ x *Brca1*$^{+/-}$ *53bp1*$^{-/-}$**			
Brca1	+/+	+/-	-/-
53bp1	-/-	-/-	-/-
Live pups (n=300)	108 (75)	166 (150)	26 (75)
Embryos (E12.5) (n=30)	6 (7.5)	17 (14)	7 (7.5)

B

***Bard1*$^{+/D700A}$ *53bp1*$^{L1616A/L1616A}$ x *Bard1*$^{+/D700A}$ *53bp1*$^{L1616A/L1616A}$**			
Bard1	+/+	+/D700A	D700A/D700A
53bp1	L1616A/L1616A	L1616A/L1616A	L1616A/L1616A
Live pups (n=135)	48 (33.75)	56 (67.5)	31 (33.75)
Embryos (E12.5) (n=15)	4 (3.75)	8 (7.5)	3 (3.75)

C

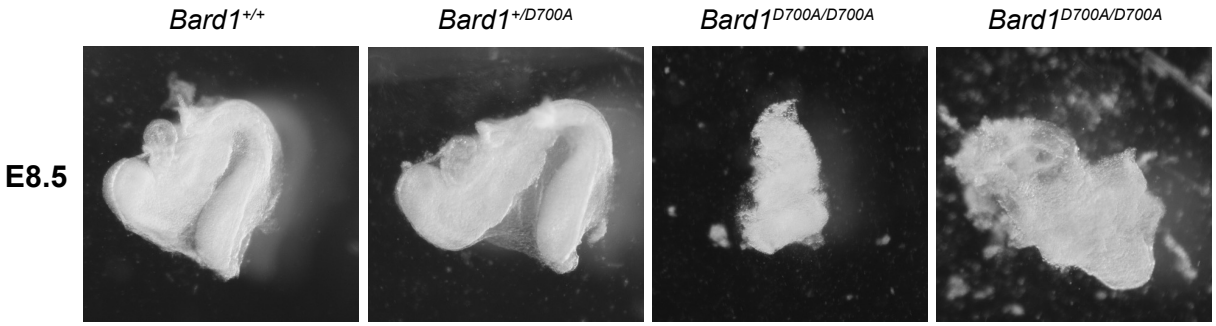


Figure 5.2 *53bp1*$^{L1616A/L1616A}$ rescues embryonic lethality of *Bard1*$^{D700A/D700A}$ mice and results in mice born at expected Mendelian ratios. (A and B) Summary of observed live mice at 3 weeks or >E12.5 embryos of indicated genotypes. (C) E8.5 embryos indicating embryonic lethality in *Bard1*$^{D700A/D700A}$ genotypes. Data obtained by Dr Jean Metson.

frequency of 25% embryos being born to *Brca1*$^{+/-}$ intercrosses in a *53bp1*-knockout background (Figure 5.2A, data obtained by Dr Jean Metson). This indicates that a significant number of *Brca1*$^{-/-}$ *53bp1*$^{-/-}$ die after E12.5, in the late gestation period of embryonic development. In comparison, interbreeding of *Bard1*$^{+/D700A}$ heterozygous mice in a homozygous *53bp1*$^{L1616A/L1616A}$ background, led to *Bard1*$^{D700A/D700A}$ *53bp1*$^{L1616A/L1616A}$

homozygous offspring born at expected Mendelian frequencies, as well as E12.5 embryos detected at expected frequencies (Figure 5.2B, data obtained by Dr Jean Metson). By contrast, homozygous *Bard1*$^{D700A/D700A}$ mice were not viable in a *53bp1*$^{+/+}$ background, where *Bard1*^{D700A} homozygosity was found to result in severe developmental delays and embryonic lethality at E8.5 (Figure 5.2C, data obtained by Dr Jean Metson). These observations indicate that the engagement of BARD1 with H2AK15ub for HR is essential during embryonic development owing to toxic 53BP1 activity. Testament to this, by mutating the corresponding ubiquitin-binding motif in 53BP1 which ablates 53BP1 chromatin recruitment via substitution of leucine 1616 to alanine (L1616A) (Raquel Cuella Martin, unpublished; (Fradet-Turcotte *et al.*, 2013), BARD1-H2AK15ub interactions are rendered non-essential, resulting in viable *Bard1*$^{D700A/D700A}$ *53bp1*$^{L1616A/L1616A}$ mice.

5.2.2 *In vivo* functions of the BARD1 dual reader domain in Homologous Recombination: Phenotypic characterisation of *Bard1*$^{D700A/D700A}$ *53bp1*$^{L1616A/L1616A}$ mutant mice

In contrast to *Brca1*$^{-/-}$ *53bp1*$^{-/-}$ mice which are smaller in size and weight compared to their *53bp1*$^{-/-}$ littermates (King *et al.*, 2024), *Brca1*$^{-/-}$ *53bp1*$^{L1616A/L1616A}$ mice display a slight growth deficiency in comparison to *53bp1*$^{L1616A/L1616A}$ mice as indicated by their weights (Figure 5.3A, data obtained by Dr Jean Metson). This suggests that the loss of *Brca1* itself, and not *53bp1*, is responsible for developmental retardation in *Brca1*$^{-/-}$ *53bp1*$^{-/-}$ mice (Figure 5.3A). By contrast, whole-body weights of *Bard1*$^{D700A/D700A}$ *53bp1*$^{L1616A/L1616A}$ mice were similar to *53bp1*$^{L1616A/L1616A}$ mice indicating that the loss of H2AK15ub-binding in *Bard1* does not cause growth defects (Figure 5.3A).

Bard1$^{D700A/D700A}$ *53bp1*$^{L1616A/L1616A}$ mice did not develop any tumours and had lifespans resembling *53bp1*$^{L1616A/L1616A}$ mice, contrary to double-knockout *Brca1*$^{-/-}$ *53bp1*$^{-/-}$ mice which developed thymic lymphomas between 12-20 weeks of age (Figure 5.3B, data obtained by Dr Jean Metson), in line with previous reports (Li *et al.*, 2016; Nacson *et al.*, 2018; Chen *et al.*, 2020). We found that BRCA1-deficient mice harbouring the *53bp1*$^{L1616A/L1616A}$ mutation also succumbed to thymic lymphoma, however, this occurred slightly later compared to the *53bp1*$^{-/-}$ mice, where the median tumour-free survival increased from 17 to 22 weeks (Figure 5.3B). To investigate if the *Bard1*$^{D700A/D700A}$ *53bp1*$^{L1616A/L1616A}$ mice had increased lifespans due to lower levels of systemic genomic instability, we analysed the levels of micronuclei from normochromatic erythrocytes (NCE). NCE from *53bp1*$^{-/-}$ and *53bp1*$^{L1616A/L1616A}$ mice had the wild-type frequencies of micronuclei (Figure 5.3C, data obtained by Dr Jean Metson). Likewise, *Bard1*$^{D700A/D700A}$ *53bp1*$^{L1616A/L1616A}$ mice displayed similar levels of micronucleation in NCE, which was in striking contrast to both *Brca1*$^{-/-}$ *53bp1*$^{-/-}$ and *Brca1*$^{-/-}$ *53bp1*$^{L1616A/L1616A}$ mice which showed similar 5-fold increases in micronuclei levels over that measured in wild-type mice (Figure 5.3C). Indeed, the high level of micronucleated NCE observed in *Brca1*$^{-/-}$ *53bp1*-deleted/mutated mice indicates that while loss of 53BP1 can restore HR and rescue embryonic development in *Brca1*-null mice, it cannot fully restore genome stability (Figure 5.3B). Interestingly, the wild-type frequencies of micronuclei observed in the erythrocytes of *Bard1*$^{D700A/D700A}$ *53bp1*$^{L1616A/L1616A}$ mice indicates a more complete phenotypic rescue that infers that BARD1 BUDR-dependent binding to H2AK15ub at DSBs primarily functions to antagonise 53BP1-dependent DNA repair activities that are dependent upon binding to the same histone modification. The fact that *Bard1*$^{D700A/D700A}$ *53bp1*$^{L1616A/L1616A}$ mice are not tumour-prone, reveals BARD1^{D700A} to be a separation of function mutant of BRCA1-BARD1,

that mediates additional important tumour suppressive functions in BRCA1/BARD1 through the formation of an intact BRCA1-BARD1$^{D700A/D700A}$ heterodimer.

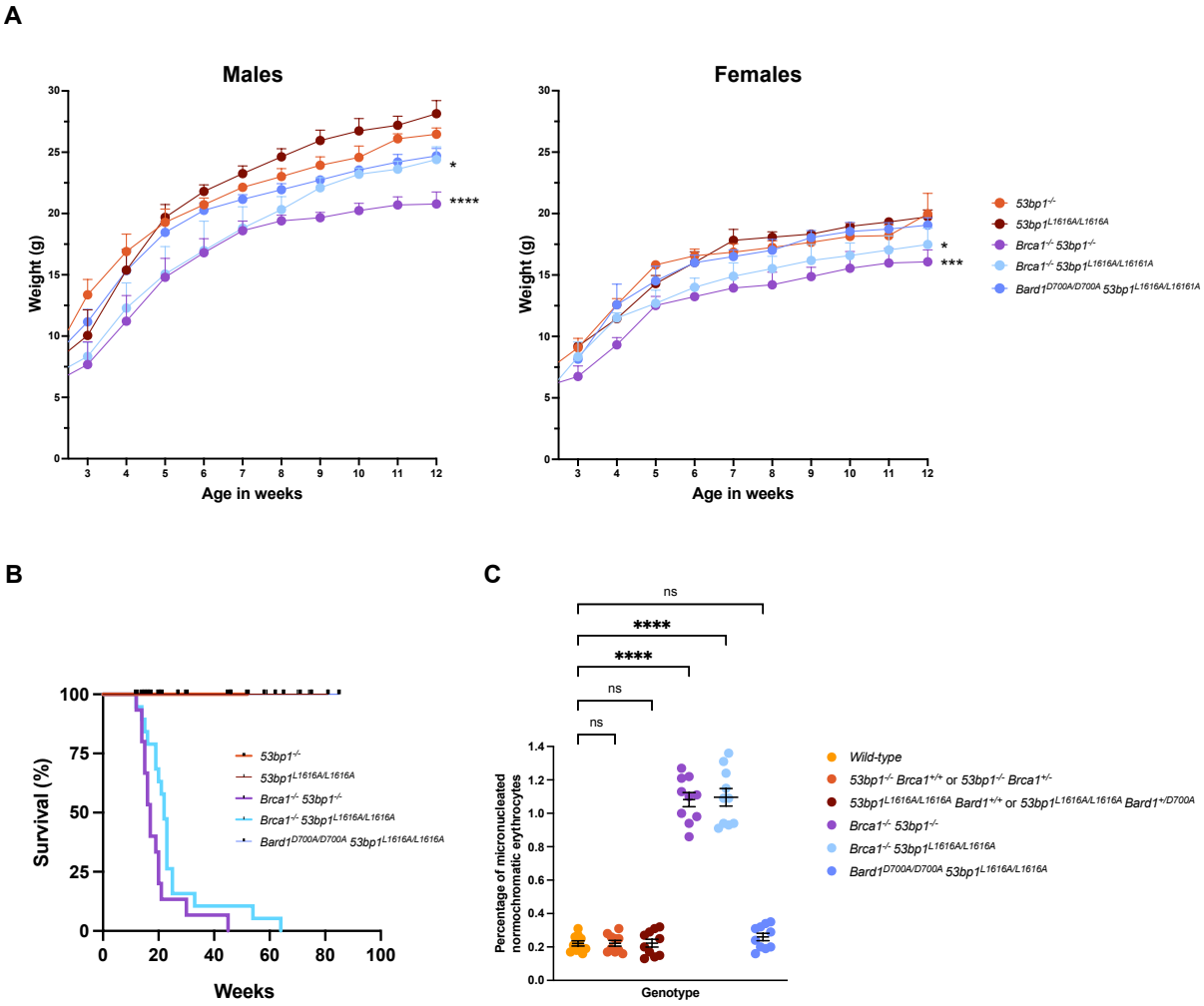


Figure 5.3 *Bard1$^{D700A/D700A}$ 53bp1$^{L1616A/L1616A}$* mice are not tumour-prone and do not accumulate systemic genomic instability. (A) Whole-body weights of male and female mice of 3-12 weeks of age of indicated genotypes. *n*=5 mice per genotype. Mean ± SEM. Ordinary one-way ANOVA with Dunnett's multiple comparison test was performed on the 12-week data point to determine statistical significance. (B) Kaplan-Meier survival curve of mice with indicated genotypes. (C) Micronuclei in normochromatic erythrocytes as a percentage of total normochromatic erythrocytes from tail vein blood of 8-12 weeks of age mice. *n*=10 mice per genotype. Mean ± SEM. Significance was determined by ordinary one-way ANOVA with Dunnett's multiple comparison test. ns, not significant; * p<0.05; *** p<0.001; **** p<0.0001. Data obtained by Dr Jean Metson.

5.2.3 *In vivo* functions of the BARD1 dual reader domain in male germline development

Next, I questioned if the BARD1 H2AK15ub-binding motif was required for male spermatogenesis, and if the male infertility resulting from *Brca1* loss is due to the loss of the BARD1-dependent binding to H2AK15ub at meiotic DSBs. We found that the testes of *Brca1*$^{-/-}$ *53bp1*$^{-/-}$ and *Brca1*$^{-/-}$ *53bp1*$^{L1616A/L1616A}$ mice were significantly smaller when compared to that of wild-type mice, or their *53bp1* single-knockout/L1616A-knockin mutant littermates (Figure 5.4A and B, data obtained by Dr Jean Metson). This is in agreement with previous findings, where 53BP1-deletion could not restore fertility to *Brca1*-mutant male mice (Broering *et al.*, 2014; Li *et al.*, 2016). Surprisingly, the testes of *Bard1*$^{D700A/D700A}$ *53bp1*$^{L1616A/L1616A}$ mice were similar in size (data not shown) and weight to that of wild-type mice, and these mice were not infertile (Figure 5.4A). Intrigued by this contrasting phenotype, I analysed the distribution of different types of meiosis prophase I cells to check if the BARD1^{D700A} mutation affected meiotic progression during spermatogenesis. Pachytene cells of *Bard1*$^{D700A/D700A}$ *53bp1*$^{L1616A/L1616A}$ male mice had no meiotic progression defects, similar to wild-type or *53bp1*-knockout/mutated pachytene cells (Figure 5.4C). Contrastingly, pachytene cells derived from *Brca1*$^{-/-}$ *53bp1*$^{-/-}$ double-mutant mice had no diplotene cells, indicating that these cells undergo apoptosis after pachytene, although *53bp1*$^{L1616A/L1616A}$ seems to have a slight rescue effect (Figure 5.4C). According to an unpaired two-tailed t-test, this rescue of *Brca1*$^{-/-}$ *53bp1*$^{L1616A/L1616A}$ diplotene population was not statistically significant to the diplotene population in wild-type spermatocytes indicating that although observed in smaller percentages, in *Brca1*$^{-/-}$ *53bp1*$^{L1616A/L1616A}$ spermatocytes, some pachytene cells escape into diplotene. Further analysis of *Brca1*$^{-/-}$ *53bp1*$^{L1616A/L1616A}$ spermatocytes will be required to

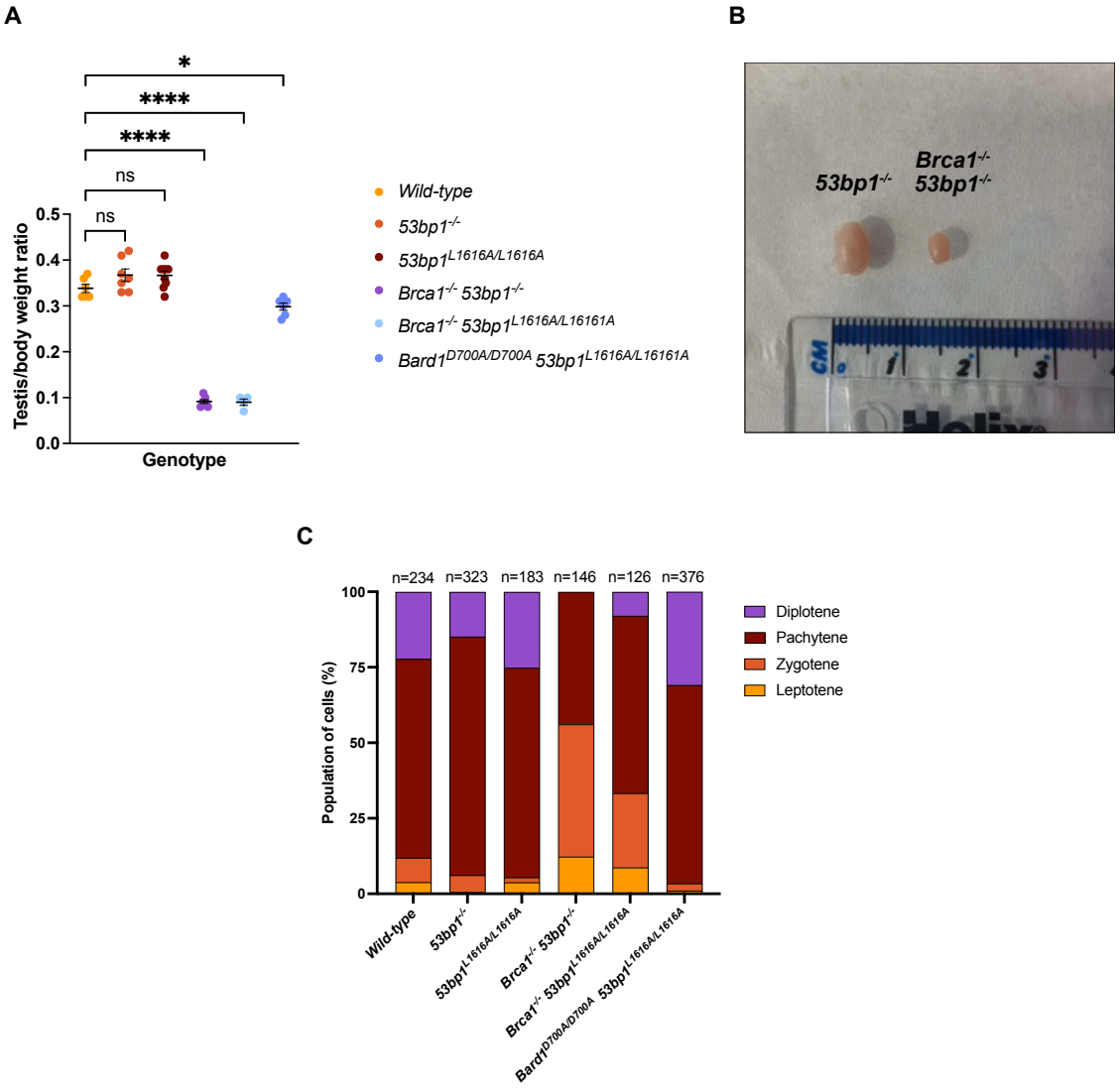


Figure 5.4 BARD1 H2AK15ub-binding ablation does not cause male germline development defects. (A) Testis/body weight ratio of mice of indicated genotypes. Wild-type *n*=6 mice; *53bp1*$^{-/-}$ *n*=4 mice; *53bp1*$^{L1616A/L1616A}$ *n*=7 mice; *Brca1*$^{-/-}$ *53bp1*$^{-/-}$ *n*=4 mice; *Brca1*$^{-/-}$ *53bp1*$^{L1616A/L1616A}$ *n*=2 mice; *Bard1*$^{D700A/D700A}$ *53bp1*$^{L1616A/L1616A}$ *n*=3 mice. Mean ± SEM. Ordinary one-way ANOVA with Dunnett's multiple comparison test was performed to determine statistical significance. ns, not significant; * p<0.05; **** p<0.0001. (B) Testes of 8-week-old *53bp1*$^{-/-}$ and *Brca1*$^{-/-}$ *53bp1*$^{-/-}$ mice showing strike difference in testis size. Data obtained by Dr Jean Metson. (C) Distribution of meiotic prophase I spermatocytes as a percentage of total analysed cells from mice in indicated genotypes. The number of analysed cells is indicated on the graph. *n*=2 mice per genotype.

determine the extent of the diplotene cell rescue. Although contradictory to the p53-mediated quality control functions which are reinstated in the *53bp1*$^{L1616A/L1616A}$ mice (Cuella-Martin *et al.*, 2016), it can be speculated that the restored 53BP1-p53 interaction in *Brca1*$^{-/-}$ *53bp1*$^{L1616A/L1616A}$ spermatocytes allows for some pachytene cells to progress into the next

stage in diplotene although the unrepaired meiotic DSBs and failed MSCI eventually lead to cell death shortly after, as testes of *Brca1*$^{-/-}$ *53bp1*$^{L1616A/L1616A}$ display atrophy like in *Brca1*$^{-/-}$ *53bp1*$^{-/-}$ mice (Figure 5.4A). This data is consistent with previous findings which showed that BRCA1-deficient mice have elevated levels of apoptotic pachytene cells and the absence of mature spermatozoa in the seminiferous tubule's lumen (Xu *et al.*, 2003; Broering *et al.*, 2014; Li *et al.*, 2016).

5.2.4 Meiotic BRCA1 recruitment does not rely on the BARD1 BUDR-dependent recruitment mechanism

The stark contrast between the spermatogenesis defects of *Brca1*$^{-/-}$ *53bp1*$^{-/-}$ or *Brca1*$^{-/-}$ *53bp1*$^{L1616A/L1616A}$ mice, and absence of apparent defects in *Bard1*$^{D700A/D700A}$ *53bp1*$^{L1616A/L1616A}$ mice prompted me to analyse the recruitment of known DNA damage response factors important for male germline development and meiotic sex chromosome inactivation (MSCI). From pachytene, γH2AX concentrates on the XY sex chromosomes, forming the γH2AX domain which is also linked to the chromatin condensation of X and Y chromosomes to form the sex body (Fernandez-Capetillo *et al.*, 2003). The formation of the sex body is required for MSCI; disruption of sex body formation or *h2ax* loss leads to failure in transcriptional silencing during male spermatogenesis resulting in infertility (Royo *et al.*, 2010). Therefore, to test the hypothesis that the BARD1 BUDR is required for meiotic sex chromosome inactivation and BRCA1 recruitment in meiosis, I performed immunostaining on meiotic chromosome spreads prepared from testes of *Brca1*$^{-/-}$ *53bp1*$^{-/-}$, *Brca1*$^{-/-}$ *53bp1*$^{L1616A/L1616A}$, and *Bard1*$^{D700A/D700A}$ *53bp1*$^{L1616A/L1616A}$ mice to analyse sex body formation in pachytene cells. Loss of 53BP1 or the H2AK15ub-binding function of the 53BP1 UDR domain did not appear to affect γH2AX

formation/immunostaining patterns, and the establishment of the sex body in spermatocytes of *Bard1*$^{D700A/D700A}$ *53bp1*$^{L1616A/L1616A}$ mice appeared to be indistinguishable from wild-type spermatocytes (Figure 5.5A and B). By contrast, *Brca1*$^{-/-}$ spermatocytes, irrespective of complete 53BP1-deleted or UDR-mutated status, were unable to form a γH2AX domain and show aberrant γH2AX immunostaining signal across autosomal chromosomes and chromatin loops (Figure 5.5A and B). The formation of the γH2AX domain depends on the recruitment of BRCA1 to the sex chromosomes (Xu *et al.*, 2003; Turner *et al.*, 2004; Broering *et al.*, 2014). Consequently, I wondered if BRCA1 was recruited to the XY chromosomes in pachytene in *Bard1*$^{D700A/D700A}$ *53bp1*$^{L1616A/L1616A}$ spermatocytes, independently of the H2AK15ub-binding by the BARD1 BUDR motif. Contrary to *Brca1*$^{-/-}$ *53bp1*$^{-/-}$ spermatocytes where all BRCA1 protein expression is lost due to deletion of exons 5-13 (Figure 5.5C), pachytene chromosomes in *Bard1*$^{D700A/D700A}$ *53bp1*$^{L1616A/L1616A}$ spermatocytes were proficient for BRCA1 recruitment to the unsynapsed regions of the X and Y chromosomes and, like in wild-type pachytene cells, exhibited normal BRCA1 recruitment patterns (Figure 5.5C).

Unrepaired meiotic DNA DSBs account for synapsis failure in autosomes which triggers the asynapsis checkpoint and meiotic progression arrest (Turner, 2015). I questioned if the pachytene arrest following loss of BRCA1 was not only due to failing the onset of MSCI but also due to the accumulation of unrepaired SPO11-induced DSBs which hinders synapsis in autosomes (Wojtasz *et al.*, 2012). The meiotic synapsis surveillance protein HORMAD2 localises to the axial elements at asynapsed chromosomes. Therefore, during pachytene, it is only recruited to the asynapsed X and Y chromosomes (Wojtasz *et al.*, 2009; Kogo *et al.*, 2012). Accordingly, in both wild-type and *Bard1*$^{D700A/D700A}$ *53bp1*$^{L1616A/L1616A}$ spermatocytes, HORMAD2 was only localised to the sex chromosomes whereas in *Brca1*$^{-/-}$ *53bp1*$^{-/-}$

spermatocytes HORMAD2 was localised aberrantly on autosomes indicating synapsis failure of homologs (Figure 5.5D).

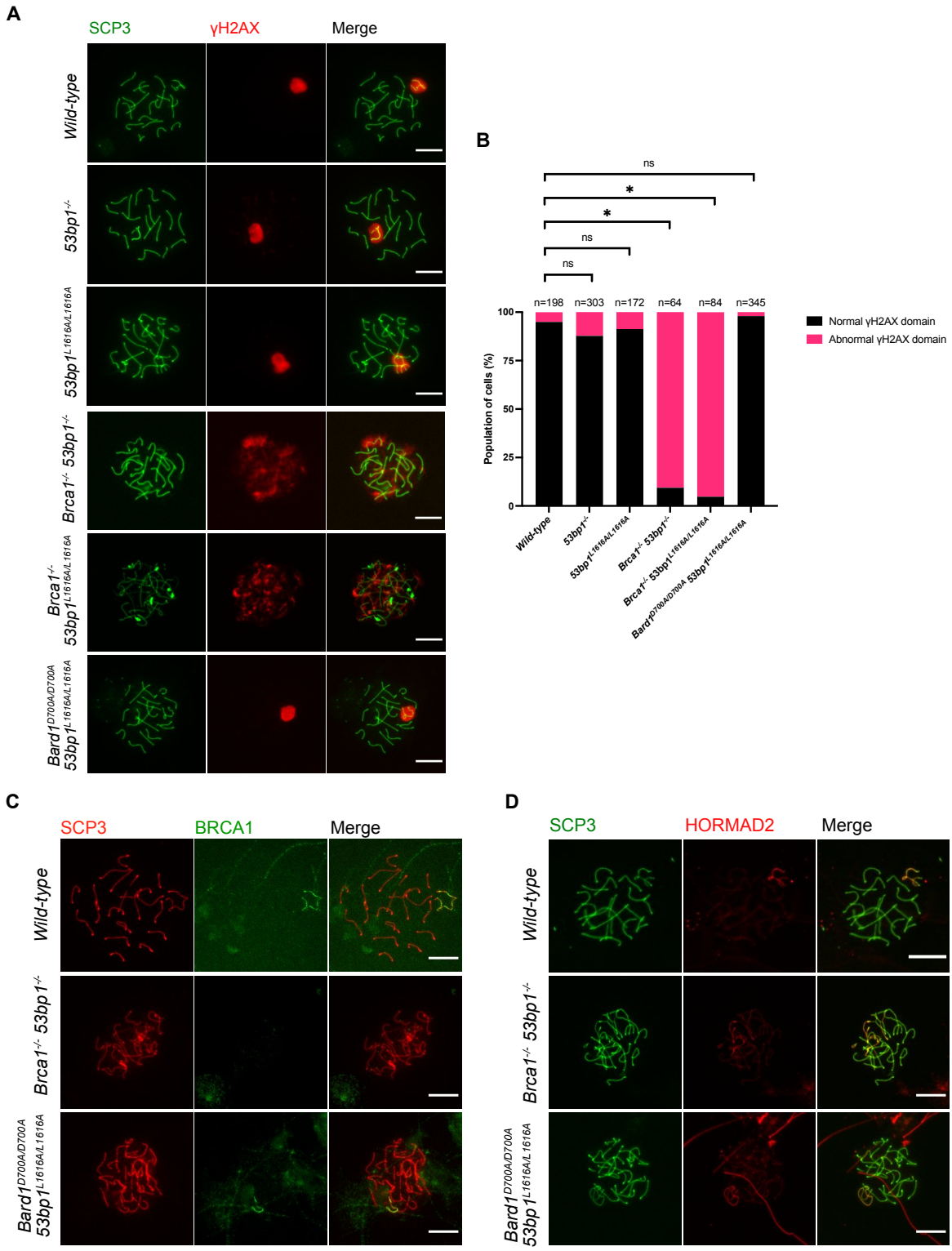


Figure 5.5 Loss of BARD1 BUDR-binding is not required for BRCA1 recruitment in germ cells and does not lead to MSCI failure or asynapsis. (A) Representative images of immunofluorescence staining of pachytene chromosome spreads from mice of indicated genotypes, stained for SCP3 to visualise chromosome axis and γH2AX. Scale bar, 10 µm. (B) Percentage of population of cells observed in (A) with normal or abnormal γH2AX domain. Number of analysed cells is indicated on the graph. *n*=2 mice per genotype. Significance was derived using ordinary one-way ANOVA with Dunnett's multiple comparison test. ns, not significant; * p<0.05. (C) Representative images of immunofluorescence analysis of BRCA1 recruitment in pachytene chromosome spreads from mice of indicated genotypes. Scale bar, 10 µm. *n*=2 mice per genotype. (D) Representative images of immunofluorescence analysis of HORMAD2 localisation in pachytene chromosomes spreads from mice of indicated genotypes. Scale bar, 10 µm. *n*=2 mice per genotype.

5.3 Concluding remarks

The remarkable finding that the *Bard1*$^{D700A/D700A}$ *53bp1*$^{L1616A/L1616A}$ male mice are fertile, and support normal MSCI functionality offers a clearcut demonstration of the versatility of the BRCA1-BARD1 complex, and its ability to use different domains and signals to mediate its recruitment to chromosomes in various contexts. Here, I demonstrate that the BARD1 BUDR is crucial for mediating chromatin binding and BRCA1-BARD1 complex recruitment to DNA DSBs in somatic cells, which we show to be vital for HR and embryonic development in mice. In contrast, my results reveal that the BARD1 BUDR is dispensable for BRCA1 recruitment to chromosomes in meiotic germ cells, nor does it appear to contribute to meiotic DNA DSB repair, nor the establishment of a γH2AX-positive sex body during MSCI. Ultimately, this indicates that BRCA1 is recruited to meiotic chromosomes via alternative mechanisms, exploiting different domains in the BRCA1-BARD1 heterodimer, that must respond to different recruitment signals. My results provide compelling insights into BRCA1-BARD1 separation-of-function *in vivo,* establishing the importance of the BARD1 dual-reader domain during HR and most likely tumour suppression, yet its dispensability for spermatogenesis and male germline function.

Unlike *Brca1*$^{-/-}$ *53bp1*$^{-/-}$ *or Brca1*$^{-/-}$ *53bp1*$^{L1616A/L1616A}$ mice, which succumb to thymic lymphoma due to elevated levels of systemic genomic instability, *Bard1*$^{D700A/D700A}$ *53bp1*$^{L1616A/L1616A}$ mice had tumour-free lifespans up until 80 weeks of age. My results showcase the ability of mutant BARD1^{D700A} to stabilise and heterodimerise with BRCA1 which clearly supports some tumour suppressive function *in vivo*. Perhaps via phospho-binding interactions mediated by the BRCA1 tandem-BRCT domain, such as with CtIP, BACH1 and/or Abraxas-mediated H2AK15ub-independent recruitment of BRCA1-BARD1 to DNA DSBs where they mediate DNA repair via different mechanisms (Shakya *et al.*, 2011; Nacson *et al.*, 2018, 2020). This suggests that the tumour suppressive functions of the BRCA1-BARD1 complex rely on an ensemble of chromatin and protein interacting domains to support high-fidelity HR repair, and potentially distinct DNA repair activities. Interestingly, although 53BP1 loss rescues RAD51 recruitment in BRCA1-deficient cells (section 4.2.2), these cells show residual PARPi hypersensitivity, indicating that the loss of 53BP1 is unable to restore other functions of the BRCA1-BARD1 complex required for DNA repair and while it can rescue HR repair, other DNA repair defects remain (Bouwman *et al.*, 2010; Becker *et al.*, 2021; King *et al.*, 2024). In contrast, 53BP1-deficient cells harbouring the BARD1^{D712A} mutation showed normal PARPi resistance (Figure 4.3 and Figure 4.5) (Becker *et al.*, 2021). These results agree with the *in vivo* data presented in this chapter which show reduced lifespans of *Brca1*$^{-/-}$ *53bp1*$^{-/-}$ mice, in comparison to the normal lifespan *Bard1*$^{D700A/D700A}$ *53bp1*$^{L1616A/L1616A}$ mice, indicating that HR-deficiency is not the only source of genome instability in BRCA1-deficient cells (Becker *et al.*, 2021; King *et al.*, 2024). Reportedly, 53BP1/BRCA1-deficient cells show increased MMEJ activity which is mutagenic as it is error-prone (Chen *et al.*, 2020). Notably, the loss of BRCA1's role in the protection of stalled replication forks might also contribute to residual genome instability (Schlacher, Wu and Jasin, 2012; Chaudhuri *et al.*, 2016). Further investigation is

needed to understand the mechanism that contributes to the genome instability in 53BP1/BRCA1-deficient cells, which causes residual PARPi sensitivity and tumour development in mice.

Brca1$^{-/-}$ *53bp1*$^{-/-}$ male mice are infertile due to MSCI failure and pachytene apoptosis which results in azoospermia, in line with previous reports that investigated spermatogenesis in genetically altered mice that were homozygous for hypomorphic *Brca1* loss-of-function alleles (Xu *et al.*, 2003). Furthermore, based on HORMAD2 localisation, BRCA1 loss leads to defects in autosomal synapsis indicating persistent unrepaired meiotic DNA DSBs (Wojtasz *et al.*, 2012). Contrastingly, mice homozygous for the BUDR mutation in *Bard1*, which were also homozygous for the equivalent ubiquitin-interacting motif mutations in *53bp1*, were fertile and had neither BRCA1 or γH2AX localisation defects during pachytene, nor meiotic DNA DSB repair defects as evidenced by the successful synapsis of the autosomal chromosomes. Interestingly, MSCI failure has been hypothesized to be caused by unrepaired DSBs on autosomes causing asynapsis, and failure in transcriptional silencing of the sex chromosomes (Baarends *et al.*, 2005; Turner *et al.*, 2005, 2006). Therefore, future investigations of interest will be to examine the basis of DSB repair dysfunction in spermatocytes of *Brca1*$^{-/-}$ *53bp1*$^{-/-}$ mice. Since the BARD1 BUDR motif is not essential for BRCA1 recruitment during spermatogenesis, how does BRCA1 get recruited to the XY chromosomes to trigger the onset of MSCI? One hypothesis is that the BRCA1 BRCT phospho-binding interactions are involved in this process as mice homozygous for the BRCT mutation S1598F in *Brca1* display male sterility (Shakya *et al.*, 2011). Additionally, the deletion of the coiled-coil domain in *Brca1* which abrogates the BRCA1-PALB2 interaction required for RAD51 loading resulted in male and female infertility (Nacson *et al.*, 2020). However, it is unclear if the infertility in these mice is caused by persistent unrepaired SPO11-induced DSBs or due to failure in transcriptional

silencing of the XY chromosomes. Interestingly, the E3 ligase activity abrogating I26A mutation in the RING domain in *Brca1* caused male sterility in mice (Shakya *et al.*, 2011). Therefore, a thought-provoking hypothesis is that the BRCA1-BARD1 RING heterodimer is crucial during spermatogenesis, for its roles in ubiquitinating H2AK125/127/129 and binding to the nucleosome acidic patch to recruit BRCA1 to unsynapsed XY chromosomes and support ATR and γH2AX signal amplification in the sex body.

Chapter 6

Discussion

The different chromatin engagement modes of the BRCA1-BARD1 complex underlie its diverse functions in distinct contexts, from maintaining genome stability to partaking in the programmed diversification of the germline. The recent discovery from our laboratory and others that BARD1 engages with histone PTM states in DSB-associated post-replicative chromatin at H4K20me0 and H2AK15ub via its ARD and tandem BRCTs domain, respectively, emphasised the role of BARD1 as an essential chromatin reader required for BRCA1 recruitment to DSB sites and 53BP1 inhibition during HR (Nakamura *et al.*, 2019; Becker *et al.*, 2021; Dai *et al.*, 2021; Hu *et al.*, 2021; Krais *et al.*, 2021). However, what roles the additional chromatin engagement domains in BARD1 play during DNA repair, and how BARD1-mediated chromatin binding supports BRCA1 functions during spermatogenesis was previously unexplored. Here, the work presented in this thesis studied the roles of the BRCA1-BARD1 RING heterodimer domain-mediated nucleosome binding in DNA repair and BRCA1-dependent functions, examined the importance of BARD1's disordered regions during DNA DSB repair, and investigated the importance of the BARD1 dual-reader module *in vivo,* during embryonic development, tumour suppression and for male germline development.

6.1 The implications of BARD1 nucleosome binding in supporting somatic DNA repair and BRCA1-dependent functions for MSCI

In addition to the H4K20me0/H2AK15ub-binding domains, recent structural work on the BRCA1-BARD1 RING-mediated nucleosome interactions showed that BARD1 can interact with

the H2B/H4 nucleosome cleft and the H2B αC helix via its RING domain (Hu *et al.*, 2021; Witus *et al.*, 2021). The nucleosome binding by the BARD1 RING domain was shown to be required for targeting the E2 ubiquitin-conjugating enzyme to histone H2A and directing the specificity of the BRCA1-BARD1 E3 ubiquitin ligase activity towards H2AK125/127/129 residues (Witus *et al.*, 2022). However, the involvement of the BARD1 RING nucleosome binding in DNA repair was previously unknown. Via separation-of-function mutants, I have shown that a BARD1^{W91A} mutation in the RING domain that impairs BARD1 RING nucleosome H2B/H4 cleft or H2B αC helix binding did not cause DNA repair defects: *BARD1*$^{\Delta/\Delta}$ cells expressing the BARD1^{W91A} mutant remained resistant to olaparib, cisplatin and camptothecin in confirmation that BRCA1-BARD1 does not utilise this to repair DNA damage caused by these genotoxic agents in the cell line model here studied. However, it could be that residual BARD1 RING nucleosome interaction is being supported by BARD1 P89, not included in the here present work (Hu *et al.*, 2021; Witus *et al.*, 2021, 2023; Wang *et al.*, 2023). Since the BARD1 RING-nucleosome binding was reported to facilitate H2A ubiquitination mediated by the E3 ligase activity in the BRCA1-BARD1 RING-heterodimer (Hu *et al.*, 2021; Witus *et al.*, 2021), my results imply that the BRCA1-BARD1 E3 ligase function supported by the W91 residue is not important for BRCA1-dependent DNA repair. The involvement of the BRCA1-BARD1 E3 ligase activity in DNA repair has been controversial as several research groups have reported that DNA repair directed by BRCA1-BARD1 relies on an intact E3 ligase activity, where it promotes DNA end resection events required for HR (Densham *et al.*, 2016; Wang *et al.*, 2023). By contrast, mice harbouring the homozygous *Brca1* isoleucine 26 to alanine mutation (*Brca1*$^{I26A/I26A}$) in the RING domain were not found to be prone to tumour development, and *Brca1*$^{-/I26A}$ embryonic stem cells showed no defects in promoting RAD51 recruitment into IRIF (Reid *et al.*, 2008; Shakya *et al.*, 2011), while 293T cells expressing BRCA1 I26A were found to be cisplatin sensitive (Anantha

et al., 2017). Furthermore, previous work from our laboratory has shown that HCT116 cells, depleted of endogenous BARD1 protein (*BARD1*$^{\Delta/\Delta}$) expressing a reported E3 ligase mutant (BARD1^{R99E}) did not display olaparib sensitivity (Nakamura *et al.*, 2019). This is also in agreement with the results presented in this thesis, that indicate that *BARD1*$^{\Delta/\Delta}$ cells expressing a minimal BARD1 RING^{R99E} fragment, did not display increased olaparib sensitivity over cells expressing a wild-type BARD1^{RING} fragment. This would suggest that the E3 ligase activity mediated by the BRCA1-BARD1 complex is not required for DNA repair functions in this cellular context, although the E3 ligase activity in the BRCA1-BARD1$^{RING\ R99E}$ heterodimer was not tested and thus it could be that BRCA1-BARD1 DNA repair functions are supported by residual ubiquitin ligase activity. Furthermore, recent findings that studied a triple BRCA1 mutant devoid of E3 ligase activity indicated that the BRCA1-BARD1 enzymatic activity is involved in cell survival following DNA-damaging agents and was required for efficient HR and end resection activity according to RPA recruitment levels in HeLa-shBRCA1 cells expressing BRCA1 I26A/L63A/K65A (Wang *et al.*, 2023).

The contrasting results regarding the importance of the BRCA1-BARD1 E3 ligase in DNA repair may be due to several factors, including differences in cells lines studied, the use of mouse models and human cell lines, the use of shRNA and siRNA technologies for BRCA1/BARD1 knockdown versus the stable degron-technology degradation of endogenous BRCA1/BARD1 protein, and the focus on point mutations that are E3 ligase-defective (e.g. BRCA1 I26A and BARD1 R99E) rather than E3-ligase dead (BRCA1 I26A/L63A/K65A) (Shakya *et al.*, 2011; Densham *et al.*, 2016; Nakamura *et al.*, 2019; Becker *et al.*, 2021; Krais *et al.*, 2021; Wang *et al.*, 2023).

My work also suggests that the BARD1 RING nucleosome binding is not involved in supporting the BARD1 dual reader functions, and could be required for biological functions

outside of somatic DNA repair, potentially during the meiotic functions of the BRCA1-BARD1 complex for MSCI. In support of this, male mice carrying the E3 ligase abrogating I26A mutation are sterile (Shakya *et al.*, 2011). Furthermore, *in vivo* work presented in this thesis which assessed the role of the BARD1 dual reader domain in BRCA1 recruitment to XY chromosomes during male meiosis and the MSCI proficiency of *Bard1*$^{D700A/D700A}$ *53bp1*$^{L1616A/L1616A}$ spermatocytes has shown that BRCA1 recruitment does not rely on the BARD1 dual reader domain. This poses the exciting question of how BRCA1 is recruited to unsynapsed regions in the XY chromosomes to initiate the MSCI process. Therefore, BARD1 RING nucleosome binding and the consequent facilitation of H2A ubiquitination might be crucial during the transcriptional silencing events of the unsynapsed XY chromosomes mediated by BRCA1. In addition, male mice harbouring mutations in the BRCA1 BRCT phosphoprotein binding domain (*Brca1*$^{S1598F/S1598F}$) and the BARD1 PAR-binding motif in the BRCT domain (*Bard1*$^{K607A/K607A}$) are infertile (Shakya *et al.*, 2011; Billing *et al.*, 2018), indicating that BRCA1 recruitment to meiotic DNA DSBs and unsynapsed chromosome regions might depend on BARD1 PAR-binding and potentially BRCA1 BRCT-binding proteins such as BACH1 or CtIP, but not on the BRCA1-A complex, since *Rap80*$^{-/-}$ male mice are fertile and display normal BRCA1 recruitment to sex chromosomes (Lu *et al.*, 2013). In addition, the observation that *Brca1*$^{-/-}$ *53bp1*$^{-/-}$ have γH2AX body formation defects and autosomal asynapsis marked by HORMAD2 staining indicates that pachytene apoptosis in *Brca1*$^{-/-}$ *53bp1*$^{-/-}$ spermatocytes and associated male infertility might be driven by 1) persistent meiotic DSBs left unrepaired and 2) failed MSCI. Future work is needed to investigate how the BRCA1-BARD1 RING-mediated nucleosome binding is involved in male germ line development and the mechanism that governs meiotic DSB repair mediated by the BRCA1-BARD1 complex.

The data presented in this chapter which showed that BARD1$^{W91A\ D712A}$ and BARD1$^{RING\ W91A}$ proteins were unable to promote BRCA1 recruitment to IR-induced DSB sites in cells, even at late time points following irradiation, indicate that the BRCA1-BARD1 RING-mediated nucleosome binding could have a secondary function external to the H2A ubiquitination events mediated by the BRCA1-BARD1 complex. These could support BRCA1-dependent functions governed by BRCT phospho-binding protein interactions, namely RAP80-dependent recruitment of BRCA1. The BRCA1-dependent functions could rely on the BARD1 RING nucleosome binding for stability at DNA damage-associated chromatin sites. This is in line with reports from the Dan Durocher laboratory that identified the BRCA1 RING nucleosome acidic patch binding to be involved in RAP80-dependent recruitment of BRCA1 (Sherker *et al.*, 2021). In addition, my work has shown that the BRCA1-BARD1 complex suppresses the recruitment of RAP80 in S and G2 phases of the cell cycle to DNA DSB sites via H2AK15ub-binding by BARD1, and that 53BP1 suppresses RAP80 recruitment in BRCA1/BARD1-proficient cells in G2. These findings support recent *in vitro* work showing that the BARD1 H2AK15ub-binding restricts K63-linked polyubiquitin chain formation required for RAP80 recruitment (Hu *et al.*, 2021), but that the BRCA1-BARD1 binding to H2AK15ub is not prevented by K63-linked polyubiquitin chains (Burdett *et al.*, 2023). Furthermore, reports indicating that 53BP1 nuclear bodies sequester under-replicated DNA that could arise from genomic regions which are difficult to replicate, to allow for whole genome duplication in the following cell cycle and limit genome instability that arises from toxic HR repair intermediates (Spies *et al.*, 2019), suggest that the regulation of RAP80 by 53BP1 could be required to prevent aberrant processing of under-replicated DNA. In addition, reports indicating that ABRAXAS-deficient cells display lower levels of SCEs (Castillo *et al.*, 2014) suggest that the BRCA1-A complex might be involved in the generation of HR-independent SCEs. The findings presented in this thesis that BRCA1-

BARD1 can support HR-dependent and HR-independent SCE formation in *BARD1*$^{\Delta/\Delta}$ +BARD1^{D712A} cells, following the loss of 53BP1, at stochastic conditions, are in line with findings showing that loss of 53BP1 is associated with increased SCE levels (Tiwari, Jones and Chan, 2018) and that the formation of HR-independent SCEs can arise from processing of under-replicated DNA (Heijink *et al.*, 2022). The newly identified hierarchy between the BRCA1-BARD1 complex, 53BP1 and RAP80 recruitment at DSB sites, presented in this thesis, provides interesting speculation regarding the physiological importance of cell-cycle dependent RAP80 suppression and the HR-independent mechanisms that it could be involved in that lead to toxic recombination intermediates which could involve BRCA1-A-dependent mitotic repair of UR-DNA.

6.2 BARD1 supports additional DNA repair roles independently of BRCA1

Previously it was not understood if BARD1 alone could support additional DNA repair functions independently from BRCA1. My findings show that in 53BP1-deficient cells, *BARD1*$^{\Delta/\Delta}$ cells expressing RING-less BARD1 (BARD1$^{\Delta RING}$) which does not support BRCA1 heterodimerisation, surprisingly rescues DNA repair to levels seen in wild-type (*BARD1*$^{\Delta/\Delta}$ +BARD1) cells, fully restoring PARPi olaparib resistance. Interestingly, *53BP1*$^{-/-}$ BRCA1-deficient cells were shown to retain residual olaparib sensitivity, despite fully restoring RAD51 recruitment to DSBs, in line with previous research (Becker *et al.*, 2021; King *et al.*, 2024). Fittingly, I showed that *Brca1*$^{-/-}$ *53bp1*$^{-/-}$ mice, despite being viable following 53BP1 loss, accumulate high levels of systemic genomic instability and succumb to thymic lymphomas within 20 weeks of age, in line with previous reports (Chen *et al.*, 2020), contrarily to *Bard1*$^{D700A/D700A}$ *53bp1*$^{L1616A/L1616A}$ mice. This indicates that the tumour suppressive roles of the BRCA1-BARD1 complex rely on additional DNA repair mechanisms which are not that of

canonical HR. Interestingly, as BRCA1-BARD1 has been reported to be required for stalled replication fork protection, one possibility is that the residual genome instability observed in *53BP1*$^{-/-}$ BRCA1-deficient cells and the susceptibility to tumour development in *53bp1*$^{-/-}$ *Brca1*$^{-/-}$ mice is due to loss of these additional DNA repair functions (Schlacher, Wu and Jasin, 2012; Chaudhuri *et al.*, 2016; Billing *et al.*, 2018). Therefore, future work is required to understand the molecular mechanism that supports additional BRCA1-BARD1 DNA repair functions and what underlines the residual toxicity to olaparib in *53BP1*$^{-/-}$ *BRCA1*$^{-/-}$ cells.

The structure-function studies undertaken on the BARD1 IDR in this thesis determined that the IDR is not crucial for DNA repair, as *BARD1*$^{\Delta/\Delta}$ cells expressing various BARD1 IDR mutant constructs were not particularly sensitive to olaparib or cisplatin, despite previous reports indicating that an identified RAD51-interacting motif within the BARD1 IDR was required for D-loop formation and HR repair (Zhao *et al.*, 2017). This suggests that the BARD1 IDR is not of fundamental importance during HR and might support some DNA repair functions in an HR-restored, *53BP1*$^{-/-}$ *BARD1*$^{\Delta/\Delta}$ background, and/or in other DNA repair contexts. Indeed, the BARD1 IDR was recently reported to contain an SLX4-interacting motif which promotes HR and DNA replication intermediates resolution via the SMX complex (Tsukada *et al.*, 2024). Additionally, the BARD1 IDR was recently shown to support BRCA1-BARD1 complex bridging over two nucleosomes, where the IDR acts as a linker between the RING and ARD-mediated nucleosome binding (Burdett *et al.*, 2023; Witus *et al.*, 2023), in line with my findings showing that the SLIMs within the IDR are not required for BARD1 recruitment to chromatin and therefore might be required for the structural conformation of the BRCA1-BARD1 chromatin binding domains on the nucleosomes. Furthermore, it was also shown that the BARD1 IDR supports the H2A ubiquitination activity of the BRCA1-BARD1 RING domain by DNA-binding motifs within the IDR (Witus *et al.*, 2023).

Perhaps the function of the BARD1 IDR in bridging BRCA1-BARD1 complexes over two nucleosomes and supporting H2A ubiquitination is required during meiosis where the localisation of the complex over two nucleosomes rather than one aids in the amplification of the MSCI cascade directed by BRCA1 (Burdett *et al.*, 2023; Witus *et al.*, 2023).

6.3 Overall Conclusions

- The distinct chromatin binding modes of the BRCA1-BARD1 complex have multifaceted functions in somatic and germ cells.
- The BRCA1-BARD1 RING-mediated nucleosome binding is dispensable for BRCA1-BARD1's roles during HR repair, but can support BRCA1-BRCT-mediated functions.
- H2AK15ub-binding by BARD1 suppresses the recruitment of BRCA1-A complex proteins at IR-induced DSB sites, and similarly, 53BP1 negatively regulates RAP80 recruitment during G2 phase.
- The intrinsically disordered region in BARD1 is not crucial for DNA repair, but can support some additional BARD1 functions, independently of BRCA1.
- The BRCA1-BARD1 complex promotes SCE formation via HR-dependent and independent mechanisms.
- BARD1 ARD-BRCT mediated chromatin binding is not required for the recruitment of BRCA1 at the XY chromosomes and meiotic sex chromosome inactivation (MSCI).

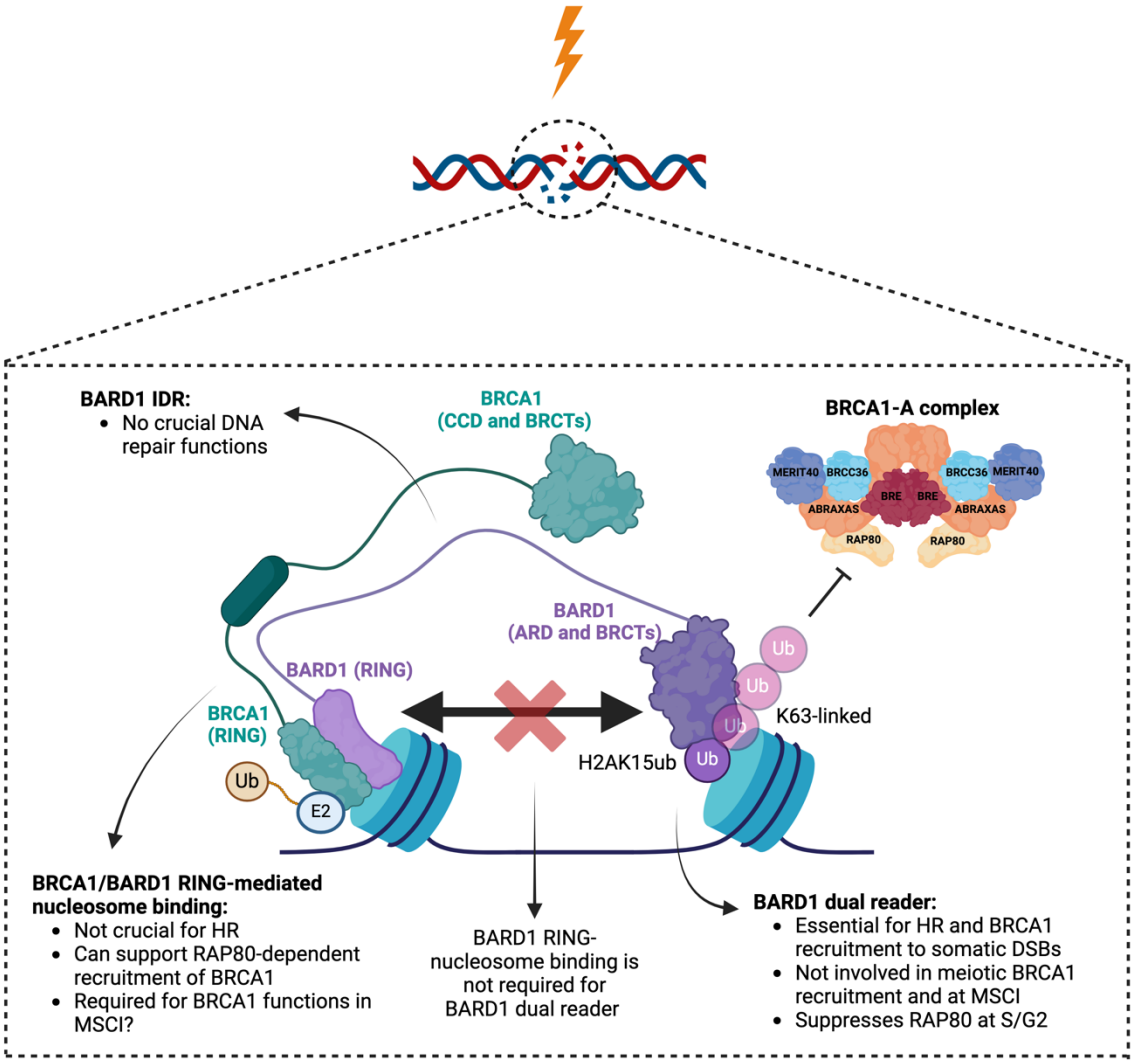


Figure 6.1. Schematic summary of the multifaceted roles of the BRCA1-BARD1 chromatin binding functions. The distinct BARD1 chromatin binding modes dictate the BRCA1-BARD1 complex DSB repair functions in somatic cells and its functions in the germline.

Chapter 7

References

Abe, H. *et al.* (2020) "The Initiation of Meiotic Sex Chromosome Inactivation Sequesters DNA Damage Signaling from Autosomes in Mouse Spermatogenesis," *Current Biology*, 30(3), pp. 408-420.e5. Available at: https://doi.org/10.1016/j.cub.2019.11.064.

Abe, H. *et al.* (2022) "Active DNA damage response signaling initiates and maintains meiotic sex chromosome inactivation," *Nature Communications*, 13(1), p. 7212. Available at: https://doi.org/10.1038/s41467-022-34295-5.

Acquaviva, L. *et al.* (2020) "Ensuring meiotic DNA break formation in the mouse pseudoautosomal region," *Nature*, 582(7812), pp. 426–431. Available at: https://doi.org/10.1038/s41586-020-2327-4.

Adams, M.M. *et al.* (2005) "53BP1 Oligomerization is Independent of its Methylation by PRMT1," *Cell Cycle*, 4(12), pp. 1854–1861. Available at: https://doi.org/10.4161/cc.4.12.2282.

Adams, P.D. *et al.* (1996) "Identification of a Cyclin-cdk2 Recognition Motif Present in Substrates and p21-Like Cyclin-Dependent Kinase Inhibitors," *Molecular and Cellular Biology*, 16(12), pp. 6623–6633. Available at: https://doi.org/10.1128/mcb.16.12.6623.

Akbari, M.R. *et al.* (2009) "Germline RAP80 mutations and susceptibility to breast cancer," *Breast Cancer Research and Treatment*, 113(2), pp. 377–381. Available at: https://doi.org/10.1007/s10549-008-9938-z.

Alagoz, M. *et al.* (2015) "SETDB1, HP1 and SUV39 promote repositioning of 53BP1 to extend resection during homologous recombination in G2 cells," *Nucleic Acids Research*, 43(16), pp. 7931–7944. Available at: https://doi.org/10.1093/nar/gkv722.

Alavattam, K.G. *et al.* (2022) "Meiotic sex chromosome inactivation and the XY body: a phase separation hypothesis," *Cellular and Molecular Life Sciences*, 79(1), p. 18. Available at: https://doi.org/10.1007/s00018-021-04075-3.

Alcorta, D.A. *et al.* (1996) "Involvement of the cyclin-dependent kinase inhibitor p16 (INK4a) in replicative senescence of normal human fibroblasts," *Proceedings of the National Academy of Sciences*, 93(24), pp. 13742–13747. Available at: https://doi.org/10.1073/pnas.93.24.13742.

An, L. *et al.* (2018) "RNF169 limits 53BP1 deposition at DSBs to stimulate single-strand annealing repair," *Proceedings of the National Academy of Sciences*, 115(35), pp. E8286–E8295. Available at: https://doi.org/10.1073/pnas.1804823115.

Anand, R. *et al.* (2016) "Phosphorylated CtIP Functions as a Co-factor of the MRE11-RAD50-NBS1 Endonuclease in DNA End Resection," *Molecular Cell*, 64(5), pp. 940–950. Available at: https://doi.org/10.1016/j.molcel.2016.10.017.

Anand, R. *et al.* (2019) "NBS1 promotes the endonuclease activity of the MRE11-RAD50 complex by sensing CtIP phosphorylation," *The EMBO Journal*, 38(7). Available at: https://doi.org/10.15252/embj.2018101005.

Anand, R.P. *et al.* (2014) "Chromosome rearrangements via template switching between diverged repeated sequences," *Genes & Development*, 28(21), pp. 2394–2406. Available at: https://doi.org/10.1101/gad.250258.114.

Anantha, R.W. *et al.* (2017) "Functional and mutational landscapes of BRCA1 for homology-directed repair and therapy resistance," *eLife*, 6, p. e21350. Available at: https://doi.org/10.7554/elife.21350.

Arter, M. and Keeney, S. (2024) "Divergence and conservation of the meiotic recombination machinery," *Nature Reviews Genetics*, 25(5), pp. 309–325. Available at: https://doi.org/10.1038/s41576-023-00669-8.

Ashworth, A. and Lord, C.J. (2018) "Synthetic lethal therapies for cancer: what's next after PARP inhibitors?," *Nature Reviews Clinical Oncology*, 15(9), pp. 564–576. Available at: https://doi.org/10.1038/s41571-018-0055-6.

Aubrey, B.J. *et al.* (2018) "How does p53 induce apoptosis and how does this relate to p53-mediated tumour suppression?," *Cell Death & Differentiation*, 25(1), pp. 104–113. Available at: https://doi.org/10.1038/cdd.2017.169.

Audebert, M., Salles, B. and Calsou, P. (2004) "Involvement of Poly(ADP-ribose) Polymerase-1 and XRCC1/DNA Ligase III in an Alternative Route for DNA Double-strand Breaks Rejoining*," *Journal of Biological Chemistry*, 279(53), pp. 55117–55126. Available at: https://doi.org/10.1074/jbc.m404524200.

Awate, S. *et al.* (2020) "FANCJ compensates for RAP80 deficiency and suppresses genomic instability induced by interstrand cross-links," *Nucleic Acids Research*, 48(16), pp. 9161–9180. Available at: https://doi.org/10.1093/nar/gkaa660.

Aymard, F. *et al.* (2014) "Transcriptionally active chromatin recruits homologous recombination at DNA double-strand breaks," *Nature Structural & Molecular Biology*, 21(4), pp. 366–374. Available at: https://doi.org/10.1038/nsmb.2796.

Baarends, W.M. *et al.* (2005) "Silencing of Unpaired Chromatin and Histone H2A Ubiquitination in Mammalian Meiosis," *Molecular and Cellular Biology*, 25(3), pp. 1041–1053. Available at: https://doi.org/10.1128/mcb.25.3.1041-1053.2005.

Baer, R. and Ludwig, T. (2002) "The BRCA1/BARD1 heterodimer, a tumor suppressor complex with ubiquitin E3 ligase activity," *Current Opinion in Genetics & Development*, 12(1), pp. 86–91. Available at: https://doi.org/10.1016/s0959-437x(01)00269-6.

Bakkenist, C.J. and Kastan, M.B. (2003) "DNA damage activates ATM through intermolecular autophosphorylation and dimer dissociation," *Nature*, 421(6922), pp. 499–506. Available at: https://doi.org/10.1038/nature01368.

Balmus, G. *et al.* (2015) "A high-throughput in vivo micronucleus assay for genome instability screening in mice," *Nature Protocols*, 10(1), pp. 205–215. Available at: https://doi.org/10.1038/nprot.2015.010.

Balmus, G. *et al.* (2019) "ATM orchestrates the DNA-damage response to counter toxic non-homologous end-joining at broken replication forks," *Nature Communications*, 10(1), p. 87. Available at: https://doi.org/10.1038/s41467-018-07729-2.

Banin, S. *et al.* (1998) "Enhanced Phosphorylation of p53 by ATM in Response to DNA Damage," *Science*, 281(5383), pp. 1674–1677. Available at: https://doi.org/10.1126/science.281.5383.1674.

Barazas, M. *et al.* (2018) "The CST Complex Mediates End Protection at Double-Strand Breaks and Promotes PARP Inhibitor Sensitivity in BRCA1-Deficient Cells," *Cell Reports*, 23(7), pp. 2107–2118. Available at: https://doi.org/10.1016/j.celrep.2018.04.046.

Bartz, S.R. *et al.* (2006) "Small Interfering RNA Screens Reveal Enhanced Cisplatin Cytotoxicity in Tumor Cells Having both BRCA Network and TP53 Disruptions," *Molecular and Cellular Biology*, 26(24), pp. 9377–9386. Available at: https://doi.org/10.1128/mcb.01229-06.

Becker, J.R. *et al.* (2018) "The ASCIZ-DYNLL1 axis promotes 53BP1-dependent non-homologous end joining and PARP inhibitor sensitivity," *Nature Communications*, 9(1), p. 5406. Available at: https://doi.org/10.1038/s41467-018-07855-x.

Becker, J.R. *et al.* (2021) "BARD1 reads H2A lysine 15 ubiquitination to direct homologous recombination," *Nature*, pp. 1–5. Available at: https://doi.org/10.1038/s41586-021-03776-w.

Belan, O. *et al.* (2022) "POLQ seals post-replicative ssDNA gaps to maintain genome stability in BRCA-deficient cancer cells," *Molecular Cell*, 82(24), pp. 4664-4680.e9. Available at: https://doi.org/10.1016/j.molcel.2022.11.008.

Belotserkovskaya, R. *et al.* (2020) "PALB2 chromatin recruitment restores homologous recombination in BRCA1-deficient cells depleted of 53BP1," *Nature Communications*, 11(1), p. 819. Available at: https://doi.org/10.1038/s41467-020-14563-y.

Benada, J. *et al.* (2015) "Polo-like kinase 1 inhibits DNA damage response during mitosis," *Cell Cycle*, 14(2), pp. 219–231. Available at: https://doi.org/10.4161/15384101.2014.977067.

Berezin, C. *et al.* (2004) "ConSeq: the identification of functionally and structurally important residues in protein sequences," *Bioinformatics*, 20(8), pp. 1322–1324. Available at: https://doi.org/10.1093/bioinformatics/bth070.

Bergerat, A. *et al.* (1997) "An atypical topoisomerase II from archaea with implications for meiotic recombination," *Nature*, 386(6623), pp. 414–417. Available at: https://doi.org/10.1038/386414a0.

Bhattacharyya, A. *et al.* (2000) "The Breast Cancer Susceptibility Gene BRCA1 Is Required for Subnuclear Assembly of Rad51 and Survival following Treatment with the DNA Cross-linking Agent Cisplatin*," *Journal of Biological Chemistry*, 275(31), pp. 23899–23903. Available at: https://doi.org/10.1074/jbc.c000276200.

Billing, D. *et al.* (2018) "The BRCT Domains of the BRCA1 and BARD1 Tumor Suppressors Differentially Regulate Homology-Directed Repair and Stalled Fork Protection," *Molecular Cell*, 72(1), pp. 127-139.e8. Available at: https://doi.org/10.1016/j.molcel.2018.08.016.

Boboila, C. *et al.* (2010) "Alternative end-joining catalyzes robust IgH locus deletions and translocations in the combined absence of ligase 4 and Ku70," *Proceedings of the National Academy of Sciences*, 107(7), pp. 3034–3039. Available at: https://doi.org/10.1073/pnas.0915067107.

Boersma, V. *et al.* (2015) "MAD2L2 controls DNA repair at telomeres and DNA breaks by inhibiting 5′ end resection," *Nature*, 521(7553), pp. 537–540. Available at: https://doi.org/10.1038/nature14216.

Boisvert, F.-M. *et al.* (2005) "The GAR Motif of 53BP1 is Arginine Methylated by PRMT1 and is Necessary for 53BP1 DNA Binding Activity," *Cell Cycle*, 4(12), pp. 1834–1841. Available at: https://doi.org/10.4161/cc.4.12.2250.

Bosse, K.R. *et al.* (2012) "Common Variation at BARD1 Results in the Expression of an Oncogenic Isoform That Influences Neuroblastoma Susceptibility and Oncogenicity," *Cancer Research*, 72(8), pp. 2068–2078. Available at: https://doi.org/10.1158/0008-5472.can-11-3703.

Bothmer, A. *et al.* (2010) "53BP1 regulates DNA resection and the choice between classical and alternative end joining during class switch recombination," *Journal of Experimental Medicine*, 207(4), pp. 855–865. Available at: https://doi.org/10.1084/jem.20100244.

Bothmer, A. *et al.* (2011) "Regulation of DNA End Joining, Resection, and Immunoglobulin Class Switch Recombination by 53BP1," *Molecular Cell*, 42(3), pp. 319–329. Available at: https://doi.org/10.1016/j.molcel.2011.03.019.

Botuyan, M.V. *et al.* (2006) "Structural Basis for the Methylation State-Specific Recognition of Histone H4-K20 by 53BP1 and Crb2 in DNA Repair," *Cell*, 127(7), pp. 1361–1373. Available at: https://doi.org/10.1016/j.cell.2006.10.043.

Botuyan, M.V.E. *et al.* (2004) "Structural Basis of BACH1 Phosphopeptide Recognition by BRCA1 Tandem BRCT Domains," *Structure*, 12(7), pp. 1137–1146. Available at: https://doi.org/10.1016/j.str.2004.06.002.

Bouwman, P. *et al.* (2010) "53BP1 loss rescues BRCA1 deficiency and is associated with triple-negative and BRCA-mutated breast cancers," *Nature Structural & Molecular Biology*, 17(6), pp. 688–695. Available at: https://doi.org/10.1038/nsmb.1831.

Brambati, A. *et al.* (2023) "RHINO directs MMEJ to repair DNA breaks in mitosis," *Science*, 381(6658), pp. 653–660. Available at: https://doi.org/10.1126/science.adh3694.

Brambati, A., Barry, R.M. and Sfeir, A. (2020) "DNA polymerase theta (Polθ) – an error-prone polymerase necessary for genome stability," *Current Opinion in Genetics & Development*, 60, pp. 119–126. Available at: https://doi.org/10.1016/j.gde.2020.02.017.

Bregenhorn, S. *et al.* (2016) "Non-canonical uracil processing in DNA gives rise to double-strand breaks and deletions: relevance to class switch recombination," *Nucleic Acids Research*, 44(6), pp. 2691–2705. Available at: https://doi.org/10.1093/nar/gkv1535.

Broering, T.J. *et al.* (2014) "BRCA1 establishes DNA damage signaling and pericentric heterochromatin of the X chromosome in male meiosis," *The Journal of Cell Biology*, 205(5), pp. 663–675. Available at: https://doi.org/10.1083/jcb.201311050.

Brown, J.P., Wei, W. and Sedivy, J.M. (1997) "Bypass of Senescence After Disruption of p21CIP1/WAF1 Gene in Normal Diploid Human Fibroblasts," *Science*, 277(5327), pp. 831–834. Available at: https://doi.org/10.1126/science.277.5327.831.

Brown, M.S. and Bishop, D.K. (2014) "DNA Strand Exchange and RecA Homologs in Meiosis," *Cold Spring Harbor Perspectives in Biology*, 7(1), p. a016659. Available at: https://doi.org/10.1101/cshperspect.a016659.

Bryant, H.E. *et al.* (2005) "Specific killing of BRCA2-deficient tumours with inhibitors of poly(ADP-ribose) polymerase," *Nature*, 434(7035), pp. 913–917. Available at: https://doi.org/10.1038/nature03443.

Brzovic, P.S. *et al.* (2001) "Structure of a BRCA1–BARD1 heterodimeric RING–RING complex," *Nature Structural Biology*, 8(10), pp. 833–837. Available at: https://doi.org/10.1038/nsb1001-833.

Brzovic, P.S. *et al.* (2003) "Binding and recognition in the assembly of an active BRCA1/BARD1 ubiquitin-ligase complex," *Proceedings of the National Academy of Sciences*, 100(10), pp. 5646–5651. Available at: https://doi.org/10.1073/pnas.0836054100.

Bugreev, D.V. *et al.* (2011) "The resistance of DMC1 D-loops to dissociation may account for the DMC1 requirement in meiosis," *Nature Structural & Molecular Biology*, 18(1), pp. 56–60. Available at: https://doi.org/10.1038/nsmb.1946.

Bunting, S.F. *et al.* (2010) "53BP1 Inhibits Homologous Recombination in Brca1-Deficient Cells by Blocking Resection of DNA Breaks," *Cell*, 141(2), pp. 243–254. Available at: https://doi.org/10.1016/j.cell.2010.03.012.

Burdett, H. *et al.* (2023) "BRCA1–BARD1 combines multiple chromatin recognition modules to bridge nascent nucleosomes," *Nucleic Acids Research*, 51(20), pp. 11080–11103. Available at: https://doi.org/10.1093/nar/gkad793.

Burgoyne, P.S., Mahadevaiah, S.K. and Turner, J.M.A. (2009) "The consequences of asynapsis for mammalian meiosis," *Nature Reviews Genetics*, 10(3), pp. 207–216. Available at: https://doi.org/10.1038/nrg2505.

Bzymek, M. *et al.* (2010) "Double Holliday junctions are intermediates of DNA break repair," *Nature*, 464(7290), pp. 937–941. Available at: https://doi.org/10.1038/nature08868.

Callen, E. *et al.* (2013) "53BP1 Mediates Productive and Mutagenic DNA Repair through Distinct Phosphoprotein Interactions," *Cell*, 153(6), pp. 1266–1280. Available at: https://doi.org/10.1016/j.cell.2013.05.023.

Cannan, W.J. and Pederson, D.S. (2016) "Mechanisms and Consequences of Double-Strand DNA Break Formation in Chromatin," *Journal of Cellular Physiology*, 231(1), pp. 3–14. Available at: https://doi.org/10.1002/jcp.25048.

Cantor, S. *et al.* (2004) "The BRCA1-associated protein BACH1 is a DNA helicase targeted by clinically relevant inactivating mutations," *Proceedings of the National Academy of Sciences*, 101(8), pp. 2357–2362. Available at: https://doi.org/10.1073/pnas.0308717101.

Cantor, S.B. *et al.* (2001) "BACH1, a Novel Helicase-like Protein, Interacts Directly with BRCA1 and Contributes to Its DNA Repair Function," *Cell*, 105(1), pp. 149–160. Available at: https://doi.org/10.1016/s0092-8674(01)00304-x.

Cantor, S.B. and Guillemette, S. (2011) "Hereditary breast cancer and the BRCA1-associated FANCJ/BACH1/BRIP1," *Future Oncology*, 7(2), pp. 253–261. Available at: https://doi.org/10.2217/fon.10.191.

Cao, L. *et al.* (2009) "A Selective Requirement for 53BP1 in the Biological Response to Genomic Instability Induced by Brca1 Deficiency," *Molecular Cell*, 35(4), pp. 534–541. Available at: https://doi.org/10.1016/j.molcel.2009.06.037.

Cao, R., Tsukada, Y. and Zhang, Y. (2005) "Role of Bmi-1 and Ring1A in H2A Ubiquitylation and Hox Gene Silencing," *Molecular Cell*, 20(6), pp. 845–854. Available at: https://doi.org/10.1016/j.molcel.2005.12.002.

Caron, M.-C. *et al.* (2019) "Poly(ADP-ribose) polymerase-1 antagonizes DNA resection at double-strand breaks," *Nature Communications*, 10(1), p. 2954. Available at: https://doi.org/10.1038/s41467-019-10741-9.

Castilla, L.H. *et al.* (1994) "Mutations in the BRCA1 gene in families with early-onset breast and ovarian cancer," *Nature Genetics*, 8(4), pp. 387–391. Available at: https://doi.org/10.1038/ng1294-387.

Castillo, A. *et al.* (2014) "The BRCA1-Interacting Protein Abraxas Is Required for Genomic Stability and Tumor Suppression," *Cell Reports*, 8(3), pp. 807–817. Available at: https://doi.org/10.1016/j.celrep.2014.06.050.

Ceccaldi, R. *et al.* (2015) "Homologous-recombination-deficient tumours are dependent on Polθ-mediated repair," *Nature*, 518(7538), pp. 258–262. Available at: https://doi.org/10.1038/nature14184.

Ceppi, I. *et al.* (2024) "Mechanism of BRCA1–BARD1 function in DNA end resection and DNA protection," *Nature*, pp. 1–9. Available at: https://doi.org/10.1038/s41586-024-07909-9.

Chan, K. and Gordenin, D.A. (2015) "Clusters of Multiple Mutations: Incidence and Molecular Mechanisms*," *Annual Review of Genetics*, 49(1), pp. 243–267. Available at: https://doi.org/10.1146/annurev-genet-112414-054714.

Chan, Y.W., Fugger, K. and West, S.C. (2018) "Unresolved recombination intermediates lead to ultra-fine anaphase bridges, chromosome breaks and aberrations," *Nature Cell Biology*, 20(1), pp. 92–103. Available at: https://doi.org/10.1038/s41556-017-0011-1.

Chang, H.H.Y. *et al.* (2017) "Non-homologous DNA end joining and alternative pathways to double-strand break repair," *Nature Reviews Molecular Cell Biology*, 18(8), pp. 495–506. Available at: https://doi.org/10.1038/nrm.2017.48.

Chaplin, A.K. *et al.* (2021) "Cryo-EM of NHEJ supercomplexes provides insights into DNA repair," *Molecular Cell*, 81(16), pp. 3400-3409.e3. Available at: https://doi.org/10.1016/j.molcel.2021.07.005.

Chapman, J.R. *et al.* (2012) "BRCA1-associated exclusion of 53BP1 from DNA damage sites underlies temporal control of DNA repair," *Journal of Cell Science*, 125(15), pp. 3529–3534. Available at: https://doi.org/10.1242/jcs.105353.

Chapman, J.R. *et al.* (2013) "RIF1 Is Essential for 53BP1-Dependent Nonhomologous End Joining and Suppression of DNA Double-Strand Break Resection," *Molecular Cell*, 49(5), pp. 858–871. Available at: https://doi.org/10.1016/j.molcel.2013.01.002.

Chapman, J.R. and Jackson, S.P. (2008) "Phospho-dependent interactions between NBS1 and MDC1 mediate chromatin retention of the MRN complex at sites of DNA damage," *EMBO reports*, 9(8), pp. 795–801. Available at: https://doi.org/10.1038/embor.2008.103.

Chapman, J.R., Taylor, M.R.G. and Boulton, S.J. (2012) "Playing the End Game: DNA Double-Strand Break Repair Pathway Choice," *Molecular Cell*, 47(4), pp. 497–510. Available at: https://doi.org/10.1016/j.molcel.2012.07.029.

Chaturvedi, P. *et al.* (1999) "Mammalian Chk2 is a downstream effector of the ATM-dependent DNA damage checkpoint pathway," *Oncogene*, 18(28), pp. 4047–4054. Available at: https://doi.org/10.1038/sj.onc.1202925.

Chaudhuri, A.R. *et al.* (2016) "Replication fork stability confers chemoresistance in BRCA-deficient cells," *Nature*, 535(7612), pp. 382–387. Available at: https://doi.org/10.1038/nature18325.

Chaudhuri, A.R. and Nussenzweig, A. (2017) "The multifaceted roles of PARP1 in DNA repair and chromatin remodelling," *Nature Reviews Molecular Cell Biology*, 18(10), pp. 610–621. Available at: https://doi.org/10.1038/nrm.2017.53.

Chen, H., Lisby, M. and Symington, L.S. (2013) "RPA Coordinates DNA End Resection and Prevents Formation of DNA Hairpins," *Molecular Cell*, 50(4), pp. 589–600. Available at: https://doi.org/10.1016/j.molcel.2013.04.032.

Chen, J. *et al.* (2020) "53BP1 loss rescues embryonic lethality but not genomic instability of BRCA1 total knockout mice," *Cell Death & Differentiation*, 27(9), pp. 2552–2567. Available at: https://doi.org/10.1038/s41418-020-0521-4.

Chen, L. *et al.* (2008) "Cell Cycle-dependent Complex Formation of BRCA1·CtIP·MRN Is Important for DNA Double-strand Break Repair*," *Journal of Biological Chemistry*, 283(12), pp. 7713–7720. Available at: https://doi.org/10.1074/jbc.m710245200.

Chen, S. *et al.* (2021) "Structural basis of long-range to short-range synaptic transition in NHEJ," *Nature*, 593(7858), pp. 294–298. Available at: https://doi.org/10.1038/s41586-021-03458-7.

Chen, S. *et al.* (2023) "Cryo-EM visualization of DNA-PKcs structural intermediates in NHEJ," *Science Advances*, 9(22), p. eadg2838. Available at: https://doi.org/10.1126/sciadv.adg2838.

Chen, Z. and Tyler, J.K. (2022) "The Chromatin Landscape Channels DNA Double-Strand Breaks to Distinct Repair Pathways," *Frontiers in Cell and Developmental Biology*, 10, p. 909696. Available at: https://doi.org/10.3389/fcell.2022.909696.

Cheng, Q. and Chen, J. (2010) "Mechanism of p53 stabilization by ATM after DNA damage," *Cell Cycle*, 9(3), pp. 472–478. Available at: https://doi.org/10.4161/cc.9.3.10556.

Chicas, A. *et al.* (2010) "Dissecting the Unique Role of the Retinoblastoma Tumor Suppressor during Cellular Senescence," *Cancer Cell*, 17(4), pp. 376–387. Available at: https://doi.org/10.1016/j.ccr.2010.01.023.

Choudhury, A.D. *et al.* (2005) "Hyperphosphorylation of the BARD1 Tumor Suppressor in Mitotic Cells*," *Journal of Biological Chemistry*, 280(26), pp. 24669–24679. Available at: https://doi.org/10.1074/jbc.m502446200.

Clark, S.L. *et al.* (2012) "STRUCTURE-FUNCTION OF THE TUMOR SUPPRESSOR BRCA1," *Computational and Structural Biotechnology Journal*, 1(1), pp. 1–8. Available at: https://doi.org/10.5936/csbj.201204005.

Clouaire, T. *et al.* (2018) "Comprehensive Mapping of Histone Modifications at DNA Double-Strand Breaks Deciphers Repair Pathway Chromatin Signatures," *Molecular Cell*, 72(2), pp. 250-262.e6. Available at: https://doi.org/10.1016/j.molcel.2018.08.020.

Coleman, K.A. and Greenberg, R.A. (2011) "The BRCA1-RAP80 Complex Regulates DNA Repair Mechanism Utilization by Restricting End Resection*," *Journal of Biological Chemistry*, 286(15), pp. 13669–13680. Available at: https://doi.org/10.1074/jbc.m110.213728.

Corneo, B. *et al.* (2007) "Rag mutations reveal robust alternative end joining," *Nature*, 449(7161), pp. 483–486. Available at: https://doi.org/10.1038/nature06168.

Couture, J.-F. *et al.* (2005) "Structural and functional analysis of SET8, a histone H4 Lys-20 methyltransferase," *Genes & Development*, 19(12), pp. 1455–1465. Available at: https://doi.org/10.1101/gad.1318405.

Cressman, V.L. *et al.* (1999) "Mammary tumor formation in p53- and BRCA1-deficient mice.," *Cell growth & differentiation : the molecular biology journal of the American Association for Cancer Research*, 10(1), pp. 1–10.

Cromie, G.A. *et al.* (2006) "Single Holliday Junctions Are Intermediates of Meiotic Recombination," *Cell*, 127(6), pp. 1167–1178. Available at: https://doi.org/10.1016/j.cell.2006.09.050.

Cruz-García, A., López-Saavedra, A. and Huertas, P. (2014) "BRCA1 Accelerates CtIP-Mediated DNA-End Resection," *Cell Reports*, 9(2), pp. 451–459. Available at: https://doi.org/10.1016/j.celrep.2014.08.076.

Cuella-Martin, R. *et al.* (2016) "53BP1 Integrates DNA Repair and p53-Dependent Cell Fate Decisions via Distinct Mechanisms," *Molecular Cell*, 64(1), pp. 51–64. Available at: https://doi.org/10.1016/j.molcel.2016.08.002.

Dai, C.Y. and Enders, G.H. (2000) "p16INK4a can initiate an autonomous senescence program," *Oncogene*, 19(13), pp. 1613–1622. Available at: https://doi.org/10.1038/sj.onc.1203438.

Dai, J. *et al.* (2017) "Meiotic Knockdown and Complementation Reveals Essential Role of RAD51 in Mouse Spermatogenesis," *Cell Reports*, 18(6), pp. 1383–1394. Available at: https://doi.org/10.1016/j.celrep.2017.01.024.

Dai, L. *et al.* (2021) "Structural insight into BRCA1-BARD1 complex recruitment to damaged chromatin," *Molecular Cell*, 81(13), pp. 2765-2777.e6. Available at: https://doi.org/10.1016/j.molcel.2021.05.010.

Davies, B. *et al.* (2016) "Re-engineering the zinc fingers of PRDM9 reverses hybrid sterility in mice," *Nature*, 530(7589), pp. 171–176. Available at: https://doi.org/10.1038/nature16931.

Daza-Martin, M. *et al.* (2019) "Isomerization of BRCA1–BARD1 promotes replication fork protection," *Nature*, 571(7766), pp. 521–527. Available at: https://doi.org/10.1038/s41586-019-1363-4.

Deans, A.J. and West, S.C. (2011) "DNA interstrand crosslink repair and cancer," *Nature Reviews Cancer*, 11(7), pp. 467–480. Available at: https://doi.org/10.1038/nrc3088.

Deng, S.K. *et al.* (2014) "RPA antagonizes microhomology-mediated repair of DNA double-strand breaks," *Nature Structural & Molecular Biology*, 21(4), pp. 405–412. Available at: https://doi.org/10.1038/nsmb.2786.

Densham, R.M. *et al.* (2016) "Human BRCA1–BARD1 ubiquitin ligase activity counteracts chromatin barriers to DNA resection," *Nature Structural & Molecular Biology*, 23(7), pp. 647–655. Available at: https://doi.org/10.1038/nsmb.3236.

Densham, R.M. and Morris, J.R. (2016) "The BRCA1 Ubiquitin ligase function sets a new trend for remodelling in DNA repair," *Nucleus*, 8(2), pp. 116–125. Available at: https://doi.org/10.1080/19491034.2016.1267092.

Derbyshire, D.J. *et al.* (2002) "Crystal structure of human 53BP1 BRCT domains bound to p53 tumour suppressor," *The EMBO Journal*, 21(14), pp. 3863–3872. Available at: https://doi.org/10.1093/emboj/cdf383.

Deshpande, M. *et al.* (2022) "Error-prone repair of stalled replication forks drives mutagenesis and loss of heterozygosity in haploinsufficient BRCA1 cells," *Molecular Cell*, 82(20), pp. 3781-3793.e7. Available at: https://doi.org/10.1016/j.molcel.2022.08.017.

Deshpande, R.A. *et al.* (2016) "Nbs1 Converts the Human Mre11/Rad50 Nuclease Complex into an Endo/Exonuclease Machine Specific for Protein-DNA Adducts," *Molecular Cell*, 64(3), pp. 593–606. Available at: https://doi.org/10.1016/j.molcel.2016.10.010.

Dev, H. *et al.* (2018) "Shieldin complex promotes DNA end-joining and counters homologous recombination in BRCA1-null cells," *Nature Cell Biology*, 20(8), pp. 954–965. Available at: https://doi.org/10.1038/s41556-018-0140-1.

Dever, S.M. *et al.* (2011) "Mutations in the BRCT binding site of BRCA1 result in hyper-recombination," *Aging (Albany NY)*, 3(5), pp. 515–532. Available at: https://doi.org/10.18632/aging.100325.

Difilippantonio, S. *et al.* (2008) "53BP1 facilitates long-range DNA end-joining during V(D)J recombination," *Nature*, 456(7221), pp. 529–533. Available at: https://doi.org/10.1038/nature07476.

Dilley, R.L. *et al.* (2016) "Break-induced telomere synthesis underlies alternative telomere maintenance," *Nature*, 539(7627), pp. 54–58. Available at: https://doi.org/10.1038/nature20099.

Dimitrova, N. *et al.* (2008) "53BP1 promotes non-homologous end joining of telomeres by increasing chromatin mobility," *Nature*, 456(7221), pp. 524–528. Available at: https://doi.org/10.1038/nature07433.

Dohrn, L. *et al.* (2012) "BRCA1-mediated repression of mutagenic end-joining of DNA double-strand breaks requires complex formation with BACH1," *Biochemical Journal*, 441(3), pp. 919–928. Available at: https://doi.org/10.1042/bj20110314.

Doil, C. *et al.* (2009) "RNF168 Binds and Amplifies Ubiquitin Conjugates on Damaged Chromosomes to Allow Accumulation of Repair Proteins," *Cell*, 136(3), pp. 435–446. Available at: https://doi.org/10.1016/j.cell.2008.12.041.

Dong, Y. *et al.* (2003) "Regulation of BRCC, a Holoenzyme Complex Containing BRCA1 and BRCA2, by a Signalosome-like Subunit and Its Role in DNA Repair," *Molecular Cell*, 12(5), pp. 1087–1099. Available at: https://doi.org/10.1016/s1097-2765(03)00424-6.

Donnianni, R.A. and Symington, L.S. (2013) "Break-induced replication occurs by conservative DNA synthesis," *Proceedings of the National Academy of Sciences*, 110(33), pp. 13475–13480. Available at: https://doi.org/10.1073/pnas.1309800110.

Drost, R. *et al.* (2011) "BRCA1 RING Function Is Essential for Tumor Suppression but Dispensable for Therapy Resistance," *Cancer Cell*, 20(6), pp. 797–809. Available at: https://doi.org/10.1016/j.ccr.2011.11.014.

Drost, R. *et al.* (2016) "BRCA1185delAG tumors may acquire therapy resistance through expression of RING-less BRCA1," *Journal of Clinical Investigation*, 126(8), pp. 2903–2918. Available at: https://doi.org/10.1172/jci70196.

Dudley, D.D. *et al.* (2005) "Mechanism and Control of V(D)J Recombination versus Class Switch Recombination: Similarities and Differences," *Advances in Immunology*, 86(Proc. Natl. Acad. Sci. USA961999), pp. 43–112. Available at: https://doi.org/10.1016/s0065-2776(04)86002-4.

Edelmann, W. *et al.* (1996) "Meiotic Pachytene Arrest in MLH1-Deficient Mice," *Cell*, 85(7), pp. 1125–1134. Available at: https://doi.org/10.1016/s0092-8674(00)81312-4.

Elango, R. *et al.* (2019) "Repair of base damage within break-induced replication intermediates promotes kataegis associated with chromosome rearrangements," *Nucleic Acids Research*, 47(18), pp. 9666–9684. Available at: https://doi.org/10.1093/nar/gkz651.

Escribano-Díaz, C. *et al.* (2013) "A Cell Cycle-Dependent Regulatory Circuit Composed of 53BP1-RIF1 and BRCA1-CtIP Controls DNA Repair Pathway Choice," *Molecular Cell*, 49(5), pp. 872–883. Available at: https://doi.org/10.1016/j.molcel.2013.01.001.

Falck, J. *et al.* (2001) "The ATM–Chk2–Cdc25A checkpoint pathway guards against radioresistant DNA synthesis," *Nature*, 410(6830), pp. 842–847. Available at: https://doi.org/10.1038/35071124.

Farmer, H. *et al.* (2005) "Targeting the DNA repair defect in BRCA mutant cells as a therapeutic strategy," *Nature*, 434(7035), pp. 917–921. Available at: https://doi.org/10.1038/nature03445.

Fedier, A. *et al.* (2003) "The effect of loss of Brca1 on the sensitivity to anticancer agents in p53-deficient cells," *International Journal of Oncology* [Preprint]. Available at: https://doi.org/10.3892/ijo.22.5.1169.

Fekairi, S. *et al.* (2009) "Human SLX4 Is a Holliday Junction Resolvase Subunit that Binds Multiple DNA Repair/Recombination Endonucleases," *Cell*, 138(1), pp. 78–89. Available at: https://doi.org/10.1016/j.cell.2009.06.029.

Feng, L., Huang, J. and Chen, J. (2009) "MERIT40 facilitates BRCA1 localization and DNA damage repair," *Genes & Development*, 23(6), pp. 719–728. Available at: https://doi.org/10.1101/gad.1770609.

Fernandez-Capetillo, O. *et al.* (2003) "H2AX Is Required for Chromatin Remodeling and Inactivation of Sex Chromosomes in Male Mouse Meiosis," *Developmental Cell*, 4(4), pp. 497–508. Available at: https://doi.org/10.1016/s1534-5807(03)00093-5.

Fishman-Lobell, J., Rudin, N. and Haber, J.E. (1992) "Two Alternative Pathways of Double-Strand Break Repair That Are Kinetically Separable and Independently Modulated," *Molecular and Cellular Biology*, 12(3), pp. 1292–1303. Available at: https://doi.org/10.1128/mcb.12.3.1292-1303.1992.

Fouquin, A. *et al.* (2017) "PARP2 controls double-strand break repair pathway choice by limiting 53BP1 accumulation at DNA damage sites and promoting end-resection," *Nucleic Acids Research*, 45(21), pp. 12325–12339. Available at: https://doi.org/10.1093/nar/gkx881.

Fradet-Turcotte, A. *et al.* (2013) "53BP1 is a reader of the DNA-damage-induced H2A Lys 15 ubiquitin mark," *Nature*, 499(7456), pp. 50–54. Available at: https://doi.org/10.1038/nature12318.

Friedman, L.S. *et al.* (1994) "Confirmation of BRCA1 by analysis of germline mutations linked to breast and ovarian cancer in ten families," *Nature Genetics*, 8(4), pp. 399–404. Available at: https://doi.org/10.1038/ng1294-399.

Fulda, S. and Debatin, K.-M. (2006) "Extrinsic versus intrinsic apoptosis pathways in anticancer chemotherapy," *Oncogene*, 25(34), pp. 4798–4811. Available at: https://doi.org/10.1038/sj.onc.1209608.

Gao, Y., Sun, Y., *et al.* (1998) "A Critical Role for DNA End-Joining Proteins in Both Lymphogenesis and Neurogenesis," *Cell*, 95(7), pp. 891–902. Available at: https://doi.org/10.1016/s0092-8674(00)81714-6.

Gao, Y., Chaudhuri, J., *et al.* (1998) "A Targeted DNA-PKcs-Null Mutation Reveals DNA-PK-Independent Functions for KU in V(D)J Recombination," *Immunity*, 9(3), pp. 367–376. Available at: https://doi.org/10.1016/s1074-7613(00)80619-6.

Garcia, V. *et al.* (2011) "Bidirectional resection of DNA double-strand breaks by Mre11 and Exo1," *Nature*, 479(7372), pp. 241–244. Available at: https://doi.org/10.1038/nature10515.

Gatti, M. *et al.* (2012) "A novel ubiquitin mark at the N-terminal tail of histone H2As targeted by RNF168 ubiquitin ligase," *Cell Cycle*, 11(13), pp. 2538–2544. Available at: https://doi.org/10.4161/cc.20919.

Gelot, C. *et al.* (2023) "Polθ is phosphorylated by PLK1 to repair double-strand breaks in mitosis," *Nature*, 621(7978), pp. 415–422. Available at: https://doi.org/10.1038/s41586-023-06506-6.

Ghezraoui, H. *et al.* (2018) "53BP1 cooperation with the REV7–shieldin complex underpins DNA structure-specific NHEJ," *Nature*, 560(7716), pp. 122–127. Available at: https://doi.org/10.1038/s41586-018-0362-1.

Goldberg, M. *et al.* (2003) "MDC1 is required for the intra-S-phase DNA damage checkpoint," *Nature*, 421(6926), pp. 952–956. Available at: https://doi.org/10.1038/nature01445.

Gong, Z. *et al.* (2009) "Accumulation of Pax2 Transactivation Domain Interaction Protein (PTIP) at Sites of DNA Breaks via RNF8-dependent Pathway Is Required for Cell Survival after DNA Damage*," *Journal of Biological Chemistry*, 284(11), pp. 7284–7293. Available at: https://doi.org/10.1074/jbc.m809158200.

Gong, Z. *et al.* (2010) "BACH1/FANCJ Acts with TopBP1 and Participates Early in DNA Replication Checkpoint Control," *Molecular Cell*, 37(3), pp. 438–446. Available at: https://doi.org/10.1016/j.molcel.2010.01.002.

Greenberg, R.A. *et al.* (2006) "Multifactorial contributions to an acute DNA damage response by BRCA1/BARD1-containing complexes," *Genes & Development*, 20(1), pp. 34–46. Available at: https://doi.org/10.1101/gad.1381306.

Grey, C. and Massy, B. de (2021) "Chromosome Organization in Early Meiotic Prophase," *Frontiers in Cell and Developmental Biology*, 9, p. 688878. Available at: https://doi.org/10.3389/fcell.2021.688878.

Grigaitis, R. *et al.* (2020) "Phosphorylation of the RecQ Helicase Sgs1/BLM Controls Its DNA Unwinding Activity during Meiosis and Mitosis," *Developmental Cell*, 53(6), pp. 706-723.e5. Available at: https://doi.org/10.1016/j.devcel.2020.05.016.

Groelly, F.J. *et al.* (2023) "Targeting DNA damage response pathways in cancer," *Nature Reviews Cancer*, 23(2), pp. 78–94. Available at: https://doi.org/10.1038/s41568-022-00535-5.

Gupta, R. *et al.* (2018) "DNA Repair Network Analysis Reveals Shieldin as a Key Regulator of NHEJ and PARP Inhibitor Sensitivity," *Cell*, 173(4), pp. 972-988.e23. Available at: https://doi.org/10.1016/j.cell.2018.03.050.

Guzzo, C.M. *et al.* (2012) "RNF4-Dependent Hybrid SUMO-Ubiquitin Chains Are Signals for RAP80 and Thereby Mediate the Recruitment of BRCA1 to Sites of DNA Damage," *Science Signaling*, 5(253), p. ra88. Available at: https://doi.org/10.1126/scisignal.2003485.

Hakem, R. *et al.* (1996) "The Tumor Suppressor Gene Brca1 Is Required for Embryonic Cellular Proliferation in the Mouse," *Cell*, 85(7), pp. 1009–1023. Available at: https://doi.org/10.1016/s0092-8674(00)81302-1.

Harper, J.W. *et al.* (1993) "The p21 Cdk-interacting protein Cip1 is a potent inhibitor of G1 cyclin-dependent kinases," *Cell*, 75(4), pp. 805–816. Available at: https://doi.org/10.1016/0092-8674(93)90499-g.

Harper, J.W. *et al.* (1995) "Inhibition of cyclin-dependent kinases by p21.," *Molecular Biology of the Cell*, 6(4), pp. 387–400. Available at: https://doi.org/10.1091/mbc.6.4.387.

Hashimoto, Y. *et al.* (2010) "Rad51 protects nascent DNA from Mre11-dependent degradation and promotes continuous DNA synthesis," *Nature Structural & Molecular Biology*, 17(11), pp. 1305–1311. Available at: https://doi.org/10.1038/nsmb.1927.

Hashimoto, Y., Puddu, F. and Costanzo, V. (2012) "RAD51- and MRE11-dependent reassembly of uncoupled CMG helicase complex at collapsed replication forks," *Nature Structural & Molecular Biology*, 19(1), pp. 17–24. Available at: https://doi.org/10.1038/nsmb.2177.

Hashizume, R. *et al.* (2001) "The RING Heterodimer BRCA1-BARD1 Is a Ubiquitin Ligase Inactivated by a Breast Cancer-derived Mutation*," *Journal of Biological Chemistry*, 276(18), pp. 14537–14540. Available at: https://doi.org/10.1074/jbc.c000881200.

Hayakawa, T. *et al.* (2010) "MRG15 binds directly to PALB2 and stimulates homology-directed repair of chromosomal breaks," *Journal of Cell Science*, 123(7), pp. 1124–1130. Available at: https://doi.org/10.1242/jcs.060178.

Heijink, A.M. *et al.* (2022) "Sister chromatid exchanges induced by perturbed replication can form independently of BRCA1, BRCA2 and RAD51," *Nature Communications*, 13(1), p. 6722. Available at: https://doi.org/10.1038/s41467-022-34519-8.

Hermeking, H. *et al.* (1997) "14-3-3σ Is a p53-Regulated Inhibitor of G2/M Progression," *Molecular Cell*, 1(1), pp. 3–11. Available at: https://doi.org/10.1016/s1097-2765(00)80002-7.

Hinch, A.G. *et al.* (2020) "The Configuration of RPA, RAD51, and DMC1 Binding in Meiosis Reveals the Nature of Critical Recombination Intermediates," *Molecular Cell*, 79(4), pp. 689-701.e10. Available at: https://doi.org/10.1016/j.molcel.2020.06.015.

Hirao, A. *et al.* (2000) "DNA Damage-Induced Activation of p53 by the Checkpoint Kinase Chk2," *Science*, 287(5459), pp. 1824–1827. Available at: https://doi.org/10.1126/science.287.5459.1824.

Ho, V. *et al.* (2020) "Aberrant Expression of RAD52, Its Prognostic Impact in Rectal Cancer and Association with Poor Survival of Patients," *International Journal of Molecular Sciences*, 21(5), p. 1768. Available at: https://doi.org/10.3390/ijms21051768.

Hoeijmakers, J.H.J. (2001) "Genome maintenance mechanisms for preventing cancer," *Nature*, 411(6835), pp. 366–374. Available at: https://doi.org/10.1038/35077232.

Hu, Q. *et al.* (2017) "Mechanisms of Ubiquitin-Nucleosome Recognition and Regulation of 53BP1 Chromatin Recruitment by RNF168/169 and RAD18," *Molecular Cell*, 66(4), pp. 473-487.e9. Available at: https://doi.org/10.1016/j.molcel.2017.04.009.

Hu, Q. *et al.* (2021) "Mechanisms of BRCA1–BARD1 nucleosome recognition and ubiquitylation," *Nature*, pp. 1–6. Available at: https://doi.org/10.1038/s41586-021-03716-8.

Hu, Qi *et al.* (2024) "Mechanisms of RNF168 nucleosome recognition and ubiquitylation," *Molecular Cell*, 84(5), pp. 839-853.e12. Available at: https://doi.org/10.1016/j.molcel.2023.12.036.

Hu, Qing *et al.* (2024) "Non-homologous end joining shapes the genomic rearrangement landscape of chromothripsis from mitotic errors," *Nature Communications*, 15(1), p. 5611. Available at: https://doi.org/10.1038/s41467-024-49985-5.

Hu, X. *et al.* (2011) "NBA1/MERIT40 and BRE Interaction Is Required for the Integrity of Two Distinct Deubiquitinating Enzyme BRCC36-containing Complexes*," *Journal of Biological Chemistry*, 286(13), pp. 11734–11745. Available at: https://doi.org/10.1074/jbc.m110.200857.

Hu, X., Paul, A. and Wang, B. (2012) "Rap80 Protein Recruitment to DNA Double-strand Breaks Requires Binding to Both Small Ubiquitin-like Modifier (SUMO) and Ubiquitin Conjugates*," *Journal of Biological Chemistry*, 287(30), pp. 25510–25519. Available at: https://doi.org/10.1074/jbc.m112.374116.

Hu, Y. *et al.* (2011) "RAP80-directed tuning of BRCA1 homologous recombination function at ionizing radiation-induced nuclear foci," *Genes & Development*, 25(7), pp. 685–700. Available at: https://doi.org/10.1101/gad.2011011.

Huang, W. *et al.* (2022) "Cellular senescence: the good, the bad and the unknown," *Nature Reviews Nephrology*, 18(10), pp. 611–627. Available at: https://doi.org/10.1038/s41581-022-00601-z.

Huertas, P. and Jackson, S.P. (2009) "Human CtIP Mediates Cell Cycle Control of DNA End Resection and Double Strand Break Repair*," *Journal of Biological Chemistry*, 284(14), pp. 9558–9565. Available at: https://doi.org/10.1074/jbc.m808906200.

Ichijima, Y. *et al.* (2011) "MDC1 directs chromosome-wide silencing of the sex chromosomes in male germ cells," *Genes & Development*, 25(9), pp. 959–971. Available at: https://doi.org/10.1101/gad.2030811.

Iijima, J. *et al.* (2010) "RAP80 Acts Independently of BRCA1 in Repair of Topoisomerase II Poison-Induced DNA Damage," *Cancer Research*, 70(21), pp. 8467–8474. Available at: https://doi.org/10.1158/0008-5472.can-10-0267.

Incorvaia, L. *et al.* (2024) "The intersection of homologous recombination (HR) and mismatch repair (MMR) pathways in DNA repair-defective tumors," *npj Precision Oncology*, 8(1), p. 190. Available at: https://doi.org/10.1038/s41698-024-00672-0.

Ip, S.C.Y. *et al.* (2008) "Identification of Holliday junction resolvases from humans and yeast," *Nature*, 456(7220), pp. 357–361. Available at: https://doi.org/10.1038/nature07470.

Jackson, S.P. and Bartek, J. (2009) "The DNA-damage response in human biology and disease," *Nature*, 461(7267), pp. 1071–1078. Available at: https://doi.org/10.1038/nature08467.

Jacquet, K. *et al.* (2016) "The TIP60 Complex Regulates Bivalent Chromatin Recognition by 53BP1 through Direct H4K20me Binding and H2AK15 Acetylation," *Molecular Cell*, 62(3), pp. 409–421. Available at: https://doi.org/10.1016/j.molcel.2016.03.031.

Janisiw, E. *et al.* (2018) "BRCA1-BARD1 associate with the synaptonemal complex and pro-crossover factors and influence RAD-51 dynamics during Caenorhabditis elegans meiosis," *PLoS Genetics*, 14(11), p. e1007653. Available at: https://doi.org/10.1371/journal.pgen.1007653.

Jasin, M. and Rothstein, R. (2013) "Repair of Strand Breaks by Homologous Recombination," *Cold Spring Harbor Perspectives in Biology*, 5(11), p. a012740. Available at: https://doi.org/10.1101/cshperspect.a012740.

Jaspers, J.E. *et al.* (2013) "Loss of 53BP1 Causes PARP Inhibitor Resistance in Brca1-Mutated Mouse Mammary Tumors," *Cancer Discovery*, 3(1), pp. 68–81. Available at: https://doi.org/10.1158/2159-8290.cd-12-0049.

Jiang, Q. *et al.* (2022) "Autologous K63 deubiquitylation within the BRCA1-A complex licenses DNA damage recognition," *Journal of Cell Biology*, 221(9), p. e202111050. Available at: https://doi.org/10.1083/jcb.202111050.

Joo, W.S. *et al.* (2002) "Structure of the 53BP1 BRCT region bound to p53 and its comparison to the Brca1 BRCT structure," *Genes & Development*, 16(5), pp. 583–593. Available at: https://doi.org/10.1101/gad.959202.

Kais, Z. *et al.* (2016) "FANCD2 Maintains Fork Stability in BRCA1/2-Deficient Tumors and Promotes Alternative End-Joining DNA Repair," *Cell Reports*, 15(11), pp. 2488–2499. Available at: https://doi.org/10.1016/j.celrep.2016.05.031.

Kalb, R. *et al.* (2014) "BRCA1 Is a Histone-H2A-Specific Ubiquitin Ligase," *Cell Reports*, 8(4), pp. 999–1005. Available at: https://doi.org/10.1016/j.celrep.2014.07.025.

Kass, E.M., Moynahan, M.E. and Jasin, M. (2010) "Loss of 53BP1 Is a Gain for BRCA1 Mutant Cells," *Cancer Cell*, 17(5), pp. 423–425. Available at: https://doi.org/10.1016/j.ccr.2010.04.021.

Kastan, M.B. and Bartek, J. (2004) "Cell-cycle checkpoints and cancer," *Nature*, 432(7015), pp. 316–323. Available at: https://doi.org/10.1038/nature03097.

Kauppi, L. *et al.* (2011) "Distinct Properties of the XY Pseudoautosomal Region Crucial for Male Meiosis," *Science*, 331(6019), pp. 916–920. Available at: https://doi.org/10.1126/science.1195774.

Keeney, S., Giroux, C.N. and Kleckner, N. (1997) "Meiosis-Specific DNA Double-Strand Breaks Are Catalyzed by Spo11, a Member of a Widely Conserved Protein Family," *Cell*, 88(3), pp. 375–384. Available at: https://doi.org/10.1016/s0092-8674(00)81876-0.

Kent, T. *et al.* (2015) "Mechanism of microhomology-mediated end-joining promoted by human DNA polymerase θ," *Nature Structural & Molecular Biology*, 22(3), pp. 230–237. Available at: https://doi.org/10.1038/nsmb.2961.

Kent, T. *et al.* (2016) "Polymerase θ is a robust terminal transferase that oscillates between three different mechanisms during end-joining," *eLife*, 5, p. e13740. Available at: https://doi.org/10.7554/elife.13740.

Khanna, K.K. and Jackson, S.P. (2001) "DNA double-strand breaks: signaling, repair and the cancer connection," *Nature Genetics*, 27(3), pp. 247–254. Available at: https://doi.org/10.1038/85798.

Kim, H., Chen, J. and Yu, X. (2007) "Ubiquitin-Binding Protein RAP80 Mediates BRCA1-Dependent DNA Damage Response," *Science*, 316(5828), pp. 1202–1205. Available at: https://doi.org/10.1126/science.1139621.

Kim, H., Huang, J. and Chen, J. (2007) "CCDC98 is a BRCA1-BRCT domain–binding protein involved in the DNA damage response," *Nature Structural & Molecular Biology*, 14(8), pp. 710–715. Available at: https://doi.org/10.1038/nsmb1277.

King, A. *et al.* (2024) "Shieldin and CST co-orchestrate DNA polymerase-dependent tailed-end joining reactions independently of 53BP1-governed repair pathway choice," *Nature Structural & Molecular Biology*, pp. 1–12. Available at: https://doi.org/10.1038/s41594-024-01381-9.

Kitevski-LeBlanc, J. *et al.* (2017) "The RNF168 paralog RNF169 defines a new class of ubiquitylated histone reader involved in the response to DNA damage," *eLife*, 6, p. e23872. Available at: https://doi.org/10.7554/elife.23872.

Kleiner, R.E. *et al.* (2015) "Chemical proteomics reveals a γH2AX-53BP1 interaction in the DNA damage response," *Nature Chemical Biology*, 11(10), pp. 807–814. Available at: https://doi.org/10.1038/nchembio.1908.

Kneitz, B. *et al.* (2000) "MutS homolog 4 localization to meiotic chromosomes is required for chromosome pairing during meiosis in male and female mice.," *Genes & development*, 14(9), pp. 1085–97.

Kogo, H. *et al.* (2012) "HORMAD2 is essential for synapsis surveillance during meiotic prophase via the recruitment of ATR activity," *Genes to Cells*, 17(11), pp. 897–912. Available at: https://doi.org/10.1111/gtc.12005.

Kolas, N.K. *et al.* (2007) "Orchestration of the DNA-Damage Response by the RNF8 Ubiquitin Ligase," *Science*, 318(5856), pp. 1637–1640. Available at: https://doi.org/10.1126/science.1150034.

Krais, J.J. *et al.* (2021) "RNF168-mediated localization of BARD1 recruits the BRCA1-PALB2 complex to DNA damage," *Nature Communications*, 12(1), p. 5016. Available at: https://doi.org/10.1038/s41467-021-25346-4.

Krais, J.J. *et al.* (2023) "Genetic separation of Brca1 functions reveal mutation-dependent Polθ vulnerabilities," *Nature Communications*, 14(1), p. 7714. Available at: https://doi.org/10.1038/s41467-023-43446-1.

Krenning, L. *et al.* (2014) "Transient Activation of p53 in G2 Phase Is Sufficient to Induce Senescence," *Molecular Cell*, 55(1), pp. 59–72. Available at: https://doi.org/10.1016/j.molcel.2014.05.007.

Kyrieleis, O.J.P. *et al.* (2016) "Three-Dimensional Architecture of the Human BRCA1-A Histone Deubiquitinase Core Complex," *Cell Reports*, 17(12), pp. 3099–3106. Available at: https://doi.org/10.1016/j.celrep.2016.11.063.

Lange, J. *et al.* (2016) "The Landscape of Mouse Meiotic Double-Strand Break Formation, Processing, and Repair," *Cell*, 167(3), pp. 695-708.e16. Available at: https://doi.org/10.1016/j.cell.2016.09.035.

LaRocque, J.R. *et al.* (2011) "Interhomolog recombination and loss of heterozygosity in wild-type and Bloom syndrome helicase (BLM)-deficient mammalian cells," *Proceedings of the National Academy of Sciences*, 108(29), pp. 11971–11976. Available at: https://doi.org/10.1073/pnas.1104421108.

Lee, Y.-H. *et al.* (2013) "HP1 promotes tumor suppressor BRCA1 functions during the DNA damage response," *Nucleic Acids Research*, 41(11), pp. 5784–5798. Available at: https://doi.org/10.1093/nar/gkt231.

Lee-Theilen, M. *et al.* (2011) "CtIP promotes microhomology-mediated alternative end joining during class-switch recombination," *Nature Structural & Molecular Biology*, 18(1), pp. 75–79. Available at: https://doi.org/10.1038/nsmb.1942.

Lemaçon, D. *et al.* (2017) "MRE11 and EXO1 nucleases degrade reversed forks and elicit MUS81-dependent fork rescue in BRCA2-deficient cells," *Nature Communications*, 8(1), p. 860. Available at: https://doi.org/10.1038/s41467-017-01180-5.

Li, M. *et al.* (2016) "53BP1 ablation rescues genomic instability in mice expressing 'RING-less' BRCA1," *EMBO reports*, 17(11), pp. 1532–1541. Available at: https://doi.org/10.15252/embr.201642497.

Li, M. and Yu, X. (2013) "Function of BRCA1 in the DNA Damage Response Is Mediated by ADP-Ribosylation," *Cancer Cell*, 23(5), pp. 693–704. Available at: https://doi.org/10.1016/j.ccr.2013.03.025.

Li, R. *et al.* (2019) "A high-resolution map of non-crossover events reveals impacts of genetic diversity on mammalian meiotic recombination," *Nature Communications*, 10(1), p. 3900. Available at: https://doi.org/10.1038/s41467-019-11675-y.

Li, S. *et al.* (2024) "Systematic investigation of BRCA1-A, -B, and -C complexes and their functions in DNA damage response and DNA repair," *Oncogene*, 43(35), pp. 2621–2634. Available at: https://doi.org/10.1038/s41388-024-03108-y.

Liang, C.-C. *et al.* (2024) "Mechanism of single-stranded DNA annealing by RAD52–RPA complex," *Nature*, 629(8012), pp. 697–703. Available at: https://doi.org/10.1038/s41586-024-07347-7.

Liang, L. *et al.* (2005) "Modulation of DNA End Joining by Nuclear Proteins*," *Journal of Biological Chemistry*, 280(36), pp. 31442–31449. Available at: https://doi.org/10.1074/jbc.m503776200.

Lieber, M.R. (2010) "The Mechanism of Double-Strand DNA Break Repair by the Nonhomologous DNA End-Joining Pathway," *Annual Review of Biochemistry*, 79(1), pp. 181–211. Available at: https://doi.org/10.1146/annurev.biochem.052308.093131.

Ling, A.K. *et al.* (2020) "SHLD2 promotes class switch recombination by preventing inactivating deletions within the Igh locus," *EMBO reports*, 21(8), p. e49823. Available at: https://doi.org/10.15252/embr.201949823.

Litman, R. *et al.* (2005) "BACH1 is critical for homologous recombination and appears to be the Fanconi anemia gene product FANCJ," *Cancer Cell*, 8(3), pp. 255–265. Available at: https://doi.org/10.1016/j.ccr.2005.08.004.

Liu, L. and Malkova, A. (2022) "Break-induced replication: unraveling each step," *Trends in Genetics*, 38(7), pp. 752–765. Available at: https://doi.org/10.1016/j.tig.2022.03.011.

Liu, X. *et al.* (2007) "Somatic loss of BRCA1 and p53 in mice induces mammary tumors with features of human BRCA1-mutated basal-like breast cancer," *Proceedings of the National Academy of Sciences*, 104(29), pp. 12111–12116. Available at: https://doi.org/10.1073/pnas.0702969104.

Liu, Z., Wu, J. and Yu, X. (2007) "CCDC98 targets BRCA1 to DNA damage sites," *Nature Structural & Molecular Biology*, 14(8), pp. 716–720. Available at: https://doi.org/10.1038/nsmb1279.

Long, D.T. *et al.* (2014) "BRCA1 Promotes Unloading of the CMG Helicase from a Stalled DNA Replication Fork," *Molecular Cell*, 56(1), pp. 174–185. Available at: https://doi.org/10.1016/j.molcel.2014.08.012.

Lottersberger, F. *et al.* (2013) "Role of 53BP1 oligomerization in regulating double-strand break repair," *Proceedings of the National Academy of Sciences*, 110(6), pp. 2146–2151. Available at: https://doi.org/10.1073/pnas.1222617110.

Lou, Z. *et al.* (2006) "MDC1 Maintains Genomic Stability by Participating in the Amplification of ATM-Dependent DNA Damage Signals," *Molecular Cell*, 21(2), pp. 187–200. Available at: https://doi.org/10.1016/j.molcel.2005.11.025.

Lu, L.-Y. *et al.* (2013) "Regulation of the DNA damage response on male meiotic sex chromosomes," *Nature Communications*, 4(1), p. 2105. Available at: https://doi.org/10.1038/ncomms3105.

Ludwig, T. *et al.* (1997) "Targeted mutations of breast cancer susceptibility gene homologs in mice: lethal phenotypes of Brca1, Brca2, Brca1/Brca2, Brca1/p53, and Brca2/p53 nullizygous embryos.," *Genes & Development*, 11(10), pp. 1226–1241. Available at: https://doi.org/10.1101/gad.11.10.1226.

Luedeman, M.E. *et al.* (2022) "Poly(ADP) ribose polymerase promotes DNA polymerase theta-mediated end joining by activation of end resection," *Nature Communications*, 13(1), p. 4547. Available at: https://doi.org/10.1038/s41467-022-32166-7.

Luijsterburg, M.S. *et al.* (2017) "A PALB2-interacting domain in RNF168 couples homologous recombination to DNA break-induced chromatin ubiquitylation," *eLife*, 6, p. e20922. Available at: https://doi.org/10.7554/elife.20922.

Lukaszewicz, A. *et al.* (2018) "Control of meiotic double-strand-break formation by ATM: local and global views," *Cell Cycle*, 17(10), pp. 1155–1172. Available at: https://doi.org/10.1080/15384101.2018.1464847.

Lydeard, J.R. *et al.* (2007) "Break-induced replication and telomerase-independent telomere maintenance require Pol32," *Nature*, 448(7155), pp. 820–823. Available at: https://doi.org/10.1038/nature06047.

Ma, J.-L. *et al.* (2003) "Yeast Mre11 and Rad1 Proteins Define a Ku-Independent Mechanism To Repair Double-Strand Breaks Lacking Overlapping End Sequences," *Molecular and Cellular Biology*, 23(23), pp. 8820–8828. Available at: https://doi.org/10.1128/mcb.23.23.8820-8828.2003.

Mailand, N. *et al.* (2007) "RNF8 Ubiquitylates Histones at DNA Double-Strand Breaks and Promotes Assembly of Repair Proteins," *Cell*, 131(5), pp. 887–900. Available at: https://doi.org/10.1016/j.cell.2007.09.040.

Manis, J.P. *et al.* (2004) "53BP1 links DNA damage-response pathways to immunoglobulin heavy chain class-switch recombination," *Nature Immunology*, 5(5), pp. 481–487. Available at: https://doi.org/10.1038/ni1067.

Manke, I.A. *et al.* (2003) "BRCT Repeats As Phosphopeptide-Binding Modules Involved in Protein Targeting," *Science*, 302(5645), pp. 636–639. Available at: https://doi.org/10.1126/science.1088877.

Mann, A. *et al.* (2022) "POLθ prevents MRE11-NBS1-CtIP-dependent fork breakage in the absence of BRCA2/RAD51 by filling lagging-strand gaps," *Molecular Cell*, 82(22), pp. 4218-4231.e8. Available at: https://doi.org/10.1016/j.molcel.2022.09.013.

Mark, W.-Y. *et al.* (2005) "Characterization of Segments from the Central Region of BRCA1: An Intrinsically Disordered Scaffold for Multiple Protein–Protein and Protein–DNA Interactions?," *Journal of Molecular Biology*, 345(2), pp. 275–287. Available at: https://doi.org/10.1016/j.jmb.2004.10.045.

Maryon, E. and Carroll, D. (1991) "Characterization of Recombination Intermediates from DNA Injected into Xenopus laevis Oocytes: Evidence for a Nonconservative Mechanism of Homologous Recombination," *Molecular and Cellular Biology*, 11(6), pp. 3278–3287. Available at: https://doi.org/10.1128/mcb.11.6.3278-3287.1991.

Mateos-Gomez, P.A. *et al.* (2015) "Mammalian polymerase θ promotes alternative NHEJ and suppresses recombination," *Nature*, 518(7538), pp. 254–257. Available at: https://doi.org/10.1038/nature14157.

Mateos-Gomez, P.A. *et al.* (2017) "The helicase domain of Polθ counteracts RPA to promote alt-NHEJ," *Nature Structural & Molecular Biology*, 24(12), pp. 1116–1123. Available at: https://doi.org/10.1038/nsmb.3494.

Matsuoka, S., Huang, M. and Elledge, S.J. (1998) "Linkage of ATM to Cell Cycle Regulation by the Chk2 Protein Kinase," *Science*, 282(5395), pp. 1893–1897. Available at: https://doi.org/10.1126/science.282.5395.1893.

Mattiroli, F. *et al.* (2012) "RNF168 Ubiquitinates K13-15 on H2A/H2AX to Drive DNA Damage Signaling," *Cell*, 150(6), pp. 1182–1195. Available at: https://doi.org/10.1016/j.cell.2012.08.005.

McCarthy, E.E. *et al.* (2003) "Loss of Bard1, the Heterodimeric Partner of the Brca1 Tumor Suppressor, Results in Early Embryonic Lethality and Chromosomal Instability," *Molecular and Cellular Biology*, 23(14), pp. 5056–5063. Available at: https://doi.org/10.1128/mcb.23.14.5056-5063.2003.

McGinty, R.K., Henrici, R.C. and Tan, S. (2014) "Crystal structure of the PRC1 ubiquitylation module bound to the nucleosome," *Nature*, 514(7524), pp. 591–596. Available at: https://doi.org/10.1038/nature13890.

McKinnon, P.J. (2013) "Maintaining genome stability in the nervous system," *Nature Neuroscience*, 16(11), pp. 1523–1529. Available at: https://doi.org/10.1038/nn.3537.

Messer, C.L. and Fox, D.T. (2024) "Broken chromosomes heading into mitosis: More than one way to patch a flat tire," *Journal of Cell Biology*, 223(4), p. e202401085. Available at: https://doi.org/10.1083/jcb.202401085.

Michelena, J. *et al.* (2021) "Replicated chromatin curtails 53BP1 recruitment in BRCA1-proficient and BRCA1-deficient cells," *Life Science Alliance*, 4(6), p. e202101023. Available at: https://doi.org/10.26508/lsa.202101023.

Mimitou, E.P. and Symington, L.S. (2008) "Sae2, Exo1 and Sgs1 collaborate in DNA double-strand break processing," *Nature*, 455(7214), pp. 770–774. Available at: https://doi.org/10.1038/nature07312.

Minocherhomji, S. *et al.* (2015) "Replication stress activates DNA repair synthesis in mitosis," *Nature*, 528(7581), pp. 286–290. Available at: https://doi.org/10.1038/nature16139.

Mirman, Z. *et al.* (2018) "53BP1–RIF1–shieldin counteracts DSB resection through CST- and Polα-dependent fill-in," *Nature*, 560(7716), pp. 112–116. Available at: https://doi.org/10.1038/s41586-018-0324-7.

Mirman, Z. *et al.* (2022) "53BP1–shieldin-dependent DSB processing in BRCA1-deficient cells requires CST–Polα–primase fill-in synthesis," *Nature Cell Biology*, 24(1), pp. 51–61. Available at: https://doi.org/10.1038/s41556-021-00812-9.

Mirman, Z. and Lange, T. de (2020) "53BP1: a DSB escort," *Genes & Development*, 34(1–2), pp. 7–23. Available at: https://doi.org/10.1101/gad.333237.119.

Morris, J.R., Keep, N.H. and Solomon, E. (2002) "Identification of Residues Required for the Interaction of BARD1 with BRCA1*," *Journal of Biological Chemistry*, 277(11), pp. 9382–9386. Available at: https://doi.org/10.1074/jbc.m109249200.

Moshous, D. *et al.* (2001) "Artemis, a Novel DNA Double-Strand Break Repair/V(D)J Recombination Protein, Is Mutated in Human Severe Combined Immune Deficiency," *Cell*, 105(2), pp. 177–186. Available at: https://doi.org/10.1016/s0092-8674(01)00309-9.

Moynahan, M.E. and Jasin, M. (1997) "Loss of heterozygosity induced by a chromosomal double-strand break," *Proceedings of the National Academy of Sciences*, 94(17), pp. 8988–8993. Available at: https://doi.org/10.1073/pnas.94.17.8988.

Nacson, J. *et al.* (2018) "BRCA1 Mutation-Specific Responses to 53BP1 Loss-Induced Homologous Recombination and PARP Inhibitor Resistance," *Cell Reports*, 24(13), pp. 3513-3527.e7. Available at: https://doi.org/10.1016/j.celrep.2018.08.086.

Nacson, J. *et al.* (2020) "BRCA1 Mutational Complementation Induces Synthetic Viability," *Molecular Cell*, 78(5), pp. 951-959.e6. Available at: https://doi.org/10.1016/j.molcel.2020.04.006.

Nakamura, K. *et al.* (2019) "H4K20me0 recognition by BRCA1–BARD1 directs homologous recombination to sister chromatids," *Nature Cell Biology*, 21(3), pp. 311–318. Available at: https://doi.org/10.1038/s41556-019-0282-9.

Nakamura, K. *et al.* (2021) "Proteome dynamics at broken replication forks reveal a distinct ATM-directed repair response suppressing DNA double-strand break ubiquitination," *Molecular Cell*, 81(5), pp. 1084-1099.e6. Available at: https://doi.org/10.1016/j.molcel.2020.12.025.

Natsume, T. *et al.* (2016) "Rapid Protein Depletion in Human Cells by Auxin-Inducible Degron Tagging with Short Homology Donors," *Cell Reports*, 15(1), pp. 210–218. Available at: https://doi.org/10.1016/j.celrep.2016.03.001.

Neale, M.J., Pan, J. and Keeney, S. (2005) "Endonucleolytic processing of covalent protein-linked DNA double-strand breaks," *Nature*, 436(7053), pp. 1053–1057. Available at: https://doi.org/10.1038/nature03872.

Noordermeer, S.M. *et al.* (2018) "The shieldin complex mediates 53BP1-dependent DNA repair," *Nature*, 560(7716), pp. 117–121. Available at: https://doi.org/10.1038/s41586-018-0340-7.

Nowsheen, S. *et al.* (2018) "L3MBTL2 orchestrates ubiquitin signalling by dictating the sequential recruitment of RNF8 and RNF168 after DNA damage," *Nature Cell Biology*, 20(4), pp. 455–464. Available at: https://doi.org/10.1038/s41556-018-0071-x.

Ochs, F. *et al.* (2016) "53BP1 fosters fidelity of homology-directed DNA repair," *Nature Structural & Molecular Biology*, 23(8), pp. 714–721. Available at: https://doi.org/10.1038/nsmb.3251.

Paiano, J. *et al.* (2020) "ATM and PRDM9 regulate SPO11-bound recombination intermediates during meiosis," *Nature Communications*, 11(1), p. 857. Available at: https://doi.org/10.1038/s41467-020-14654-w.

Paigen, K. and Petkov, P. (2010) "Mammalian recombination hot spots: properties, control and evolution," *Nature Reviews Genetics*, 11(3), pp. 221–233. Available at: https://doi.org/10.1038/nrg2712.

Palek, M. *et al.* (2024) "RAD18 directs DNA double-strand break repair by homologous recombination to post-replicative chromatin," *Nucleic Acids Research*, 52(13), pp. 7687–7703. Available at: https://doi.org/10.1093/nar/gkae499.

Panier, S. and Boulton, S.J. (2014) "Double-strand break repair: 53BP1 comes into focus," *Nature Reviews Molecular Cell Biology*, 15(1), pp. 7–18. Available at: https://doi.org/10.1038/nrm3719.

Pannunzio, N.R., Watanabe, G. and Lieber, M.R. (2018) "Nonhomologous DNA end-joining for repair of DNA double-strand breaks," *Journal of Biological Chemistry*, 293(27), pp. 10512–10523. Available at: https://doi.org/10.1074/jbc.tm117.000374.

Pathania, S. *et al.* (2014) "BRCA1 haploinsufficiency for replication stress suppression in primary cells," *Nature Communications*, 5(1), p. 5496. Available at: https://doi.org/10.1038/ncomms6496.

Paull, T.T. and Gellert, M. (1998) "The 3' to 5' Exonuclease Activity of Mre11 Facilitates Repair of DNA Double-Strand Breaks," *Molecular Cell*, 1(7), pp. 969–979. Available at: https://doi.org/10.1016/s1097-2765(00)80097-0.

Pellegrino, S. *et al.* (2017) "Replication-Coupled Dilution of H4K20me2 Guides 53BP1 to Pre-replicative Chromatin," *Cell Reports*, 19(9), pp. 1819–1831. Available at: https://doi.org/10.1016/j.celrep.2017.05.016.

Pittman, D.L. *et al.* (1998) "Meiotic Prophase Arrest with Failure of Chromosome Synapsis in Mice Deficient for Dmc1, a Germline-Specific RecA Homolog," *Molecular Cell*, 1(5), pp. 697–705. Available at: https://doi.org/10.1016/s1097-2765(00)80069-6.

Piwko, W. *et al.* (2016) "The MMS22L–TONSL heterodimer directly promotes RAD51-dependent recombination upon replication stress," *The EMBO Journal*, 35(23), pp. 2584–2601. Available at: https://doi.org/10.15252/embj.201593132.

Pogliano, C.B. *et al.* (2022) "The CDK1-TOPBP1-PLK1 axis regulates the Bloom's syndrome helicase BLM to suppress crossover recombination in somatic cells," *Science Advances*, 8(5), p. eabk0221. Available at: https://doi.org/10.1126/sciadv.abk0221.

Polato, F. *et al.* (2014) "CtIP-mediated resection is essential for viability and can operate independently of BRCA1," *Journal of Experimental Medicine*, 211(6), pp. 1027–1036. Available at: https://doi.org/10.1084/jem.20131939.

Poon, R.Y.C. *et al.* (1996) "Cyclin-dependent Kinases Are Inactivated by a Combination of p21 and Thr-14/Tyr-15 Phosphorylation after UV-induced DNA Damage*," *Journal of Biological Chemistry*, 271(22), pp. 13283–13291. Available at: https://doi.org/10.1074/jbc.271.22.13283.

Poulsen, M. *et al.* (2012) "Human RNF169 is a negative regulator of the ubiquitin-dependent response to DNA double-strand breaks," *Journal of Cell Biology*, 197(2), pp. 189–199. Available at: https://doi.org/10.1083/jcb.201109100.

Pulver, E.M. *et al.* (2021) "A BRCA1 coiled-coil domain variant disrupting PALB2 interaction promotes the development of mammary tumors and confers a targetable defect in homologous recombination repair," *Cancer Research*, 81(24), p. canres.1415.2021. Available at: https://doi.org/10.1158/0008-5472.can-21-1415.

Quaas, M., Müller, G.A. and Engeland, K. (2012) "p53 can repress transcription of cell cycle genes through a p21WAF1/CIP1-dependent switch from MMB to DREAM protein complex binding at CHR promoter elements," *Cell Cycle*, 11(24), pp. 4661–4672. Available at: https://doi.org/10.4161/cc.22917.

Rabl, J. *et al.* (2019) "Structural Basis of BRCC36 Function in DNA Repair and Immune Regulation," *Molecular Cell*, 75(3), pp. 483-497.e9. Available at: https://doi.org/10.1016/j.molcel.2019.06.002.

Rafnar, T. *et al.* (2011) "Mutations in BRIP1 confer high risk of ovarian cancer," *Nature Genetics*, 43(11), pp. 1104–1107. Available at: https://doi.org/10.1038/ng.955.

Rahman, N. *et al.* (2007) "PALB2, which encodes a BRCA2-interacting protein, is a breast cancer susceptibility gene," *Nature Genetics*, 39(2), pp. 165–167. Available at: https://doi.org/10.1038/ng1959.

Rahman, N. and Stratton, M.R. (1998) "THE GENETICS OF BREAST CANCER SUSCEPTIBILITY," *Genetics*, 32(1), pp. 95–121. Available at: https://doi.org/10.1146/annurev.genet.32.1.95.

Reczek, C.R. *et al.* (2013) "The interaction between CtIP and BRCA1 is not essential for resection-mediated DNA repair or tumor suppression," *Journal of Cell Biology*, 201(5), pp. 693–707. Available at: https://doi.org/10.1083/jcb.201302145.

Refolio, E. *et al.* (2011) "The Ddc2/ATRIP checkpoint protein monitors meiotic recombination intermediates," *Journal of Cell Science*, 124(14), pp. 2488–2500. Available at: https://doi.org/10.1242/jcs.081711.

Reid, L.J. *et al.* (2008) "E3 ligase activity of BRCA1 is not essential for mammalian cell viability or homology-directed repair of double-strand DNA breaks," *Proceedings of the National Academy of Sciences*, 105(52), pp. 20876–20881. Available at: https://doi.org/10.1073/pnas.0811203106.

Rodriguez, M. *et al.* (2003) "Phosphopeptide Binding Specificities of BRCA1 COOH-terminal (BRCT) Domains*," *Journal of Biological Chemistry*, 278(52), pp. 52914–52918. Available at: https://doi.org/10.1074/jbc.c300407200.

Rogakou, E.P. *et al.* (1998) "DNA Double-stranded Breaks Induce Histone H2AX Phosphorylation on Serine 139*," *Journal of Biological Chemistry*, 273(10), pp. 5858–5868. Available at: https://doi.org/10.1074/jbc.273.10.5858.

Rogakou, E.P. *et al.* (1999) "Megabase Chromatin Domains Involved in DNA Double-Strand Breaks in Vivo," *The Journal of Cell Biology*, 146(5), pp. 905–916. Available at: https://doi.org/10.1083/jcb.146.5.905.

Ronson, G.E. *et al.* (2023) "Mechanisms of synthetic lethality between BRCA1/2 and 53BP1 deficiencies and DNA polymerase theta targeting," *Nature Communications*, 14(1), p. 7834. Available at: https://doi.org/10.1038/s41467-023-43677-2.

Rose, M. *et al.* (2020) "PARP Inhibitors: Clinical Relevance, Mechanisms of Action and Tumor Resistance," *Frontiers in Cell and Developmental Biology*, 8, p. 564601. Available at: https://doi.org/10.3389/fcell.2020.564601.

Roumelioti, F. *et al.* (2016) "Alternative lengthening of human telomeres is a conservative DNA replication process with features of break-induced replication," *EMBO reports*, 17(12), pp. 1731–1737. Available at: https://doi.org/10.15252/embr.201643169.

Royo, H. *et al.* (2010) "Evidence that Meiotic Sex Chromosome Inactivation Is Essential for Male Fertility," *Current Biology*, 20(23), pp. 2117–2123. Available at: https://doi.org/10.1016/j.cub.2010.11.010.

Royo, H. *et al.* (2013) "ATR acts stage specifically to regulate multiple aspects of mammalian meiotic silencing," *Genes & Development*, 27(13), pp. 1484–1494. Available at: https://doi.org/10.1101/gad.219477.113.

Russo, A.A. *et al.* (1998) "Structural basis for inhibition of the cyclin-dependent kinase Cdk6 by the tumour suppressor p16INK4a," *Nature*, 395(6699), pp. 237–243. Available at: https://doi.org/10.1038/26155.

Ryser, S. *et al.* (2009) "Distinct Roles of BARD1 Isoforms in Mitosis: Full-Length BARD1 Mediates Aurora B Degradation, Cancer-Associated BARD1β Scaffolds Aurora B and BRCA2," *Cancer Research*, 69(3), pp. 1125–1134. Available at: https://doi.org/10.1158/0008-5472.can-08-2134.

Sakofsky, C.J. *et al.* (2014) "Break-Induced Replication Is a Source of Mutation Clusters Underlying Kataegis," *Cell Reports*, 7(5), pp. 1640–1648. Available at: https://doi.org/10.1016/j.celrep.2014.04.053.

Salas-Lloret, D. *et al.* (2024) "BRCA1/BARD1 ubiquitinates PCNA in unperturbed conditions to promote continuous DNA synthesis," *Nature Communications*, 15(1), p. 4292. Available at: https://doi.org/10.1038/s41467-024-48427-6.

Salunkhe, S. *et al.* (2024) "Promotion of DNA end resection by BRCA1–BARD1 in homologous recombination," *Nature*, 634(8033), pp. 482–491. Available at: https://doi.org/10.1038/s41586-024-07910-2.

Sartori, A.A. *et al.* (2007) "Human CtIP promotes DNA end resection," *Nature*, 450(7169), pp. 509–514. Available at: https://doi.org/10.1038/nature06337.

Schimmel, J. *et al.* (2017) "Mutational signatures of non-homologous and polymerase theta-mediated end-joining in embryonic stem cells," *The EMBO Journal*, 36(24), pp. 3634–3649. Available at: https://doi.org/10.15252/embj.201796948.

Schlacher, K. *et al.* (2011) "Double-Strand Break Repair-Independent Role for BRCA2 in Blocking Stalled Replication Fork Degradation by MRE11," *Cell*, 145(4), pp. 529–542. Available at: https://doi.org/10.1016/j.cell.2011.03.041.

Schlacher, K., Wu, H. and Jasin, M. (2012) "A Distinct Replication Fork Protection Pathway Connects Fanconi Anemia Tumor Suppressors to RAD51-BRCA1/2," *Cancer Cell*, 22(1), pp. 106–116. Available at: https://doi.org/10.1016/j.ccr.2012.05.015.

Schotta, G. *et al.* (2004) "A silencing pathway to induce H3-K9 and H4-K20 trimethylation at constitutive heterochromatin," *Genes & Development*, 18(11), pp. 1251–1262. Available at: https://doi.org/10.1101/gad.300704.

Schrempf, A. *et al.* (2022) "POLθ processes ssDNA gaps and promotes replication fork progression in BRCA1-deficient cells," *Cell Reports*, 41(9), p. 111716. Available at: https://doi.org/10.1016/j.celrep.2022.111716.

Schreuder, A. *et al.* (2024) "(Single-stranded DNA) gaps in understanding BRCAness," *Trends in Genetics*, 40(9), pp. 757–771. Available at: https://doi.org/10.1016/j.tig.2024.04.013.

Scully, R. *et al.* (1997) "Association of BRCA1 with Rad51 in Mitotic and Meiotic Cells," *Cell*, 88(2), pp. 265–275. Available at: https://doi.org/10.1016/s0092-8674(00)81847-4.

Setiaputra, D. *et al.* (2022) "RIF1 acts in DNA repair through phosphopeptide recognition of 53BP1," *Molecular Cell*, 82(7), pp. 1359-1371.e9. Available at: https://doi.org/10.1016/j.molcel.2022.01.025.

Sfeir, A. and Symington, L.S. (2015) "Microhomology-Mediated End Joining: A Back-up Survival Mechanism or Dedicated Pathway?," *Trends in Biochemical Sciences*, 40(11), pp. 701–714. Available at: https://doi.org/10.1016/j.tibs.2015.08.006.

Shabbeer, S. *et al.* (2013) "BRCA1 targets G2/M cell cycle proteins for ubiquitination and proteasomal degradation," *Oncogene*, 32(42), pp. 5005–5016. Available at: https://doi.org/10.1038/onc.2012.522.

Shakya, R. *et al.* (2011) "BRCA1 Tumor Suppression Depends on BRCT Phosphoprotein Binding, But Not Its E3 Ligase Activity," *Science*, 334(6055), pp. 525–528. Available at: https://doi.org/10.1126/science.1209909.

Shao, G. *et al.* (2009) "MERIT40 controls BRCA1–Rap80 complex integrity and recruitment to DNA double-strand breaks," *Genes & Development*, 23(6), pp. 740–754. Available at: https://doi.org/10.1101/gad.1739609.

Shao, Z. *et al.* (2012) "Persistently bound Ku at DNA ends attenuates DNA end resection and homologous recombination," *DNA Repair*, 11(3), pp. 310–316. Available at: https://doi.org/10.1016/j.dnarep.2011.12.007.

Sharma, S. *et al.* (2015) "Homology and enzymatic requirements of microhomology-dependent alternative end joining," *Cell Death & Disease*, 6(3), pp. e1697–e1697. Available at: https://doi.org/10.1038/cddis.2015.58.

Sherker, A. *et al.* (2021) "Two redundant ubiquitin-dependent pathways of BRCA1 localization to DNA damage sites," *EMBO reports*, 22(12), p. e53679. Available at: https://doi.org/10.15252/embr.202153679.

Shiozaki, E.N. *et al.* (2004) "Structure of the BRCT Repeats of BRCA1 Bound to a BACH1 Phosphopeptide Implications for Signaling," *Molecular Cell*, 14(3), pp. 405–412. Available at: https://doi.org/10.1016/s1097-2765(04)00238-2.

Silverman, J. *et al.* (2004) "Human Rif1, ortholog of a yeast telomeric protein, is regulated by ATM and 53BP1 and functions in the S-phase checkpoint," *Genes & Development*, 18(17), pp. 2108–2119. Available at: https://doi.org/10.1101/gad.1216004.

Simhadri, S. *et al.* (2014) "Male Fertility Defect Associated with Disrupted BRCA1-PALB2 Interaction in Mice*," *Journal of Biological Chemistry*, 289(35), pp. 24617–24629. Available at: https://doi.org/10.1074/jbc.m114.566141.

Simsek, D. *et al.* (2011) "DNA Ligase III Promotes Alternative Nonhomologous End-Joining during Chromosomal Translocation Formation," *PLoS Genetics*, 7(6), p. e1002080. Available at: https://doi.org/10.1371/journal.pgen.1002080.

Sobhian, B. *et al.* (2007) "RAP80 Targets BRCA1 to Specific Ubiquitin Structures at DNA Damage Sites," *Science*, 316(5828), pp. 1198–1202. Available at: https://doi.org/10.1126/science.1139516.

Solyom, S. *et al.* (2012) "Breast Cancer–Associated Abraxas Mutation Disrupts Nuclear Localization and DNA Damage Response Functions," *Science Translational Medicine*, 4(122), p. 122ra23. Available at: https://doi.org/10.1126/scitranslmed.3003223.

Spies, J. *et al.* (2019) "53BP1 nuclear bodies enforce replication timing at under-replicated DNA to limit heritable DNA damage," *Nature Cell Biology*, 21(4), pp. 487–497. Available at: https://doi.org/10.1038/s41556-019-0293-6.

Spies, M. and Fishel, R. (2015) "Mismatch Repair during Homologous and Homeologous Recombination," *Cold Spring Harbor Perspectives in Biology*, 7(3), p. a022657. Available at: https://doi.org/10.1101/cshperspect.a022657.

Stewart, G.S. *et al.* (2003) "MDC1 is a mediator of the mammalian DNA damage checkpoint," *Nature*, 421(6926), pp. 961–966. Available at: https://doi.org/10.1038/nature01446.

Stewart, G.S. *et al.* (2009) "The RIDDLE Syndrome Protein Mediates a Ubiquitin-Dependent Signaling Cascade at Sites of DNA Damage," *Cell*, 136(3), pp. 420–434. Available at: https://doi.org/10.1016/j.cell.2008.12.042.

Stewart, M.D. *et al.* (2017) "Tuning BRCA1 and BARD1 activity to investigate RING ubiquitin ligase mechanisms," *Protein Science*, 26(3), pp. 475–483. Available at: https://doi.org/10.1002/pro.3091.

Stucki, M. *et al.* (2005) "MDC1 Directly Binds Phosphorylated Histone H2AX to Regulate Cellular Responses to DNA Double-Strand Breaks," *Cell*, 123(7), pp. 1213–1226. Available at: https://doi.org/10.1016/j.cell.2005.09.038.

Sun, Y. *et al.* (2009) "Histone H3 methylation links DNA damage detection to activation of the tumour suppressor Tip60," *Nature Cell Biology*, 11(11), pp. 1376–1382. Available at: https://doi.org/10.1038/ncb1982.

Sy, S.M.H., Huen, M.S.Y. and Chen, J. (2009) "PALB2 is an integral component of the BRCA complex required for homologous recombination repair," *Proceedings of the National Academy of Sciences*, 106(17), pp. 7155–7160. Available at: https://doi.org/10.1073/pnas.0811159106.

Taccioli, G.E. *et al.* (1998) "Targeted Disruption of the Catalytic Subunit of the DNA-PK Gene in Mice Confers Severe Combined Immunodeficiency and Radiosensitivity," *Immunity*, 9(3), pp. 355–366. Available at: https://doi.org/10.1016/s1074-7613(00)80618-4.

Tang, J. *et al.* (2013) "Acetylation limits 53BP1 association with damaged chromatin to promote homologous recombination," *Nature Structural & Molecular Biology*, 20(3), pp. 317–325. Available at: https://doi.org/10.1038/nsmb.2499.

Tarsounas, M. *et al.* (1999) "Rad51 and Dmc1 Form Mixed Complexes Associated with Mouse Meiotic Chromosome Cores and Synaptonemal Complexes," *The Journal of Cell Biology*, 147(2), pp. 207–220. Available at: https://doi.org/10.1083/jcb.147.2.207.

Tarsounas, M. and Sung, P. (2020) "The antitumorigenic roles of BRCA1–BARD1 in DNA repair and replication," *Nature Reviews Molecular Cell Biology*, 21(5), pp. 284–299. Available at: https://doi.org/10.1038/s41580-020-0218-z.

Tham, K.-C. *et al.* (2013) "Mismatch Repair Inhibits Homeologous Recombination via Coordinated Directional Unwinding of Trapped DNA Structures," *Molecular Cell*, 51(3), pp. 326–337. Available at: https://doi.org/10.1016/j.molcel.2013.07.008.

Thorslund, T. *et al.* (2015) "Histone H1 couples initiation and amplification of ubiquitin signalling after DNA damage," *Nature*, 527(7578), pp. 389–393. Available at: https://doi.org/10.1038/nature15401.

Tiwari, A., Jones, O.A. and Chan, K.-L. (2018) "53BP1 can limit sister-chromatid rupture and rearrangements driven by a distinct ultrafine DNA bridging-breakage process," *Nature Communications*, 9(1), p. 677. Available at: https://doi.org/10.1038/s41467-018-03098-y.

Truong, L.N. *et al.* (2013) "Microhomology-mediated End Joining and Homologous Recombination share the initial end resection step to repair DNA double-strand breaks in mammalian cells," *Proceedings of the National Academy of Sciences*, 110(19), pp. 7720–7725. Available at: https://doi.org/10.1073/pnas.1213431110.

Tsukada, K. *et al.* (2024) "BLM and BRCA1-BARD1 coordinate complementary mechanisms of joint DNA molecule resolution," *Molecular Cell* [Preprint]. Available at: https://doi.org/10.1016/j.molcel.2023.12.040.

Tubbs, A. and Nussenzweig, A. (2017) "Endogenous DNA Damage as a Source of Genomic Instability in Cancer," *Cell*, 168(4), pp. 644–656. Available at: https://doi.org/10.1016/j.cell.2017.01.002.

Turner, J.M.A. *et al.* (2004) "BRCA1, Histone H2AX Phosphorylation, and Male Meiotic Sex Chromosome Inactivation," *Current Biology*, 14(23), pp. 2135–2142. Available at: https://doi.org/10.1016/j.cub.2004.11.032.

Turner, J.M.A. *et al.* (2005) "Silencing of unsynapsed meiotic chromosomes in the mouse," *Nature Genetics*, 37(1), pp. 41–47. Available at: https://doi.org/10.1038/ng1484.

Turner, J.M.A. *et al.* (2006) "Pachytene Asynapsis Drives Meiotic Sex Chromosome Inactivation and Leads to Substantial Postmeiotic Repression in Spermatids," *Developmental Cell*, 10(4), pp. 521–529. Available at: https://doi.org/10.1016/j.devcel.2006.02.009.

Turner, J.M.A. (2007) "Meiotic sex chromosome inactivation," *Development*, 134(10), pp. 1823–1831. Available at: https://doi.org/10.1242/dev.000018.

Turner, J.M.A. (2015) "Meiotic Silencing in Mammals," *Annual Review of Genetics*, 49(1), pp. 395–412. Available at: https://doi.org/10.1146/annurev-genet-112414-055145.

Uckelmann, M. *et al.* (2018) "USP48 restrains resection by site-specific cleavage of the BRCA1 ubiquitin mark from H2A," *Nature Communications*, 9(1), p. 229. Available at: https://doi.org/10.1038/s41467-017-02653-3.

Vekariya, U. *et al.* (2024) "PARG is essential for Polθ-mediated DNA end-joining by removing repressive poly-ADP-ribose marks," *Nature Communications*, 15(1), p. 5822. Available at: https://doi.org/10.1038/s41467-024-50158-7.

Vincendeau, E. *et al.* (2022) "SHLD1 is dispensable for 53BP1-dependent V(D)J recombination but critical for productive class switch recombination," *Nature Communications*, 13(1), p. 3707. Available at: https://doi.org/10.1038/s41467-022-31287-3.

Virgilio, M.D. *et al.* (2013) "Rif1 Prevents Resection of DNA Breaks and Promotes Immunoglobulin Class Switching," *Science*, 339(6120), pp. 711–715. Available at: https://doi.org/10.1126/science.1230624.

Wang, B. *et al.* (2007) "Abraxas and RAP80 Form a BRCA1 Protein Complex Required for the DNA Damage Response," *Science*, 316(5828), pp. 1194–1198. Available at: https://doi.org/10.1126/science.1139476.

Wang, B. *et al.* (2009) "NBA1, a new player in the Brca1 A complex, is required for DNA damage resistance and checkpoint control," *Genes & Development*, 23(6), pp. 729–739. Available at: https://doi.org/10.1101/gad.1770309.

Wang, B. and Elledge, S.J. (2007) "Ubc13/Rnf8 ubiquitin ligases control foci formation of the Rap80/Abraxas/Brca1/Brcc36 complex in response to DNA damage," *Proceedings of the*

National Academy of Sciences, 104(52), pp. 20759–20763. Available at: https://doi.org/10.1073/pnas.0710061104.

Wang, H. *et al.* (2018) "PLK1 targets CtIP to promote microhomology-mediated end joining," *Nucleic Acids Research*, 46(20), pp. 10724–10739. Available at: https://doi.org/10.1093/nar/gky810.

Wang, M. *et al.* (2006) "PARP-1 and Ku compete for repair of DNA double strand breaks by distinct NHEJ pathways," *Nucleic Acids Research*, 34(21), pp. 6170–6182. Available at: https://doi.org/10.1093/nar/gkl840.

Wang, M. *et al.* (2023) "Crucial roles of the BRCA1-BARD1 E3 ubiquitin ligase activity in homology-directed DNA repair," *Molecular Cell*, 83(20), pp. 3679-3691.e8. Available at: https://doi.org/10.1016/j.molcel.2023.09.015.

Wang, X.S., Lee, B.J. and Zha, S. (2020) "The recent advances in non-homologous end-joining through the lens of lymphocyte development," *DNA Repair*, 94, p. 102874. Available at: https://doi.org/10.1016/j.dnarep.2020.102874.

Wang, X.W. *et al.* (1999) "GADD45 induction of a G2/M cell cycle checkpoint," *Proceedings of the National Academy of Sciences*, 96(7), pp. 3706–3711. Available at: https://doi.org/10.1073/pnas.96.7.3706.

Wang, Y.-G. *et al.* (2004) "Phosphorylation and Regulation of DNA Ligase IV Stability by DNA-dependent Protein Kinase*," *Journal of Biological Chemistry*, 279(36), pp. 37282–37290. Available at: https://doi.org/10.1074/jbc.m401217200.

Ward, I. *et al.* (2006) "The Tandem BRCT Domain of 53BP1 Is Not Required for Its Repair Function*," *Journal of Biological Chemistry*, 281(50), pp. 38472–38477. Available at: https://doi.org/10.1074/jbc.m607577200.

Ward, I.M. *et al.* (2003) "p53 Binding Protein 53BP1 Is Required for DNA Damage Responses and Tumor Suppression in Mice," *Molecular and Cellular Biology*, 23(7), pp. 2556–2563. Available at: https://doi.org/10.1128/mcb.23.7.2556-2563.2003.

Ward, I.M. *et al.* (2004) "53BP1 is required for class switch recombination," *The Journal of Cell Biology*, 165(4), pp. 459–464. Available at: https://doi.org/10.1083/jcb.200403021.

Wassing, I.E. *et al.* (2021) "The RAD51 recombinase protects mitotic chromatin in human cells," *Nature Communications*, 12(1), p. 5380. Available at: https://doi.org/10.1038/s41467-021-25643-y.

Weber-Lassalle, N. *et al.* (2019) "Germline loss-of-function variants in the BARD1 gene are associated with early-onset familial breast cancer but not ovarian cancer," *Breast Cancer Research*, 21(1), p. 55. Available at: https://doi.org/10.1186/s13058-019-1137-9.

Weinberg, R.A. (1995) "The retinoblastoma protein and cell cycle control," *Cell*, 81(3), pp. 323–330. Available at: https://doi.org/10.1016/0092-8674(95)90385-2.

West, K.L. *et al.* (2019) "LC8/DYNLL1 is a 53BP1 effector and regulates checkpoint activation," *Nucleic Acids Research*, 47(12), pp. 6236–6249. Available at: https://doi.org/10.1093/nar/gkz263.

West, S.C. (2003) "Molecular views of recombination proteins and their control," *Nature Reviews Molecular Cell Biology*, 4(6), pp. 435–445. Available at: https://doi.org/10.1038/nrm1127.

West, S.C. *et al.* (2015) "Resolution of Recombination Intermediates: Mechanisms and Regulation," *Cold Spring Harbor Symposia on Quantitative Biology*, 80, pp. 103–109. Available at: https://doi.org/10.1101/sqb.2015.80.027649.

Whelan, D.R. *et al.* (2018) "Spatiotemporal dynamics of homologous recombination repair at single collapsed replication forks," *Nature Communications*, 9(1), p. 3882. Available at: https://doi.org/10.1038/s41467-018-06435-3.

Widger, A. *et al.* (2018) "ATR is a multifunctional regulator of male mouse meiosis," *Nature Communications*, 9(1), p. 2621. Available at: https://doi.org/10.1038/s41467-018-04850-0.

Williams, R.S., Green, R. and Glover, J.N.M. (2001) "Crystal structure of the BRCT repeat region from the breast cancer-associated protein BRCA1," *Nature Structural Biology*, 8(10), pp. 838–842. Available at: https://doi.org/10.1038/nsb1001-838.

Wilson, D.M. and Thompson, L.H. (2007) "Molecular mechanisms of sister-chromatid exchange," *Mutation Research/Fundamental and Molecular Mechanisms of Mutagenesis*, 616(1–2), pp. 11–23. Available at: https://doi.org/10.1016/j.mrfmmm.2006.11.017.

Wilson, M.D. *et al.* (2016) "The structural basis of modified nucleosome recognition by 53BP1," *Nature*, 536(7614), pp. 100–103. Available at: https://doi.org/10.1038/nature18951.

Witus, S.R. *et al.* (2021) "BRCA1/BARD1 site-specific ubiquitylation of nucleosomal H2A is directed by BARD1," *Nature Structural & Molecular Biology*, 28(3), pp. 1–10. Available at: https://doi.org/10.1038/s41594-020-00556-4.

Witus, S.R. *et al.* (2022) "BRCA1/BARD1 is a nucleosome reader and writer," *Trends in Biochemical Sciences*, 47(7), pp. 582–595. Available at: https://doi.org/10.1016/j.tibs.2022.03.001.

Witus, S.R. *et al.* (2023) "BRCA1/BARD1 intrinsically disordered regions facilitate chromatin recruitment and ubiquitylation," *The EMBO Journal*, 42(15), p. e113565. Available at: https://doi.org/10.15252/embj.2023113565.

Witus, S.R., Stewart, M.D. and Klevit, R.E. (2021) "The BRCA1/BARD1 ubiquitin ligase and its substrates," *Biochemical Journal*, 478(18), pp. 3467–3483. Available at: https://doi.org/10.1042/bcj20200864.

Wojtasz, L. *et al.* (2009) "Mouse HORMAD1 and HORMAD2, Two Conserved Meiotic Chromosomal Proteins, Are Depleted from Synapsed Chromosome Axes with the Help of

TRIP13 AAA-ATPase," *PLoS Genetics*, 5(10), p. e1000702. Available at: https://doi.org/10.1371/journal.pgen.1000702.

Wojtasz, L. *et al.* (2012) "Meiotic DNA double-strand breaks and chromosome asynapsis in mice are monitored by distinct HORMAD2-independent and -dependent mechanisms," *Genes & Development*, 26(9), pp. 958–973. Available at: https://doi.org/10.1101/gad.187559.112.

Wu, J. *et al.* (2012) "RAP80 Protein Is Important for Genomic Stability and Is Required for Stabilizing BRCA1-A Complex at DNA Damage Sites in Vivo *," *Journal of Biological Chemistry*, 287(27), pp. 22919–22926. Available at: https://doi.org/10.1074/jbc.m112.351007.

Wu, L.C. *et al.* (1996) "Identification of a RING protein that can interact in vivo with the BRCA1 gene product," *Nature Genetics*, 14(4), pp. 430–440. Available at: https://doi.org/10.1038/ng1296-430.

Wu, Q. *et al.* (2016) "Structure of BRCA1-BRCT/Abraxas Complex Reveals Phosphorylation-Dependent BRCT Dimerization at DNA Damage Sites," *Molecular Cell*, 61(3), pp. 434–448. Available at: https://doi.org/10.1016/j.molcel.2015.12.017.

Wu, W. *et al.* (2015) "Interaction of BARD1 and HP1 Is Required for BRCA1 Retention at Sites of DNA Damage," *Cancer Research*, 75(7), pp. 1311–1321. Available at: https://doi.org/10.1158/0008-5472.can-14-2796.

Wu, X. and Wang, B. (2021) "Abraxas suppresses DNA end resection and limits break-induced replication by controlling SLX4/MUS81 chromatin loading in response to TOP1 inhibitor-induced DNA damage," *Nature Communications*, 12(1), p. 4373. Available at: https://doi.org/10.1038/s41467-021-24665-w.

Wyatt, H.D.M. *et al.* (2013) "Coordinated Actions of SLX1-SLX4 and MUS81-EME1 for Holliday Junction Resolution in Human Cells," *Molecular Cell*, 52(2), pp. 234–247. Available at: https://doi.org/10.1016/j.molcel.2013.08.035.

Xie, A., Kwok, A. and Scully, R. (2009) "Role of mammalian Mre11 in classical and alternative nonhomologous end joining," *Nature Structural & Molecular Biology*, 16(8), pp. 814–818. Available at: https://doi.org/10.1038/nsmb.1640.

Xu, G. *et al.* (2015) "REV7 counteracts DNA double-strand break resection and affects PARP inhibition," *Nature*, 521(7553), pp. 541–544. Available at: https://doi.org/10.1038/nature14328.

Xu, X. *et al.* (2001) "Genetic interactions between tumor suppressors Brca1 and p53 in apoptosis, cell cycle and tumorigenesis," *Nature Genetics*, 28(3), pp. 266–271. Available at: https://doi.org/10.1038/90108.

Xu, X. *et al.* (2003) "Impaired meiotic DNA-damage repair and lack of crossing-over during spermatogenesis in BRCA1 full-length isoform deficient mice," *Development*, 130(9), pp. 2001–2012. Available at: https://doi.org/10.1242/dev.00410.

Yamada, S. *et al.* (2020) "Molecular structures and mechanisms of DNA break processing in mouse meiosis," *Genes & Development*, 34(11–12), pp. 806–818. Available at: https://doi.org/10.1101/gad.336032.119.

Yamamoto, H. and Hirasawa, A. (2021) "Homologous Recombination Deficiencies and Hereditary Tumors," *International Journal of Molecular Sciences*, 23(1), p. 348. Available at: https://doi.org/10.3390/ijms23010348.

Yan, C.T. *et al.* (2007) "IgH class switching and translocations use a robust non-classical end-joining pathway," *Nature*, 449(7161), pp. 478–482. Available at: https://doi.org/10.1038/nature06020.

Yan, J., Kim, Y.-S., Yang, X.-P., Li, L.-P., *et al.* (2007) "The Ubiquitin-Interacting Motif–Containing Protein RAP80 Interacts with BRCA1 and Functions in DNA Damage Repair Response," *Cancer Research*, 67(14), pp. 6647–6656. Available at: https://doi.org/10.1158/0008-5472.can-07-0924.

Yan, J., Kim, Y.-S., Yang, X.-P., Albers, M., *et al.* (2007) "Ubiquitin-interaction motifs of RAP80 are critical in its regulation of estrogen receptor α," *Nucleic Acids Research*, 35(5), pp. 1673–1686. Available at: https://doi.org/10.1093/nar/gkl1112.

Yan, J. *et al.* (2008) "RAP80 Responds to DNA Damage Induced by Both Ionizing Radiation and UV Irradiation and Is Phosphorylated at Ser205," *Cancer Research*, 68(11), pp. 4269–4276. Available at: https://doi.org/10.1158/0008-5472.can-07-5950.

Yata, K. *et al.* (2012) "Plk1 and CK2 Act in Concert to Regulate Rad51 during DNA Double Strand Break Repair," *Molecular Cell*, 45(3), pp. 371–383. Available at: https://doi.org/10.1016/j.molcel.2011.12.028.

Yata, K. *et al.* (2014) "BRCA2 Coordinates the Activities of Cell-Cycle Kinases to Promote Genome Stability," *Cell Reports*, 7(5), pp. 1547–1559. Available at: https://doi.org/10.1016/j.celrep.2014.04.023.

Yilmaz, D. *et al.* (2021) "Activation of homologous recombination in G1 preserves centromeric integrity," *Nature*, 600(7890), pp. 748–753. Available at: https://doi.org/10.1038/s41586-021-04200-z.

Yin, X. *et al.* (2017) "Cryo-EM structure of human DNA-PK holoenzyme," *Cell Research*, 27(11), pp. 1341–1350. Available at: https://doi.org/10.1038/cr.2017.110.

Yoshida, K. *et al.* (1998) "The Mouse RecA-like Gene Dmc1 Is Required for Homologous Chromosome Synapsis during Meiosis," *Molecular Cell*, 1(5), pp. 707–718. Available at: https://doi.org/10.1016/s1097-2765(00)80070-2.

You, Z. *et al.* (2005) "ATM Activation and Its Recruitment to Damaged DNA Require Binding to the C Terminus of Nbs1," *Molecular and Cellular Biology*, 25(13), pp. 5363–5379. Available at: https://doi.org/10.1128/mcb.25.13.5363-5379.2005.

Youle, R.J. and Strasser, A. (2008) "The BCL-2 protein family: opposing activities that mediate cell death," *Nature Reviews Molecular Cell Biology*, 9(1), pp. 47–59. Available at: https://doi.org/10.1038/nrm2308.

Yu, W. *et al.* (2020) "Repair of G1 induced DNA double-strand breaks in S-G2/M by alternative NHEJ," *Nature Communications*, 11(1), p. 5239. Available at: https://doi.org/10.1038/s41467-020-19060-w.

Yu, X. *et al.* (2003) "The BRCT Domain Is a Phospho-Protein Binding Domain," *Science*, 302(5645), pp. 639–642. Available at: https://doi.org/10.1126/science.1088753.

Yu, X. *et al.* (2006) "BRCA1 ubiquitinates its phosphorylation-dependent binding partner CtIP," *Genes & Development*, 20(13), pp. 1721–1726. Available at: https://doi.org/10.1101/gad.1431006.

Yu, X. and Chen, J. (2004) "DNA Damage-Induced Cell Cycle Checkpoint Control Requires CtIP, a Phosphorylation-Dependent Binding Partner of BRCA1 C-Terminal Domains," *Molecular and Cellular Biology*, 24(21), pp. 9478–9486. Available at: https://doi.org/10.1128/mcb.24.21.9478-9486.2004.

Zgheib, O. *et al.* (2008) "An Oligomerized 53BP1 Tudor Domain Suffices for Recognition of DNA Double-Strand Breaks ▿," *Molecular and Cellular Biology*, 29(4), pp. 1050–1058. Available at: https://doi.org/10.1128/mcb.01011-08.

Zhang, B. *et al.* (2020) "NBS1 is required for SPO11-linked DNA double-strand break repair in male meiosis," *Cell Death & Differentiation*, 27(7), pp. 2176–2190. Available at: https://doi.org/10.1038/s41418-020-0493-4.

Zhang, Fan *et al.* (2009) "PALB2 Functionally Connects the Breast Cancer Susceptibility Proteins BRCA1 and BRCA2," *Molecular Cancer Research*, 7(7), pp. 1110–1118. Available at: https://doi.org/10.1158/1541-7786.mcr-09-0123.

Zhang, Feng *et al.* (2009) "PALB2 Links BRCA1 and BRCA2 in the DNA-Damage Response," *Current Biology*, 19(6), pp. 524–529. Available at: https://doi.org/10.1016/j.cub.2009.02.018.

Zhang, T. *et al.* (2023) "Break-induced replication orchestrates resection-dependent template switching," *Nature*, 619(7968), pp. 201–208. Available at: https://doi.org/10.1038/s41586-023-06177-3.

Zhang, Y. and Jasin, M. (2011) "An essential role for CtIP in chromosomal translocation formation through an alternative end-joining pathway," *Nature Structural & Molecular Biology*, 18(1), pp. 80–84. Available at: https://doi.org/10.1038/nsmb.1940.

Zhao, W. *et al.* (2017) "BRCA1–BARD1 promotes RAD51-mediated homologous DNA pairing," *Nature*, 550(7676), pp. 360–365. Available at: https://doi.org/10.1038/nature24060.

Zhou, J. *et al.* (2021) "A first-in-class polymerase theta inhibitor selectively targets homologous-recombination-deficient tumors," *Nature Cancer*, 2(6), pp. 598–610. Available at: https://doi.org/10.1038/s43018-021-00203-x.

Zhu, Z. *et al.* (2008) "Sgs1 Helicase and Two Nucleases Dna2 and Exo1 Resect DNA Double-Strand Break Ends," *Cell*, 134(6), pp. 981–994. Available at: https://doi.org/10.1016/j.cell.2008.08.037.

Zimmermann, M. *et al.* (2013) "53BP1 Regulates DSB Repair Using Rif1 to Control 5' End Resection," *Science*, 339(6120), pp. 700–704. Available at: https://doi.org/10.1126/science.1231573.

Zong, D. *et al.* (2019) "BRCA1 Haploinsufficiency Is Masked by RNF168-Mediated Chromatin Ubiquitylation," *Molecular Cell*, 73(6), pp. 1267-1281.e7. Available at: https://doi.org/10.1016/j.molcel.2018.12.010.